Natural products from some filamentous fungi and other sources

Nirmal Kumar Chaudhary

Master of Pharmacy (Pharmaceutical Chemistry)

Bachelor of Pharmaceutical Sciences

This thesis is submitted in the partial fulfilment of the requirements for the degree of

Doctor of Philosophy

Department of Molecular Sciences

Faculty of Science and Engineering

MACQUARIE University

Sydney, Australia

December 2017

Acknowledgement

First and foremost, I would like to thank my supervisor, Prof. Peter Karuso for giving me the opportunity to carry out this research. Without his continuous support and supervision, the completion of this thesis would not have been possible. I would also like to thank my assosciate supervisor Dr. Andrew Piggott for his advice and encouragement during the course of this research. I express my sincere thanks to Dr. Ernest Lacey, Microbial Screening Technologies for providing me the crude fungal extracts and performing the bioassays.

I am thankful to the current and past members of our research group Kavita, Ketan, Imam, Jenny, Andre, Wendy, Girish and Tahnim for their help and support during my stay at Macquarie University. I would also like to thank current and past members of other research groups- Mohammad, Haq, Shahjahan, Shalini, Michael, Tareq and Fuyan.

I extend my sincere thanks to all the staff members of the Department of Molecular Sciences, especially, Prof. Alison Rodger, Dr. Erika Davies, Dr. Mathew McKay, Anthony Gurlica, Mark Tran and Tony Wang.

I am grateful to my family members for their continuous support and encouragement.

Declaration

I declare that this thesis entitled "*Natural products from some filamentous fungi and other sources*" is a presentation of my original work. No part of this thesis has been submitted to any other university or institution for award of any degree. To the best of my knowledge and belief, this thesis contains no material previously published or written by another person except where due references are made.

Nirmal Chaudhary

December 2017

Notes for readers

This thesis is drafted as a compilation of published article and four other preliminary manuscripts hence may have inconsistencies in formatting from chapter to chapter arising from variations in the requirements of the journals to which they are submitted or intended to be submitted.

List of Abbreviations and Symbols

1D	One dimensional
2D	Two dimensional
amu	atomic mass unit
Å	Angstrom
BGC	Biosynthetic gene clusters
BCRP	Breast cancer resistance protein
°C	degree Celsius
$[\alpha]^{T}_{D}$	Specific rotary power, sodium D-line (589 nm); T: temperature
br	broad (in connection with NMR data)
c	concentration
CCK	cholecystokinin
cm	centimeter
CD	Circular dichroism
$CDCl_3$	deutero-chloroform
CoA	Coenzyme A
COSY	Correlation spectroscopy
δ	NMR chemical shift [ppm]
d	doublet
dd	doublet of doublets
ddd	doublet of doublet of doublet
dq	doublet of quartet
dt	doublet of triplet
DMSO-d_6	dimethyl sulfoxide-d_6
DNA	Deoxyribonucleic acid

ECD	Electronic circular dichroism
ESIMS	Electron spray ionization mass spectrometry
IR	Infrared spectroscopy
FDA	Food and Drug Administration
g	gram
h	hour
HMBC	Heteronuclear multiple bond correlation
HPLC	High performance liquid chromatography
HSQC	Heteronuclear single quantum correlation
HTS	High-throughput screening
HRESIMS	High-resolution electron-spray ionization mass spectrometry
Hz	Hertz
J	coupling constant
L	liter
m	*meta*
m	multiplet
mdeg	millidegrees
MeOH	Methanol
mg	milligram
MHz	Megahertz
MIC	Minimum inhibitory concentration
MOE	Molecular Operating Environment
min	minute
MRSA	Methicillin resistant *Staphylococcus aureus*

m/z	mass-to-charge ratio (in connection with mass spectrometry)
nm	nanometer
NMR	Nuclear magnetic resonance
o	*ortho*
p	*para*
PKS	polyketide synthase
ppm	parts per million
q	quartet
ROESY	Rotating-frame overhause effect spectroscopy
RP	Reversed phase
s	singlet
SAM	S-Adenosyl methionine
t	triplet
tt	triplet of triplet
TDDFT	Time dependent density functional theory
TFA	Trifluoroacetic acid
TLC	Thin layer chromatography
UV	Ultraviolet
VRE	Vancomycin resistant *Enterococci*
µ	micro
ν	wave number [cm^{-1}]
λ_{abs}	Absorption wavelength

Abstract

Natural products remain a major source for new drugs and drug leads owing to their unparalleled structural and chemical diversity and "drug-likeness" because of their evolutionary optimization to interact with living systems, unlike synthetic libraries. However, a combination of tedious isolation, repetitive isolation of known compounds, poor yields (supply) and structural complexities hindering total synthesis are some major bottlenecks in the process of drug discovery and development from natural products. Microorganisms offer a relatively unexplored source of new natural products by virtue of their vast biodiversity that can address the supply issue through fermentation. Moreover, microorganisms are amenable to selection and genetic manipulation for overproduction of the desired metabolite(s).

The primary aim of this thesis is the isolation, characterization and biological screening of the secondary metabolites of some filamentous fungal species. Secondary metabolites of three filamentous fungi – *Aspergillus banksianus*, *Aspergillus luteorubrus* and *Talaromyces stipitatus* were characterized and screened. A total of 15 polyketide derived natural products were isolated from *A. banksianus* of which 10 were new metabolites. Among these, were the first isochromanone-orsellinic acid conjugates, isochromanone-anthraquininone conjugate and sulphur containing isochromanones including a rare sulfoxide metabolite. Chemical investigation of *A. luteorubrus* resulted in six metabolites including two new molecules, one was known but is a new natural product. *Talaromyces stipitatus* led to the isolation of 21 molecules among which nine were new molecules. Among the new metabolites of *T. stipitatus* were 5 natural talauxins, which are condensation products of duclauxin with various L-amino acids. The semi-synthesis of new analogues of talauxins derived from D- and L-amino acids (except proline) and duclauxin is described.

In addition, four new molecules from an Australian rainforest tree *Galbulimima baccata* were isolated and characterized.

The structures of the isolated compounds were established by 2D NMR spectroscopy. Absolute stereochemistry of the isolated compounds was determined based on optical rotations, ECD, NMR, molecular modelling and TDDFT calculations. Plausible biogenetic pathway leading to these secondary metabolites are proposed wherever possible which can help in the design of biomimetic synthesis of these compounds.

Table of Contents

Chapter one

INTRODUCTION

Natural products, generally referred to the secondary metabolites, are formed in living organisms in response to some external stimulus such as environmental and nutritional changes, infection and competition with other organisms. Secondary metabolites, unlike primary metabolites are not essential for normal growth, development or reproducibility of the organism directly but can have important ecological and other functions.[1] Most living beings produce some sort of secondary metabolites. The role of secondary metabolites in animals including human beings which live by physical means is not so apparent. However, the role of secondary metabolites is conspicuous in plants, invertebrates, microorganisms and some other organisms which need to compensate for one or more challenges or inherent limitations including restricted movement, lack of physical defenses (e.g., a shell), extreme competition for food and space.[2] Not only do secondary metabolites have a definite role in the producing organism, but also many of them are capable of exhibiting some sort of biological activity in human beings or other organisms. Mankind has been able to exploit the properties exhibited by secondary metabolites, either directly or indirectly, knowingly or unknowingly for their own benefit since the beginning of human civilization itself.[3] Natural products have since then found important applications as medicines, herbicides, insecticides, reagents and probes for cellular and biological processes, nutraceuticals, and so on, the most remarkable application being their use as medicines.[4]

Medicine has been closely linked with natural products for thousands of years through the various traditional systems of medicines practiced across the globe.[3,5] These traditional medicines were mostly dependent on plant derived extracts in some form.[3,5] The bioactive principles of many of the early traditional medicines (Figure 1) such as morphine,

artemisnin, quinine, digitoxin, salicin and pilocarpine are in fact still being used albeit in their pure form rather than as crude extracts.[6] The first natural product to be commercially used as a medicine in pure chemical form was the opioid analgesic morphine introduced by Merck in 1826 whereas the first semi-synthetic pure drug aspirin, based on a natural product salicin was introduced by Bayer in 1899.[7] However, the seminal point in the use of natural products as therapeutic agents is the serendipitous discovery of the antibacterial penicillin by Alexander Fleming in 1928.[8] The subsequent isolation and introduction of penicillin G in clinical use by Florey and Chain in 1941 heralded the beginning of the golden age of antibiotics.[9] A post penicillin hunt for further antibiotics from various microbes was followed by the subsequent discovery of many other antibacterial agents such as streptomycin from *Streptomyces griseus* in 1943,[10] chlortetracycline from *S. aureofaciens* in 1945,[11] chloramphenicol from *S. venezuelae* in 1947,[12] erythromycin from *Sachharopolyspora erythreae* in 1952,[13] vancomycin from *Amycolatopsis orientalis* in 1953;[14] antitumor agents such as dactinomycin from *Streptomyces parvullus* in 1940,[15] bleomycin from *S. verticillus* in 1962,[16] daunorubicin from *S. peucetius* in 1962,[16] doxorubicin from a mutant strain of *S. peucetius* in 1967;[17] and antifungal drugs such as nystatin from *S. noursei* in 1950,[18] amphotericin B from *S. nodosus* in 1953[19] (Figure 2). These natural products discovered in the period 1940-1970, widely heralded as the golden age of antibiotics, not only remain in clinical use till date but their discovery laid the foundation for modern drug discovery and development. Thousands of novel bioactive secondary metabolites with a wide range of biological activities have been discovered since then.

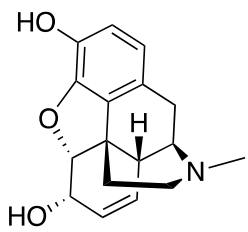

Morphine

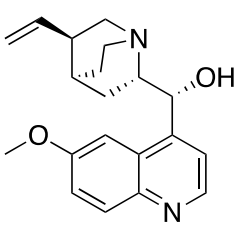

Quinine

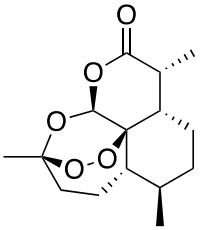

Artemisnin

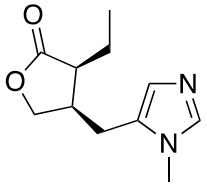

Pilocarpine

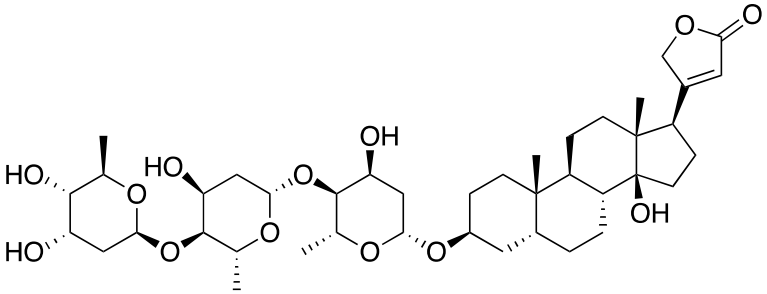

Digitoxin

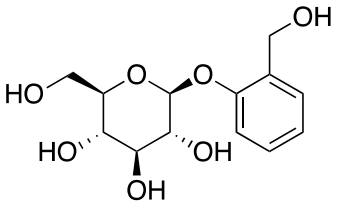

Salicin

Figure 1: Active principles involved in some traditional medicines

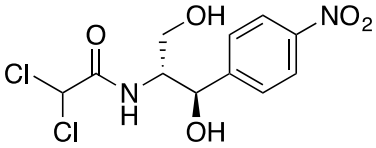

Chloramphenicol

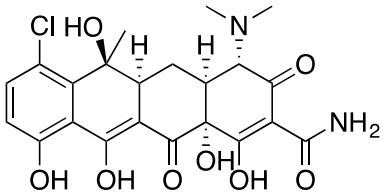

Chlortetracycline

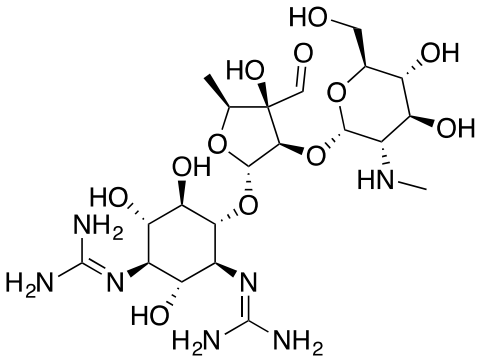

Streptomycin

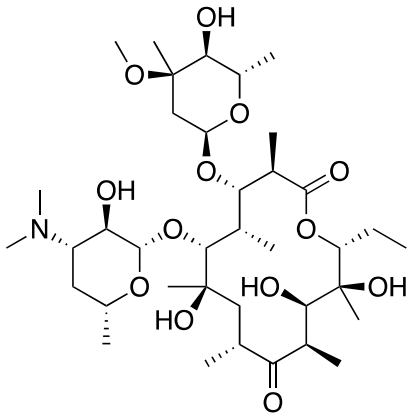

Erythromycin

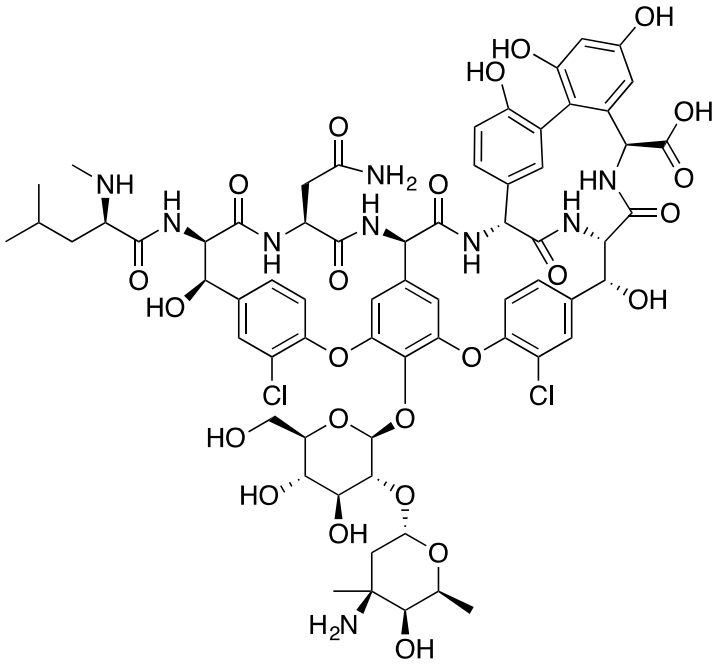

Vancomycin

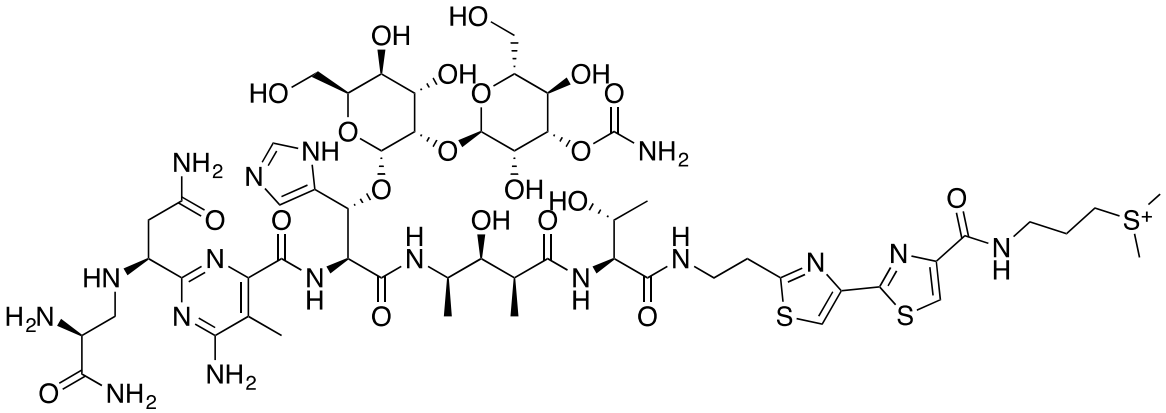

Bleomycin

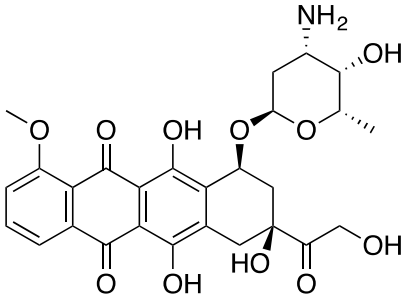

Doxorubicin

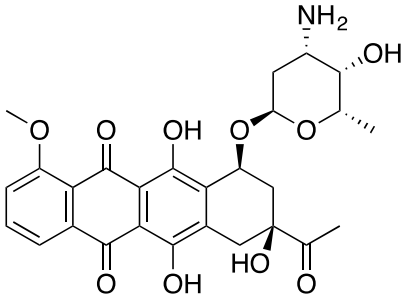

Daunorubicin

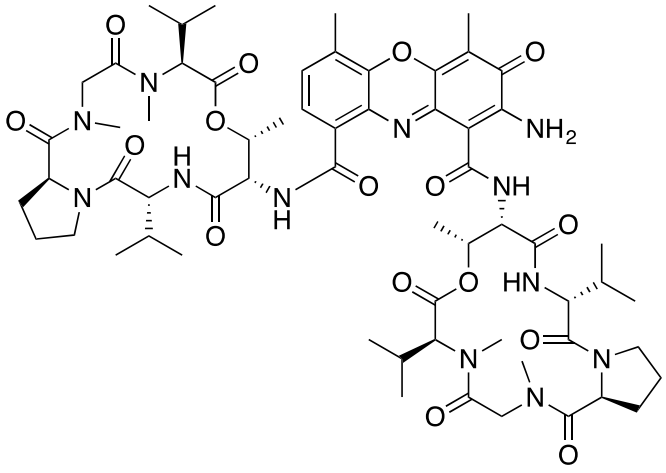

Dactinomycin

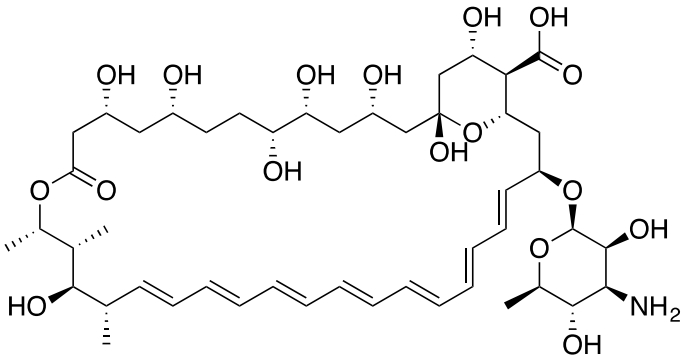

Amphotericin B

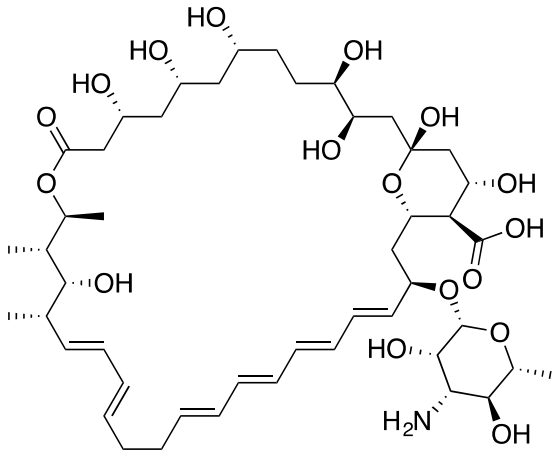

Nystatin

Figure 2: Some antibiotics discovered during the golden era of antibiotics (1940-1970)

1.1 Status of natural products in drug discovery and development

Despite of the long history of the use of natural products as sources of drugs and drug leads, the last two decades have witnessed substantial downscaling of natural product research by pharmaceutical companies.[20] One major contributing cause was the belief that natural products are somehow incompatible with drug discovery approaches that are based on high-throughput screening (HTS) directed towards molecular targets.[21] Another major factor is the ownership of natural products discovered from traditional medicines. Beside these other conventional bottlenecks in drug discovery from natural products such as rigorous isolation processes, poor yields, repetitive isolation of known compounds and structural complexities hindering total synthesis/structural modifications were the other contributing factors. However, the failure of combinatorial chemistry to deliver new drugs along with the growing appreciation of functional assays and phenotypic screens are likely to revive the natural product research for drug discovery in the near future.[22] This can be attributed to two main pros of natural products in contrast to the synthetic libraries, firstly because they possess incredible structural and chemical diversity in terms of pharmacophore and stereochemistry and secondly because they possess "drug-likeness" owing to their tendency to interact with living systems.[23] This can be further justified by the fact that in spite of the diminished focus on natural product research, an analysis of the total number of small molecule drugs approved by US Food and Drug Administration (FDA) from 1981 to 2010 revealed that 34% of them were based on natural products or direct derivatives of natural products.[24] This proportion is even higher when considering only antibiotics (49%) or anticancer compounds (61%).[24]

The historical success of natural products in drug discovery and development is remarkable considering the fact that the vast majority end up being confined to the research laboratory

in which they were discovered with little or no biological assessment. It is estimated that a mere 2% of the nearly 50,000 microbial metabolites isolated to date have been available to the wider research community.[25] Since natural products are designed to interact with living systems, it is logical to assume that even those natural products which are currently regarded as inactive could have some sort of biological activity or ecological role to play, yet to be unraveled. Many natural products initially reported as inactive were later found to be bioactive or possessed bioactivity in addition to that originally reported (polypharmacology).[25] For example, the fungal metabolite mycophenolic acid, the first crystalline antibiotic, was shown to possess antibacterial activity as early as 1893 by Italian physician Gossi whereas its clinical use as an immunosuppressant, as the prodrug mycophenolate mofetil, was approved by the FDA as late as 1995.[26] Similarly, certain mycotoxins such as the cytochalasins, aflatoxins, fumitremorgin C and fumonisins, which were earlier identified as hazards to humans and livestocks have been re-discovered as important molecular reagents.[27] For example, cytochalasins have played important role in understanding cytoskeletal movement and many other biological processes.[28] Also, cytochalasins, particularly cytochalasin D has practical application in thromboelastometry whole blood assays for assessment of fibrinogen and fibrin polymerization disorders.[29] Fumitremorgin C reverses multidrug resistance in cells mediated by breast cancer resistance protein (BCRP) and is a pharmacological probe for the expression and molecular action of the transporter BCRP.[30] Natural products will continue to play a vital role in drug discovery, agriculture and understanding of biological processes as long as there are untapped sources of new natural products and advances in the instrumentation and techniques involved to access and utilize them for potential applications. The challenge is to find their intended target(s) and to subvert this natural activity to our advantage.

1.2 Microbial natural products

Microorganisms are a relatively unexplored source of natural products and hence the vast biodiversity of microorganisms presents a potential source of new drug leads. It is estimated that only around 0.1 ~ 1.0% of microorganisms can be cultured using current techniques.[31] Moreover, microorganisms offers several advantages as a source of secondary metabolites compared to the other sources of natural products such as plants and marine organisms. Firstly, microbes can be subjected to large-scale culture and can be stored indefinitely ensuring sustained availability of the source organism, and their metabolites. Secondly, microbes are amenable to genetic manipulation for the overproduction of the desired metabolite(s) thereby overcoming the yield limitations often encountered with other sources such as marine natural products.[27] Moreover, microbial natural products are not just notable for their biological activities but equally known for their desired pharmacokinetic properties making them suitable for direct clinical use without any structural modifications.[6] Streptomycin, erythromycin, vancomycin, chloramphenicol, natamycin, kanamycin A, tetracycline, fusidic acid, cyclosporine, rapamycin, bleomycin, dactinomycin, mitomycin C, amphotericin B, griseofulvin, nystatin and lovastatin are some examples of the many microbial metabolites that are used clinically without any structural modification.

Microorganisms produce secondary metabolites which confer upon them some competitive advantage in their native environments. For controlling the competing bacteria, microbes produce antibiotics such as penicillin, tetracyclines, gentamicin, erythromycin, mupirocin, rifamycins, teicoplanin, capreomycin. Against competing fungi they produce antifungals such as natamycin, nystatin, amphotericin, griseofulvin and cycloheximide; against protozoa spiramycin, paramomycin, monensin, salinomycin, lasalocid A and maduramycin, and against plants herbicides like herbicidin, glufosinate and bialophos.[32] Similarly, to curb

predation by larger organisms such as worms and insects they produce antihelminthics such as the avermectins and paraherquamide, and insecticides such as the milbemectins, piericidins, versimide and spinosads.[6] To encourage plants and animals beneficial for them, they produce growth stimulants and metabolites that inhibit pathogens such as candicidin[33] and valinomycin.[34]

During the early years, testing of microbial metabolites were almost exclusively limited to antibacterial activities and later for their antifungal, antiparasitic and anticancer activities. However, with the improved understanding of the pathophysiology of diseases, the therapeutic utility of microbial metabolites has moved beyond controlling infections. For example, the discovery of selective inhibition by lovastatin and compactin of the enzyme 3-hydroxy-3-methylglutaryl-CoA reductase, an enzyme essential for sterol biosynthesis led to the development of a new class of hypolipidemic drugs, the statins.[35] Similarly, understanding the pathophysiology involved in organ rejection led to the discovery of immunosuppressants such as cyclosporine A, mycophenolic acid, FK506 and rapamycin.[6] Understanding the mechanism of β-lactamase (penicillinase) resistance, led to the discovery of the β-lactamase inhibitor clavulanic acid.[36] Similarly, an α-glucosidase inhibitor, acarbose, isolated from the filamentous bacterium *Actinoplanes* sp. is used in treatment of diabetes mellitus type II.[37] Optimization of the lead compound, asperlicin, a fungal natural product led to the discovery of cholecystokinin (CCK) antagonists of the benzodiazepines and quinazolidinone class, used for the treatment of anxiety and insomnia.[38]

Macro-organisms such as plants and sponges are considered by some to be massive consortium of microbes that produces the natural products we see. Many natural products previously reported from plants and sponges are now known to be in fact produced by an

associated microorganism and in some cases, both by the host organism and associated microbes. For example, lassomycin, a mycobacterial protease inhibitor,[39] and many other diverse secondary metabolites including the antitumor polyketide onnamides and theopederins present in the marine sponge *Theonella swinhoei,* are actually made by an unculturable symbiont *Entotheonella* sp.[40] Similarly, bryostatin 1, pederin, mycalamide A, mazamine A and theopalauamide are suggested to be derived from microbial symbionts.[41,42] Also, the anticancer drugs taxol and podophyllotoxin are considered to be produced by endophytic microbes. For example, taxol isolated from the plant *Taxus brevifolia* is reportedly produced by the endophytic fungus *Taxomyces andreanae*.[43] Similarly, podophyllotoxin, the precursor for semi-synthetic anticancer drugs etoposide and teniposide, and isolated from the rhizomes of *Podophyllum peltatum* is reported to be produced by the endophyte *Phialocephela fortinii*.[44] However, because these claims have not been verified by genetic studies and they have not led to commercial or even research commodity chemical production, these stories may have no basis in fact. For example, the genes responsible for nearly every step of taxol biosynthesis have been isolated from plant and functionally characterized. No such gene has been identified in *Taxaomyces andreanea* or any other fungus. Finding these biosynthetic genes in fungi is technically much less demanding than plants.[45]

1.3 Bioactive natural products of fungal origin

Fungi are ubiquitous eukaryotic organisms that yield a broad range of secondary metabolites and their biological activities also have a long history. It has been estimated that some 1.5 - 3 million fungal species exist of which only around 100,000 species have been described so far.[46] This estimate reveals that the fungal world has only been scratched so far. A multitude of new fungal species are likely to be discovered in the future from diverse habitats. Apart

from the untapped biodiversity, recent sequencing of complete fungal genomes has revealed that many natural product gene clusters are silent, suggesting the possibility of many more compounds yet to be discovered in common organisms.[47] Despite efforts to stimulate such pathways using epigenetic modifiers,[48,49] it is evident that the full biosynthetic potential, even of the well-studied model organism *Aspergillus nidulans*, is not completely understood strongly reflecting Nature's potential as a source of new promising bioactive small molecules.[50]

The discovery, and successful clinical use of the fungal metabolite penicillin G was a revolution in medicinal chemistry. This was the first natural antibiotic to be successfully introduced to clinical use and prompted the hunt for other bioactive fungal metabolites that has led to several novel metabolites with diverse structures and functions. This has culminated in several clinically and commercially successful fungal metabolites (**Fig. 3**) that has the hypolipidemic lovastatin isolated from *Aspergillus terreus*,[51] immunosuppressants cyclosporine A isolated from *Tolypocladium inflatum,*[52] and mycophenolic acid from *Penicillium brevicompactum*[26] and antifungal agents fusidic acid from *Fusidium coccineum*[53] and griseofulvin from *Penicillium griseofulvum.*[54]

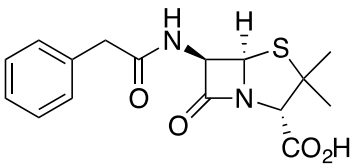

Penicillin G

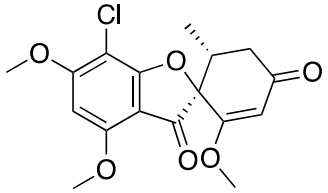

Griseofulvin

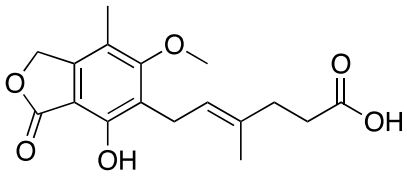

Mycophenolic acid

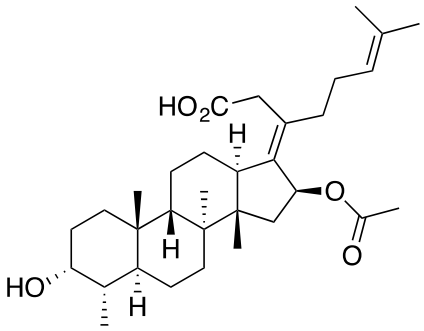

Fusidic acid

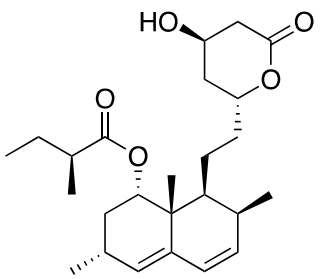

Lovastatin

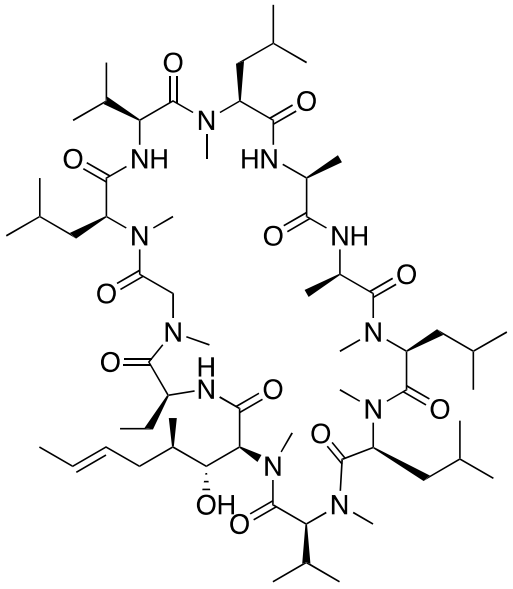

Cyclosporin A

A number of bioactive fungal metabolites though themselves not used clinically are progenitor or precursor to a number of clinically used drugs. For example, cephalosporin C, an antibacterial fungal metabolite from the filamentous fungus *Acremonium chrysogenum,* is the progenitor of an important class of antibacterial drugs, the cephalosporins such as cephalexin.[55,56] Similarly, pleuromutilin, discovered as an antibiotic in 1950 from the fungus *Clitopilus passeckerianus* (formerly *Pleurotus passeckerianus*), is the progenitor of the clinically used drug retapamulin and veterinary drugs valnemulin and tiamulin.[57] Pneumocandin B_0 from the filamentous fungus *Glarea lozoyensis,* although itself not used clinically is the precursor for the antifungal drug caspofungin.[58] Similarly, FR901379 from

the filamentous fungus *Coleophoma empetri,* though itself not in clinical use, is the precursor for the antifungal drug micafungin.[59]

1.4 Recent trends in microbial natural products

The vast majority of microbes (> 99%) are not easily cultured in the standard laboratory conditions using synthetic media and remains unexplored.[60] Hence, exploration of new culture methods to allow cultivation of hitherto neglected microbes can unravel several new bioactive natural products with potentially new mode of actions. This has recently led to a number of innovative culturing methods. One such method is the use of an isolation chip (iChip) which involves growing of microbes inside diffusion chambers incubated *in situ* which provides microorganisms with their naturally occurring growth factors. The iChip is composed of several hundred miniature diffusion chambers, each inoculated with a single environmental cell.[60] The iChip method is expected to expand the fraction of culturable microbes from 1 to 50%.[61] Teixobactin is a novel depsipeptide antibiotic produced from a new species of β-proteobacteria *Elefthera terrae* using the iChip method.[61] Similarly, novel antibiotics neocitreamicin I and II, from a novel *Nocardia* strain with in-vitro activity against Gram-positive bacteria including MRSA and VRE[62] and Novo10, an antibiotic candidate with potential anti-neoplastic properties from *Oerskovia paurometabola* are other natural products isolated using a diffusion chamber, the prototype of iChip.[63]

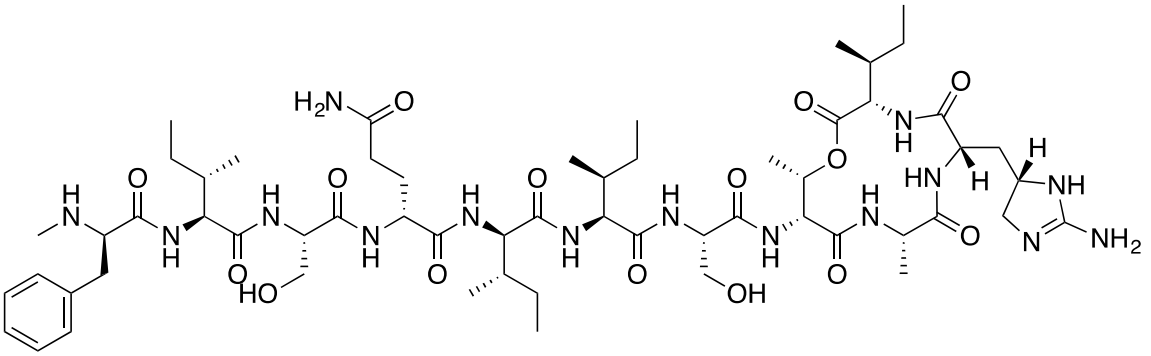

Teixobactin

Accessing the metagenome from environmental samples is another recent trend utilized as a tool for the discovery of novel cryptic bioactive compounds from otherwise uncultivable microbial species.[64,65] Metagenomics offering access to the genetic information present in these uncultured microbes by screening of libraries constructed from DNA isolated from different habitats. Antibacterials such as violacein, nocardamine, indigo and turbomycins were all developed from soil libraries using metagenomics.[66]

Rapid advances in genomics and bioinformatics has revealed that the biosynthetic potential and metabolic capabilities of microbes extend much beyond than was expected from classical biological screens.[67] Genome sequencing has revealed the presence of several cryptic biosynthetic gene clusters (BGC) in microbes.[68] Heterologous gene expression, epigenetic perturbation, manipulation of biosynthetic pathway specific regulators are some important methods of activating silent BGC.[67] Activation of these silent gene clusters has resulted in several new natural products[68] including asperfuranone, aspyridones, terrequinone, stabomycin, kanamycin, gaburedins, burkholdacs, thailindamide, chladochromes, nygerone A, closthioamides B-H and pulvomycin.[67] Heterologous gene expression involves expression of a single gene, a cassette of genes, or an entire biosynthetic gene cluster in a genetically tractable host[68] and is a remarkably practical alternative route for identifying and engineering the corresponding natural products.[69,70] Heterologous gene expression have led to the discovery of natural products such as haloduracin, avermitilol, epiisozizaene and terferol analogues.[67]

1.5 Aim and significance of the study

Filamentous fungi such as *Aspergillus, Penicillium* and *Talaromyces* are historically known to harbor genes responsible for an arsenal of diverse array of natural products. The primary aim of this thesis was isolation and characterization of the secondary metabolites from some

filamentous fungal species. Structure elucidation of purified compounds were determined by NMR spectroscopy in conjunction with mass spectrometry. The purified compounds were subjected to antimicrobial, antifungal, antiprotozoal and cytotoxicity bioassays to test their pharmaceutical potential.

Additionally, new *Galbulimima* alkaloids, were to be isolated and characterized from the bark of the rainforest tree, *G. baccata* that could act as either the potential intermediates/links or unravel new pathways in the biosynthesis of these unique and complex group of alkaloids.

References

(1) Croteau, R.; Kutchan, T. M.; Lewis, N. G., *Natural products (secondary metabolites)*. 2000; Vol. 24, p 1250-1319.

(2) Verpoorte, R., *Drug Discov. Today* **1998,** 3, (5), 232-238.

(3) Lahlou, M., *Pharmacol. Pharm.* **2013,** 4, (3A), 17-31.

(4) Kiuru, P.; D'Auria, M. V.; Muller, C. D.; Tammela, P.; Vuorela, H.; Yli-Kauhaluoma, J., *Planta Med.* **2014,** 80, (14), 1234-1246.

(5) Butler, M. S., *J. Nat. Prod.* **2004,** 67, (12), 2141-2153.

(6) Brahmachari, G., *Bioactive Natural Products: Chemistry and Biology*. John Wiley & Sons: 2015.

(7) Newman, D. J.; Cragg, G. M.; Snader, K. M., *Nat. Prod. Rep.* **2000,** 17, (3), 215-234.

(8) Haven, K., *Marvels of Science: 50 Fascinating 5-minute Reads*. ERIC: 1994.

(9) Aldridge, S.; Parascandola, J.; Sturchio, J. L.; Society, A. C.; Chemistry, R. S. o., *The Discovery and Development of Penicillin 1928-1945: The Alexander Fleming*

Laboratory Museum, London, UK, November 19, 1999 : an International Historic Chemical Landmark. American Chemical Society: 1999.

(10) Schatz, A.; Bugle, E.; Waksman, S. A., *Proc. Soc. Exp. Biol. Med.* **1944,** 55, (1), 66-69.

(11) Ochsendorf, F., *Am. J. Clin. Dermatol.* **2010,** 11, (5), 327-341.

(12) Wiest, D. B.; Cochran, J. B.; Tecklenburg, F. W., *J. Pediatr. Pharmacol. Ther.* **2012,** 17, (2), 182-188.

(13) Ma, Z.; Nemoto, P. A., *Curr. Med. Chem.: Anti-Infect. Agents* **2002,** 1, (1), 15-34.

(14) Shnayerson, M.; Plotkin, M. J., *The Killers Within: The Deadly Rise of Drug-resistant Bacteria*. Little, Brown: 2002.

(15) Hollstein, U., *Chem. Rev.* **1974,** 74, (6), 625-652.

(16) Sneader, W., *Drug discovery: a history*. John Wiley & Sons: 2005.

(17) Raviña, E., *The evolution of drug discovery: from traditional medicines to modern drugs*. John Wiley & Sons: 2011.

(18) Razonable, R. R.; Henault, M.; Watson, H. L.; Paya, C. V., *Antimicrob. Agents Chemother.* **2005,** 49, (8), 3546-3549.

(19) Dutcher, J. D., *Chest* **1968,** 54, (Supplement_1), 296-298.

(20) Li, J. W.-H.; Vederas, J. C., *Science* **2009,** 325, (5937), 161-165.

(21) Rishton, G. M., *Am. J. Cardiol.* **2008,** 101, (10), S43-S49.

(22) Harvey, A. L.; Edrada-Ebel, R.; Quinn, R. J., *Nat. Rev. Drug Discov.* **2015,** 14, (2), 111.

(23) Shen, B., *Cell* **2015,** 163, (6), 1297-1300.

(24) Newman, D. J.; Cragg, G. M., *J. Nat. Prod.* **2012,** 75, (3), 311-335.

(25) Berdy, J., *J. Antibiot.* **2005,** 58, (1), 1-26.

(26) Bentley, R., *Chem. Rev.* **2000,** 100, (10), 3801-3826.

(27) http://www.bioaustralis.com/metabolites.htm

(28) Haidle, A. M.; Myers, A. G., *Proc. Natl. Acad. Sci.* **2004,** 101, (33), 12048-12053.

(29) Glenn, J. M. H. R. J.; Heptinstall, W. L. P. S. S., *Platelets* **1998,** 9, (3-4), 227-232.

(30) Rabindran, S. K.; Ross, D. D.; Doyle, L. A.; Yang, W.; Greenberger, L. M., *Cancer Res.* **2000,** 60, (1), 47-50.

(31) Galvão, T. C.; Mohn, W. W.; de Lorenzo, V., *Trends Biotechnol.* **2005,** 23, (10), 497-506.

(32) Vining, L. C., *Annu. Rev. Microbial.* **1990,** 44, (1), 395-427.

(33) Haeder, S.; Wirth, R.; Herz, H.; Spiteller, D., *Proc. Natl. Acad. Sci.* **2009,** 106, (12), 4742-4746.

(34) Schoenian, I.; Spiteller, M.; Ghaste, M.; Wirth, R.; Herz, H.; Spiteller, D., *Proc. Natl. Acad. Sci.* **2011,** 108, (5), 1955-1960.

(35) Endo, A.; Kuroda, M.; Tsujita, Y., *J. Antibiot.* **1976,** 29, (12), 1346-1348.

(36) Higgens, C.; Kastner, R., *Int. J. Syst. Evol. Microbiol.* **1971,** 21, (4), 326-331.

(37) Schwientek, P.; Szczepanowski, R.; Rückert, C.; Kalinowski, J.; Klein, A.; Selber, K.; Wehmeier, U. F.; Stoye, J.; Pühler, A., *BMC genomics* **2012,** 13, (1), 112.

(38) Herranz, R., *Med. Res. Rev.* **2003,** 23, (5), 559-605.

(39) Gavrish, E.; Sit, C. S.; Cao, S.; Kandror, O.; Spoering, A.; Peoples, A.; Ling, L.; Fetterman, A.; Hughes, D.; Bissell, A., *Chem. Biol.* **2014,** 21, (4), 509-518.

(40) Wilson, M. C.; Mori, T.; Rückert, C.; Uria, A. R.; Helf, M. J.; Takada, K.; Gernert, C.; Steffens, U. A.; Heycke, N.; Schmitt, S., *Nature* **2014,** 506, (7486), 58.

(41) Piel, J., *Nat. Prod. Rep.* **2004,** 21, (4), 519-538.

(42) König, G. M.; Kehraus, S.; Seibert, S. F.; Abdel-Lateff, A.; Müller, D., *Chem. Bio. Chem.* **2006,** 7, (2), 229-238.

(43) Stierle, A.; Strobel, G.; Stierle, D., *Science* **1993,** 260, 214-214.

(44) Eyberger, A. L.; Dondapati, R.; Porter, J. R., *J. Nat. Prod.* **2006,** 69, (8), 1121-1124.

(45) Morita, M.; Schmidt, E. W., *Nat. Prod. Rep.* **2018,** 35, (4), 357-378.

(46) Hawksworth, D. L., *Stud. Mycol.* **2004,** 50, 9-18.

(47) Klejnstrup, M. L.; Frandsen, R. J.; Holm, D. K.; Nielsen, M. T.; Mortensen, U. H.; Larsen, T. O.; Nielsen, J. B., *Metabolites* **2012,** 2, (1), 100-133.

(48) Williams, R. B.; Henrikson, J. C.; Hoover, A. R.; Lee, A. E.; Cichewicz, R. H., *Org. Biomol. Chem.* **2008,** 6, (11), 1895-1897.

(49) Henrikson, J. C.; Hoover, A. R.; Joyner, P. M.; Cichewicz, R. H., *Org. Biomol. Chem.* **2009,** 7, (3), 435-438.

(50) Bladt, T. T.; Frisvad, J. C.; Knudsen, P. B.; Larsen, T. O., *Molecules* **2013,** 18, (9), 11338-11376.

(51) Endo, A., *J. Antibiot.* **1979,** 32, (8), 852-854.

(52) Kobel, H.; Traber, R., *Eur. J. Appl. Microbiol. Biotechnol.* **1982,** 14, (4), 237-240.

(53) Leclercq, R.; Bismuth, R.; Casin, I.; Cavallo, J.; Croize, J.; Felten, A.; Goldstein, F.; Monteil, H.; Quentin-Noury, C.; Reverdy, M., *J. Antimicrob. Chemother.* **2000,** 45, (1), 27-29.

(54) Grove, J. F.; MacMillan, J.; Mulholland, T.; Rogers, M. T., *J. Chem. Soc.* **1952**, 3977-3987.

(55) Abraham, E., *Rev. Infect. Dis.* **1979,** 1, (1), 99-105.

(56) Murdoch, J. M.; Speirs, C.; Geddes, A.; Wallace, E., *Br. Med. J.* **1964,** 2, (5419), 1238.

(57) Novak, R.; Shlaes, D. M., *Curr. Opin. Investig. Drugs* **2010,** 11, (2), 182-191.

(58) Vicente, M.; Basilio, A.; Cabello, A.; Peláez, F., *Clin. Microbiol. Infect.* **2003,** 9, (1), 15-32.

(59) Yamada, M.; Yawata, K.; Orino, Y.; Ueda, S.; Isogai, Y.; Taguchi, G.; Shimosaka, M.; Hashimoto, S., *Curr. Genet.* **2009,** 55, (6), 623.

(60) Nichols, D.; Cahoon, N.; Trakhtenberg, E.; Pham, L.; Mehta, A.; Belanger, A.; Kanigan, T.; Lewis, K.; Epstein, S., *Appl. Environ. Microbiol.* **2010,** 76, (8), 2445-2450.

(61) Ling, L. L.; Schneider, T.; Peoples, A. J.; Spoering, A. L.; Engels, I.; Conlon, B. P.; Mueller, A.; Schaberle, T. F.; Hughes, D. E.; Epstein, S.; Jones, M.; Lazarides, L.; Steadman, V. A.; Cohen, D. R.; Felix, C. R.; Fetterman, K. A.; Millett, W. P.; Nitti, A. G.; Zullo, A. M.; Chen, C.; Lewis, K., *Nature* **2015,** 517, (7535), 455-459.

(62) Peoples, A. J.; Zhang, Q.; Millett, W. P.; Rothfeder, M. T.; Pescatore, B. C.; Madden, A. A.; Ling, L. L.; Moore, C. M., *J. Antibiot.* **2008,** 61, (7), 457.

(63) Stackebrandt, E.; Breymann, S.; Steiner, U.; Prauser, H.; Weiss, N.; Schumann, P., *Int. J. Syst. Evol. Microbiol.* **2002,** 52, (4), 1105-1111.

(64) Daniel, R., *Curr. Opin. Biotechnol.* **2004,** 15, (3), 199-204.

(65) Riesenfeld, C. S.; Schloss, P. D.; Handelsman, J., *Annu. Rev. Genet.* **2004,** 38, 525-552.

(66) Banik, J. J.; Brady, S. F., *Curr. Opin. Microbiol.* **2010,** 13, (5), 603-609.

(67) Rutledge, P. J.; Challis, G. L., *Nature Rev. Microbiol.* **2015,** 13, (8), 509.

(68) Luo, Y.; Enghiad, B.; Zhao, H., *Nat. Prod. Rep.* **2016,** 33, (2), 174-182.

(69) Way, J. C.; Collins, J. J.; Keasling, J. D.; Silver, P. A., *Cell* **2014,** 157, (1), 151-161.

(70) Du, J.; Shao, Z.; Zhao, H., *J. Ind. Microbiol. Biotechnol.* **2011,** 38, (8), 873-890.

Chapter Two

Chapter 2: Authors contribution

Nirmal Chaudhary- Isolation and purification of the crude extract, characterization, structure elucidation, manuscript draft

John Pitt- Identification of the fungus

Dr. Ernest Lacey- Fungal culture and extraction, Manuscript revision

Andrew Crombie & Daniel Vuong – Bioassay of the purified samples

Dr. Andrew Piggott – Manuscript revision/Project co-supervision

Prof. Peter Karuso – DFT calculation, Manuscript revision, Project supervision

Pages 20-90 of this thesis have been removed as they contain published material. Please refer to the following citation for details of the article contained in these pages.

Chaudhary, N. K., Pitt, J. I., Lacey, E., Crombie, A., Vuong, D., Piggott, A. M., & Karuso, P. (2018). Banksialactones and banksiamarins: isochromanones and isocoumarins from an Australian fungus, Aspergillus banksianus. *Journal of Natural Products*, 81(7), 1517-1526.

DOI: 10.1021/acs.jnatprod.7b00816

Chapter Three

Chapter 3: Authors contribution

Nirmal Chaudhary- Isolation and purification of the crude extract, characterization, structure elucidation, manuscript draft

Dr. Ernest Lacey – Fungal culture and extraction, bioassay

Andrew Crombie & Daniel Vuong – Bioassay of the purified samples

Dr. Andrew Piggott – Manuscript revision/Project co-supervision

Prof. Peter Karuso – Molecular modelling, Manuscript revision, Project supervision

Talauxins from *Talaromyces stipitatus* and the semi-synthesis of talauxin analogues from their common biogenetic precursor duclauxin

Nirmal K. Chaudhary,[†] John I. Pitt,[‡] Ernest Lacey,[§,†] Andrew Crombie,[§] Daniel Vuong,[§] Andrew M. Piggott,[†] Peter Karuso[†,]*

[†]Department of Molecular Sciences, Macquarie University, NSW 2109, Australia

[‡]Commonwealth Scientific and Industrial Research Organisation, North Ryde, NSW 2113, Australia,

[§]Microbial Screening Technologies Pty. Ltd., Smithfield, NSW 2164, Australia

ABSTRACT

Cultivation and extraction of the fungus *Talaromyces stipitatus* led to the isolation of five new oxyphenalenone–amino acid hybrids, talauxins E, Q, V, L and I (**2**-**6**), along with their putative biosynthetic precursor, duclauxin (**1**). The spontaneous reaction of duclauxin with amino acids to produce talauxins and epitalauxins was demonstrated *in vitro* and exploited to generate a small library of semi-synthetic analogues. An unusual degradation product of talauxin V, desacetyldesmethyltalauxin V (**9**), was also identified. All the natural talauxins and the semi-synthetic compounds prepared were tested for cytotoxicity, antibacterial and antifungal activities.

Filamentous fungi, such as species of *Aspergillus*, *Penicillium* and *Talaromyces*, are a rich source of biologically active secondary metabolites.[1] Continuing our pursuit of unique secondary metabolites from filamentous fungi,[2-4] herein we report the isolation of duclauxin (**1**)[5] as the major metabolite of *Talaromyces stipitatus* along with five new talauxins (**2**-**6**), *O*-desmethylfunalenone (**7**) and 9-demethyl FR-901235 (**8**). Talauxins are unusual azaphenalenone heterodimers that are most closely related to duclauxamide A1, which was isolated from *Penicillium manginii* by Cao *et al*. in 2015.[6] An X-ray crystal structure of duclauxamide A1 led to a revision of the long-standing incorrect configuration at the C-9' position of duclauxin and its analogues from *R* to *S*. Additionally, we describe a facile semi-synthesis of talauxins from their putative biosynthetic precursor, duclauxin.

RESULTS AND DISCUSSION

We recently reported the chemical analysis of a new species of Australian fungus, *Aspergillus banksianus*.[2] During our initial media optimization studies on *A. banksianus*, we discovered the presence of a quiescent fungus, which we subsequently identified as a strain of *T. stipitatus*. LC-MS analysis of an initial small-scale culture of *T. stipitatus* revealed an interesting natural product profile that was distinct from any of our existing fungal cultures. *T. stipitatus* grew readily on all common fungal growth media, with production being much higher on grains than in liquids or agars. Pearl barley was selected for large-scale cultivation, which resulted in luxuriant growth of the fungus after 14 days at 24 °C. The pooled mycelial mass was extracted with acetone, the solvent removed, and the aqueous residue was partitioned with ethyl acetate to give a crude extract. The crude extract was defatted, and the resulting fraction was subjected to size exclusion chromatography on Sephadex LH-20 to yield four fractions. Fractions 2-4 were then purified by preparative and semi-preparative reversed phase HPLC to yield metabolites **1**-

8.

Duclauxin (**1**) was obtained as a pale-yellow solid. The ESI-MS revealed a protonated molecule $[M+H]^+$ at *m/z* 547, indicating a monoisotopic mass of 546. The ^1H and ^{13}C NMR spectra of **1** revealed 22 and 29 resonances respectively, suggesting a probable molecular formula of $C_{29}H_{22}O_{11}$. The UV spectrum of **1** (Supporting Information, Figure S19) was characteristic of an oxyphenalenone dimer.[7] The ^1H and ^{13}C NMR spectra of **1** (Table 1 and Supporting Information Table S1) were a close match for duclauxin and an observed specific optical rotation of +197 confirmed that the compound was (+)-duclauxin, which has previously been reported with a specific rotation of +164.5[8] and +271.5[5] Duclauxin was first isolated from *P. duclauxii*[5] and more recently from *P. stipitatum,*[9] *P. herquei*,[8] *T. bacillisporus*,[7, 10] *T. stipitatus*[1] and *P. manginii*.[6] The latter paper proposed a revision of the configuration at the C-9' position of the entire duclauxin family based on unequivocal results from an X-ray crystal structure and coupling constant analysis of duclauxamide A1. Specifically, the NMR data for duclauxamide A1 revealed a small coupling constant between H-8'/H-9' (< 1 Hz), which modeling of the literature structure suggested should be 6-7 Hz (Karplus equation).[11] Our sample of duclauxin similarly had a small coupling between H-8' and H-9' and moreover, our measurement of inter-proton distances from DFT calculations (Figure 1) compared favorably to the ROESY correlations observed. For example, the absence of a ROESY correlation between H-9' and H8 (3.76 Å) (Supporting Information, Figure S1), supported the *S*-configuration at C-9', *c.f.* C-9' *R* isomer would have a strong NOE to H-8 (2.56 Å).

Of the minor metabolites, talauxin E (**2**) was the most abundant and isolated as a yellow solid. The UV spectrum (Supporting Information, Figure S20) was very similar to that of **1**, with absorbance maxima at 210, 238 and 350 nm. The IR spectrum (Supporting Information, Figure S42) showed strong broad bands around 3177 cm^{-1} indicating the

presence of chelated hydroxy groups, which were observed in the ^{1}H NMR spectrum (δ_H 10.71 and 11.72). At least three different carbonyl groups were indicated by the presence of sharp and strong absorption bands at 1748 and 1667 cm^{-1}. The HR-ESI(+)MS spectrum of **2** revealed an adduct ion $[M+Na]^+$ at *m/z* 698.1477, suggesting a molecular formula $C_{34}H_{29}NO_{14}$ (Δmmu= –0.3). Compared to **1** ($C_{29}H_{22}O_{11}$), this represents an additional $C_5H_7NO_3$. The only duclauxins known to contain nitrogen are the semisynthetic derivatives reported in 1966[12] and the recently reported duclauxamide A1.[6] The ^{1}H NMR spectrum of **2** showed 25 non-exchangeable and 4 exchangeable protons. Compared to **1**, a new –CH-CH_2-CH_2- spin-system was identified in the COSY spectrum, with the central CH_2 (δ_H 2.21/2.32) showing HMBC correlations to two different carboxylic acid carbons (δ_C 169.9 and 173.6), suggesting the additional fragment was glutamic acid. Notable differences in the chemical shifts between **1** and **2** (Table 1 and Supporting Information Table S2) occur around C-3. In particular, the chemical shifts of C-1, C-3 and C-3a in **2** are shifted by 12, 3 and 5 ppm respectively compared to **1** in the ^{13}C NMR spectrum. The remaining ^{1}H and ^{13}C NMR resonances were very similar to those in **1**. With consideration to the known reactivities of pyranones, we postulated that the structure of **2** was as shown. This assignment was supported by key HMBC correlations from H-11 to C-1 and C-3 and a ROESY correlation between H-11 and H-1 (Supporting Information, Figure S2).

Talauxin Q (**3**) had a molecular formula of $C_{34}H_{30}N_2O_{13}$ as determined by HR-ESI(+)MS of the $[M+Na]^+$ adduct ion (Δmmu –0.9). The IR spectrum showed strong broad absorption bands around 3193 cm^{-1} indicating the presence of chelated hydroxy groups. The presence of bands at 3354 cm^{-1} and 3445 cm^{-1} together with absorptions between 1650-1580 cm^{-1} indicated the possible presence of primary amines/amides. The presence of at least two different carbonyl groups was also suggested by the IR spectrum (ν_{max} 1744 and 1676 cm^{-1}). The UV spectrum showed absorbances at 212, 235 and 347 nm and were

very similar to **2** suggesting they shared the same chromophore. In addition, **3** showed a similar –CH-CH_2-CH_2- spin-system as in **2**, but the molecular formula indicated an extra nitrogen and one less oxygen, suggesting a glutamine adduct instead of glutamic acid. This was confirmed by identifying the amide protons in the ^{1}H NMR spectrum of **3** (δ_H 6.84 and 7.21), both of which showed HMBC correlations to the amide carbonyl carbon (δ_C 173.0). One amide proton (δ_H 6.84) showed an additional HMBC correlation to C-13. Like **2**, **3** showed HMBC correlations from H-11 to C-1 and C-3, and a ROESY correlation between H-11 and H-1, confirming the attachment point of the glutamine between C-1 and C-3 (Supporting Information, Table S3).

Talauxin V (**4**) showed a UV spectrum very similar to **2** and **3**. The IR spectrum showed strong broad bands in the region around 3200 cm^{-1} indicating the presence of chelated hydroxy groups. At least two different carbonyl groups present were observable at 1748 and 1667 cm^{-1}. A molecular formula of $C_{34}H_{31}NO_{12}$ was determined by HR-ESI(+)MS of the $[M+Na]^+$ adduct ion (Δmmu –1.3). Compared to **1**, this represents a gain of C_5H_5NO over duclauxin. The COSY spectrum showed correlations for an additional isobutyl spin system, $(CH_3)_2$-CH-CH-, compared to **1**. Both the methine protons from this spin system showed strong HMBC correlations with a carbonyl carbon at δ_C 169.5. As the methine proton (δ_H 4.77) of this spin system, showed additional HMBC correlations with C-1 and C-3 and a ROESY correlation was observed between H-11 and H-1 (Supporting Information, Table S4), it was clear that this analogue had a valine side-chain at position 2.

Talauxins L (**5**) and I (**6**) were isolated as an inseparable mixture in a ratio of 2.4:1 (Supporting Information, Figure S3). The mixture had very similar IR and UV spectra to **2**-**4**, suggesting they were closely related analogues. HR-ESI(+)MS analysis of the mixture suggested **5** and **6** both had a molecular formula $C_{35}H_{33}NO_{12}$, representing an additional $C_6H_{11}NO$ compared to **1**. Analysis of the COSY spectrum of **5** revealed the presence of

correlations for an additional 3-isopentyl spin systems compared to **1**. The methine proton of this isopentenyl side chain at δ_H 5.11 showed HMBC correlations to carbonyl carbons at δ_C 170.0 and 169.6, suggesting the presence of a leucine moiety. Additional HMBC and ROESY correlations (Supporting Information, Table S5) allowed **5** to be identified as the leucine adduct of **1**. Similarly, COSY analysis of **6** revealed correlations for an additional 2-isopentyl spin system compared to **1**. The methine proton of this isopentenyl system at δ_H 4.88 showed HMBC correlations to carbonyl carbons at δ_C 169.7 and 169.5, suggesting the presence of an isoleucine moiety. Again, additional HMBC and ROESY correlations (Supporting Information, Table S6) allowed **6** to be identified as the isoleucine adduct of **1**. Independent characterization of pure samples of **5** and **6** was achieved following their independent semi-synthesis from **1** (*vide infra*). In addition to talauxins **2**-**6**, several additional minor talauxins were also observed in the crude extract but there was insufficient material for full characterization. However, from LC-MS/UV-Vis, the minor talauxins observed were the alanine, arginine, phenylalanine and tyrosine analogues of **2**.

HMBC correlations from H-1 to C-11 and from H-11 to C-1 and C-3 were important in establishing the connectivity of the duclauxin moiety with the amino acid side chain in the hybrid metabolites, whereas HMBC correlations from H-8 to C-1', C-8', C-9', C-9a' and H-8' to C-6a, C-7, C-8 were crucial in establishing the connectivity and the structural architecture of the two monomeric oxyphenalenone units of the duclauxin moiety. The generalized key HMBC, COSY and ROESY correlations are represented in Figure 2.

O-Desmethylfunalenone (**7**) was isolated as yellow solid. The UV spectrum showed absorbance maxima at 218, 252 and 332 nm, which are indicative of a phenalenone monomer.[13] The IR spectrum showed broad bands in the region between 3100-3650 cm^{-1} indicating the presence of free and chelated hydroxy groups. A band at 1671 cm^{-1} indicated the presence of a carbonyl group. The ESIMS revealed $[M+H]^+$ and $[M–H]^–$ ions

at *m/z* 275 and 273 respectively, indicating a monoisotopic mass of 274. *O*-Desmethylfunalenone showed just two aromatic protons and one methyl group in the ^{1}H NMR spectrum but 14 carbons in the ^{13}C NMR spectrum, suggesting a probable molecular formula of $C_{14}H_{10}O_{6}$. Of the 14 carbon resonances, one was a methyl, two were methines and eleven were non-protonated aromatic carbon resonances. Five of the non-protonated carbons were oxygenated as evident from their chemical shifts. Also, four hydrogens were not observed in the ^{1}H NMR spectrum and hence they were assumed to be exchangeable hydroxy groups. The index of hydrogen deficiency was ten, whereas the number of double bonds was seven, requiring **7** to be a tricyclic aromatic system similar to funalenone.[14] A methoxy group observed in funalenone as a singlet at δ_H 3.80 in the ^{1}H NMR spectrum and at δ_C 59.7 in the ^{13}C NMR spectrum was missing in **7**, suggesting a desmethyl analogueue of funalenone. Key 2D NMR correlations (Supporting Information, Table S7) confirmed the structure of **7** as indicated.

9-Demethyl FR-901235 (**8**) was isolated as a yellow solid. The UV spectrum, the ^{1}H NMR spectrum and the ^{13}C NMR spectrum (Supporting Information, Table S8) of **8** showed a close match with the literature data for 9α-demethyl FR-901235, which has been previously reported from the endophytic fungus *Penicillium* sp. JP-1, originating from the inner bark of a mangrove tree *Aegiceras corniculatum.*[13] Compound **8**, despite previously being reported as a natural product,[13] appears to be an aldol adduct between **8a** and acetone. This adduct may have been formed because acetone was employed during our extraction of the culture, but the original paper[13] does not mention the solvent used for extraction. Acetone adducts of natural products, including some phenalenones, have been reported. For example, the acetone adduct rousselianone A' was isolated from *Phaeosphaeria rousseliana* when acetone was employed as solvent for extraction of the culture broth, while the genuine natural product rousselianone A is isolated when other

extraction solvents are employed.[15] Rousselianone A was shown to possess broad spectrum antifungal activities against some plant pathogens, but its acetone adduct was devoid of activity. Subsequently, rousselianone A' was also isolated from *Coniothyrium cereale*.[16] Similarly, the acetone adduct of atrovenetinone has been reported from the ascomycetes fungus *Gremmeniella abietina*[17] and the soil fungus *P. herquei*.[18] Ayer *et al.*, showed that the acetone adduct of atrovenetonone (as a mixture of epimers) was only formed when acetone was employed for chromatography from the natural product atrovenetinone which could be isolated when acetone was avoided. They also showed that even low concentrations of acetone converted atrovenetonone into its acetone adduct. FR-901235, an immunoactive substance produced by an imperfect fungus *Paecilomyces carneus* is also an acetone adduct.[19] Similarly, flaviphenalenone A, isolated from the wetland fungus *A. flavipes*, is an acetone adduct of the corresponding triketone and is reported to possess cytotoxic activity against A549 and MCF-7 cell-lines.[20] These examples emphasize the inherent electrophilicity of the natural products and are likely to be important in the biological activity and ecological role of these metabolites.

During the course of this research, we noticed that **4** is unstable. HPLC re-purification of **4** led to the isolation of desacetyldesmethyltalauxin V (**9**), a new molecule. Since duclauxin and talauxins are susceptible to degradation in acidic/alkaline conditions, the possibility that some of the reported phenalenone dimers based on neoclauxin or acetylneoclauxin skeleton are in fact degradation products cannot be ignored.

The degradation product of talauxin V, desacetyldesmethyltalauxin V (**9**) was isolated as a yellow solid. HR-ESI(+)MS analysis of **9** revealed a protonated molecule $[M+H]^+$ at 572.1548, suggesting a molecular formula $C_{31}H_{25}NO_{10}$ (Δmmu –0.3). The ^1H and ^{13}C NMR spectra in comparison to **4** showed no corresponding resonances for an acetyl group and methoxy group, but an additional hydroxy group was observed. Further, the molecular

mass deficit of 74 Da compared to **4**, suggested that **9** was formed by elimination of methyl acetate. Notable differences in the NMR chemical shifts (Supporting Information, Table S9) between **4** and its degradation product **9** were observed around C-1, C-3, C-7, C-8 and C-9. The most significant deviation of ^{13}C NMR chemical shifts were observed for C-7 and C-8 due to the introduction of an additional double bond. This in turn caused a significant upfield chemical shift of the C-9 ketone (now an α,β-unsaturated ketone). This extended conjugated system, analogous to a quinonoid system, was responsible for an absorbance around 450 nm in the UV-visible spectrum (Supporting Information Figure S27). The remaining ^{1}H and ^{13}C NMR resonances were quite similar to **4**, allowing the structure of **9** to be assigned as desacetyldesmethyltalauxin V.

Azaphilones are known to react with primary amines to form pyridones.[21] Therefore, to determine whether the talauxins could be formed abiotically from **1** (Figure 4), we reacted **1** with L-glutamine in DMSO-d_6 at room temperature. NMR analysis of the reaction mixture revealed the formation of the expected product **3** within minutes (yield in excess of 50% by NMR), which was confirmed by LC-MS. The reaction was repeated for L-leucine and L-isoleucine to generate pure samples of **5** and **6** for full characterization. Additional talauxin analogues were prepared by reaction of **1** with D-leucine, D-isoleucine and D-phenylalanine to give epitalauxins L (**10**), I (**11**) and F (**12**) respectively. The ^{1}H and ^{13}C NMR data for **10**-**12** are provided in Table 2 and Supporting Information Tables S10-S12. Finally, we generated an analytical library of the remaining talauxin standards by reacting all the natural L-amino acids (except proline) with **1** in DMSO on a 50 μg scale. It is noteworthy that the amino acids reacted with **1** readily in DMSO but not at all in water. This kind of chemical behaviour of **1** along with the no evidence of an open ring aldehyde form in the careful examination of 1D NMR spectra of **1** in turn helped us to propose the mechanism of reaction of **1** as shown in Figure 3.

To determine the absolute configurations of the amino acids in the talauxins, the retention times of the naturally occurring talauxins were compared with those of the semi-synthetic talauxins, prepared by reacting **1** with the corresponding L- and D-amino acids (Supporting Information, Figure S5). In each case, the retention times of the L-amino acid derivatives of duclauxin matched the corresponding natural talauxin. The absolute configurations at all other stereocenters of talauxins were assumed to be the same as those of **1** based on the identical electronic circular dichroism (ECD) spectra for all compounds (Supporting Information, Figures S31-S36).

All the natural and semi-synthetic compounds were tested for *in vitro* cytotoxicity against mouse myeloma NS-1 cells (ATCC TIB-18), antibacterial activity against *Bacillus subtilis* (ATCC 6633) and *Escherichia coli* (ATCC 25922), and antifungal activity against *Saccharomyces cerevisiae* (ATCC 9763) and *Candida albicans* (ATCC 10231). Compounds **1** and **7** exhibited weak cytotoxic activities (MIC 100 and 25 μg/mL, respectively), while **7** also exhibited weak antibacterial activity against *B. subtilis* (MIC 100 μg/mL). All other compounds tested were inactive up to 100 μg/mL.

Oligophenalenone dimers, such as duclauxin, are natural products first isolated during the golden era of antibiotic discovery (1945-1965).[5] These compounds have demonstrated significant cytotoxic activities linked to oxidative phosphorylation in mitochondria[22] and protein synthesis in tumor cells,[23] although the actual biological target remains unknown. Many other phenalenone analogues, such as bacillisporins A-E, also have significant cytotoxic activities, amongst which bacillisporin A is reported to be the most active.[10] Despite being known for over five decades and possessing noteworthy biological activities, no total synthesis of duclauxin or its analogues has been reported to date.

Biosynthetic studies carried on the metabolites of *Gremmeniella abietina* using acetate labeling showed sclerodin and related analogues originate from a heptaketide precursor

that cyclizes to the tricyclic aromatic ring system of phenalenone.[24] In 2016, Tang and colleagues identified the *phn* biosynthetic gene cluster in *P. herquei*, which is responsible for herqueinone biosynthesis.[25] They have shown that a non-reducing polyketide synthase PhnA is responsible for the cyclization of the heptaketide backbone into an angular hemiketal-containing naptho-γ-pyrone, prephenalenone. The transformation of prephenalenone to phenalenone requires a FAD-dependent monooxygenase PhnB, which catalyzes the C-2 hydroxylation of prephenalenone and ring opening of the γ-pyrone simultaneously.

Recently, Tang and colleagues[26] identified the *dux* biosynthetic pathway for **1** in *Talaromyces stipitatus* and reconstituted parts of the pathway in *Saccharomyces cerevisiae* and *Aspergillus nidulans* heterologous hosts. The authors demonstrated that the cupin family dioxygenase, DuxM, performs oxidative cleavage of phenalenone to afford a common hemiketal-oxaphenalenone intermediate, which can either be oxidatively decarboxylated by DuxM to give the anhydride, or further processed by redox enzymes DuxJ (maleylacetate reductase), DuxD (P450 monooxygenase) and DuxG (isoflavone reductase) to give the dihydrocoumarin. Oxidative homodimerization of two dihydrocoumarin oxaphenalenone monomers was shown to be catalyzed by DuxL (P450 monooxygenase), giving rise to the bacillisporins and duclauxins. Similarly, it was proposed that heterodimerization of the dihydrocoumarin and anhydride oxaphenalenone monomers gives rise to the cryptoclauxins, although the P450 monooxygenase responsible for catalyzing the dimerization could not be located in the *dux* cluster. From ducluaxin, either enzyme catalyzed or abiotic reaction with amino acids would give rise to the talauxins.

CONCLUSION

Chemical investigation of the fungus *T. stipitatus* led to the isolation of five new duclauxin analogue, the talauxins. The spontaneous reactivity of duclauxin with amino acids suggests that the biosynthesis of talauxins could be non-enzymatic similar to the discoipyrroles.[27] However, as dimethylsulfoxide was necessary for the reaction of duclauxin with amino acids under abiotic condition, the presence of a specific enzyme that catalyzes the condensation of amino acids with duclauxin in the fungus as a possible "detoxification" mechanism cannot be discounted. The bioassay results for the talauxins identified no significant activities, with **1** and **7** displaying only weak *in vitro* cytotoxicity, while **7** also showed weak antibacterial activity. The semi-synthetic conversion of duclauxin to talauxins was utilized to show that compounds **2**-**6** can be formed from the respective L-amino acids and allowed us to unequivocally, in conjunction with ORD and ECD measurements, determine the stereochemistry of the talauxins. The inherent reactivity of duclauxin[22, 23, 28] could further be utilized for the preparation of analogue libraries for further medicinal chemistry.

EXPERIMENTAL SECTION

General experimental procedures. Size exclusion chromatography (SEC) was performed using Sephadex LH-20 (GE Healthcare Bio-Sciences Corp.). Thin-layer chromatography (TLC) was performed using pre-coated silica gel GF254 plates (Merck, Darmstadt, Germany) with various solvent systems and spots were visualized with UV light (254 nm). Preparative and semi-preparative HPLC separations were performed on a Gilson HPLC system, equipped with a Gilson 215 liquid handler, 819 injection module, 322 pump, 506C system interface and Gilson single variable wavelength UV-Vis 152 detector by reverse phase chromatography using a gradient of acetonitrile (Sigma Aldrich,

USA) and water containing 0.025% HPLC grade TFA (Sigma Aldrich, USA) unless mentioned otherwise. UV-visible spectra were recorded on an Eppendorf UV-visible spectrophotometer (Model-Biospectrometer® Kinetic). Optical rotations were recorded in MeOH using a JASCO P-1020 polarimeter (Jasco Corp., Japan). ECD spectra were recorded on a Jasco J-810 spectropolarimeter; model CDF-426S/426L Peltier-type ECD/fluorescence simultaneous measurement attachment (Jasco Corp., Japan). The IR spectra were measured on a Thermo Scientific Nicolet iS10 ATR FTIR spectrometer. ^{1}H NMR, ^{13}C NMR and 2D NMR spectra were recorded in deuterated DMSO using an AVANCE II 600 MHz NMR spectrometer equipped with a cryoprobe (Bruker Corp.). The ESIMS spectra were recorded using Agilent 6130B single quadrupole mass spectrometer (Agilent Corp., USA). HR-ESIMS data were obtained using a Q Exactive Plus hybrid quadrupole-orbitrap mass spectrometer (Thermo Scientific, Germany).

Biological Material. *Talaromyces stipitatus* was isolated from a soil sample collected in Collaroy, New South Wales, Australia in 2004 as part of an investigation of the diversity of the fungal family Trichocomaceae in the Sydney basin and was accessioned into the Commonwealth Scientific and Industrial Research Organisation (CSIRO) fungal collection as FRR 6047 and into the Microbial Screening Technologies (MST) fungal collection as FP2248C.

T. stipitatus was cultivated for extraction on pearl barley in Erlenmeyer flasks (100 g per flask; 40 × 250 mL) at 24 °C for 14 days. The cultures were pooled (3,900 g) and extracted with acetone (2 × 5 L) for 2 h on a rotatory platform at 100 rpm. The macerated solid was removed by filtration and the filtrate was reduced to an aqueous concentrate (146 g) by rotatory evaporation. The concentrate was partitioned against ethyl acetate (2 × 2 L) then evaporated to dryness to provide an organic extract (56.9 g). The extract was dissolved in methanol (360 mL), diluted with distilled water (140 mL) and de-fatted by partitioning

against hexane (2 × 500 mL) to provide a crude extract (34.5 g). The extract was dissolved in methanol (360 mL), diluted with distilled water (140 mL) and de-fatted by partitioning against hexane (2 × 500 mL) to provide a crude extract (34.5 g).

Isolation. A portion of the crude extract (9.0 g) was dissolved in 50:50% *v/v* MeOH/$CHCl_3$ (5 mL) and loaded onto a Sephadex LH-20 column (24 × 2.2 cm). The column was developed with 50:50% *v/v* MeOH/$CHCl_3$ at a flow rate of 1 mL/min for approximately 40 h and 180 fractions were collected. The fractions were combined into four initial sub-fractions, S1 to S4, based on TLC analysis. Fraction S1 contained mostly viscous polymeric material and was not further investigated. Fractions S2-S4 were pre-treated on a C18 SPE cartridge by washing with 10% methanol/water and eluting with 90% methanol/water, before further fractionation by reversed phase HPLC.

The Sephadex fractions were purified by reversed phase HPLC on a 250 × 22.4 mm Phenomenex Hydro-RP (10 μm) preparative column using a gradient of 10-100% acetonitrile/water (each containing 0.025% TFA) at 14 mL/min over 40 min. Fraction S2 yielded talauxin E (**2**; 20 mg; t_R 17.7 min), talauxin Q (**3**; 17 mg; t_R 15.1 min), talauxin V (**4**; 15 mg; t_R 25.6 min), talauxin I/L (**5/6**; 14 mg; t_R 26.8 min). Fraction S3 yielded duclauxin (**1**; 6 mg; t_R 28.1 min). Fraction S4 yielded *O*-desmethylfunalenone (**7**; 29 mg; t_R 12.4 min) and 9-demethyl FR-901235 (**12**; 27 mg; t_R 16.3 min).

Semi-synthesis of talauxin derivatives. The semi-synthetic talauxins were prepared by reacting duclauxin (2 mg) with the corresponding amino acid (1 mg) in DMSO (0.5 mL) at room temperature. Following the spontaneous formation of talauxins, as evidenced by an immediate change in color and by LC-MS analysis, the products were purified by reversed phase HPLC under the same conditions as the natural analogues.

Bioassays. Test compounds were dissolved in DMSO to provide 10 mg/mL stock solutions (or 1 mg/mL for compounds of limited quantities). An aliquot of each stock

solution was transferred to the first lane of rows B to G in a 96-well microtiter plate and two-fold serially diluted across the 12 lanes of the plate to provide a 2,048-fold concentration gradient. Bioassay medium was added to an aliquot of each test solution to provide a 100-fold dilution into the final bioassay, thus yielding a test range of 100 to 0.05 μg/mL in 1% DMSO. Row A was used as the negative control (no inhibition) and Row H was used as the positive control (uninoculated).

CyTOX,[4] NS-1 (ATCC TIB-18) mouse myeloma cells were inoculated in 96-well microtiter plates (190 μL) at 50,000 cells/mL in DMEM (Dulbecco's Modified Eagle Medium + 10% fetal bovine serum (FBS) + 1% penicillin/streptomycin (10 mL/L, Life Technologies)) and incubated in 37 °C (5% CO_2) incubator. At 48 h, resazurin (250 μg/mL; 10 μL) was added to each well and the plates were incubated for a further 48 h. MIC end points were determined visually.

ProTOX,[4] *Bacillus subtilis* (ATCC 6633) and *Escherichia coli* (ATCC 25922) were used as indicative species for Gram positive and negative antibacterial activity, respectively. A bacterial suspension (50 mL in 250 mL flask) was prepared in nutrient broth by cultivation for 24 h at 100 rpm 250 rpm, 28 °C. The suspension was diluted to an absorbance of 0.01 absorbance units per mL, and 10 μL aliquots were added to the wells of a 96-well microtiter plate, which contained the test compounds dispersed in nutrient agar (Amyl) with resazurin (12.5 μg/mL). The plates were incubated at 28 °C for 48 h during which time the negative control wells change from a blue to light pink color. MIC end points were determined visually.

EuTOX,[4] The yeasts *Candida albicans* (ATCC 10231) and *Saccharomyces cerevisiae* (ATCC 9763) were used as indicative species for antifungal activity. A yeast suspension (50 mL in 250 mL flask) was prepared in 1% malt extract broth by cultivation for 24 h at 250 rpm, 24 °C. The suspension was diluted to an absorbance of 0.005 and 0.03

absorbance units per mL for *C. albicans* and S. *cerevisiae*, respectively. Aliquots (20 μL and 30 μL) were applied to the wells of a 96-well microtiter plate, which contained the test compounds dispersed in malt extract agar containing bromocresol green (50 μg/mL). The plates were incubated at 24 °C for 48 h during which time the negative control wells change from a blue to yellow color. MIC end points were determined visually.

TriTOX,[4] *Tritrichomonas foetus* (strain KV-1) were inoculated in 96-well microtiter plates (200 μL) at 4×10^4 cells/mL in *T. foetus* medium (0.2% tryptone, Oxoid; 0.1% yeast extract, Difco; 0.25% glucose; 0.1% l-cysteine; 0.1% K_2HPO_4; 0.1% KH_2PO_4; 0.1% ascorbic acid; 0.01% $FeSO_4.7H_2O$; 1% penicillin/streptomycin (10 mL/L), 10% new born calf serum (NBCS), Life Technologies). The plates were incubated in anaerobic jars (Oxoid AG25)

Molecular modeling. Models of (9'*S*)-duclauxin and (9'*R*)-duclauxin were built in Molecular Operating Environment 2017 (MOE2017; Chemical Computing Group) and were energy-minimized (MMFF94x). A conformational search using low-mode molecular dynamics identified the global minimum energy structures. The structures were then minimized using density functional theory (DFT//PBE0/TZVP) in DMSO (COSMO) using Turbomole 7.1 (Cosmologic GmbH).[29]

Spectroscopic data

*Talauxin E (**2**):* Pale yellow solid; $[\alpha]^{24}_D$ +243 (*c* 0.39, MeOH); ECD (*c* 2.9×10^{-5} mg/mL, MeOH) λ_{max} ($\Delta\varepsilon$): 210 (–59.81), 242 (+73.22), 312 (–24.23), 361(+22.41); UV (MeCN) λ_{max} (log ε): 215 (4.62), 238 (4.69), 350 (3.90) nm; IR (ATR) ν_{max} 3445, 3177, 1748, 1716, 1667, 1602, 1568, 1507, 1455, 1362, 1319, 1267, 1215, 1161, 1128, 1091, 1046, 867, 816, 762, 726, 602, 581 cm^{-1}; NMR (600 MHz, DMSO-d_6) see Table 1 and

Table S2, Supporting Information; HR-ESI(+)MS $[M + Na]^+$ *m/z* 698.1477 (calcd for $C_{34}H_{29}NO_{14}Na^+$, 698.1480).

Talauxin Q ***(3)****:* Pale yellow solid; $[\alpha]^{24}_D$ +234 (*c* 0.47, MeOH); ECD (*c* 8.1×10^{-5} mg/mL, MeOH) λ_{max} ($\Delta\varepsilon$): 212 (–70.49), 244 (75.61), 296 (–17.84), 378 (14.68); UV (MeCN) λ_{max} (log ε): 212 (4.65), 235 (4.74), 347 (3.92) nm; IR (ATR) ν_{max} 3596, 3445, 3354, 3193, 1744, 1676, 1638, 1604, 1584, 1508, 1458, 1421, 1338, 1274, 1211, 1160, 1106, 1075, 1043, 1021, 963, 905, 873, 814, 795, 760, 707, 695, 657, 643, 610, 599 cm^{-1}; NMR (600 MHz, DMSO-d_6) see Table 1 and Table S3, Supporting Information; HR-ESI(+)MS $[M + Na]^+$ *m/z* 697.1631 (calcd for $C_{34}H_{30}N_2O_{13}Na^+$, 697.1640).

Talauxin V ***(4)****:* Pale yellow solid; $[\alpha]^{24}_D$ +247 (*c* 0.53, MeOH); ECD (*c* 3.9×10^{-5} mg/mL, MeOH) λ_{max} ($\Delta\varepsilon$): 210 (–66.01), 242 (+89.29), 310 (–20.94), 370 (+17.04); UV (MeCN) λ_{max} (log ε): 215 (4.59), 239 (4.70), 348 (3.89) nm; IR (ATR) ν_{max} 3446, 3176, 1748, 1717, 1667, 1602, 1568, 1507, 1471, 1455, 1431, 1362, 1321, 1268, 1213, 1161, 1127, 1090, 1045, 1023, 898, 868, 816, 762, 726, 614, 606, 574 cm^{-1}; NMR (600 MHz, DMSO-d_6) see Table 1 and Table S4, Supporting Information; HR-ESI(+)MS $[M + Na]^+$ *m/z* 668.1725 (calcd for $C_{34}H_{31}NO_{12}Na^+$, 668.1738).

Talauxin L ***(5)****:* Pale yellow solid; $[\alpha]^{23}_D$ +146 (*c* 0.20, MeOH); ECD (*c* 2.8×10^{-5} mg/mL, MeOH) λ_{max} ($\Delta\varepsilon$): 242 (+64.02), 293 (–21.23), 362 (+9.75); UV (MeCN) λ_{max} (log ε): 208 (4.63), 228 (4.71), 349 (3.93) nm; IR (ATR) ν_{max} 3670, 2970, 2084, 1747, 1674, 1640, 1570, 1463, 1338, 1273, 1216, 1129, 1046, 1022, 904, 815, 762, 667 cm^{-1}; NMR (600 MHz, DMSO-d_6) see Table 2 and Table S5, Supporting Information; HR-ESI(+)MS $[M + H]^+$ *m/z* 660.2067 (calcd for $C_{35}H_{34}NO_{12}^+$, 660.2076).

Talauxin I ***(6)****:* Pale yellow solid; $[\alpha]^{23}_D$ +172 (*c* 0.17, MeOH); ECD (*c* 1.5×10^{-5} mg/mL, MeOH) λ_{max} ($\Delta\varepsilon$): 243 (+31.98), 294 (–10.77), 362 (+4.91); UV (MeCN) λ_{max} (log

ε): 209 (4.68), 227 (4.80), 351 (3.98) nm; IR (ATR) ν_{max} 3672, 2971, 1747, 1679, 1641, 1572, 1459, 1415, 1335, 1277, 1217, 1129, 1076, 1046, 1022, 904, 816, 757, 668 cm^{-1}; NMR (600 MHz, DMSO-d_6) see Table 2 and Table S6, Supporting Information; HR-ESI(+)MS $[M + H]^+$ *m/z* 660.2070 (calcd for $C_{35}H_{34}NO_{12}^+$, 660.2076).

*Desacetyldemetalauxin V (**9**):* Yellow solid; $[\alpha]^{23}_D$ –12 (*c* 0.69, MeOH); ECD (*c* 2.7×10^{-5} mg/mL, MeOH) λ_{max} (Δε): 218 (–58.99), 242 (+88.63), 286 (–7.84), 297 (–6.44), 336 (14.05), 378 (17.7), 400 (–1.21); UV (MeCN) λ_{max} (log ε): 220 (4.76), 318 (4.22), 374 (4.04), 450 (4.06) nm; IR (ATR) ν_{max} 3442, 3178, 2969, 2359, 2340, 1715, 1659, 1608, 1559, 1470, 1403, 1375, 1326, 1269, 1213, 1230, 1159, 1130, 1092, 1037, 830, 797, 764, 733, 699, 668, 652, 647 cm^{-1}; NMR (600 MHz, DMSO-d_6) see Table S9, Supporting Information; HR-ESI(+)MS $[M + H]^+$ *m/z* 572.1548 (calcd for $C_{31}H_{26}NO_{10}^+$, 572.1551).

*Epitalauxin L (**10**):* Pale yellow solid; $[\alpha]^{23}_D$ +202 (*c* 0.35, MeOH); ECD (*c* 3.1×10^{-5} mg/mL, MeOH) λ_{max} (Δε): 243 (+63.29), 292 (–21.47), 363 (+29.26); UV (MeCN) λ_{max} (log ε): 207 (4.67), 228 (4.78), 351 (3.97) nm; IR (ATR) ν_{max} 3649, 2964, 1747, 1679, 1639, 1575, 1459, 1336, 1274, 1210, 1129, 1076, 1049, 1022, 905, 868, 815, 760, 666 cm^{-1}; NMR (600 MHz, DMSO-d_6) see Table 2 and Table S10, Supporting Information; HR-ESI(+)MS $[M + H]^+$ *m/z* 660.2067 (calcd for $C_{35}H_{34}NO_{12}^+$, 660.2076).

*Epitalauxin I (**11**):* Pale yellow solid; $[\alpha]^{23}_D$ +200 (c 0.32, MeOH); ECD (*c* 4.2×10^{-5} mg/mL, MeOH) λ_{max} (Δε): 243 (+94.67), 292 (–31.09), 362 (+14.54); UV (MeCN) λ_{max} (log ε): 208 (4.65), 228 (4.74), 353 (3.93) nm; IR (ATR) ν_{max} 3670, 2971, 1746, 1679, 1639, 1574, 1457, 1419, 1336, 1277, 1215, 1130, 1075, 1045, 1022, 960, 905, 815, 760, 613 cm^{-1}; NMR (600 MHz, DMSO-d_6) see Table 2 and Table S11, Supporting Information; HR-ESI(+)MS $[M + H]^+$ *m/z* 660.2069 (calcd for $C_{35}H_{34}NO_{12}^+$, 660.2076).

*Epitalauxin F (**12**):* Pale yellow solid; $[\alpha]^{23}_D$ +209 (*c* 0.30, MeOH); ECD (*c* 1.4×10^{-5}

mg/mL, MeOH) λ_{max} ($\Delta\varepsilon$): 243 (+32.15), 292 (–11.03), 365 (+5.04); UV (MeCN) λ_{max} (log ε): 208 (4.70), 232 (4.73), 356 (3.92) nm; IR (ATR) ν_{max} 3650, 2985, 1746, 1677, 1640, 1575, 1457, 1419, 1338, 1273, 1211, 1129, 1076, 1046, 962, 906, 872, 813, 753, 699, 659, 612 cm^{-1}; NMR (600 MHz, DMSO-d_6) see Table 2 and Table S12, Supporting Information; HR-ESI(+)MS $[M + H]^+$ *m/z* 694.1913 (calcd for $C_{38}H_{32}NO_{12}^+$, 694.1919).

ASSOCIATED CONTENT

Supporting Information. The Supporting Information is available free of charge on the ACS Publications website at DOI: 10.1021/acs.jnatprod.XXXX.

Tabulated full NMR data, NMR spectra, CD spectra, UV-Visible spectra, biological activity data and details of DFT calculations (PDF)

AUTHOR INFORMATION

Corresponding Author

*Author to whom correspondence should be addressed; e-mail: peter.karuso@mq.edu.au;

Tel.: +61-2-9850-8290; Fax: +61-2-9850-8313.

ACKNOWLEDGMENT

We thank Dr. M. McKay (APAF, Macquarie University) for the acquisition of HRMS data. This research was funded, in part, by the Australian Research Council (DP130103281 to PK and AMP; FT130100142 to AMP) and Macquarie University (iMQRES scholarship to NC).

REFERENCES

(1) Zang, Y.; Genta-Jouve, G.; Retailleau, P.; Escargueil, A.; Mann, S.; Nay, B.; Prado, S., *Org. Biomol. Chem.* **2016,** 14, (9), 2691-2697.

(2) Chaudhary, N. K.; Pitt, J. I.; Lacey, E.; Crombie, A.; Vuong, D.; Piggott, A. M.; Karuso, P., *J. Nat. Prod.* **2018**.

(3) Pitt, J. I.; Lange, L.; Lacey, A. E.; Vuong, D.; Midgley, D. J.; Greenfield, P.; Bradbury, M. I.; Lacey, E.; Busk, P. K.; Pilgaard, B.; Chooi, Y.-H.; Piggott, A. M., *PLoS One* **2017,** 12, (4), e0170254.

(4) Lacey, H. J.; Vuong, D.; Pitt, J. I.; Lacey, E.; Piggott, A. M., *Aust. J. Chem.* **2016,** 69, (2), 152-160.

(5) Shibata, S.; Ogihara, Y.; Tokutake, N.; Tanaka, O., *Tetrahedron Lett.* **1965,** 6, (18), 1287-1288.

(6) Cao, P.; Yang, J.; Miao, C.-P.; Yan, Y.; Ma, Y.-T.; Li, X.-N.; Zhao, L.-X.; Huang, S.-X., *Org. Lett.* **2015,** 17, (5), 1146-1149.

(7) Yamazaki, M.; Okuyama, E., *Chem. Pharm. Bull.* **1980,** 28, (12), 3649-55.

(8) Bryant, F. O.; Cutler, H. G.; Jacyno, J. M., *J. Pharm. Sci.* **1993,** 82, (12), 1214-1217.

(9) Kuhr, I.; Fuska, J., *J. Antibiot.* **1973,** 26, (9), 535-536.

(10) Dethoup, T.; Manoch, L.; Kijjoa, A.; Nascimento, M. S. J.; Puaparoj, P.; Silva, A. M. S.; Eaton, G.; Herz, W., *Planta Med.* **2006,** 72, (10), 957-960.

(11) Haasnoot, C.; de Leeuw, F. A.; Altona, C., *Tetrahedron* **1980,** 36, (19), 2783-2792.

(12) Ogihara, Y.; Tanaka, O.; Shibata, S., *Tetrahedron Lett.* **1966**, (25), 2867-73.

(13) Lin, Z.; Zhu, T.; Fang, Y.; Gu, Q.; Zhu, W., *Phytochemistry* **2008,** 69, (5), 1273-1278.

(14) Inokoshi, J.; Shiomi, K.; Masuma, R.; Tanaka, H.; Yamada, H.; Omura, S., *J. Antibiot.* **1999,** 52, (12), 1095-1100.

(15) Xiao, J.-z.; Kumazawa, S.; Tomita, H.; Yoshikawa, N.; Kimura, C.; Mikawa, T., *J. Antibiot.* **1993,** 46, (10), 1570-1574.

(16) Elsebai, M. F.; Ghabbour, H. A.; Mehiri, M., *Molecules* **2016,** 21, (2), 178.

(17) Ayer, W. A.; Hoyano, Y.; Pedras, M. S.; Altena, I. v., *Can. J. Chem.* **1986,** 64, (8), 1585-1589.

(18) Tansakul, C.; Rukachaisirikul, V.; Maha, A.; Kongprapan, T.; Phongpaichit, S.; Hutadilok-Towatana, N.; Borwornwiriyapan, K.; Sakayaroj, J., *Nat. Prod. Res.* **2014,** 28, (20), 1718-1724.

(19) Shibata, T.; Nishikawa, M.; Tsurumi, Y.; Takase, S.; Terano, H.; Kohsaka, M., *J. Antibiot.* **1989,** 42, (9), 1356-1361.

(20) Zhang, L.-H.; Feng, B.-M.; Sun, Y.; Wu, H.-H.; Li, S.-G.; Liu, B.; Liu, F.; Zhang, W.-Y.; Chen, G.; Bai, J., *Tetrahedron Lett.* **2016,** 57, (6), 645-649.

(21) Achard, M.; Beeler, A. B.; Porco, J. A., *ACS Combi. Sci.* **2012,** 14, (3), 236-244.

(22) Kawai, K.; Shiojiri, H.; Nakamaru, T.; Nozawa, Y.; Sugie, S.; Mori, H.; Kato, T.; Ogihara, Y., *Cell Biol. Toxicol.* **1985,** 1, (2), 1-10.

(23) Fuskova, A.; Proksa, B.; Fuska, J., *Pharmazie* **1977,** 32, (5), 291-293.

(24) Ayer, W. A.; Pedras, M. S.; Ward, D. E., *Can. J. Chem.* **1987,** 65, (4), 760-764.

(25) Gao, S.-S.; Duan, A.; Xu, W.; Yu, P.; Hang, L.; Houk, K.; Tang, Y., *J. Am. Chem. Soc.* **2016,** 138, (12), 4249-4259.

(26) Gao, S.-S.; Zhang, T.; Garcia-Borràs, M.; Hung, Y.-S.; Billingsley, J. M.; Houk, K. N.; Hu, Y.; Tang, Y., *J. Am. Chem. Soc.* **2018,** 140, (22), 6991-6997.

(27) Colosimo, D. A.; MacMillan, J. B., *J. Am. Chem. Soc.* **2016,** 138, (7), 2383-2388.

(28) Fuska, I.; Ivanitskaia, L.; Makukho, L.; Volkova, L., *Antibiotiki* **1974,** 19, (10), 890.

(29) TURBOMOLE V7.1.1,. In a development of the University of Karlsruhe and Forschungszentrum Karlsruhe GmbH:2016.

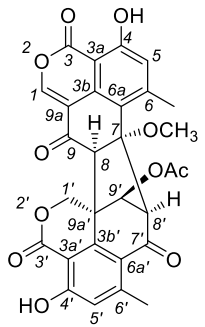

1

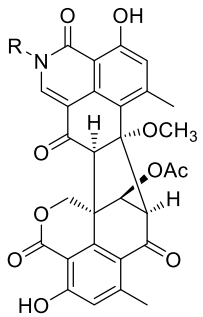

R = Asp **2** R = D-Leu **10**
Asn **3** D-Ile **11**
Val **4** D-Phe **12**
Leu **5**
Ile **6**

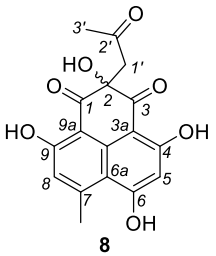

8

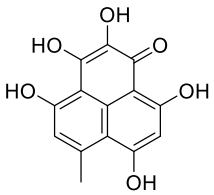

7

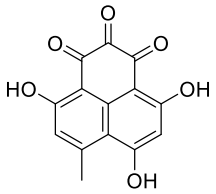

8a

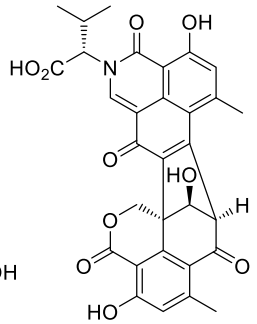

9

Table 1: ^{1}H and ^{13}C NMR data of talauxins and duclauxin in DMSO-d_6

Position	Talauxin E (**2**)		Talauxin Q (**3**)		Talauxin V (**4**)		Talauxin L (**5**)*		Talauxin I (**6**)*		Duclauxin (**1**)	
	δ_C	δ_H, multi (*J*, Hz)	δ_C	δ_H, multi (*J*, Hz)	δ_C	δ_H, multi (*J*, Hz)	δ_C	δ_H, multi (*J*, Hz)	δ_C	δ_H, multi (J, Hz)	δ_C	δ_H, multi (*J*, Hz)
1	137.2 br	7.93, s	136.9 br	7.93, s	138.0 br	8.11, s	137.7 br	8.08, s	137.5 br	8.06, s	149.7	7.92, s
3	164.8		164.7		164.7		164.7		164.8		161.6	
3a	106.6		106.5		106.3		106.6		106.6		101.5	
3b	134.6		134.5		134.6		134.4		134.5		133.5	
4	160.7		160.5		160.6		160.6		160.6		160.6	
5	117.7	6.84, br s	117.4	6.84, br s	117.4	6.83, br s	117.3	6.84, br s	117.4	6.83, br s	120.2	6.98, br s
6	148.8		148.5		148.6		148.5		148.6		150.4	
6a	117.1		116.8		116.8		116.7		117.4		118.1	
7	88.1		87.9		87.8		87.7		88.8		88.4	
8	63.5	3.97, s	63.3	3.98, s	63.3	3.98, s	63.2	4.00, s	63.2	3.98, s	63.2	4.00, s
9	193.5		193.2		193.2		193.0		193.1		193.8	
9a	111.0		110.7		110.3		110.4		110.4		112.7	
6-CH_3	21.6	2.62, br s	21.4	2.63, br s	21.4	2.63, br s	21.4	2.64, br s	21.4	2.63, br s	21.5	2.61, br s
7-OCH_3	51.4	2.87, s	51.2	2.88, s	51.2	2.87, s	51.1	2.88, s	51.2	2.87, s	51.4	2.90, s
4-OH		12.11, s		12.18, s		12.16, s		12.120, s		12.17, s		11.72, s
1'	71.0	5.00, d (*12.2*) 5.13, d (*12.2*)	70.8	5.00, d (*12.2*) 5.14, d (*12.2*)	70.9	5.00, d (*12.1*) 5.14, d (*12.1*)	70.9	5.01, d (*11.9*) 5.15, d (*11.9*)	70.9	5.01, d (*12.1*) 5.11, d (*12.1*)	70.7	5.00, d (*12.3*) 5.12, d (*12.3*)
3'	167.3		166.9		167.1		167.1		167.2		166.7	
3a'	105.2		105.1		105.0		105.0		105		105.5	
3b'	143.5		143.3		143.4		143.4		143.4		143.4	

4'	163.8		163.5		163.5		163.5		163.6		163.6	
5'	120.1	6.60, d (*0.7*)	120.0	6.61, br s	120.2	6.58, d (*0.7*)	119.8	6.60 d (*0.7*)	119.9	6.60, d (*0.7*)	120.0	6.78, d (*0.8*)
6'	150.3		150.1		150.0		150.1		150.1		150.3	
6a'	121.0		120.9		120.8		120.7		120.8		120.8	
7'	191.6		191.4		191.3		191.3		191.3		191.4	
8'	67.4	4.03, br s	67.2	4.03, br s	67.2	4.03, br s	67.1	4.04 br s	67.2	4.03, br s	66.9	4.00, br s
9'	78.6	5.16, br s	78.5	5.17, br s	78.5	5.16, br s	78.5	5.16 br s	78.5	5.12, br s	78.4	5.20, br s
9a'	51.1		50.9		50.9		50.8		51.2		51.0	
6'-CH_3	21.7	1.90, d (*0.7*)	21.5	1.92, br s	21.5	1.92, (*0.7*)	21.5	1.93, br s	21.6	1.93, br s	21.5	1.97, d (*0.8*)
9'-$\underline{C}OCH_3$	169.8		169.7		169.7		169.6		169.6		169.7	
9'-CO$\underline{C}H_3$	20.9	2.16, s	20.8	2.17, s	20.8	2.17, s	20.7	2.17, s	20.8	2.17, s	20.8	2.17, s
4'-OH		11.68, s		11.70, s		11.65, s		11.70, s		11.68, s		10.71, s
10	169.8		169.7		169.5		170.0		169.7			
11	61.9, br s	5.17, dd (*10.2, 5.1*)	61.5, br s	5.17, dd (*10.2, 5.1*)	67.6, br s	4.77, d (*9.3*)	61.5, br s	5.11, dd (*5.2*)	66.4, br s	4.87, d (*9.4*)		
12	24.7	2.21, m 2.32, m	25.1	2.20, m 2.31, m	27.6	2.50, m	37.3	1.82, m 2.01, m	33.9	2.26, m		
13	30.3	1.83, m 2.12, m	31.3	1.72, m 1.98, m	19.1	0.49, d (*6.8*)	24.5	1.00, m	24.7	1.50, m		
13'					20.9	1.10, d (*6.8*)			16.7	1.04, d (6.5)		
14	173.6		173.0				23.0	0.88, m (6.9)	10.9	0.82, d (6.8)		
14'							21.3	0.89, m (7.2)				
14-NH_2/OH		–		6.84, br s		7.21, br s						
10-OH		α		α		α		α		α		

α- Not observed, *In the mixture of **5** and **6**

Table 2: ^{1}H and ^{13}C NMR data of talauxins and epitalauxins (semi-synthetic) in DMSO-*d*$_6$

Position	Talauxin L (**5**)		Talauxin I (**6**)		Epitalauxin L (**10**)		Epitalauxin I (**11**)		Epitalauxin F (**12**)	
	δ_C	δ_H, multi (*J*, Hz)	δ_C	δ_H, multi (J, Hz)	δ_C	δ_H, multi (*J*, Hz)	δ_C	δ_H, multi (*J*, Hz)	δ_C	δ_H, multi (*J*, Hz)
1	137.7 br	8.06, s	137.4 br	8.06, s	134.3 br	7.77, s	134.6 br	7.83, s	136.6 br	7.67, s
3	164.6		164.8		164.8		164.8		164.7	
3a	106.6		106.2		106.1		106.0		106.5	
3b	134.4		134.4		134.1		133.9		134.2	
4	160.5		160.6		160.6		160.7		160.5	
5	117.3	6.83, br s	117.3	6.83, br s	117.6	6.85, br s	117.6	6.86, br s	117.4	6.82, br s
6	148.5		148.6		148.6		148.7		148.5	
6a	116.7		116.7		116.7		116.7		116.4	
7	87.7		87.8		87.8		87.8		87.8	
8	63.2	3.99, s	63.2	3.98, s	63.2	3.99, s	63.1	4.00, s	63.3	3.91, s
9	193.0		193.1		193.0		193.0		192.8	
9a	110.4		110.3		110.7		110.3		110.5	
6-CH_3	21.4	2.64, br s	21.4	2.63, br s	21.4	2.63, br s	21.4	2.64, br s	21.4	2.62, br s
7-OCH_3	51.1	2.87, s	51.1	2.88, s	51.2	2.88, s	51.1	2.88, s	51.0	2.81, s
4-OH		12.22, s		12.20, s		12.25, s		12.26, s		12.20 s
1'	70.9	5.01, d (*11.9*) 5.15, d (*11.9*)	70.9	5.00, d (*12.1*) 5.14, d (*12.1*)	70.9	5.00, d (*12.2*) 5.14, d (*12.2*)	70.9	5.01, d (*12.1*) 5.15, d (*12.1*)	70.8	4.99, d (*12.0*) 5.11, d (*12.0*)
3'	167.1		167.0		167.1		167.0		167.0	
3a'	105.0		105.0		105.0		105.1		104.9	
3b'	143.4		143.4		143.3		143.4		143.4	
4'	163.5		163.6		163.4		163.4		163.6	
5'	119.8	6.60, br s	119.9	6.60, d (*0.7*)	119.8	6.59, br s	120.0	6.62, d (*0.7*)	120.3	6.57, d (*0.7*)
6'	150.1		150.0		150.1		150.1		149.8	
6a'	120.7		120.7		120.8		120.8		120.5	

7'	191.3		191.3		191.2		191.2		191.2	
8'	67.1	4.04, br s	67.1	4.03, br s	67.1	4.03, br s	67.1	4.05, br s	66.9	4.03, br s
9'	78.5	5.16, br s	78.5	5.16, br s	78.4	5.16, br s	78.4	5.17, br s	78.5	5.14, br s
9a'	50.8		50.8		50.9		50.9		50.6	
6'-CH_3	21.5	1.93, br s	21.5		21.4	1.91, br s	21.4	1.93, s	21.6	1.90, br s
9'-$\underline{C}OCH_3$	169.6		169.5		169.6		169.7		169.7	
9'-CO$\underline{C}H_3$	20.7	2.17, s	20.7	2.17, s	20.7	2.16, s	20.7	2.17, s	20.7	2.15, s
4'-OH		11.70, s		11.68, s		11.67, s		11.64, s		11.72, s
10	170.0		169.7		170.7		170.2		169.5	
11	61.5, br s	5.11, dd *(11.0, 4.2)*	66.1, br s	4.88, d (*9.0*)	55.7 br s	5.34, dd (*10.3, 6.2*)	60.2, br s	5.31, d (*8.2*)	62.8, br s	5.45, dd (*10.2, 5.6*)
12	37.3	1.82, m 2.00, m	34.0	0.80, m	38.0	1.90, m	35.8	2.13, m	35.0	3.20, m 3.42, dd (14.3, 5.5)
13	24.5	1.03, m	24.6	1.50, m	24.4	1.12, m	24.4	0.83, m 1.18, m	136.7	
13'			16.6	1.04, d (*6.6*)		0.82, d (*6.6*)	15.3	0.91, d (*6.7*)		
14	23.0	0.88, m (*7.0*)	10.9	0.82, t (*6.6*)	23.0	0.91, d (*6.6*)	10.5	0.85, t (*6.7*)	128.8	7.05, m
14'	21.3	0.89, m (*7.0*)			20.4					
15									128.3	7.16, m
16									126.7	7.12, m
17									128.3	7.16, m
18									128.8	7.05, m
10-OH		13.15, br s		13.1 3, br s		13.58, br s		13.71, br s		13.29, br s

Table 3: Antibacterial (ProTOX), antifungal (EuTOX) and cytotoxicity (CyTOX) minimum inhibitory concentrations (MICs) of compounds **1** - **12.** Compounds **3** and **9** were insufficient for bioassay.

Compound	ProTOX[a] (μg/mL)	EuTOX[b] (μg/mL)	CyTOX[c] (μg/mL)
1	>100	>100	10+0
2	>100	>100	-
3	-	-	-
4	>100	>100	-
5	>100	>100	>100
6	>100	>100	>100
7	100	>100	25
8	>100	>100	>100
9	-	-	-
10	>100	>100	>100
11	>100	>100	>100
12	>100	>100	>100
C[d]	0.4	0.2	0.8

[a] *Bacillus subtilis* (ATCC 6633), no activity for *Escherichia coli* (ATCC 25922)
[b] *Saccharomyces cerevisiae* (ATCC 9763), no activity for *Candida albicans* (ATCC 10231)
[c] mouse myeloma NS-1 cell line (ATCC TIB-18)
[d] Positive controls: ampicillin; clotrimazole; 5-fluorouracil; respectively

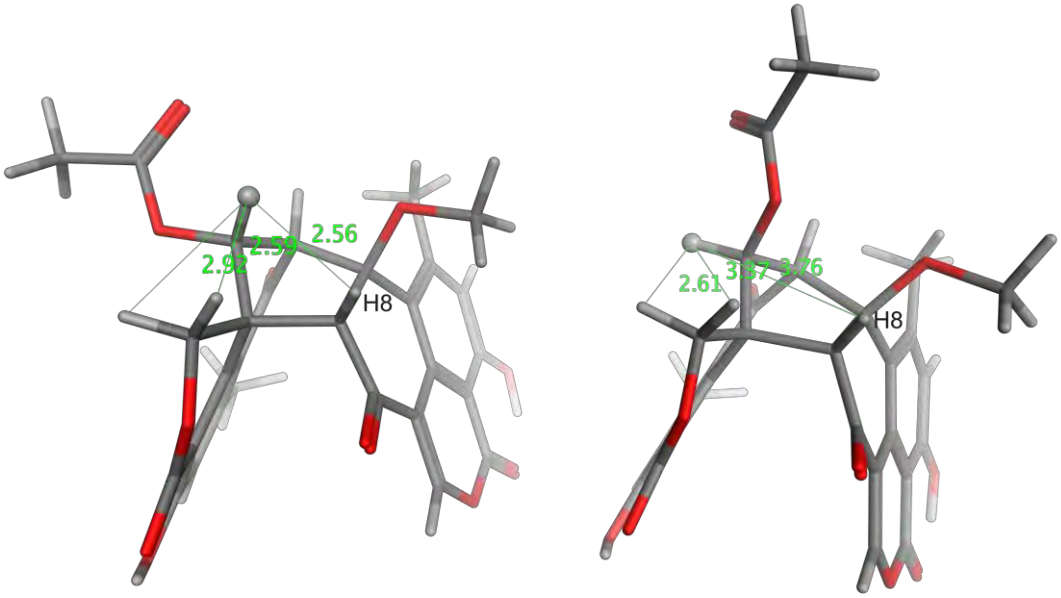

Figure 1: Measurement of inter-proton distances for C-9' epimers of **1** from DFT//BPE0/TZVP geometry optimization. (*R*)-**1** (left), a H-9'–H-8 distance of 2.56 Å would suggest a strong ROE; for (*S*)-**1** (right) a distance of 3.76 Å suggests a weak ROE.

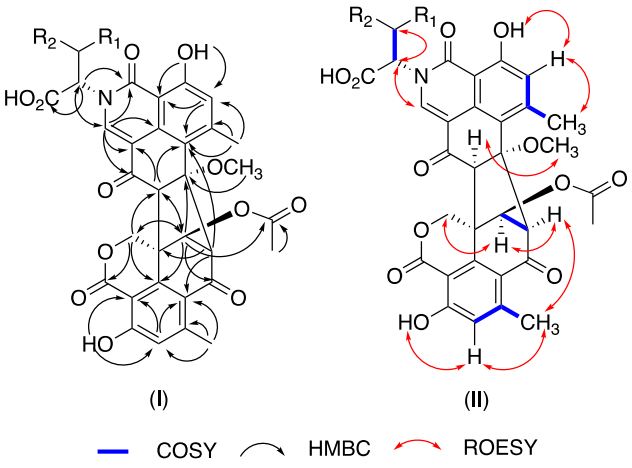

Figure 2: Key (I) HMBC correlations and (II) ROESY, COSY correlations in talauxins

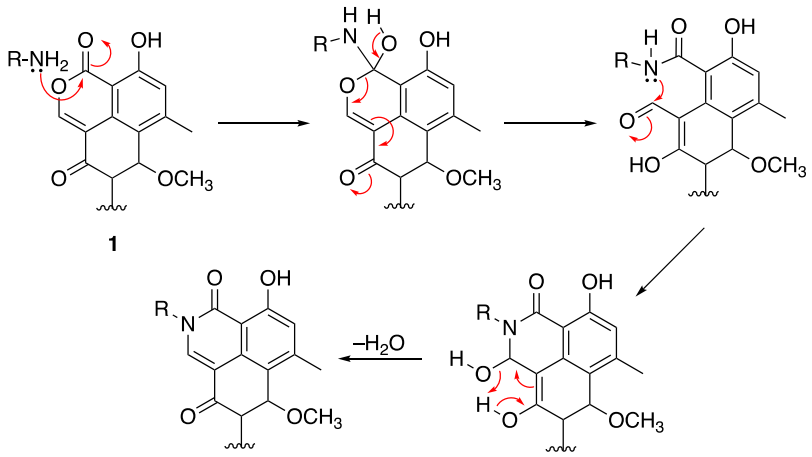

Figure 3: Proposed mechanism for the reaction of duclauxin (**1**) with amino acids to yield talauxins

Supporting Information

Talauxins from *Talaromyces stipitatus* and the semi-synthesis of talauxin analogs from their common biogenetic precursor duclauxin

Nirmal K. Chaudhary,[†] John I. Pitt,[‡] Ernest Lacey,[§,†] Andrew Crombie,[§] Daniel Vuong,[§] Andrew M. Piggott,[†] Peter Karuso[†,]*

[†]Department of Molecular Sciences, Macquarie University, NSW 2109, Australia

[‡]Commonwealth Scientific and Industrial Research Organisation, North Ryde, NSW 2113, Australia,

[§]Microbial Screening Technologies Pty. Ltd., Smithfield, NSW 2164, Australia

Table of Contents

A. NMR tables

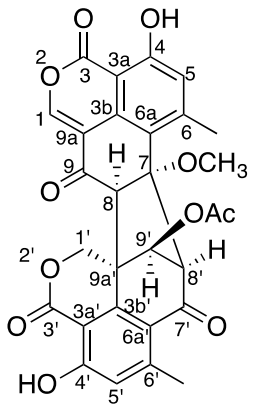

Duclauxin (**1**)

Table 1: NMR data of duclauxin (**1**) in DMSO-d_6

Position	δ_H, mult (*J*, Hz)	δ_C	^1H-^{13}C HMBC	COSY	ROESY
1	7.92, s	149.7	3, 3b, 9, 6a, 9a		
3		161.6			
3a		101.5			
3b		133.5			
4		160.6			
5	6.98, br s	120.2	3a, 6a, 6-CH_3, 3 (w)		6-CH_3, 4-OH
6		150.4			
6a		118.1			
7		88.4			
8	4.00, s	63.2	6a, 7, 9, 9a, 1', 3b', 8', 9', 9a'		1', 7-OCH_3
9		193.8			
9a		112.7			
6-CH_3	2.61, br s	21.5	5, 6, 6a	5 (w)	5, 8'
7-OCH_3	2.90, s	51.4	7		8
4-OH	11.72, s		3a, 4, 5		5
1'	5.00, d (*12.3*) 5.12, d (*12.3*)	70.7	3', 3b', 6a', 9', 9a'		8, 9'
3'		166.7			
3a'		105.5			
3b'		143.4			
4'		163.6			
5'	6.78, d (*0.8*)	120.0	3a', 6a', 6-CH_3', 3' (w)		6-CH_3', 4-OH'
6'		150.3			
6a'		120.8			

7'		191.4			
8'	4.00, br s	66.9	6a, 7, 8, 6a', 9', 9a', 5', 7', 1' (w), 6' (w)	9'	6-CH_3, 9'
9'	5.20, br s	78.4	7, 8, 1', 7', 3b', 8', 9'-$\underline{C}OCH_3$	8'	1', 8'
9a'		51.0			
6'-CH_3	1.97, d (*0.8*)	21.5	5', 6', 6a'	5' (w)	5'
9'- $\underline{C}OCH_3$		169.7			
9'-$CO\underline{CH_3}$	2.17, s	20.8	9'- $\underline{C}OCH_3$		
4'-OH	10.71, s		3a', 4', 5'		5'

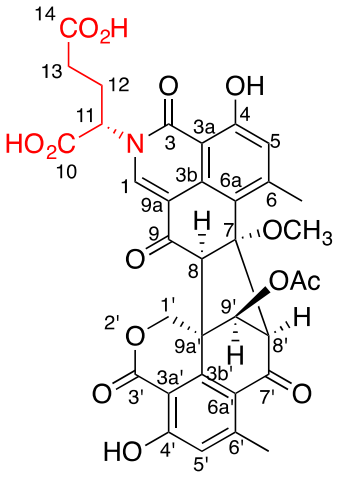

Talauxin E (**2**)

Table 2: NMR data of talauxin E (**2**) in DMSO-d_6

Position	δ_H, mult (*J*, Hz)	δ_C	^1H-^{13}C HMBC	COSY	ROESY
1	7.93, s	137.2 br	3, 3b, 9, 6a, 11, 9a (w)		11
3		164.8			
3a		106.6			
3b		134.6			
4		160.7			
5	6.84, br s	117.7	3a, 6a, 6-CH_3, 3 (w)		6-CH_3, 4-OH
6		148.8			
6a		117.1			
7		88.1			
8	3.97, s	63.5	6a, 7, 9, 9a, 1', 3b', 8', 9', 9a'		1', 7-OCH_3
9		193.5			

9a		111.0			
6-CH_3	2.62, br s	21.6	5, 6, 6a	5 (w)	5
7-OCH_3	2.87, s	51.4	7		8
4-OH	12.11, s		3a, 4, 5		5
1'	5.00, d (*12.2*) 5.13, d (*12.2*)	71.0	3', 3b', 6a', 8, 9', 9a', 7 (w)		8, 9'
3'		167.3			
3a'		105.2			
3b'		143.5			
4'		163.8			
5'	6.60, d (*0.7*)	120.1	3a', 6a', 6-CH_3', 3' (w)		6-CH_3', 4-OH'
6'		150.3			
6a'		121.0			
7'		191.6			
8'	4.03, br s	67.4	6a, 7, 8, 6a', 9', 9a', 5', 7', 1'(w), 6'(w)	9'	6-CH_3, 9'
9'	5.16, br s	78.6	7, 8, 1', 7', 3b', 8', 9'- $\underline{C}OCH_3$	8'	1', 8'
9a'		51.1			
6'-CH_3	1.90, d (*0.7*)	21.7	5', 6', 6a'	5' (w)	5'
9'- $\underline{C}OCH_3$		169.8			
9'- $CO\underline{CH_3}$	2.16, s	20.9	9'- $\underline{C}OCH_3$		
4'-OH	11.68, s		3a', 4', 5'		5'
10		169.9			
11	5.17, dd (*10.2, 5.1*)	61.9 br	1, 3, 13	12	1, 12, 13
12	2.21, m 2.32, m	24.7	10, 14	11, 13	11, 13
13	1.83, m 2.12, m	30.3	11	12	12
14		173.6			
14-OH	[a]				
10-OH	[a]				

[a] Not observed or not assignable

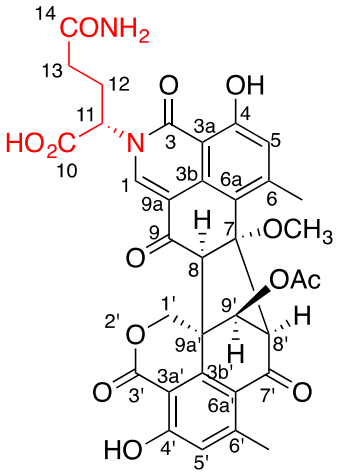

Talauxin Q (**3**)

Table 3: NMR data of talauxin Q (**3**) in DMSO-d_6

Position	δ_H, mult (*J*, Hz)	δ_C	^{1}H-^{13}C HMBC	COSY	ROESY
1	7.93, s	136.9 br	3, 3b, 9, 6a, 11, 9a (w)		11
3		164.7			
3a		106.5			
3b		134.5			
4		160.6			
5	6.84, br s	117.4	3a, 6a, 6-CH_3, 3 (w)		6-CH_3, 4-OH
6		148.5			
6a		116.8			
7		87.9			
8	3.98, s	63.3	6a, 7, 9, 9a, 1', 3b', 8', 9', 9a'		1', 7-OCH_3
9		193.2			
9a		110.7			
6-CH_3	2.63, br s	21.4	5, 6, 6a	5 (w)	5, 8'
7-OCH_3	2.88, s	51.2	7		8
4-OH	12.18, s		3a, 4, 5		5
1'	5.00, d (*12.2*) 5.14, d (*12.2*)	70.8	3', 3b', 6a', 8, 9, 9a', 7 (w)		8, 9'
3'		166.9			
3a'		105.1			
3b'		143.3			
4'		163.5			
5'	6.61, br s	120.0	3a', 6a', 6-CH_3', 3' (w)		6-CH_3', 4-OH'
6'		150.1			
6a'		120.9			
7'		191.4			

8'	4.03, br s	67.2	6a, 7, 8, 5', 6a', 7', 9', 9a', 1' (w), 6' (w)	9'	6-CH_3, 9'
9'	5.17, br s	78.5	7, 8, 1', 3b', 7', 8', 9'- $\underline{C}OCH_3$	8'	1', 8'
9a'		50.9			
6'-CH_3	1.92, br s	21.5	5', 6', 6a'	5' (w)	5'
9'- $\underline{C}OCH_3$		169.7			
9'- $CO\underline{CH_3}$	2.17, s	20.8	9'- $\underline{C}OCH_3$		
4'-OH	11.70, s		3a', 4', 5'		5'
10		169.8			
11	5.17, dd (*10.2, 5.1*)	61.5 br	1, 3, 13	12	
12	2.20, m 2.31, m	25.1	10, 14	11, 13	
13	1.72, m 1.98, m	31.3	11	12	
14		173.0			
14-NH_2	6.84, br s 7.21, br s		13		
10-OH	[a]				

[a] Not observed or not assignable

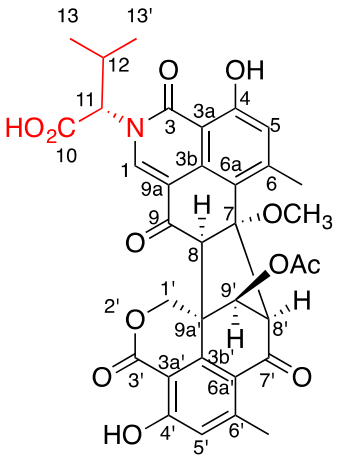

Talauxin V (**4**)

Table 4: NMR data of talauxin V (**4**) in DMSO-d_6

Position	δ_H, mult (*J*, Hz)	δ_C	^1H-^{13}C HMBC	COSY	ROESY
1	8.11, s	138.0 br	3, 3b, 9, 6a, 11, 9a (w)		11
3		164.7			
3a		106.3			
3b		134.6			
4		160.6			
5	6.83, br s	117.4	3a, 6a, 6-CH_3, 3 (w)	6-CH_3 (w)	6-CH_3, 4-OH
6		148.6			
6a		116.8			
7		87.8			
8	3.98, s	63.3	6a, 7, 9, 9a, 1', 3b', 8', 9', 9a'		1', 7-OCH_3
9		193.2			
9a		110.3			
6-CH_3	2.63, br s	21.4	5, 6, 6a	5 (w)	5, 8'
7-OCH_3	2.87, s	51.2	7		8
4-OH	12.16, s		3a, 4, 5		5
1'	5.00, d (*12.1*) 5.14, d (*12.1*)	70.9	3', 3b', 6a', 8, 9, 9a', 7 (w)		8, 9'
3'		167.1			
3a'		105			
3b'		143.4			
4'		163.5			
5'	6.58, d (*0.7*)	120.2	3a', 6a', 6-CH_3', 3' (w)	6-CH_3' (w)	6-CH_3' (w), 4-OH'
6'		150			
6a'		120.8			
7'		191.3			
8'	4.03, br s	67.2	6a, 7, 8, 5', 6a', 7', 9', 9a', 1' (w), 6' (w)	9'	9', 6-CH_3
9'	5.16, br s	78.5	7, 8, 1', 3b', 7', 8', 9'-$\underline{C}OCH_3$	8'	1', 8'
9a'		50.9			
6'-CH_3	1.92, (*0.7*)	21.5	5', 6', 6a'	5' (w)	5'
9'-$\underline{C}OCH_3$		169.7			
9'-CO$\underline{C}H_3$	2.17, s	20.8	9'-$\underline{C}OCH_3$		
4'-OH	11.65, s		3a', 4', 5'		5'
10		169.5			

11	4.77, d (*9.3*)	67.6 br	1, 3, 13, 13'	12	1, 12, 13, 13'
12	2.50, m	27.6	10	11, 13, 13'	11, 13, 13'
13	0.49, d (*6.8*)	19.1	11, 13'	12	12
13'	1.10, d (*6.8*)	20.9	11, 13	12	12
10-OH	[a]				

[a] - Not observed or not assignable

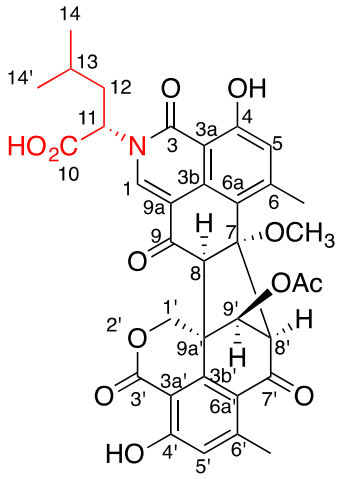

Talauxin L (**5**)

Table 5: NMR data of talauxin L (**5**) in DMSO-d_6

Position	δ_H, mult (*J*, Hz)	δ_C	^1H-^{13}C HMBC	COSY	ROESY
1	8.06, s	137.7 br	3, 3b, 9, 6a, 11, 9a (w)		11
3		164.6			
3a		106.6			
3b		134.4			
4		160.5			
5	6.83, br s	117.3	3a, 6a, 6-CH_3, 3 (w)		6-CH_3, 4-OH
6		148.5			
6a		116.7			
7		87.7			
8	3.99, s	63.2	6a, 7, 9, 9a, 1', 3b', 8', 9', 9a'		1', 7-OCH_3
9		193.0			
9a		110.4			
6-CH_3	2.64, br s	21.4	5, 6, 6a	5 (w)	5, 8'
7-OCH_3	2.87, s	51.1	7		8
4-OH	12.22, s		3a, 4, 5		5
1'	5.01, d (*11.9*) 5.15, d (*11.9*)	70.9	3', 3b', 6a', 8, 9, 9a', 7 (w)		11

3'		167.1			
3a'		105.0			
3b'		143.4			
4'		163.5			
5'	6.60, br s	119.8	3a', 6a', 6-CH_3', 3' (w)		6-CH_3', 4-OH'
6'		150.1			
6a'		120.7			
7'		191.3			
8'	4.04, br s	67.1	6a, 7, 8, 5', 6a', 7', 9', 9a', 1' (w), 6' (w)	9'	6-CH_3, 9'
9'	5.16, br s	78.5	7, 8, 1', 3b', 7', 8', 9'- $\underline{C}OCH_3$	8'	1', 8'
9a'		50.8			
6'-CH_3	1.93, br s	21.5	5', 6', 6a'	5' (w)	5'
9'- $\underline{C}OCH_3$		169.6			
9'- CO$\underline{C}H_3$	2.17, s	20.7	9'- $\underline{C}OCH_3$		
4'-OH	11.70, s		3a', 4', 5'		5'
10		170.0			
11	5.11, dd (*11.0, 4.2*)	61.5 br	1, 3, 13	12	1, 12, 13, 14'
12	1.84, m 2.00, m	37.3	10, 11, 13, 14, 14'	11, 13	11, 13, 14, 14'
13	1.03, m	24.5	11, 13'	12	12
14	0.88, m (*7.0*)	23.0			
14'	0.89, m (*7.0*)	21.3			
10-OH	13.15, br s				

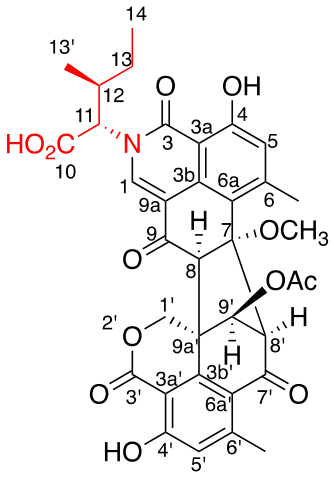

Talauxin I (**6**)

Table 6: NMR data of talauxin I (**6**) in DMSO-d_6

Position	δ_H, mult (*J*, Hz)	δ_C	^1H-^{13}C HMBC	COSY	ROESY
1	8.07, s	137.4 br	3, 3b, 9, 6a, 11, 9a (w)		11
3		164.8			
3a		106.2			
3b		134.4			
4		160.6			
5	6.83, br s	117.3	3a, 6a, 6-CH_3, 3 (w)		6-CH_3, 4-OH
6		148.6			
6a		116.7			
7		87.8			
8	3.98, s	63.2	6a, 7, 9, 9a, 1', 3b', 8', 9', 9a'		1', 7-OCH_3
9		193.1			
9a		110.3			
6-CH_3	2.63, br s	21.4	5, 6, 6a	5 (w)	5, 8'
7-OCH_3	2.88, s	51.1	7		8
4-OH	12.20, s		3a, 4, 5		5
1'	5.00, d (*12.1*) 5.14, d (*12.1*)	70.9	3', 3b', 6a', 8, 9, 9a', 7 (w)		11
3'		167.0			
3a'		105.0			
3b'		143.4			
4'		163.6			
5'	6.60, d (*0.7*)	119.9	3a', 6a', 6-CH_3', 3' (w)		6-CH_3', 4-OH'
6'		150.0			
6a'		120.7			
7'		191.3			
8'	4.03, br s	67.1	6a, 7, 8, 5', 6a', 7', 9', 9a', 1' (w), 6' (w)	9'	6-CH_3, 9'
9'	5.16, br s	78.5	7, 8, 1', 3b', 7', 8', 9'- $\underline{C}OCH_3$	8'	1', 8'
9a'		50.8			
6'-CH_3		21.5	5', 6', 6a'	5' (w)	5'
9'- $\underline{C}OCH_3$		169.5			
9'- CO$\underline{CH_3}$	2.17, s	20.7	9'- $\underline{C}OCH_3$		
4'-OH	11.69, s		3a', 4', 5'		5'
10		169.7			
11	4.88, d (*9.0*)	66.1 br	1, 3, 13, 13'	12	1, 12, 13, 13'
12	2.25, m	34.0	10	11, 13, 13'	11, 13, 13'

13	0.80, m	24.6	11, 13'	12	12
13'	1.04, d (*6.6*)	16.6	11, 13	12	12, 13
14	0.82, t (*6.6*)	10.9	12, 13	13	13
10-OH	13.13, br s				

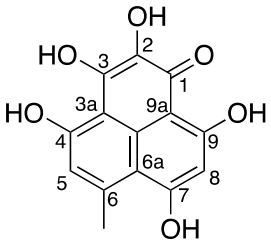

O-desmethylfunalenone (**7**)

Table 7: NMR data of *O*-desmethylfunalenone (**7**) in DMSO-d_6

Position	δ_H, multi (J, Hz)	δ_C	^1H-^{13}C HMBC	COSY	ROESY
1		170.4			
2		131.3			
3		154.8 br			
3a		105.1			
3b		124.9			
4		162.7			
5	6.82 br s	116.6	3a, 4, 6, 6a	6-CH_3 (w)	6-CH_3 (w)
6		145.6			
6a		110.8			
7		166.1			
8	6.43 s	99.8	6a, 7, 9, 9a		7-OH
9		1665.9			
9a		102.3			
6-CH_3	2.81, br s	25.3	5, 6, 6a	5 (w)	5 (w)
1-OH	[a]				
2-OH	[a]				
4-OH	[a]				
6-OH	[a]				
7-OH	11.69		6a, 7, 8		

[a] Not observed

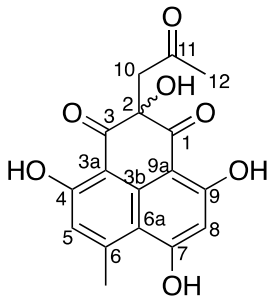

9-demethyl FR 901235 (**8**)

Table 8: NMR data of 9-demethyl FR 901235 (**8**) in DMSO-d_6

Position	δ_H, multi (J, Hz)	δ_C	^1H-^{13}C HMBC	COSY	ROESY
1		200.7			
2		73.3			
3		198.1			
3a		105.4			
3b		137.6			
4		165.2			
5	6.87 (0.8)	117.9	3a, 4, 6a, 6-CH_3	6-CH_3	6-CH_3
6		149.7			
6a		112.5			
7		1668.0			
8	6.40	99.2	7, 9, 9a, 6a		7-OH
9		168.3			
9a		101.2			
6-CH_3	2.83, d (0.7)	25.6	5, 6, 6a	5	5, 7-OH
10	3.57 d (*17.7*) 3.61 d (*17.7*)	49.3			
11		208.0			
12	2.11 s	29.3	10, 11		
4-OH	13.21 s				
7-OH	12.08 s		6a, 7, 8		6-CH_3
9-OH	13.71 s				
2-OH	6.97 s				

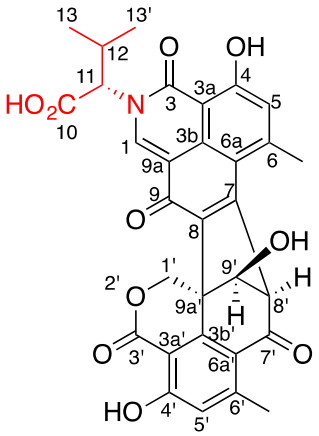

Desacetyldesmethyltalauxin V (**9**)

Table 9: NMR data of desacetyldesmethyltalauxin V (**9**) in DMSO-d_6

Position	δ_H, mult (*J*, Hz)	δ_C	^1H-^{13}C HMBC	COSY	ROESY
1	8.76, s	142.3 br	3, 3b, 9, 6a, 11, 9a (w)		11
3		164.8			
3a		107.6			
3b		134.2			
4		163.5			
5	7.02, br s	118.0	3a, 6a, 6-CH_3, 3 (w)	6-CH_3 (w)	6-CH_3, 4-OH
6		149.1			
6a		114.7			
7		152.4			
8		139.7			
9		177.4			
9a		113.7			
6-CH_3	2.98, br s	24.4	5, 6, 6a	5 (w)	5, 8'
4-OH	12.64, s		3a, 4, 5		5
1'	4.85, d (*12.1*) 5.02, d (*12.1*)	69.3	3', 3b', 6a', 8, 9, 9a', 7 (w)		9'
3'		167.8			
3a'		104.3			
3b'		147.6			
4'		163.3			
5'	6.85, br s	119.6	3a', 6a', 6-CH_3', 3' (w)	6-CH_3' (w)	6-CH_3' (w), 4-OH'
6'		152.3			
6a'		117.0			
7'		191.5			

8'	4.75, br s	66.3	6a, 7, 8, 5', 6a', 7', 9', 9a', 1' (w), 6' (w)	9'	6-CH_3, 9'
9'	4.68, d (*5.4*)	84.4	7, 8, 1', 3b', 7', 8'	8', 9'-OH	1', 8', 9'-OH
9a'		49.3			
6'-CH_3	2.50, s [b]	23.3	5', 6', 6a'	5' (w)	5'
4'-OH	12.02, s		3a', 4', 5'		5'
9'-OH	6.33, d (*5.4*)		8', 9', 9a',	9'	9'
10		169.9			
11	5.20, d (*9.1*)	65.0 br	1, 3, 13, 13'	12	1, 12, 13, 13'
12	2.60, m	29.1	10	11, 13, 13'	11, 13, 13'
13	0.75, d (*6.8*)	19.0	11, 13'	12	12
13'	1.13, d (*6.8*)	20.2	11, 13	12	12
10-OH	[a]				

[a] Not observed or not assignable; [b]signal masked under DMSO-d_6 peak

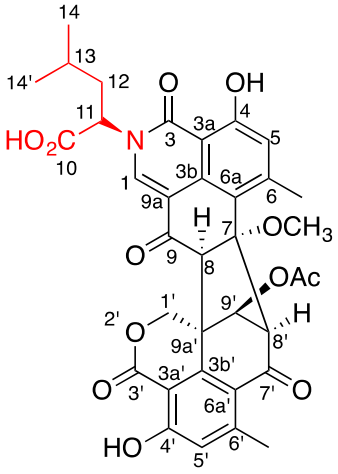

Epitalauxin L (**10**)

Table 10: NMR data of epitalauxin L (**10**) in DMSO-d_6

Position	δ_H, mult (*J*, Hz)	δ_C	^1H-^{13}C HMBC	COSY	ROESY
1	7.77, s	134.3 br	3, 3b, 9, 6a, 11, 9a (w)		11
3		164.8			
3a		106.1			
3b		134.1			
4		160.6			
5	6.85, br s	117.6	3a, 6a, 6-CH_3, 3 (w)		6-CH_3, 4-OH

6		148.6			
6a		116.7			
7		87.8			
8	3.99, s	63.2	6a, 7, 9, 9a, 1', 3b', 8', 9', 9a'		1', 7-OCH_3
9		193.0			
9a		110.7			
6-CH_3	2.63, br s	21.4	5, 6, 6a	5 (w)	5, 8'
7-OCH_3	2.88, s	51.2	7		8
4-OH	12.25, s		3a, 4, 5		5
1'	5.00, d (*12.2*) 5.14, d (*12.2*)	70.9	3', 3b', 6a', 8, 9, 9a', 7 (w)		11
3'		167.1			
3a'		105.0			
3b'		143.3			
4'		163.4			
5'	6.59, br s	119.8	3a', 6a', 6-CH_3', 3' (w)		6-CH_3', 4-OH'
6'		150.1			
6a'		120.8			
7'		191.2			
8'	4.03, br s	67.1	6a, 7, 8, 5', 6a', 7', 9', 9a', 1' (w), 6' (w)	9'	6-CH_3, 9'
9'	5.16, br s	78.4	7, 8, 1', 3b', 7', 8', 9'- $\underline{C}OCH_3$	8'	1', 8'
9a'		50.9			
6'-CH_3	1.91, br s	21.4	5', 6', 6a'	5' (w)	5'
9'- $\underline{C}OCH_3$		169.6			
9'- CO$\underline{C}H_3$	2.16, s	20.7	9'- $\underline{C}OCH_3$		
4'-OH	11.67, s		3a', 4', 5'		5'
10		170.7			
11	5.34, dd (*10.3, 6.2*)	55.7 br	1, 3, 13	12	1, 12
12	1.90, m	38.0	10, 11, 13, 14, 14'	11, 13	11, 13, 14, 14'
13	1.12, m	24.4	11, 13'	12	12, 14, 14'
14	0.82, d (*6.6*)	23.0			
14'	0.91, d (*6.6*)	20.4			
10-OH	13.58, br s				

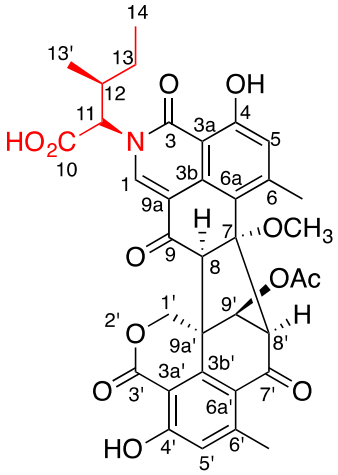

Epitalauxin I (**11**)

Table 11: NMR data of epitalauxin I (**11**) in DMSO-d_6

Position	δ_H, mult (*J*, Hz)	δ_C	^1H-^{13}C HMBC	COSY	ROESY
1	7.83, s	134.6 br	3, 3b, 9, 6a, 11, 9a (w)		11
3		164.8			
3a		106.0			
3b		133.9			
4		160.7			
5	6.86, br s	117.6	3a, 6a, 6-CH_3, 3 (w)		6-CH_3, 4-OH
6		148.7			
6a		116.7			
7		87.8			
8	4.00, s	63.1	6a, 7, 9, 9a, 1', 3b', 8', 9', 9a'		1', 7-OCH_3
9		193.0			
9a		110.3			
6-CH_3	2.64, br s	21.4	5, 6, 6a	5 (w)	5, 8'
7-OCH_3	2.88, s	51.1	7		8
4-OH	12.26, s		3a, 4, 5		5
1'	5.01, d (*12.1*) 5.15, d (*12.1*)	70.9	3', 3b', 6a', 8, 9, 9a', 7 (w)		11
3'		167.0			
3a'		105.1			
3b'		143.4			
4'		163.4			
5'	6.62, d (*0.7*)	120.0	3a', 6a', 6-CH_3', 3' (w)		6-CH_3', 4-OH'
6'		150.1			

6a'		120.8			
7'		191.2			
8'	4.05, br s	67.1	6a, 7, 8, 5', 6a', 7', 9', 9a', 1' (w), 6' (w)	9'	6-CH_3, 9'
9'	5.17, br s	78.4	7, 8, 1', 3b', 7', 8', 9'- $\underline{C}OCH_3$	8'	1', 8'
9a'		50.9			
6'-CH_3	1.93, s	21.5	5', 6', 6a'	5' (w)	5'
9'- $\underline{C}OCH_3$		169.7			
9'- $CO\underline{CH_3}$	2.17, s	20.7	9'- $\underline{C}OCH_3$		
4'-OH	11.64, s		3a', 4', 5'		5'
10		170.2			
11	5.31, d (*8.2*)	60.2 br	1, 3, 13, 13'	12	12
12	2.13, m	35.8	10	11, 13, 13'	11, 13, 13'
13	0.83, m 1.18, m	24.4	11, 13'	12	12, 13', 14
13'	0.91, d (*6.7*)	15.3	11, 13	12	12, 13
14	0.85, t (*6.7*)	10.5	12, 13	13	13
10-OH	13.71, br s				

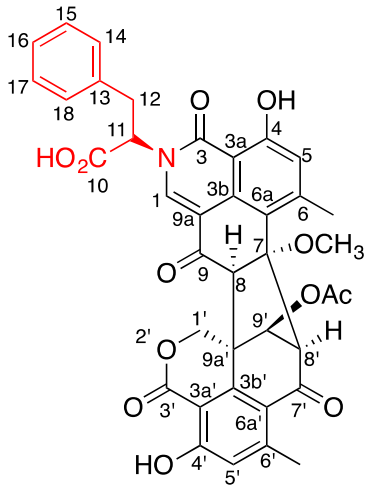

Epitalauxin F (**12**)

Table 12: NMR data of epitalauxin F (**12**) in DMSO-d_6

Position	δ_H, mult (*J*, Hz)	δ_C	^1H-^{13}C HMBC	COSY	ROESY
1	7.67, s	136.6 br	3, 3b, 9, 6a, 11, 9a (w)		11
3		164.7			
3a		106.4			
3b		134.2			
4		160.5			
5	6.82, br s	117.4	3a, 6a, 6-CH_3, 3 (w)		6-CH_3, 4-OH
6		148.5			
6a		116.4			
7		87.8			
8	3.91, s	63.3	6a, 7, 9, 9a, 1', 3b', 8', 9', 9a'		1', 7-OCH_3
9		192.8			
9a		110.4			
6-CH_3	2.62, br s	21.4	5, 6, 6a	5 (w)	5, 8'
7-OCH_3	2.81, s	51.0	7		8
4-OH	12.20 s		3a, 4, 5		5
1'	4.99, d (*12.0*) 5.11, d (*12.0*)	70.8	3', 3b', 6a', 8, 9, 9a', 7 (w)		11
3'		167.0			
3a'		104.9			
3b'		143.4			
4'		163.6			
5'	6.57, d (*0.7*)	120.3	3a', 6a', 6-CH_3', 3' (w)		6-CH_3', 4-OH'
6'		149.8			
6a'		120.5			
7'		191.2			
8'	4.03, br s	66.9	6a, 7, 8, 5', 6a', 7', 9', 9a', 1' (w), 6' (w)	9'	6-CH_3, 9'
9'	5.14, br s	78.5	7, 8, 1', 3b', 7', 8', 9'- $\underline{C}OCH_3$	8'	1', 8'
9a'		50.6			
6'-CH_3	1.90, br s	21.6	5', 6', 6a'	5' (w)	5'
9'- $\underline{C}OCH_3$		169.7			
9'- $CO\underline{CH_3}$	2.15, s	20.7	9'- $\underline{C}OCH_3$		
4'-OH	11.72, s		3a', 4', 5'		5'
10		169.5			
11	5.45, dd (*10.2, 5.6*)	62.8 br	1, 3, 13	12	12

12	3.20, m 3.42, dd (*14.3*, *5.5*)	35.0	10	11	11, 14, 18
13		136.7			
14	7.05, m	128.8	12, 16	15, 16, 18	12, 15
15	7.16, m	128.3	13, 17	14, 16, 17	14, 16
16	7.12, m	126.7	14, 18	14, 15, 17, 18	15, 17
17	7.16, m	128.3	13, 17	15, 16, 18	16, 18
18	7.05, m	128.8	12, 16	15, 16, 14	12, 17
10-OH	13.29, br s				

B. Figures

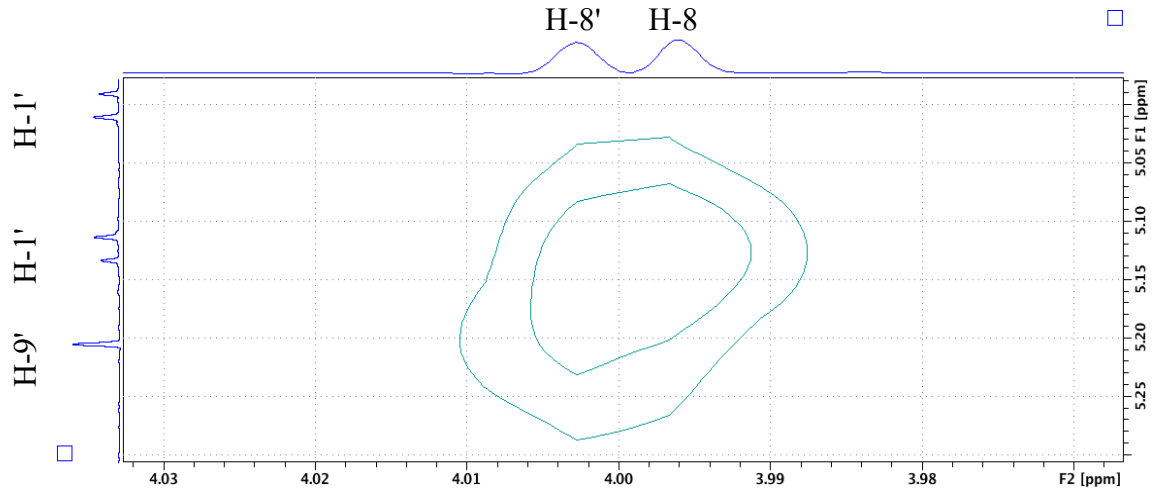

Figure S1: Figure showing observed ROESY correlations between H-8' and H-9'; H-8 and H-1' but more importantly absence of ROESY correlation between H-8 and H-9' in duclauxin (**1**) suggesting *S*-configuration at C-9'

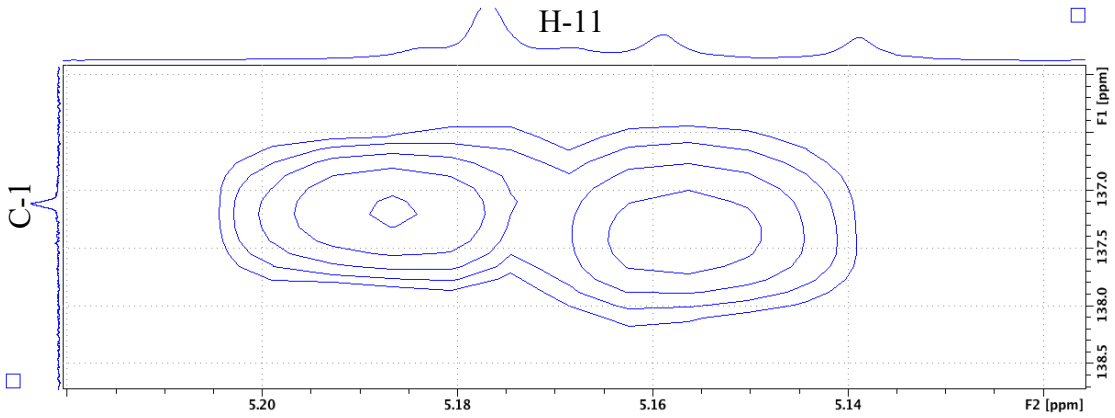

(a)

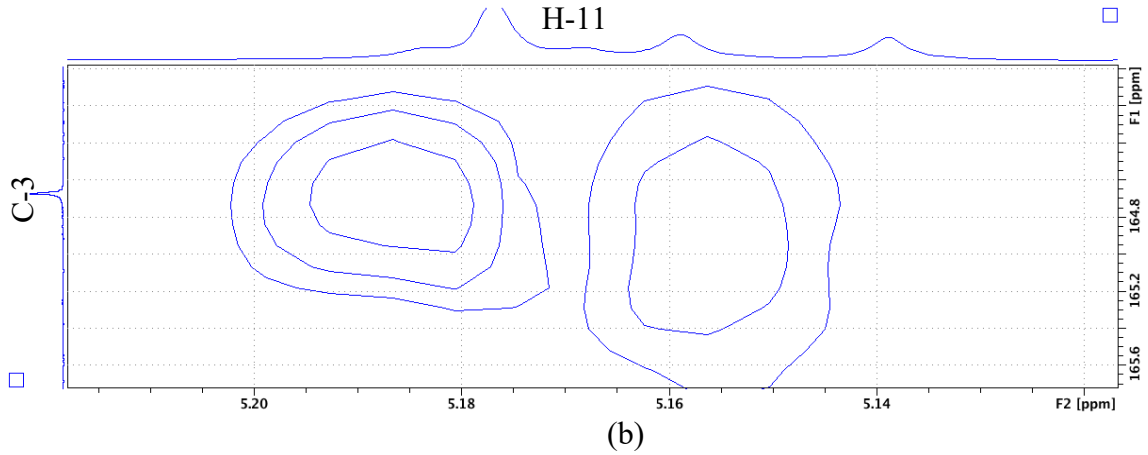

Figure S2 (a): HMBC correlation from H-11 doublet of doublet proton to (a) C-1 and (b) C-3 in talauxin E (**2**)

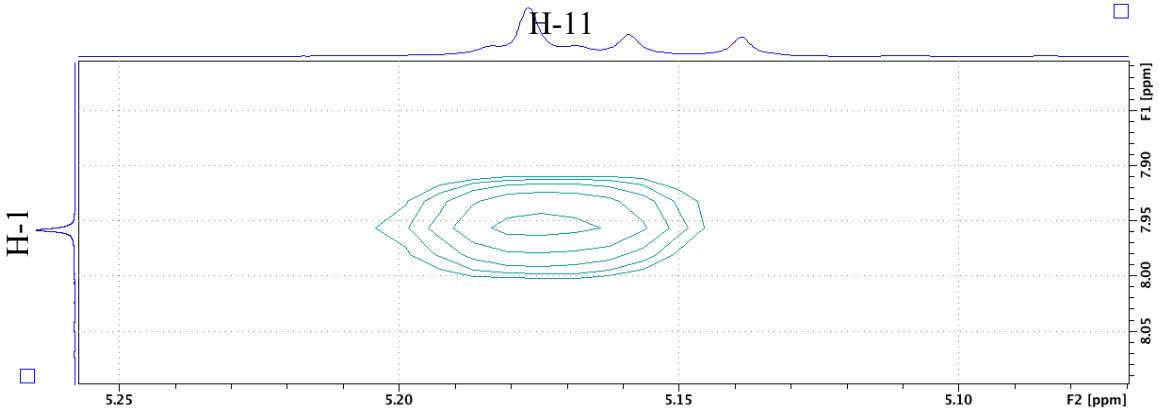

Figure S2 (b): ROESY correlation between H-1 singlet proton and H-11 doublet of doublet proton in talauxin E (**2**)

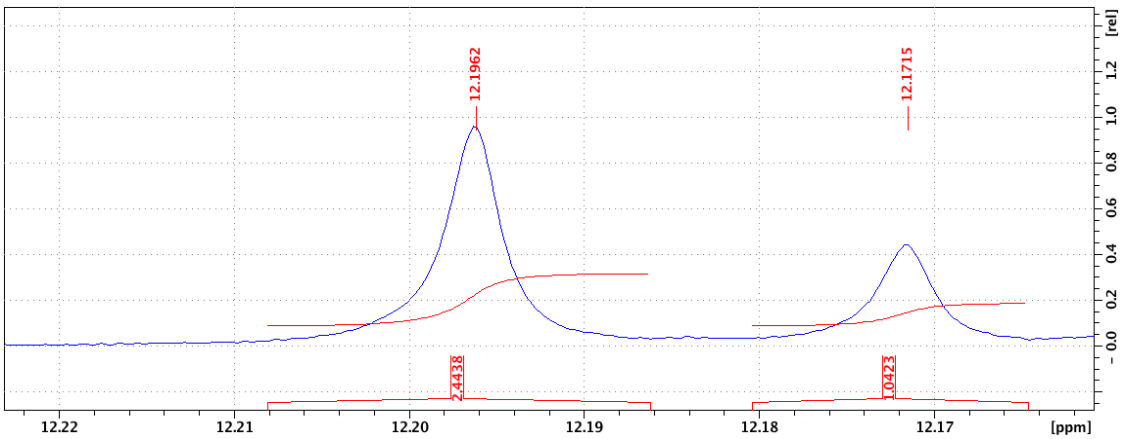

Figure S3: Expansion of the ^{1}H NMR spectrum of talauxin L/I (**5/6**) showing the 4-OH ratio of the two isomers as 2.3:1 in DMSO-d_6

Semisynthetic talauxins

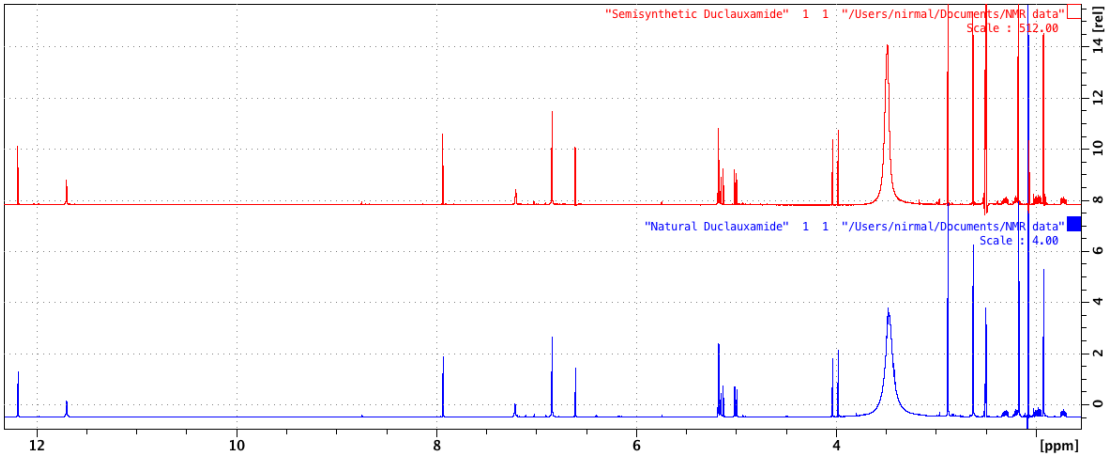

Figure S4: NMR comparison of the natural talauxin Q and the semisynthetic talauxin Q prepared by reacting duclauxin with L-glutamine

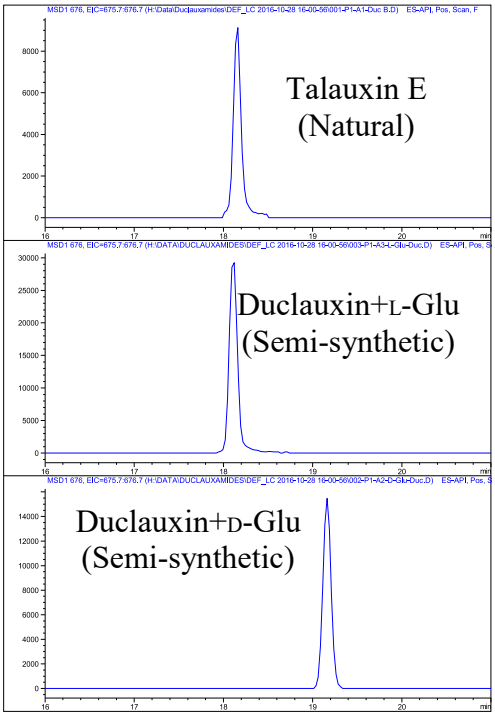

(a)

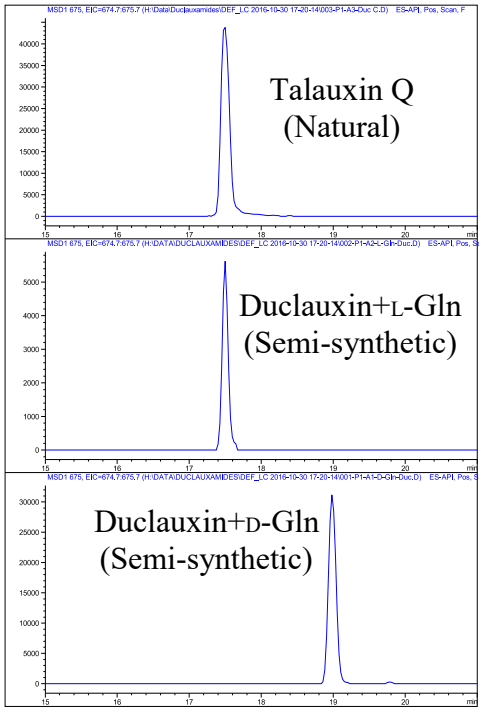

(b)

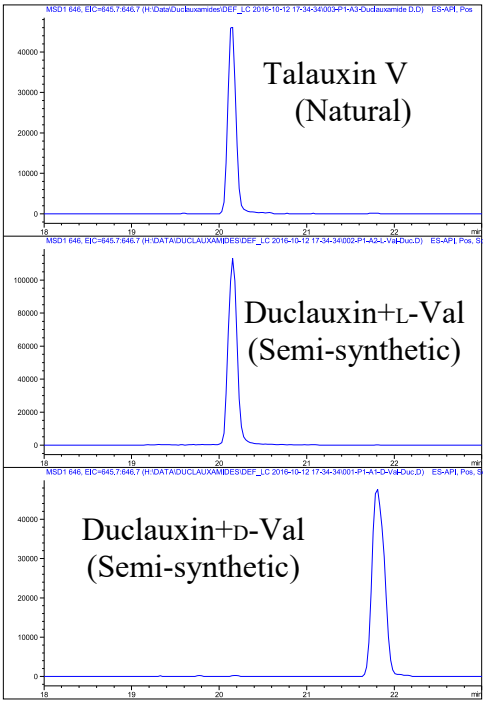

(c)

Figure S5: Figure showing a comparison of the retention time of the natural talauxins (top) with their semi-synthetic counterparts obtained from reaction of duclauxin with the corresponding L-amino acids (middle) and D-amino acids (bottom); (a) glutamic acid (b) glutamine (c) valine

C. ^{1}H (600 MHz) and ^{13}C NMR (150 MHz) NMR spectra

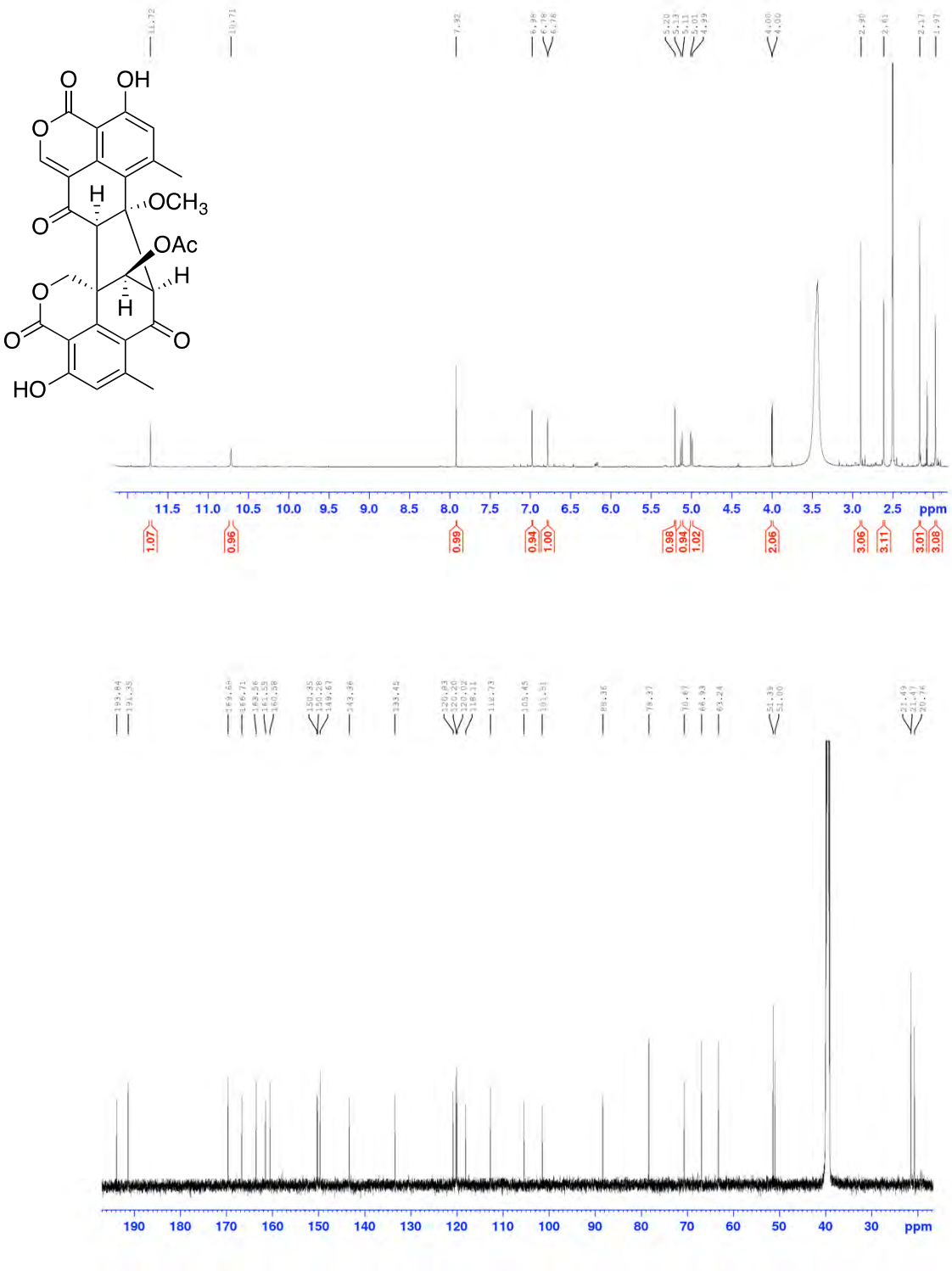

Figure S6: ^{1}H and ^{13}C NMR spectra of duclauxin (**1**) in DMSO-d_6

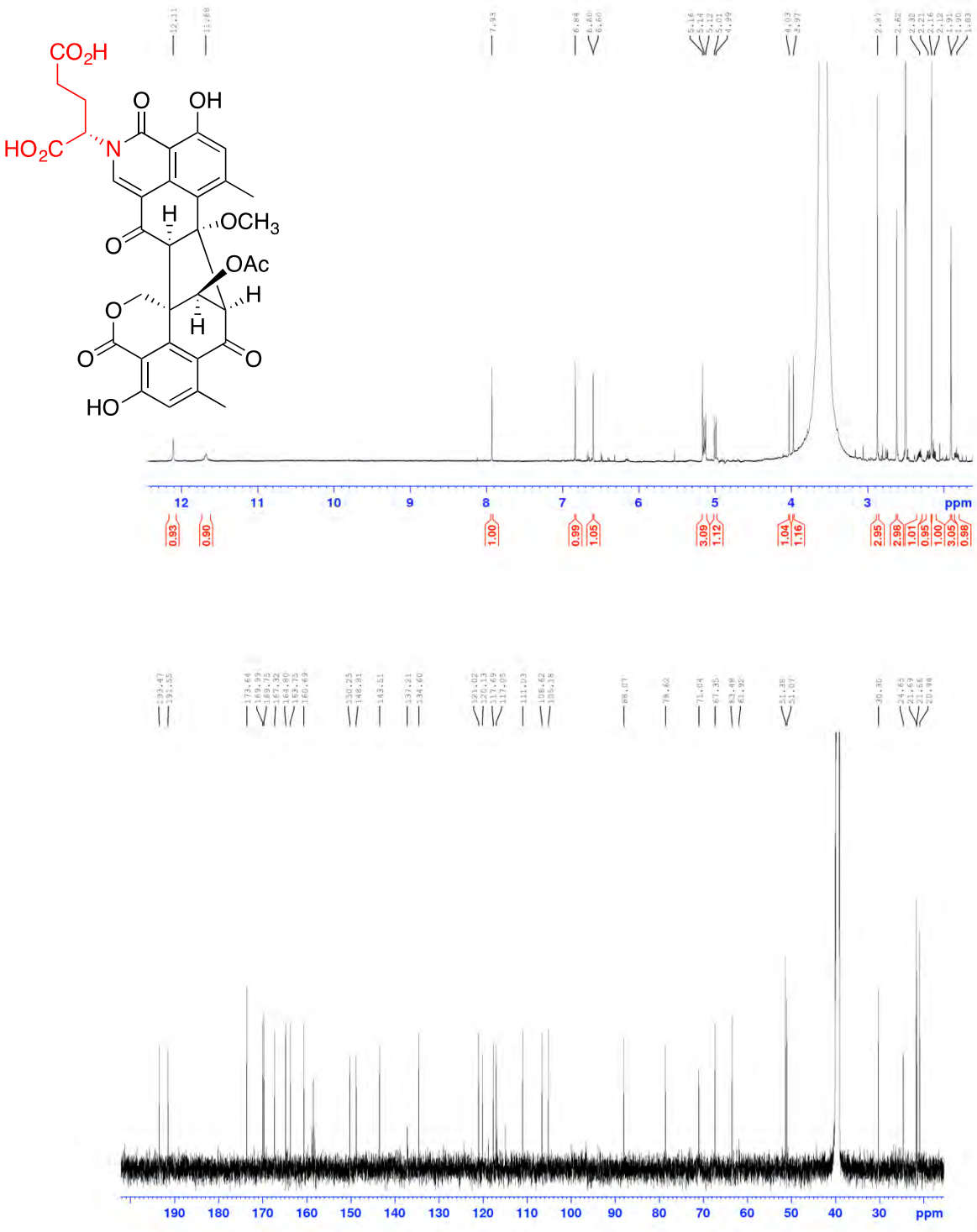

Figure S7: ^{1}H and ^{13}C NMR spectra of talauxin E (**2**) in DMSO-*d*$_6$

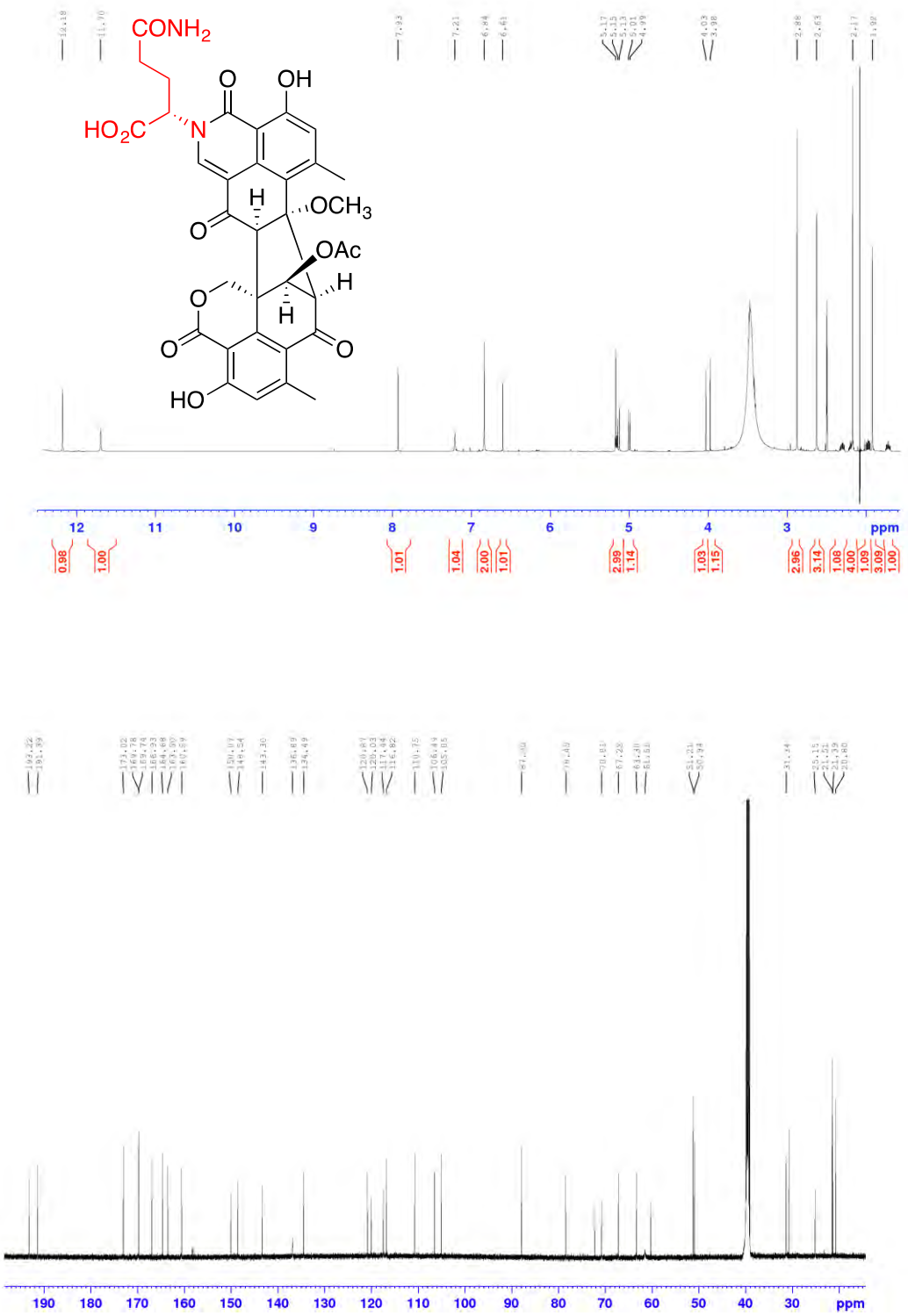

Figure S8: ^{1}H and ^{13}C NMR spectra of talauxin Q (**3**) in DMSO-d_6

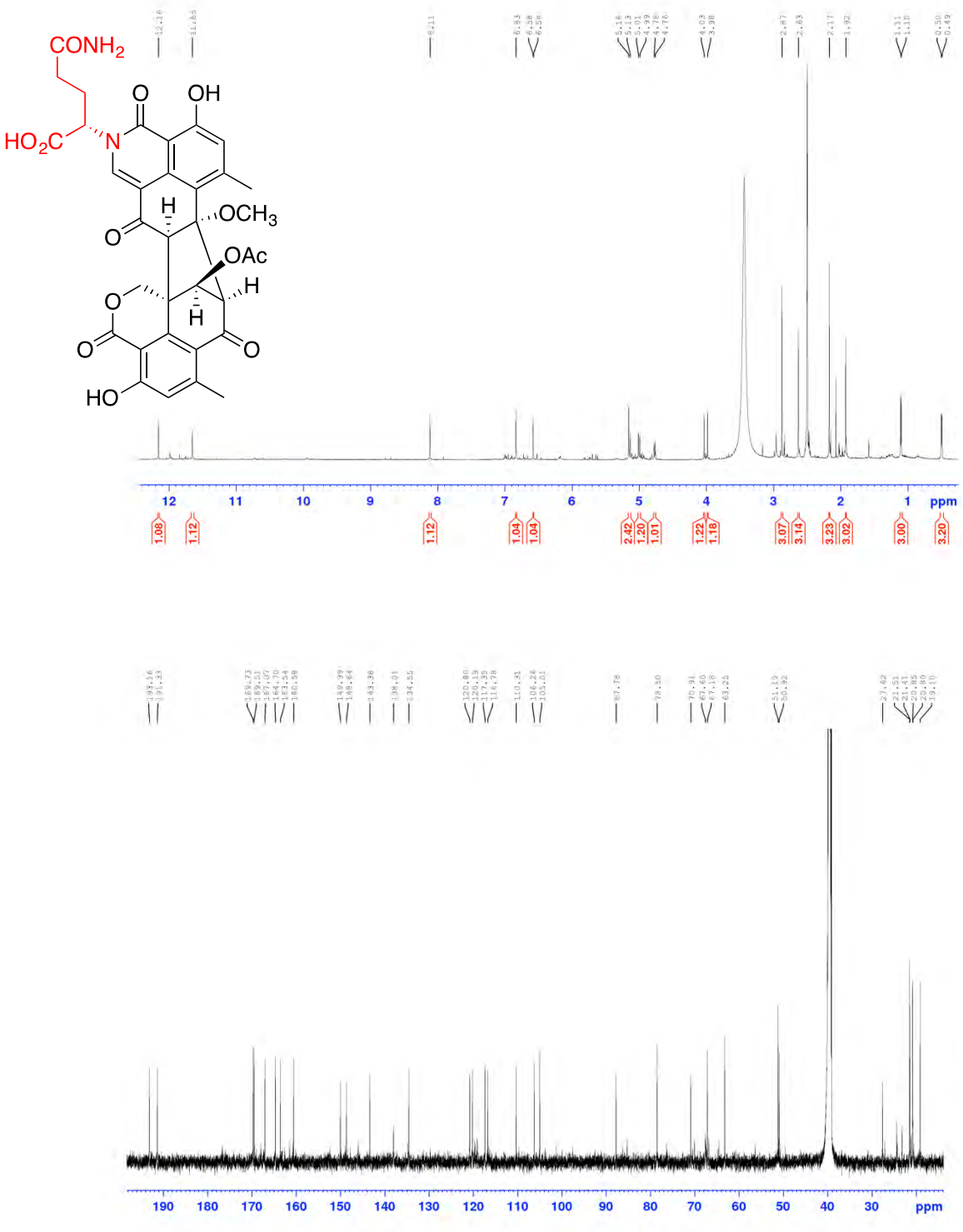

Figure S9: ^{1}H and ^{13}C NMR spectra of talauxin V (**4**) in DMSO-d_6

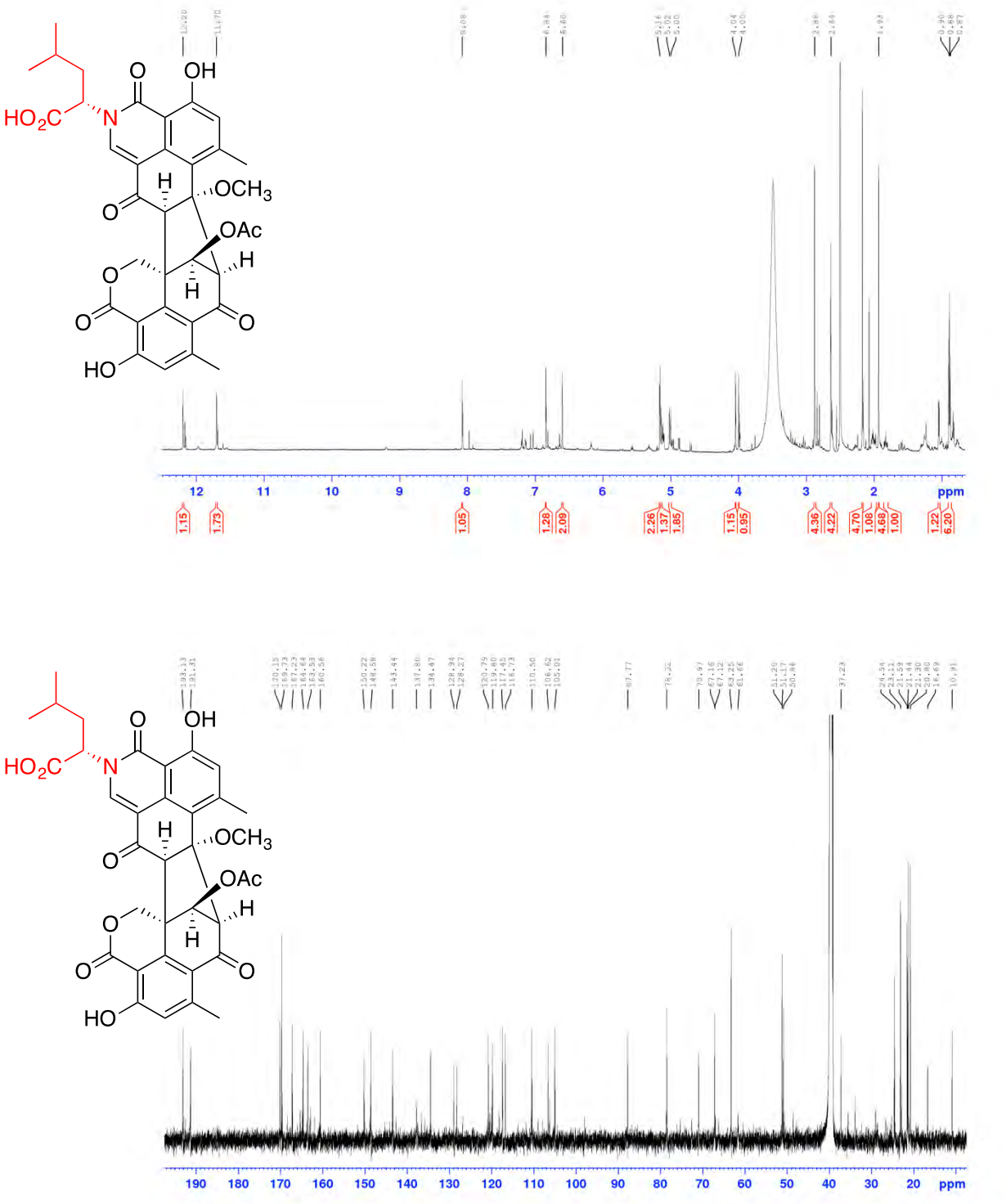

Figure S10: ^{1}H and ^{13}C NMR spectra of inseparable talauxin L and I (**5/6**) mixture in DMSO-d_6

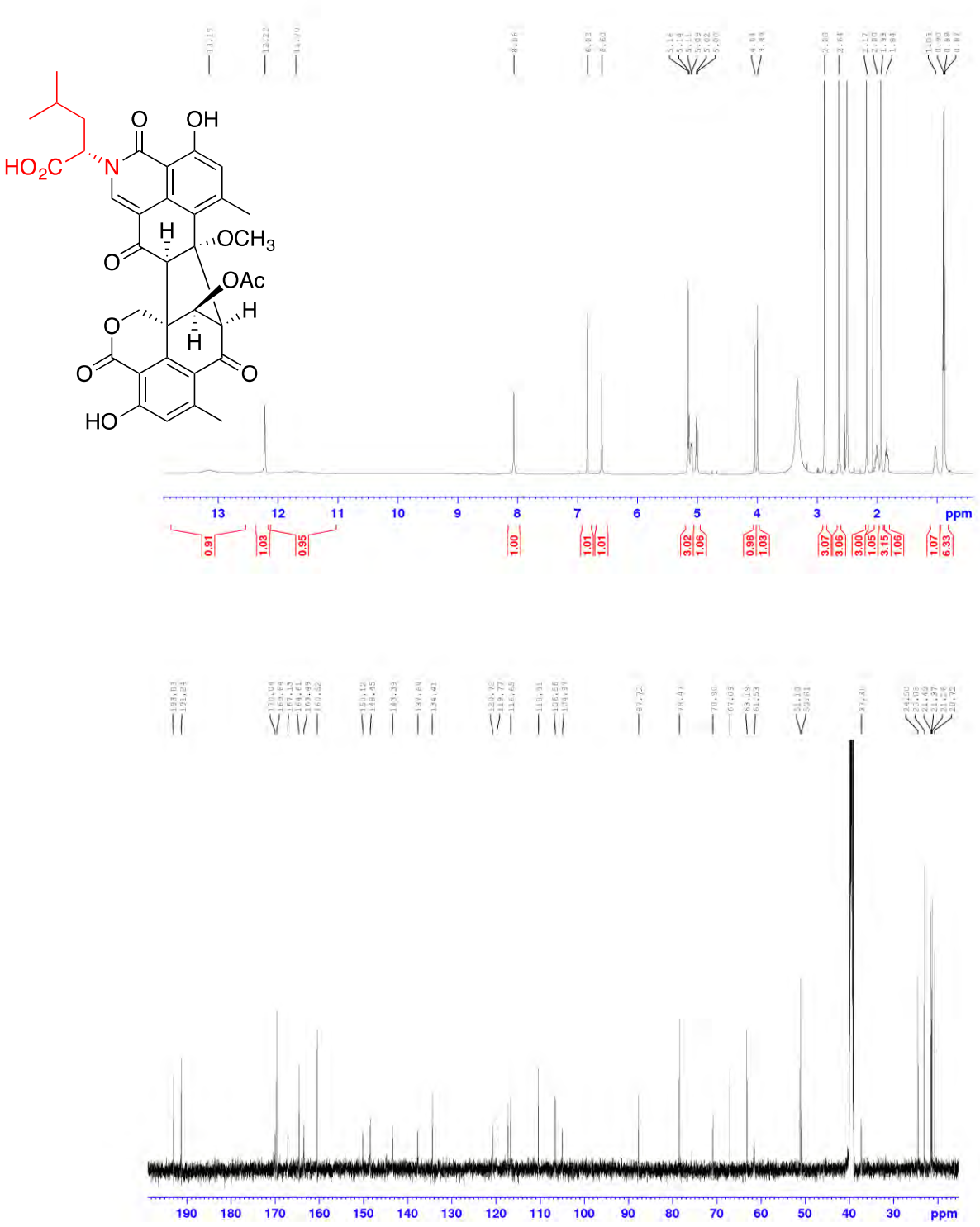

Figure S11: ^{1}H and ^{13}C NMR spectra of talauxin L (**5**) in DMSO-d_6

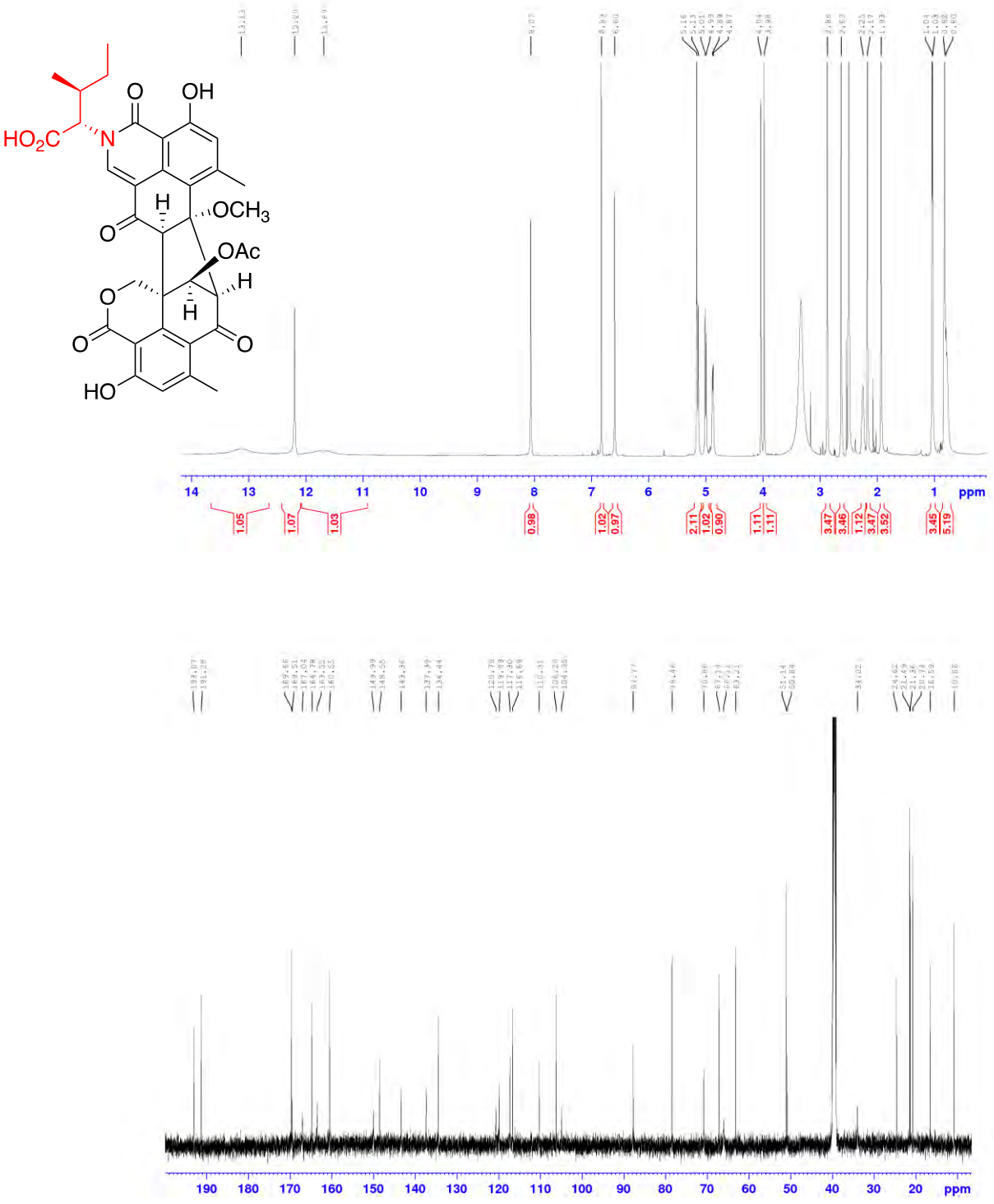

Figure S12: ^{1}H and ^{13}C NMR spectra of talauxin I (**6**) in DMSO-d_6

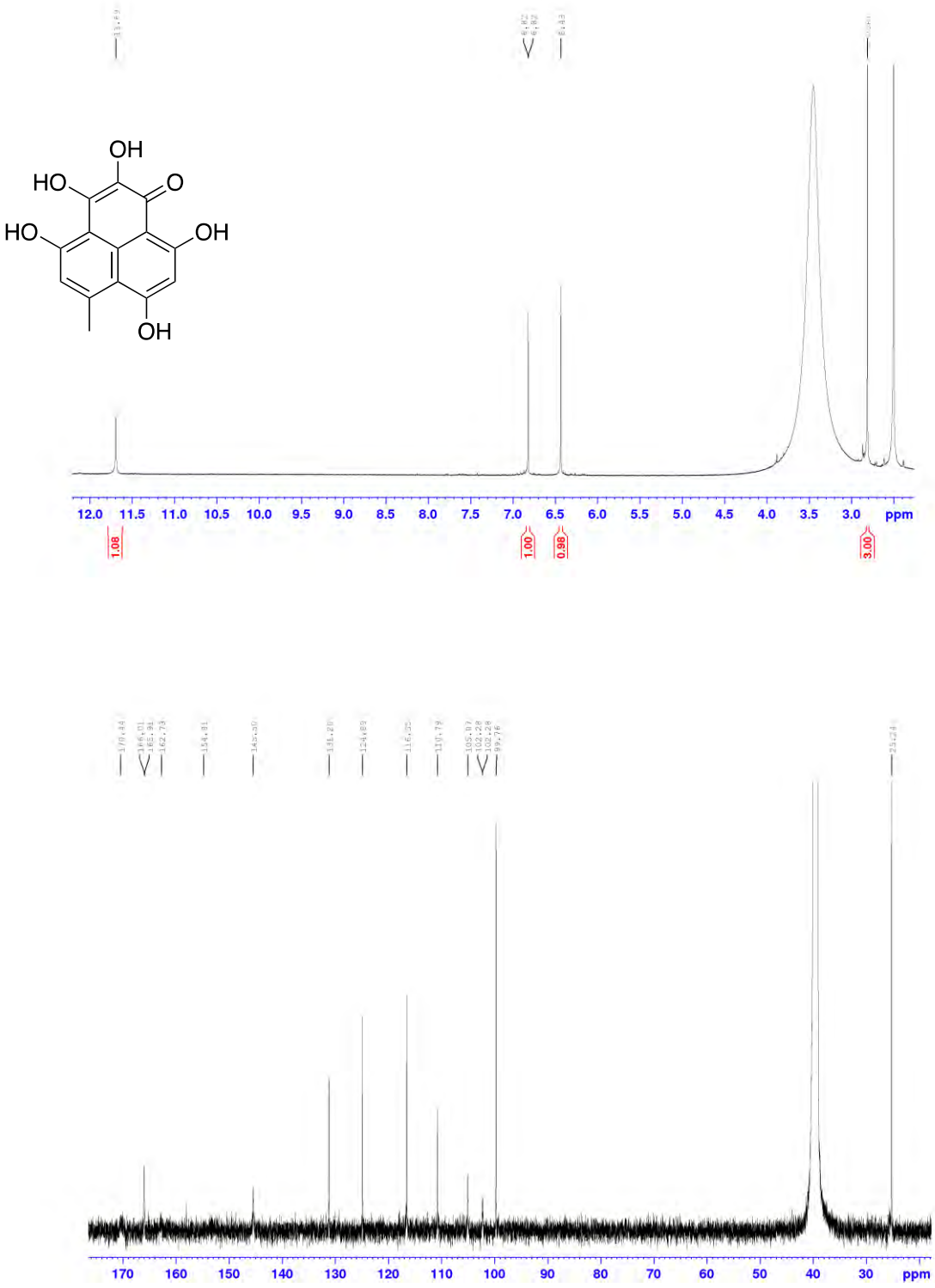

Figure S13: ^{1}H and ^{13}C NMR spectra of *O*-desmethylfunalenone (**7**) in DMSO-d_6

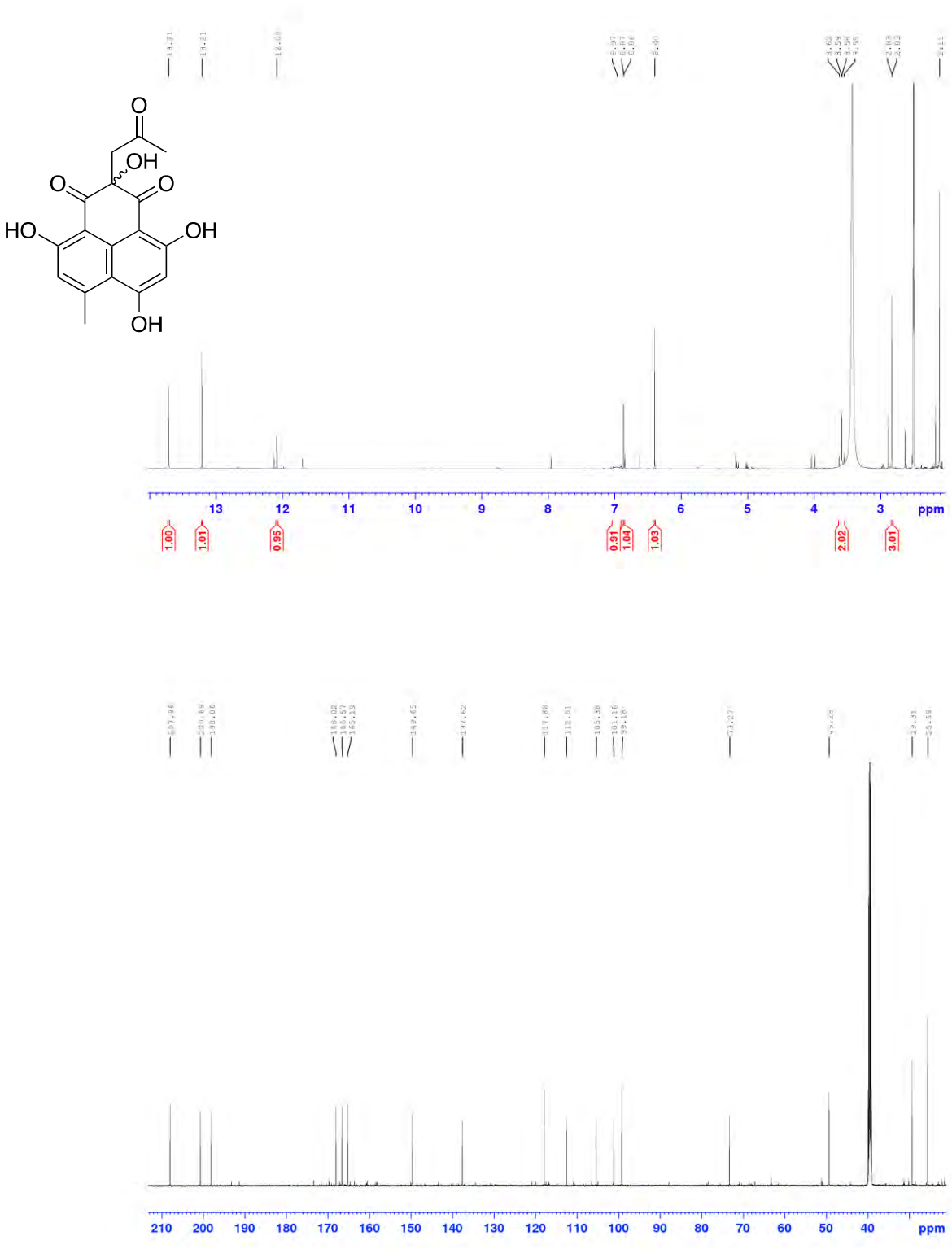

Figure S14: ^{1}H and ^{13}C NMR spectra of 9-demethyl FR 901235 (**8**) in DMSO-d_6

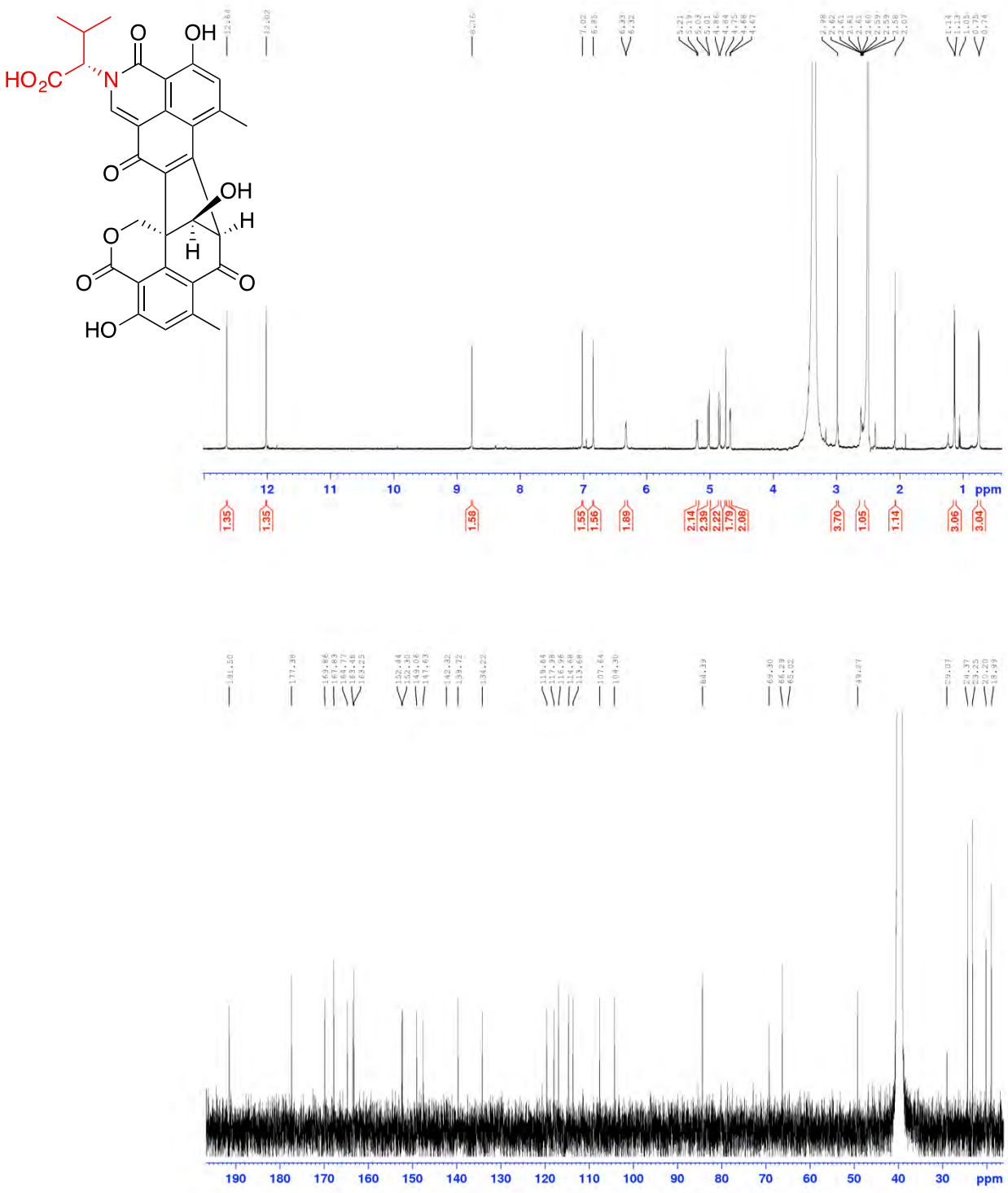

Figure S15: ^{1}H and ^{13}C NMR spectra of desacetyldesmethyltalauxin V (**9**) in DMSO-d_6

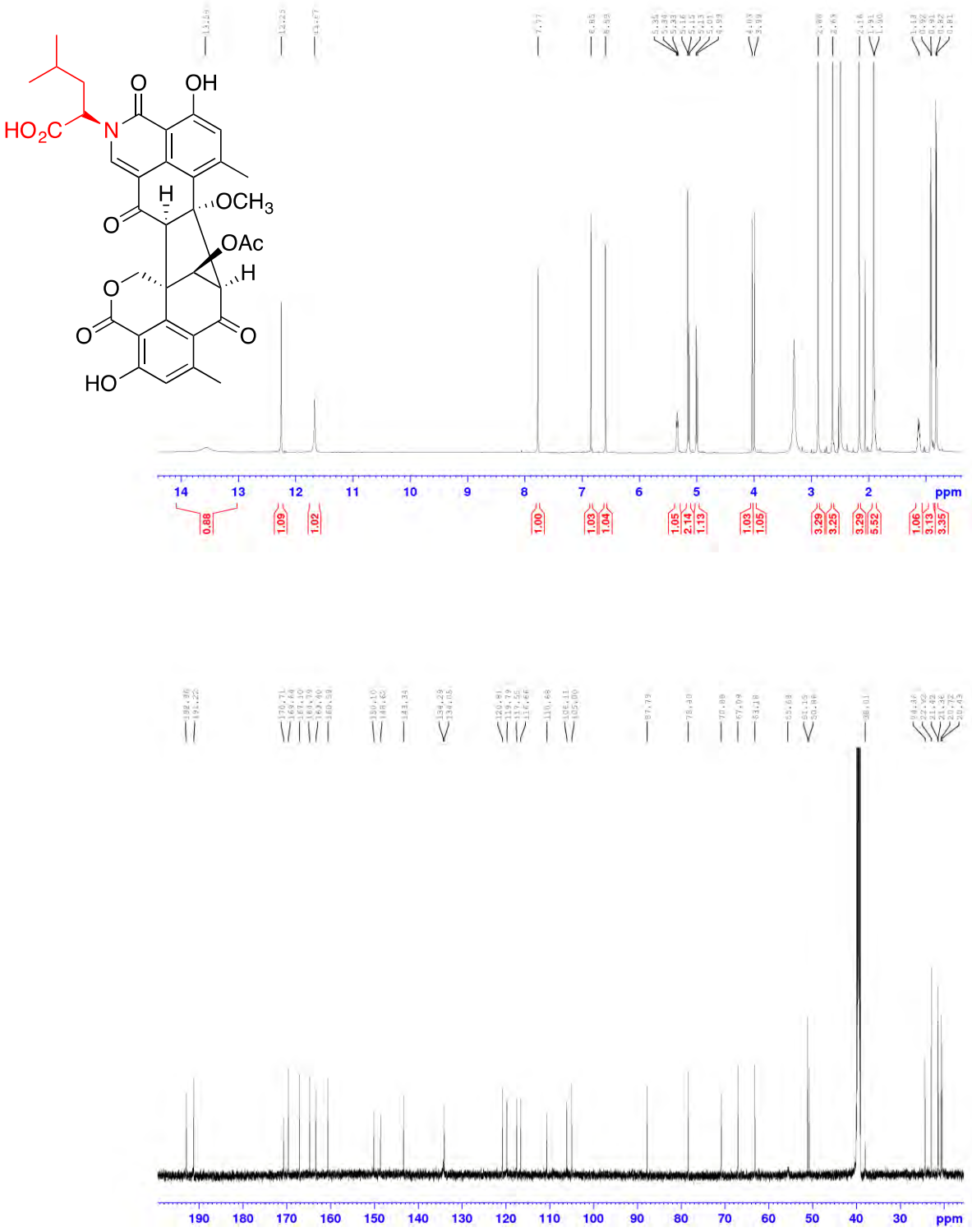

Figure S16: ^{1}H and ^{13}C NMR spectra of epitalauxin L (**10**) in DMSO-d_6

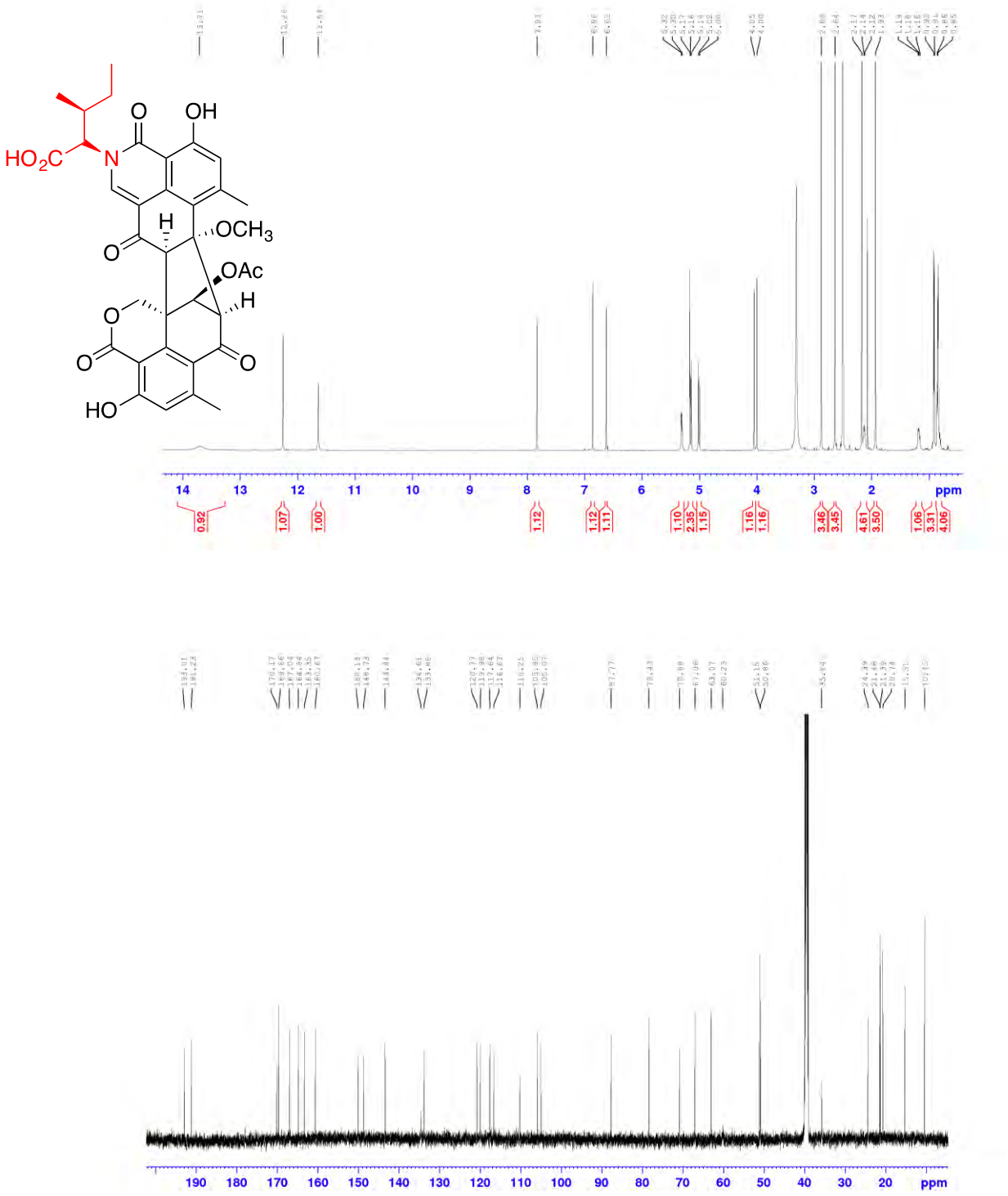

Figure S17: ^{1}H and ^{13}C NMR spectra of epitalauxin I (**11**) in DMSO-d_6

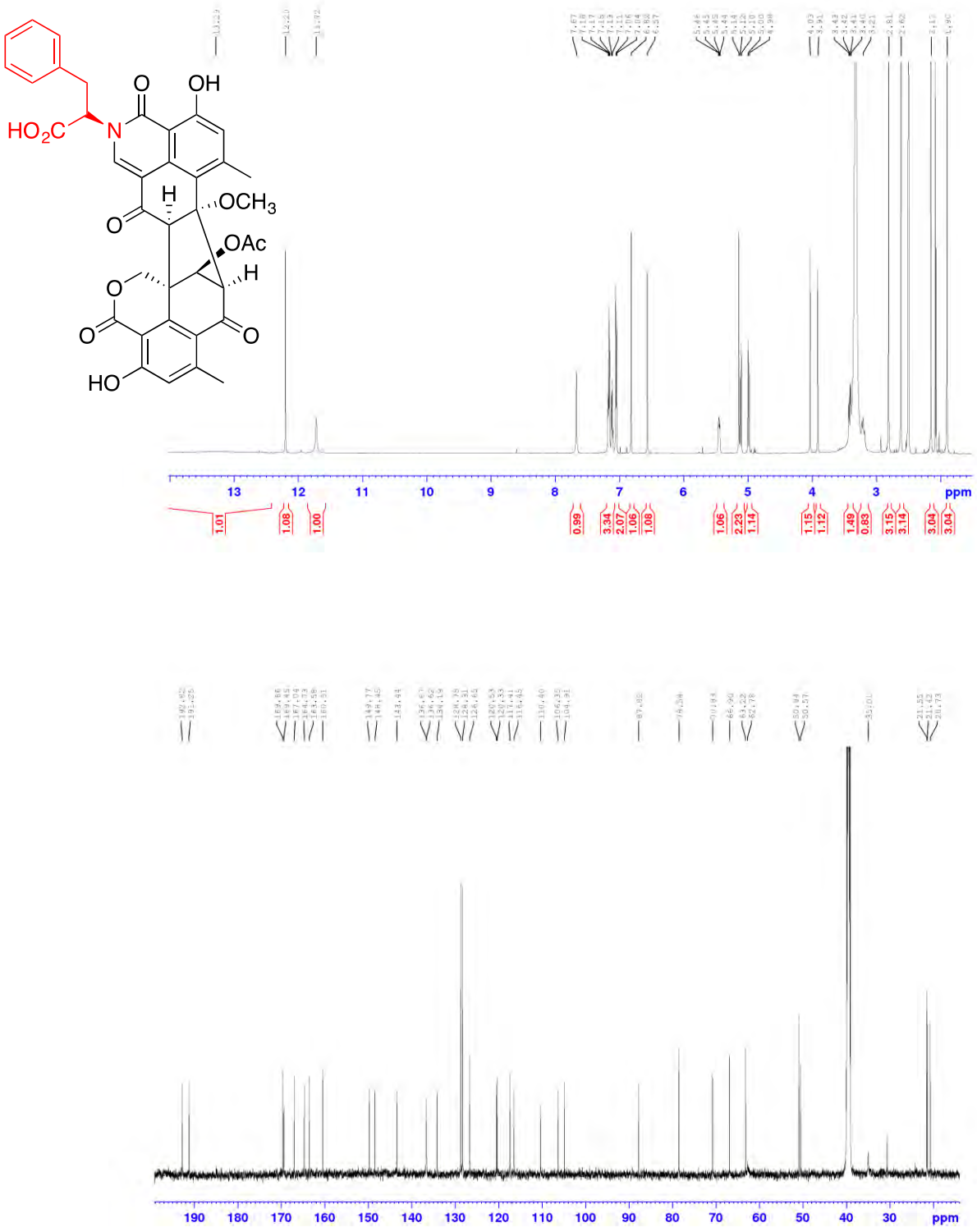

Figure S18: ^{1}H and ^{13}C NMR spectra of epitalauxin F (**12**) in DMSO-d_6

D. UV-visible spectra

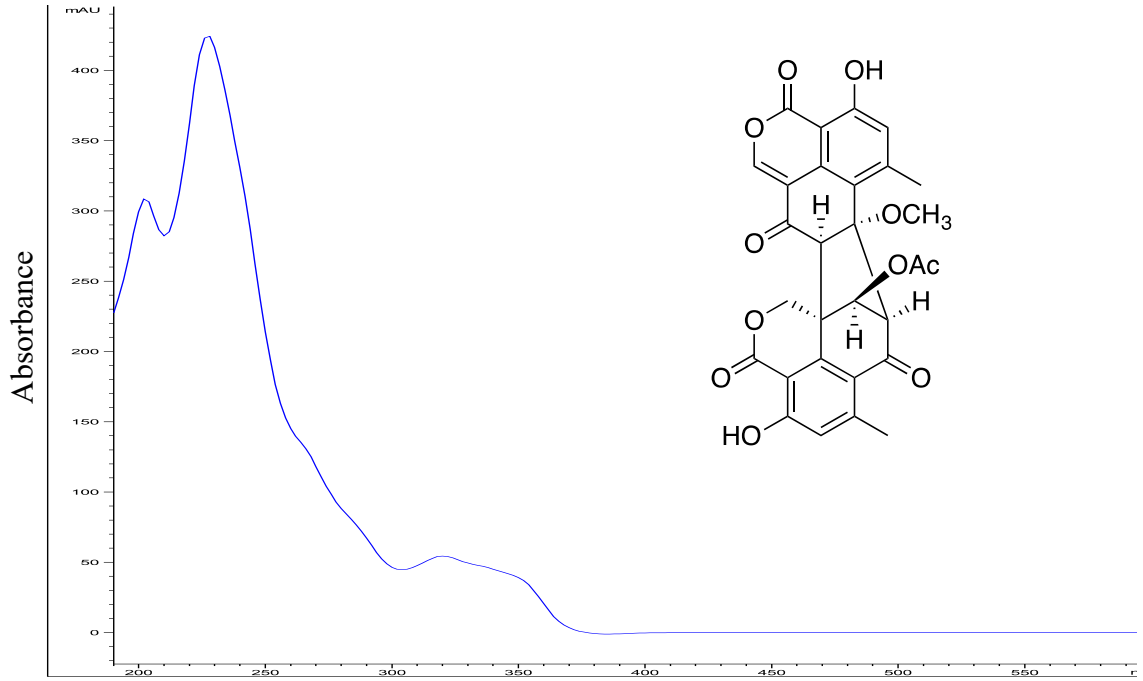

Figure S19: UV-visible spectrum of duclauxin (**1**)

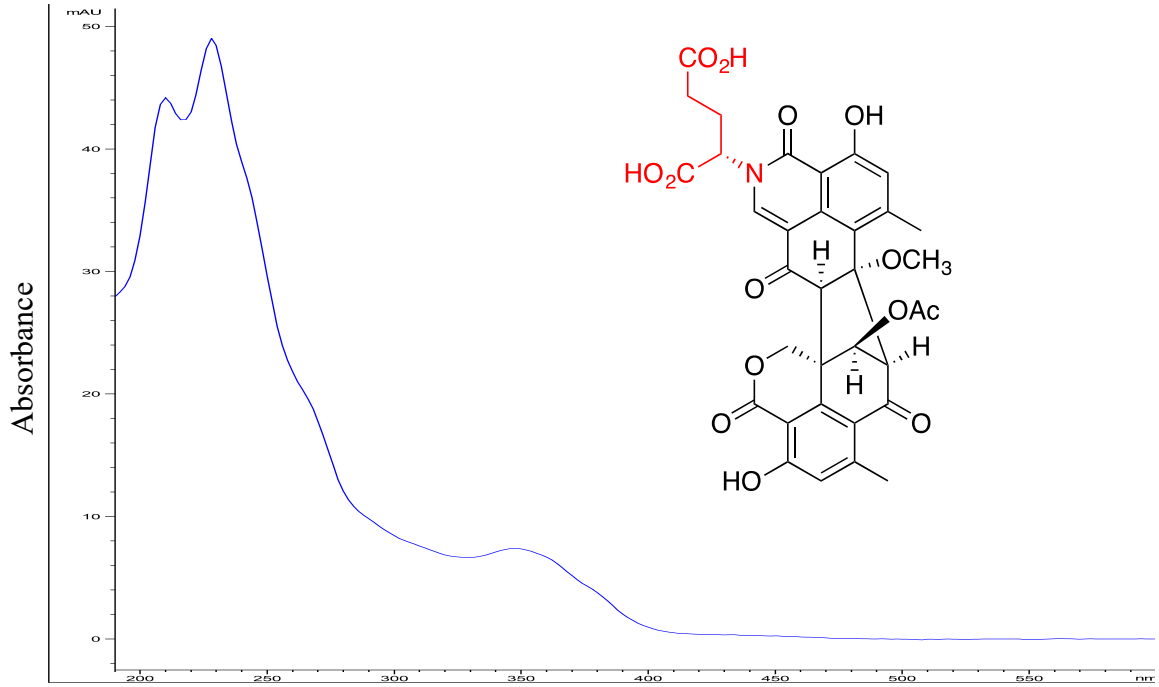

Figure S20: UV-visible spectrum of talauxin E (**2**)

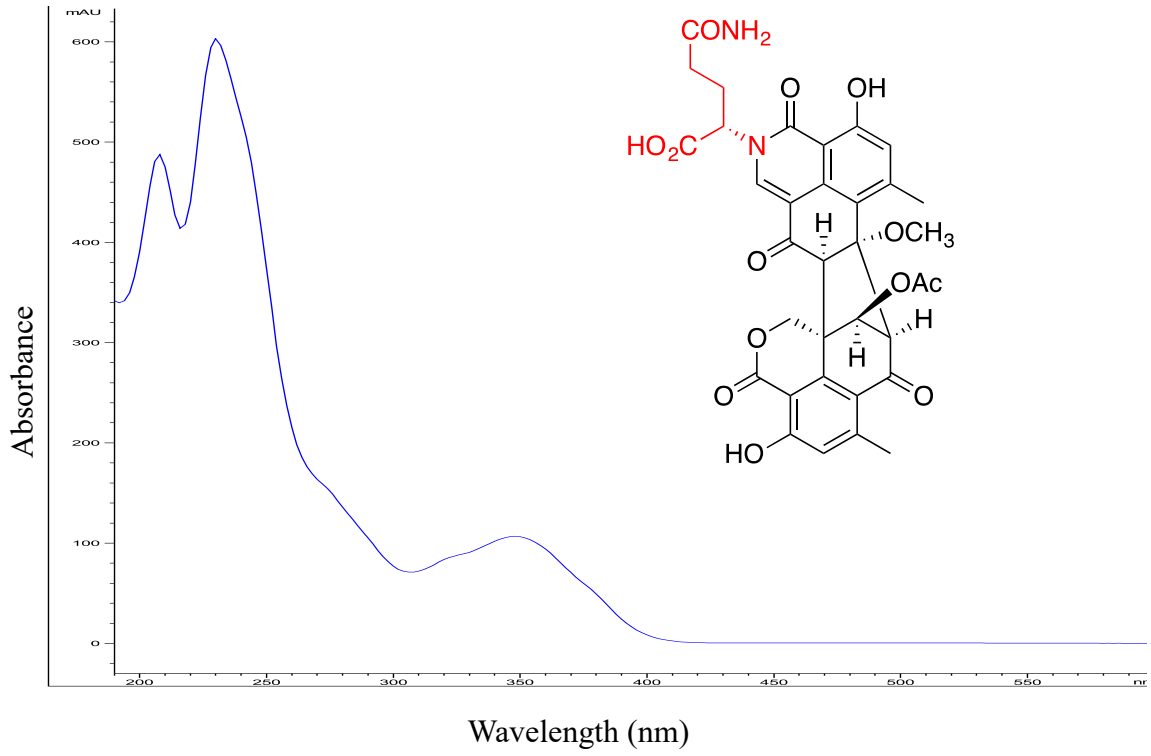

Figure S21: UV-visible spectrum of talauxin Q (**3**)

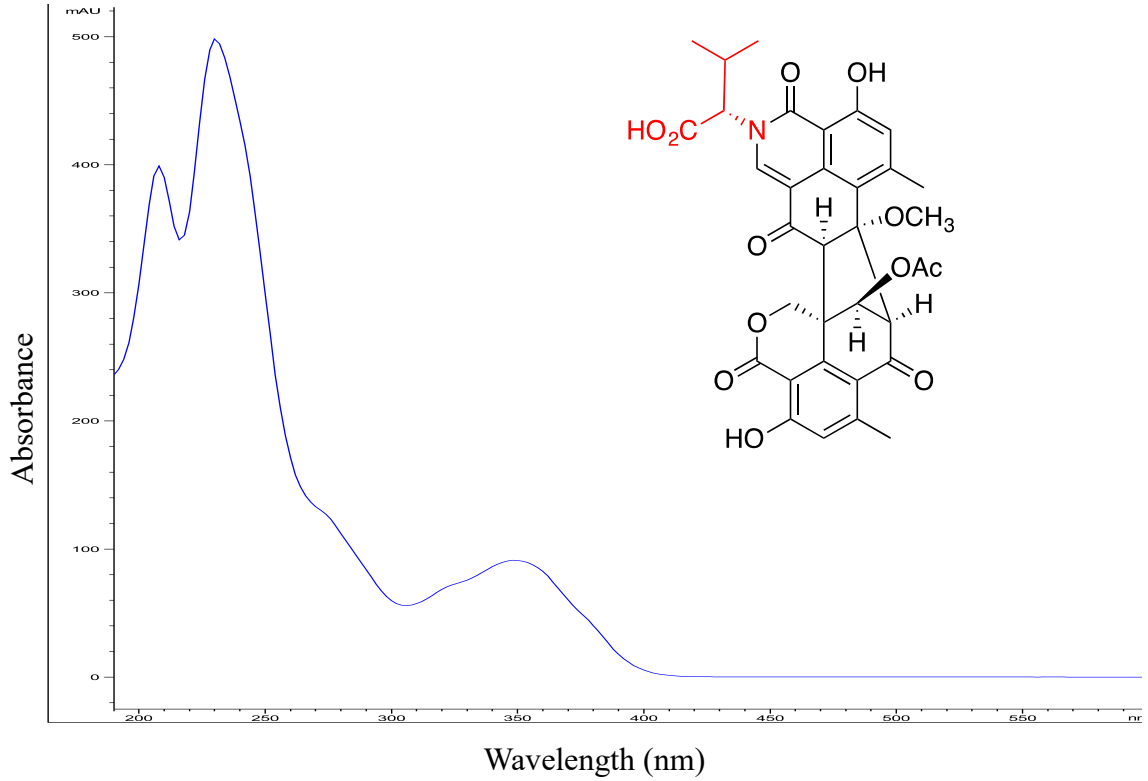

Figure S22: UV-visible spectrum of talauxin V (**4**)

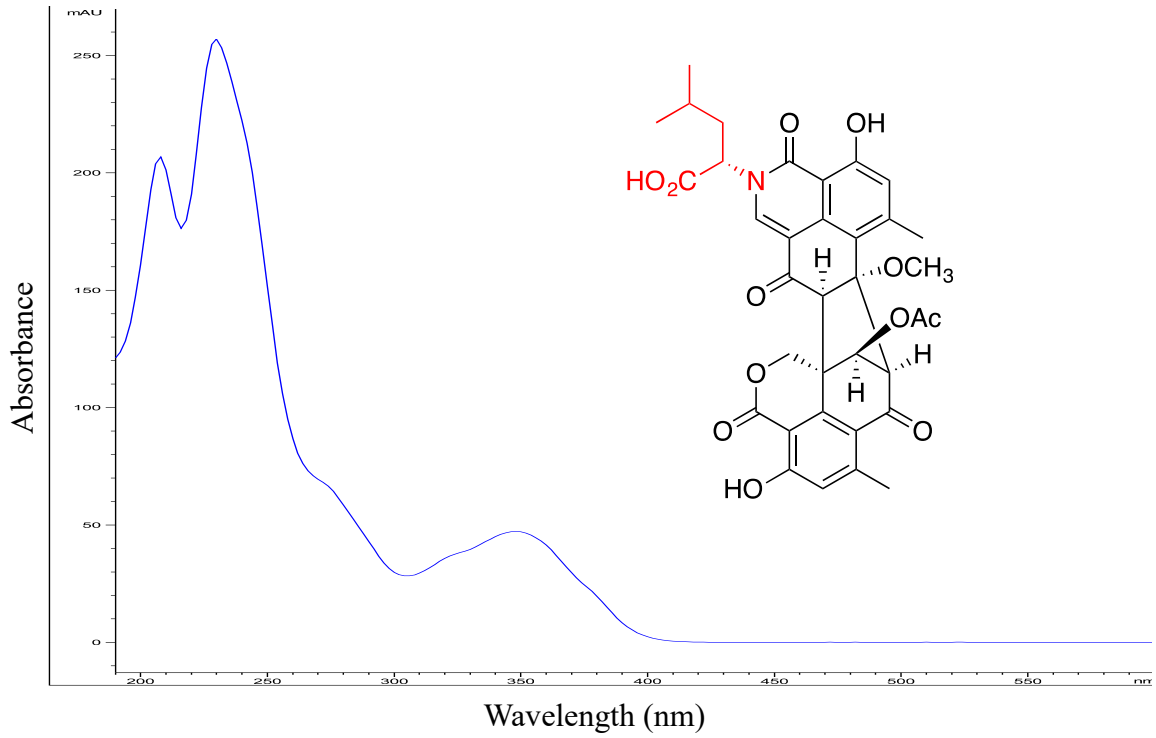

Figure S23: UV-visible spectrum of talauxin L (**5**)

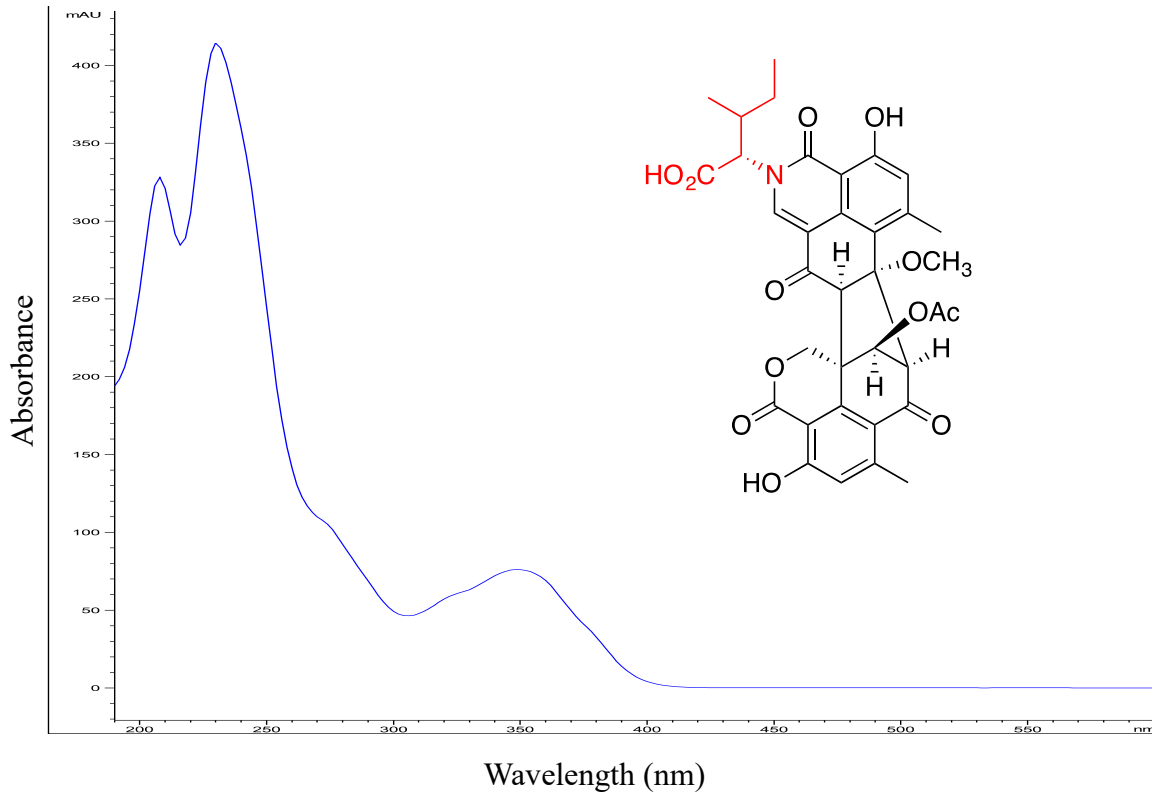

Figure S24: UV-visible spectrum of talauxin I (**6**)

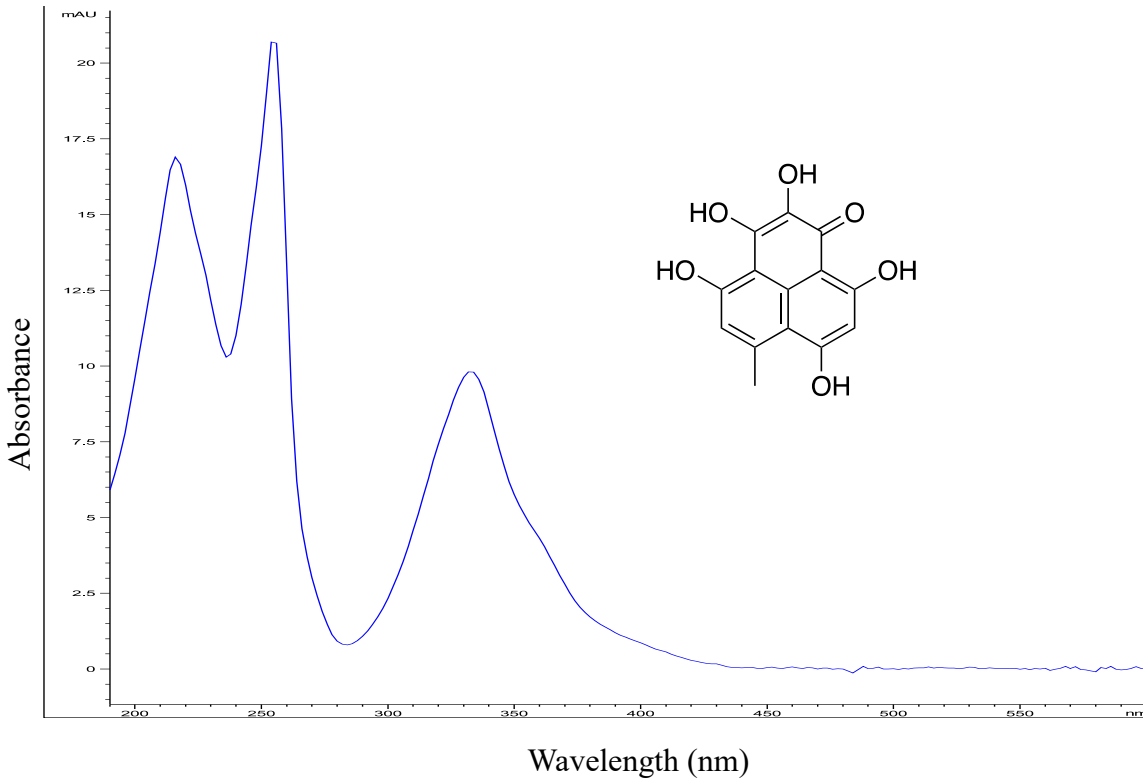

Figure S25: UV-visible spectrum of *O*-desmethylfunalenone (**7**)

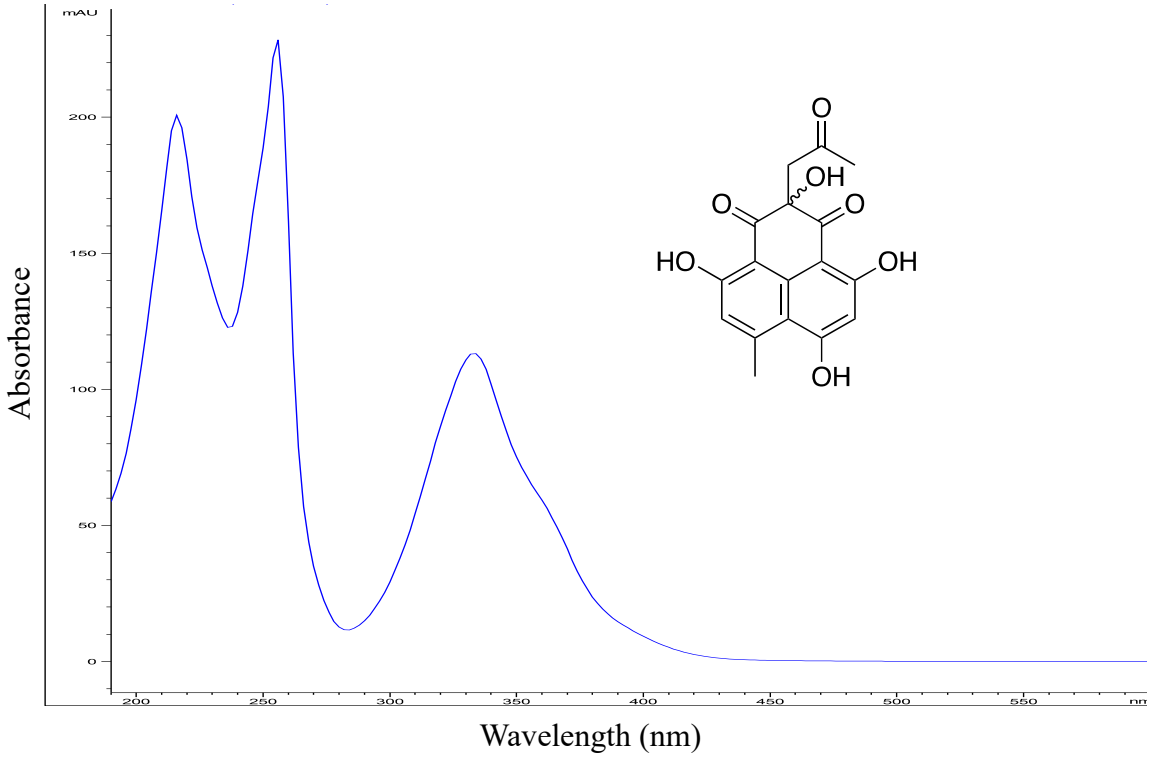

Figure S26: UV-visible spectrum of *O*-desmethylfunalenone (**8**)

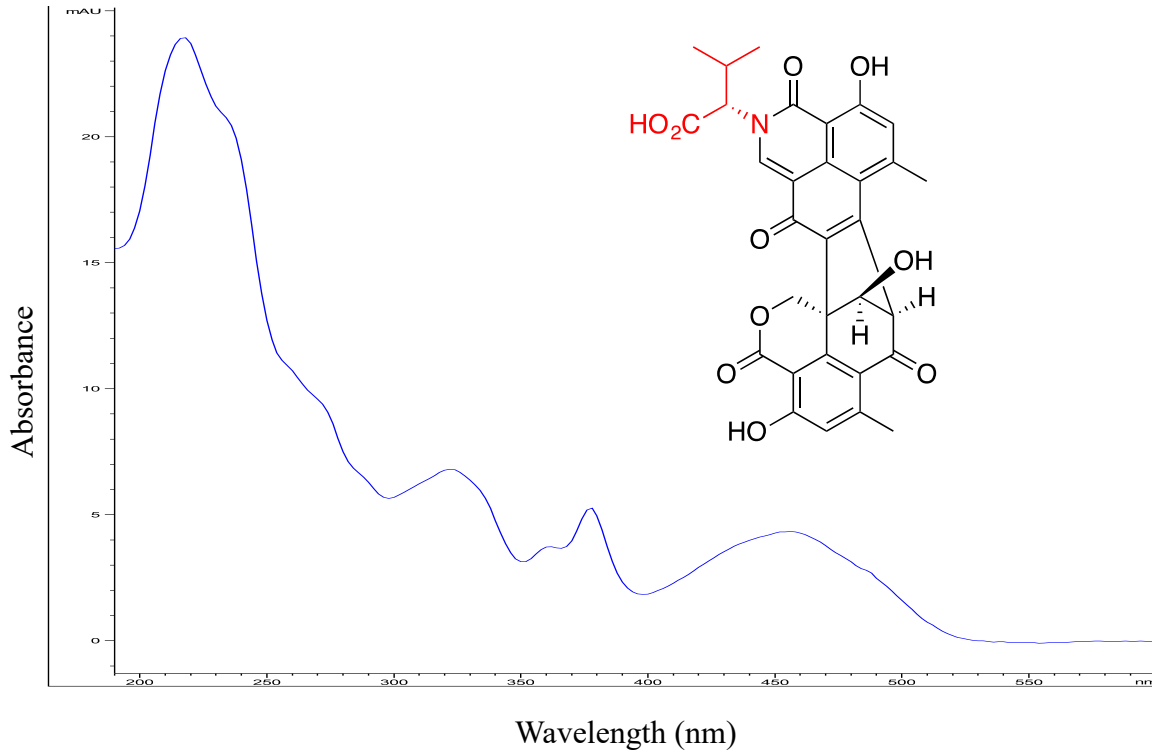

Figure S27: UV-visible spectrum of desacetyldesmethyltalauxin (**9**)

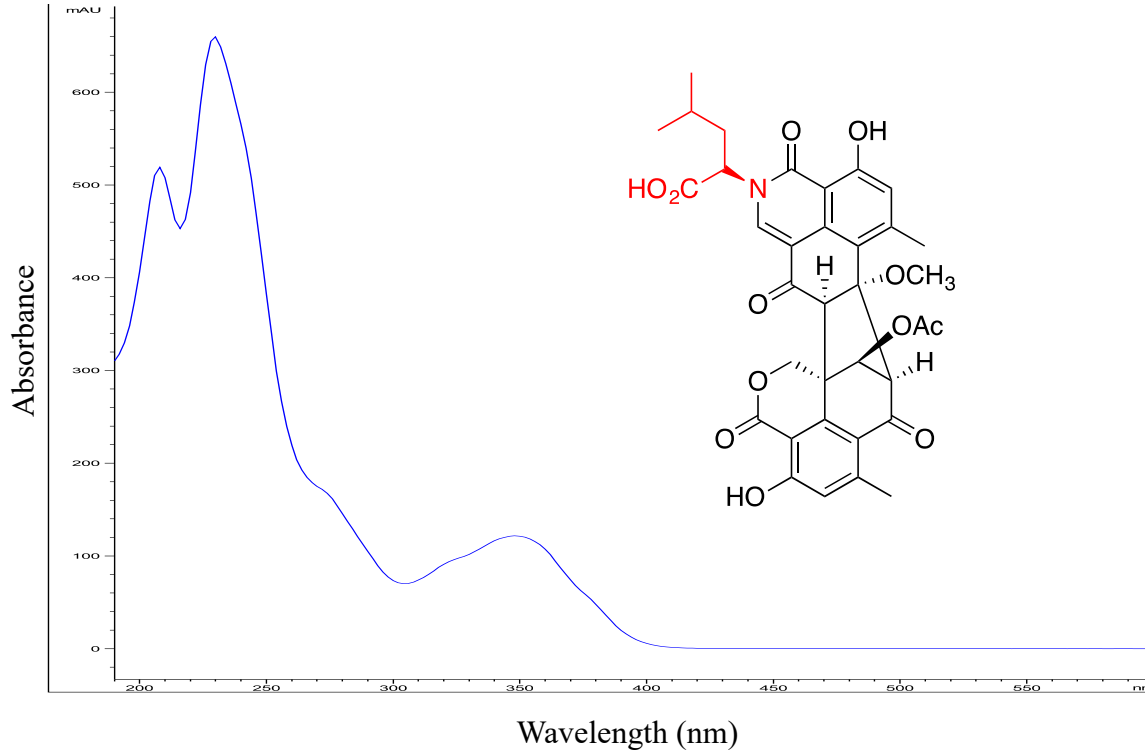

Figure S28: UV-visible spectrum of epitalauxin L (**10**)

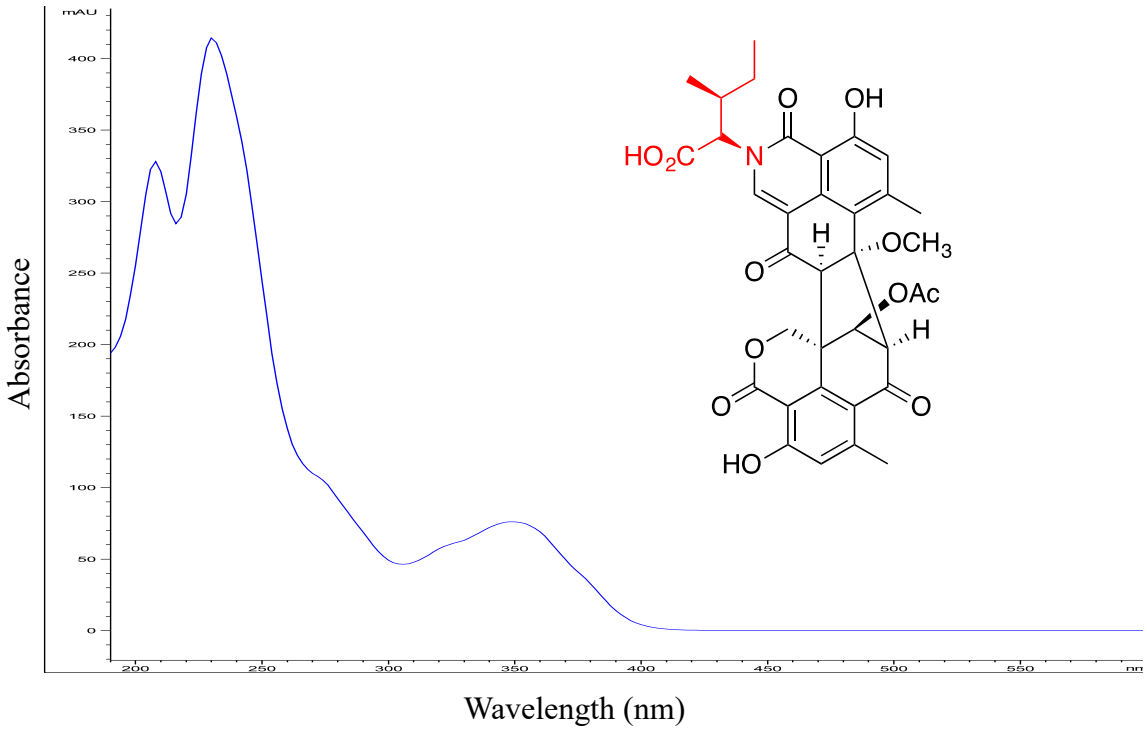

Figure S29: UV-visible spectrum of epitalauxin I (**11**)

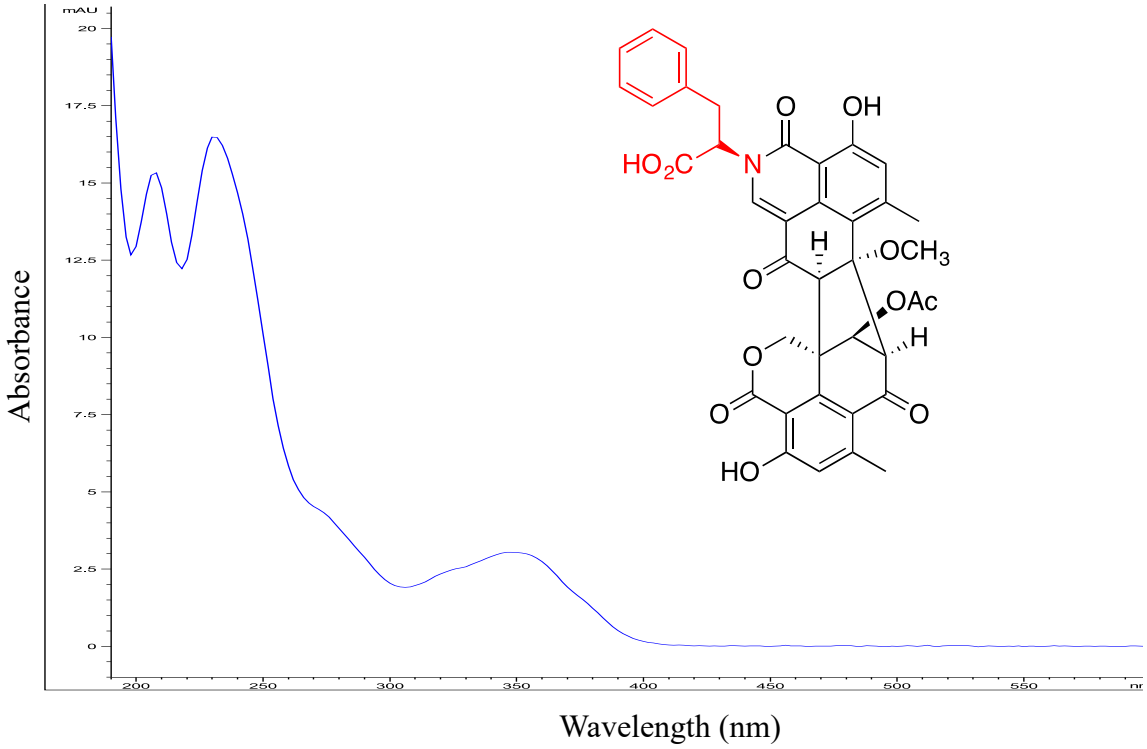

Figure S30: UV-visible spectrum of epitalauxin F (**12**)

E. ECD spectra

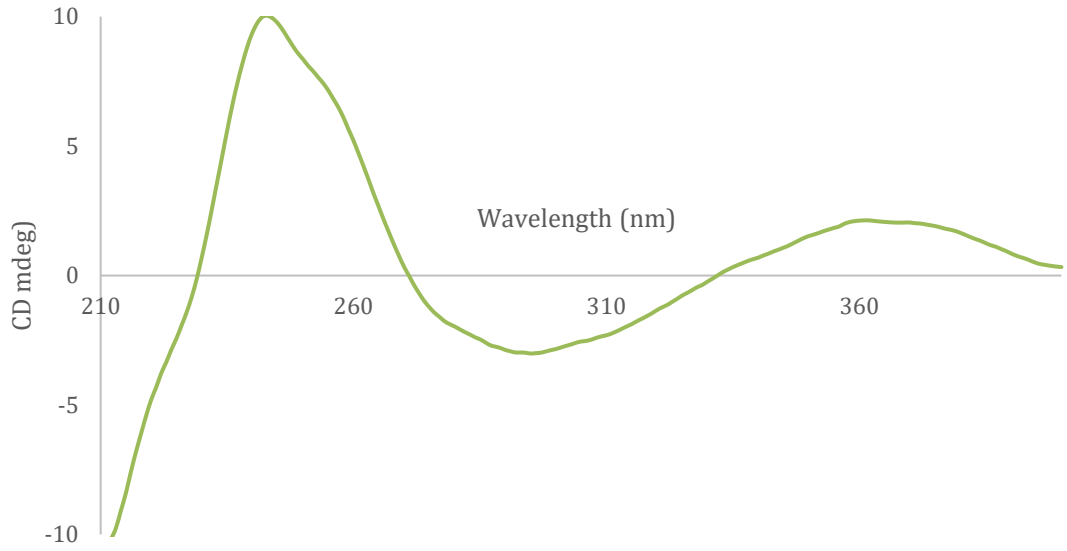

Figure S31: ECD spectrum of duclauxin (**1**) in MeOH

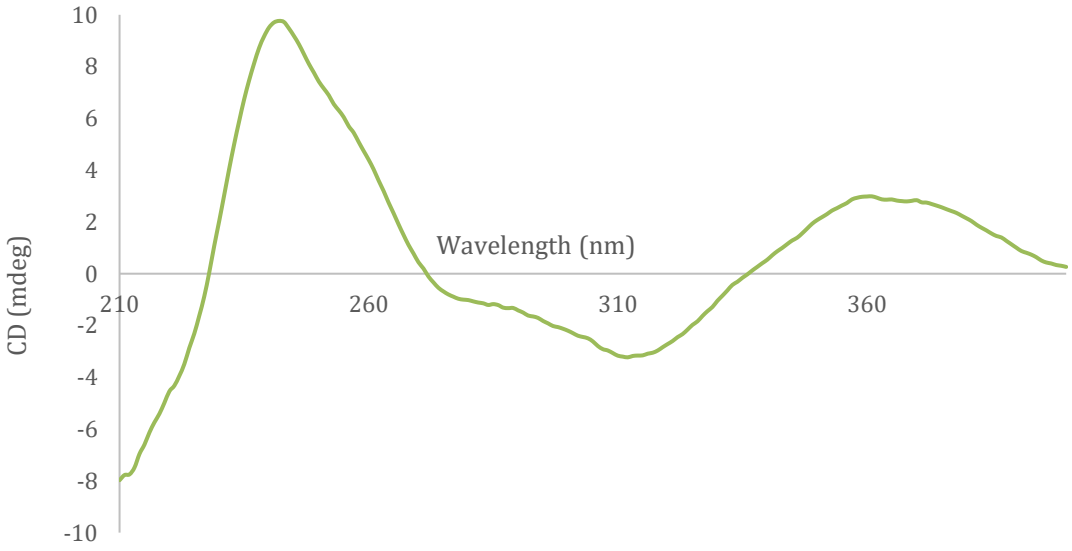

Figure S32: ECD spectrum of talauxin E (**2**) in MeOH

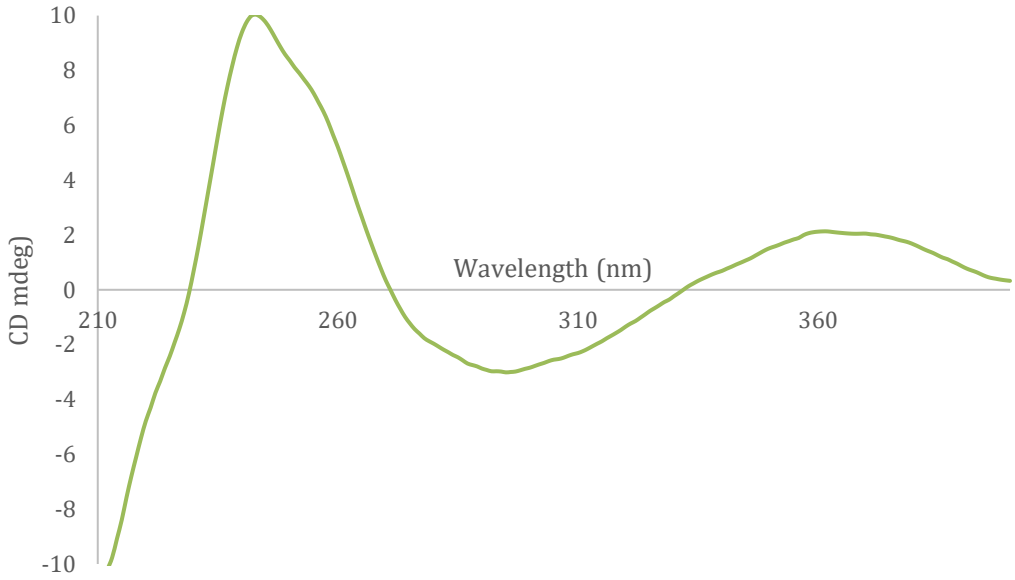

Figure S33: ECD spectrum of talauxin Q (**3**) in MeOH

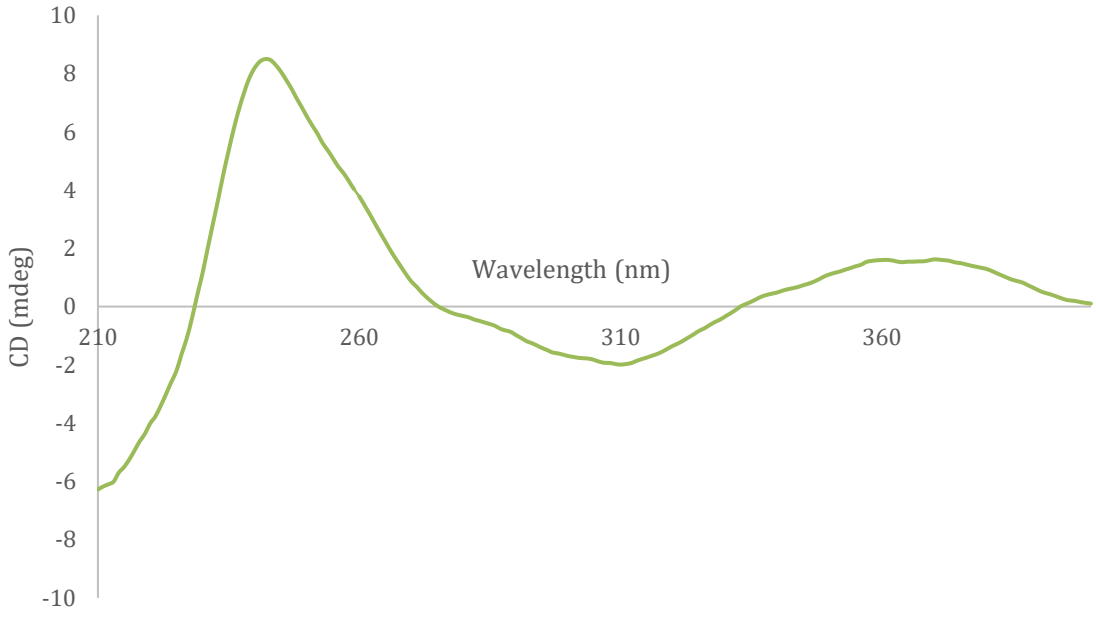

Figure S34: ECD spectrum of talauxin V (**4**) in MeOH

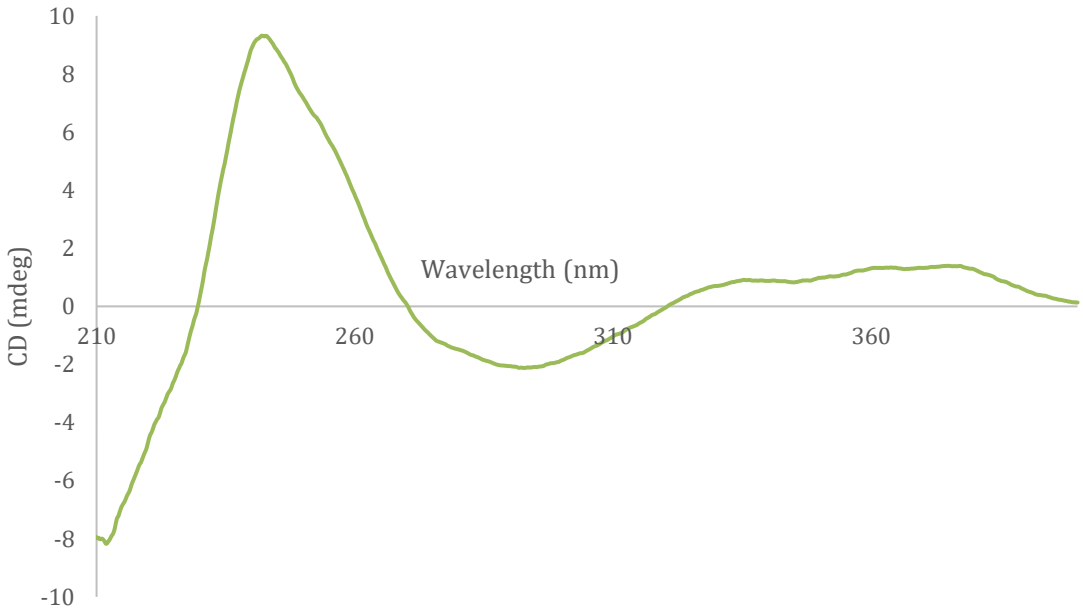

Figure S35: ECD spectrum of semi-synthetic talauxin L (**5**) in MeOH

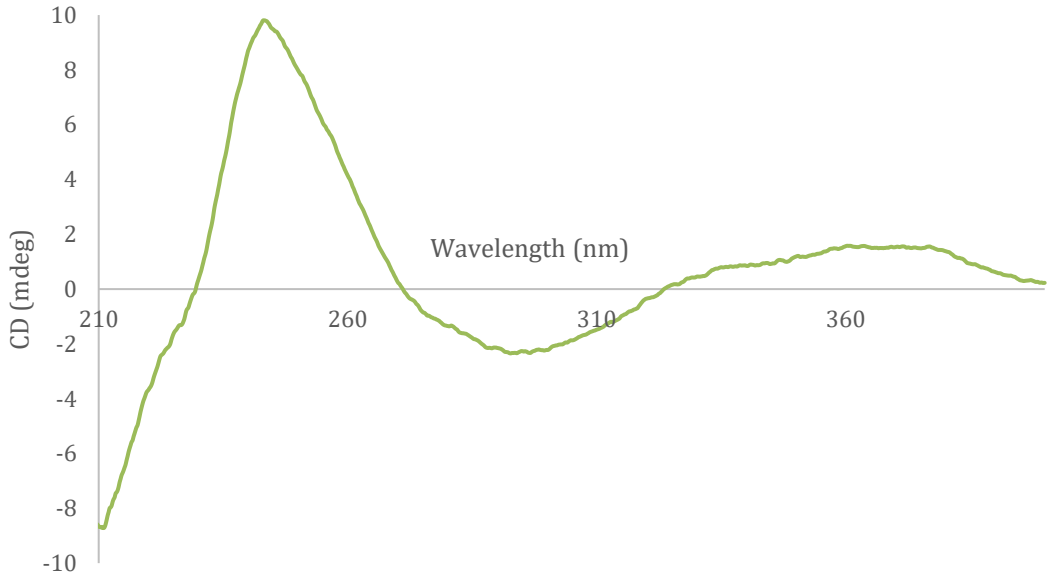

Figure S36: ECD spectrum of semi-synthetic talauxin I (**6**) in MeOH

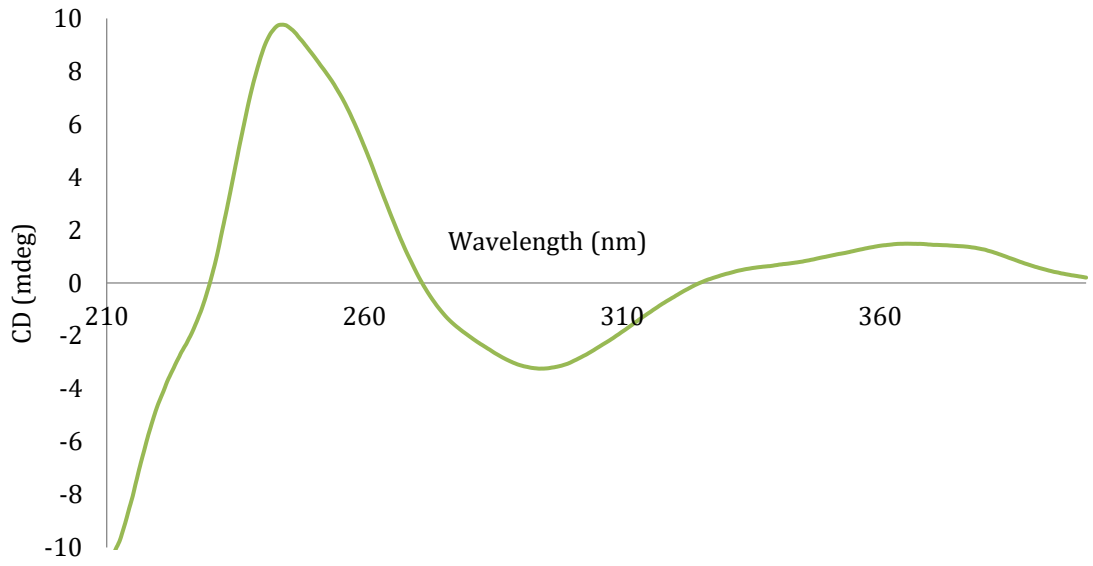

Figure S37: ECD spectrum of talauxin L and I (**5**/**6**) mixture in MeOH

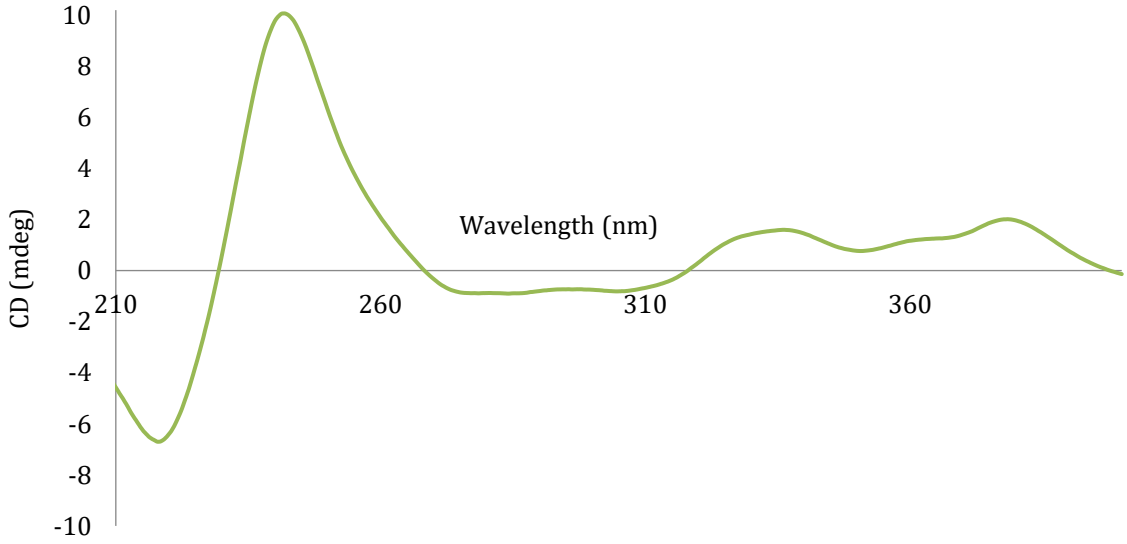

Figure S38: ECD spectrum of desacetyldesmethyltalauxin V (**9**) in MeOH

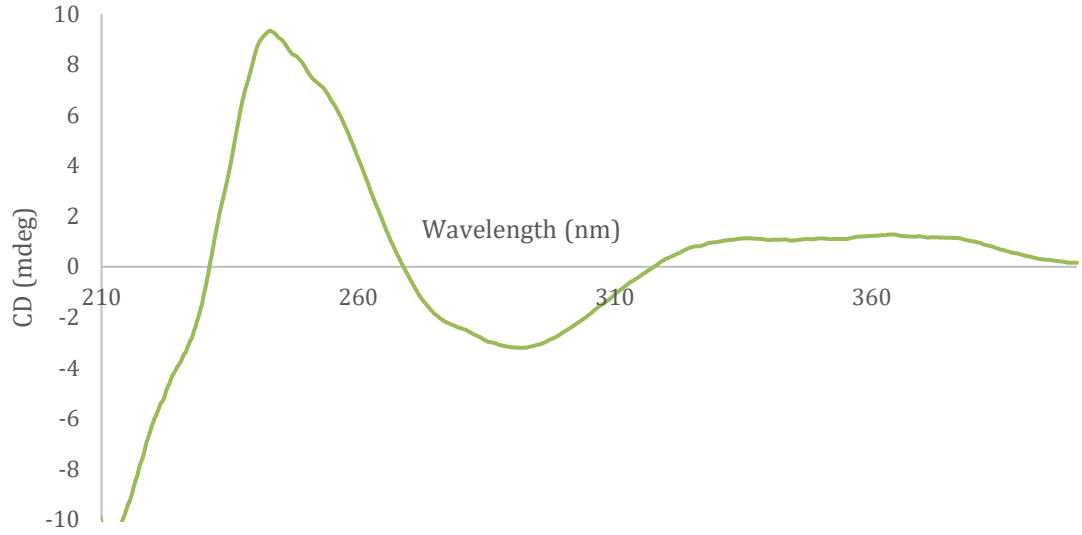

Figure S39: ECD spectrum of epitalauxin L (**10**) in MeOH

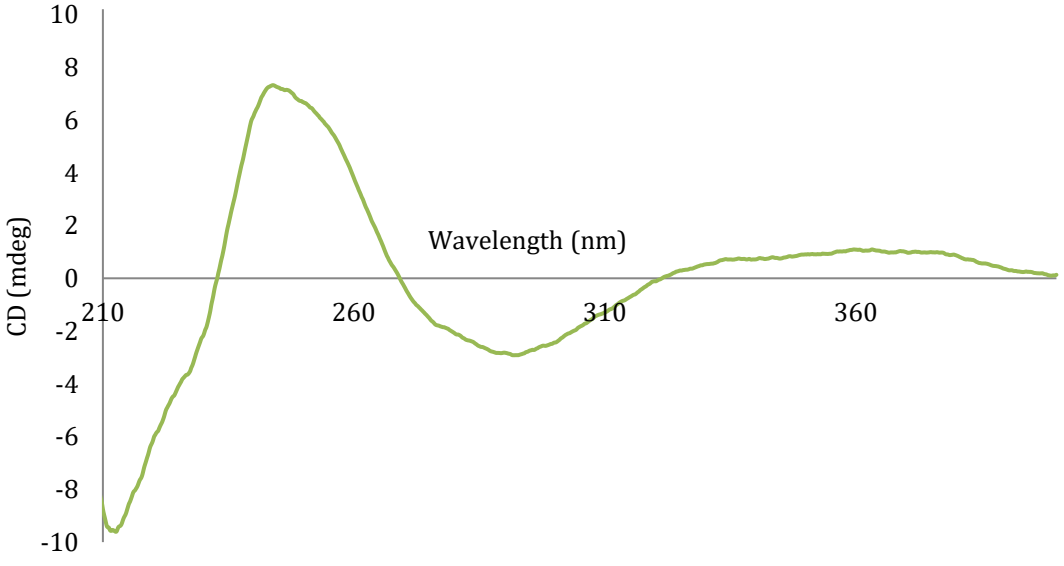

Figure S40: ECD spectrum of epitalauxin I (**11**) in MeOH

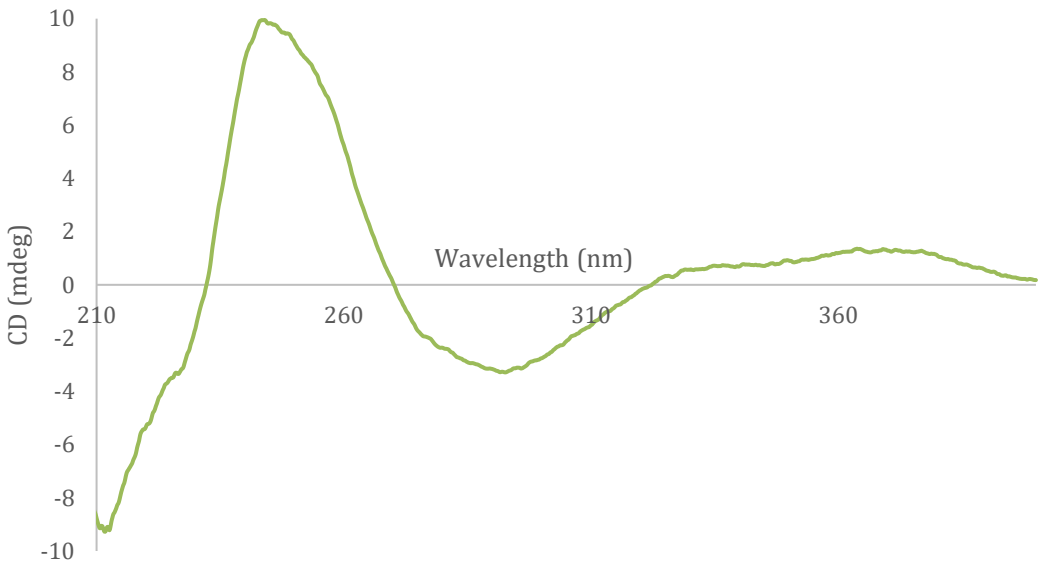

Figure S41: ECD spectrum of epitalauxin F (**12**) in MeOH

F. IR spectra

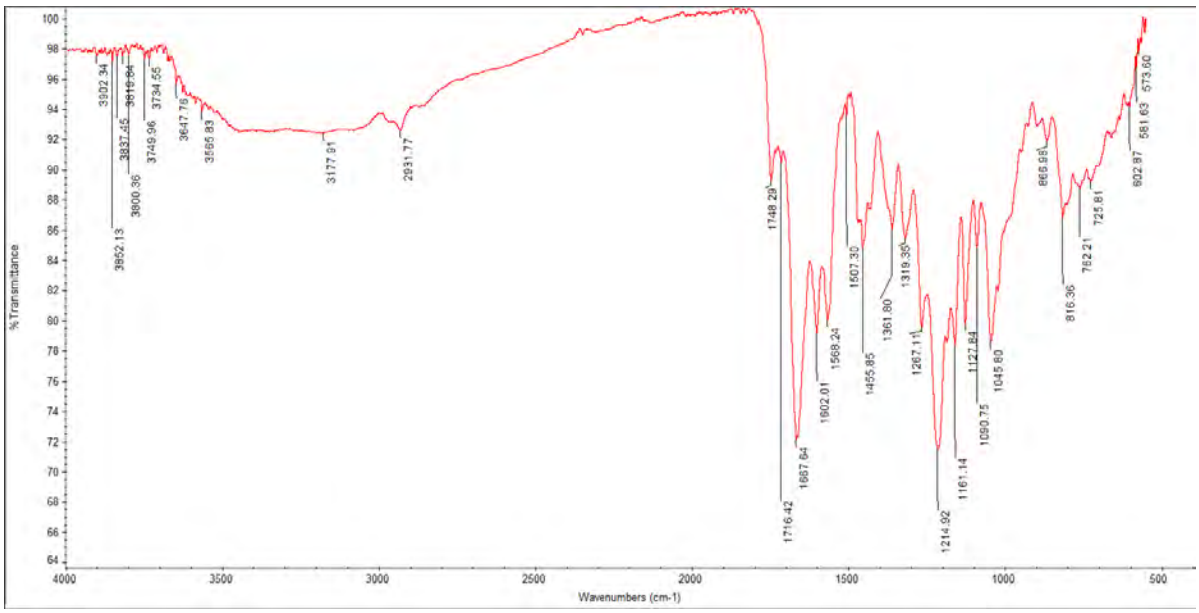

Figure S42: IR spectrum of talauxin E (**2**)

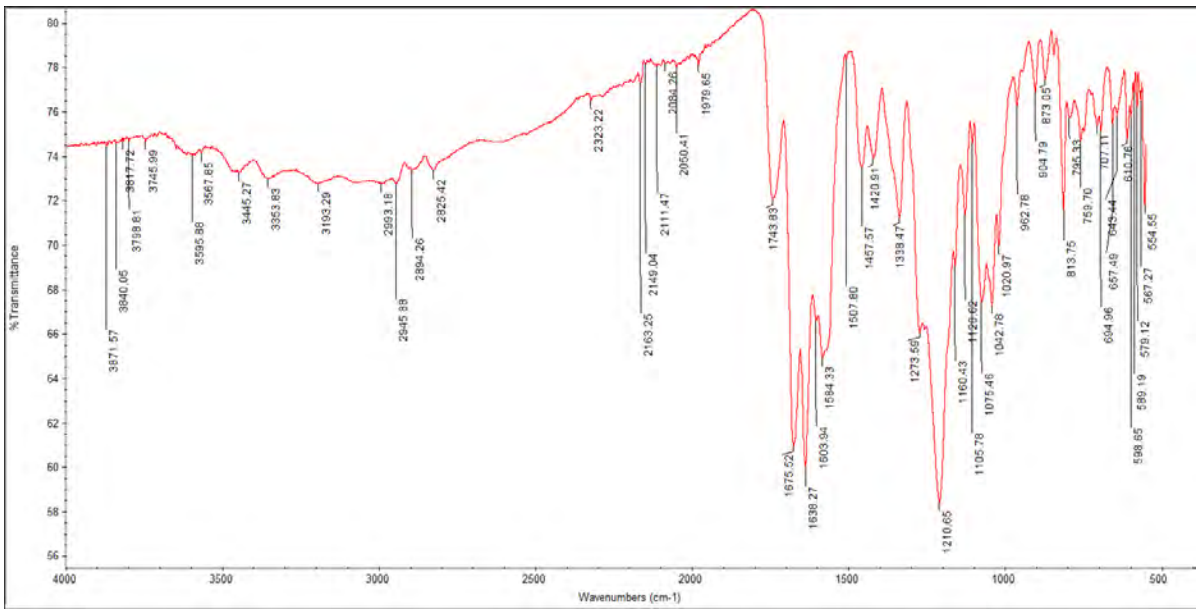

Figure S43: IR spectrum of talauxin Q (**3**)

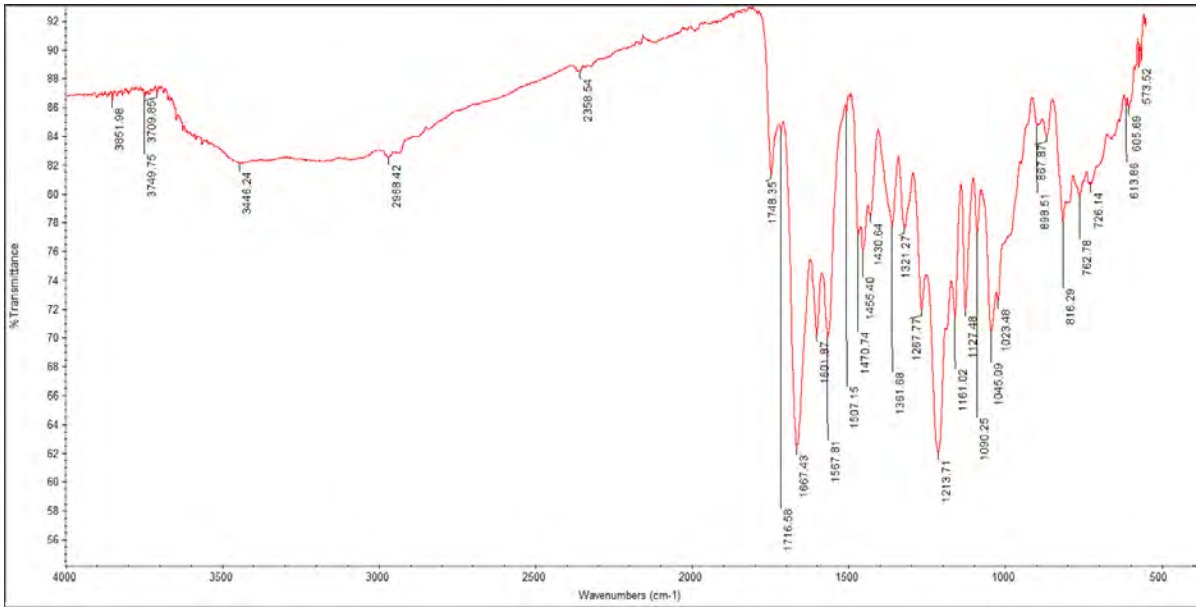

Figure S44: IR spectrum of talauxin V (**4**)

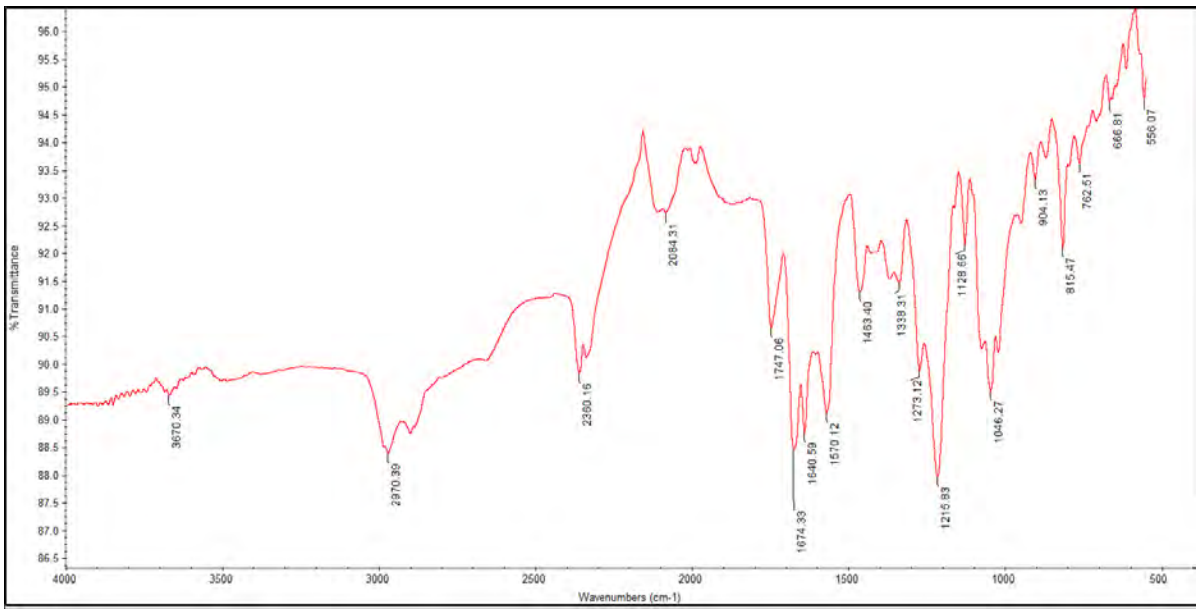

Figure S45: IR spectrum of talauxin L (**5**)

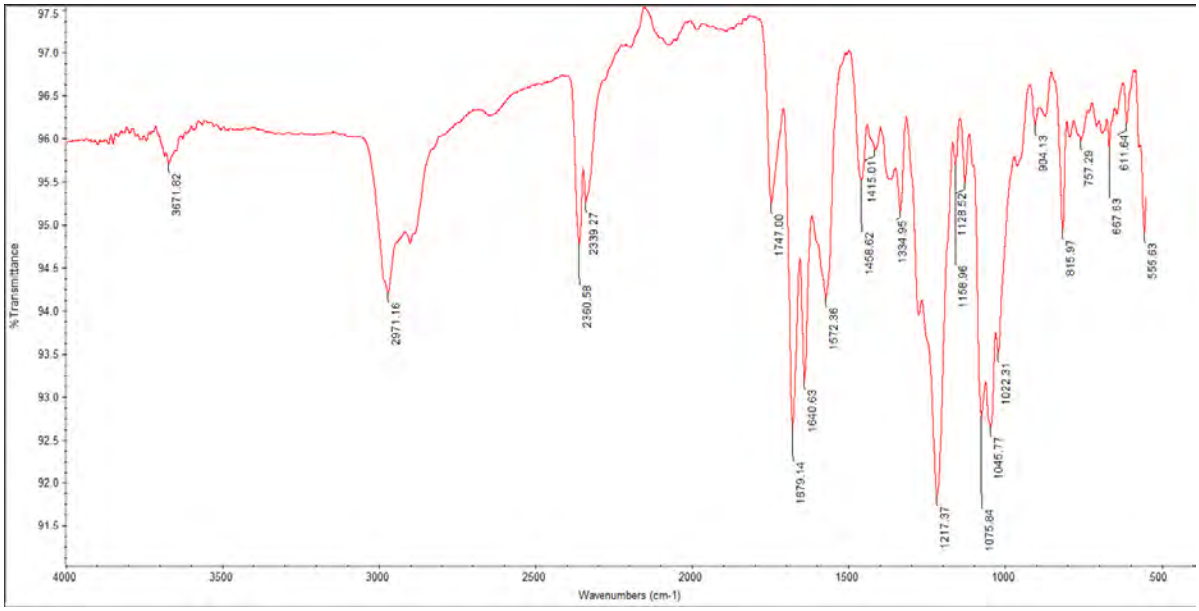

Figure S46: IR spectrum of talauxin I (**6**)

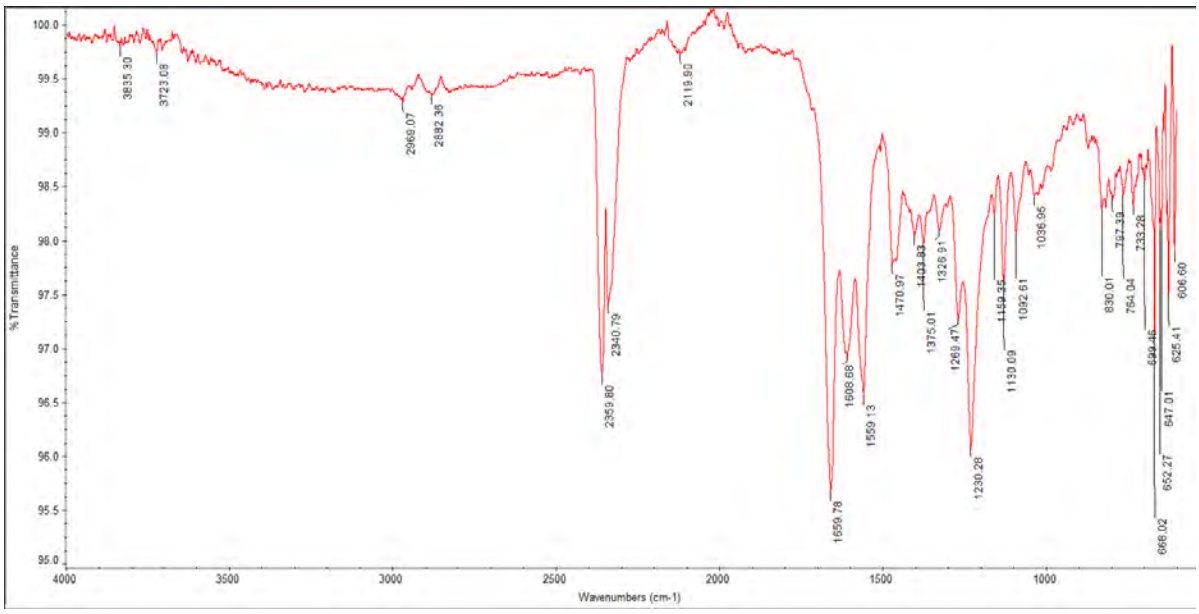

Figure S47: IR spectrum of desacetyldesmethyltalauxin V (**9**)

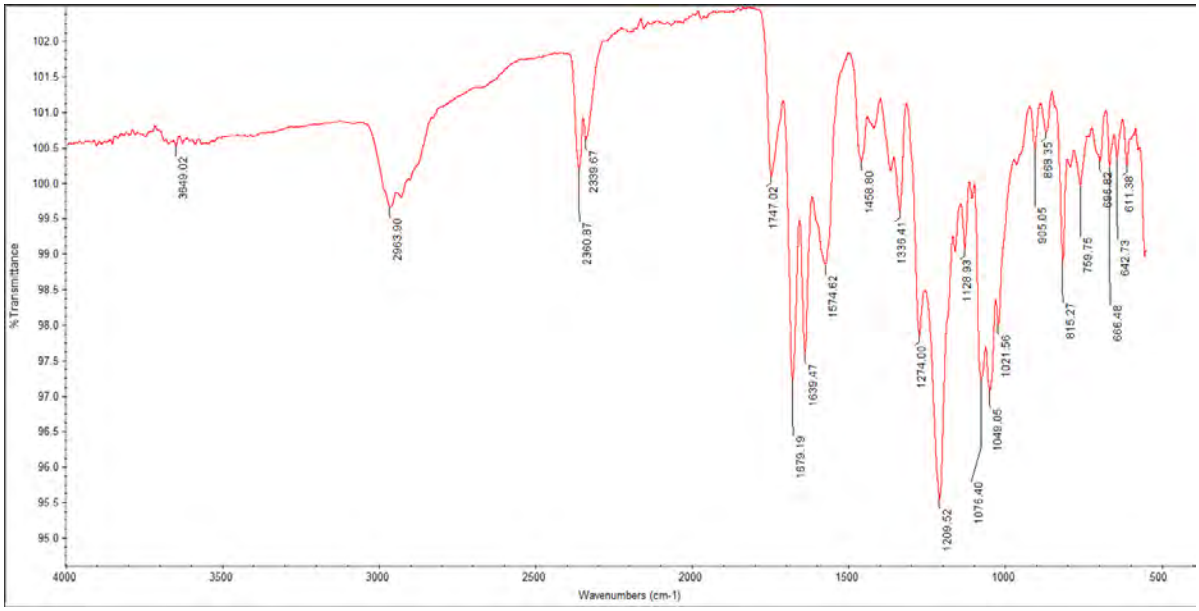

Figure S48: IR spectrum of epitalauxin L (**10**)

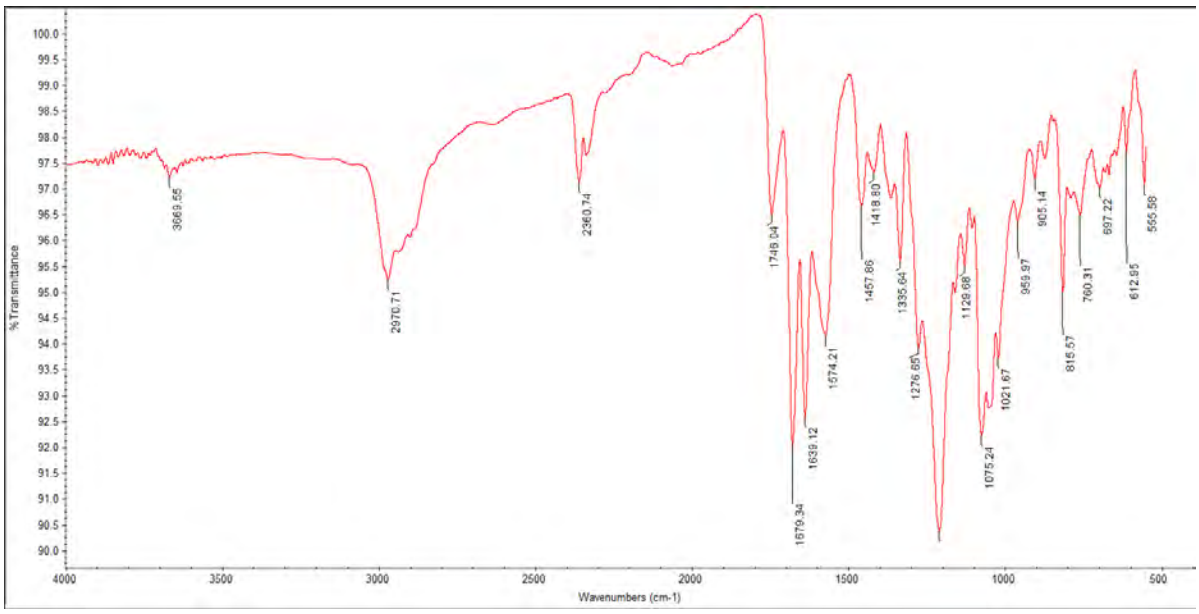

Figure S49: IR spectrum of epitalauxin I (**11**)

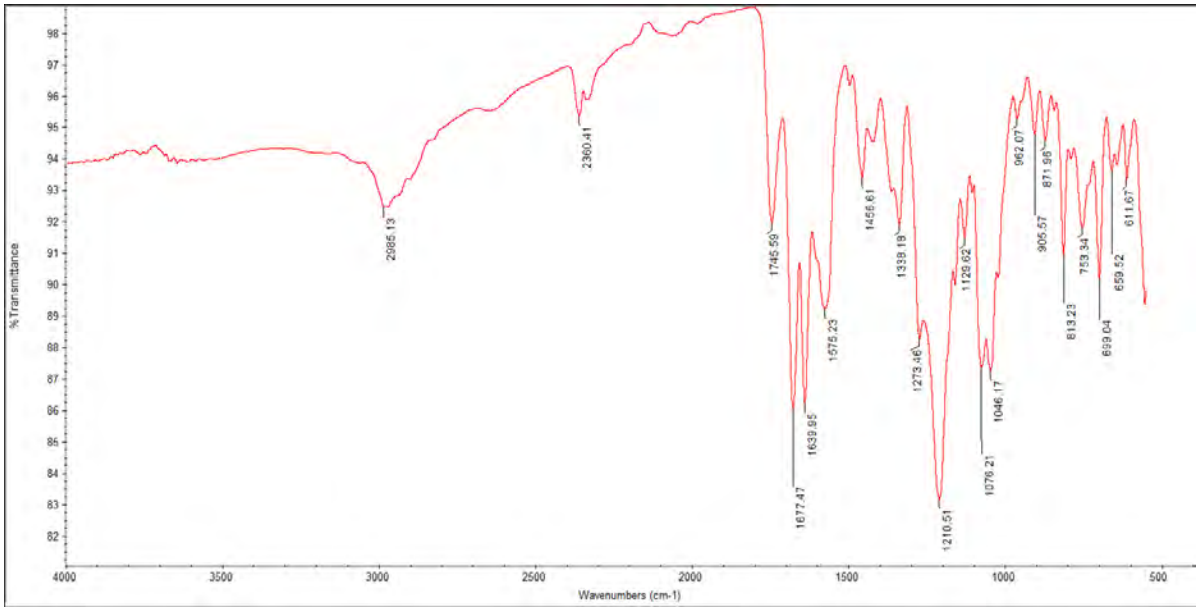

Figure S50: IR spectrum of epitalauxin F (**12**)

G. Spectroscopic data (Reported compounds)

Duclauxin (1): Yellow solid, $[M+H]^+$ *m/z* 546.1; $[\alpha]^{24}_D$: +197 (*c* 0.08, $CHCl_3$); NMR (600 MHz, DMSO-d_6) see Table 1 and Supporting Information, Table S1.

***O*-desmethylfunalenone** (**7**): Green-yellow solid. ESI(+)MS $[M+H]^+$ *m/z* 274.0; NMR (600 MHz, DMSO-d_6) see Supporting Information, Table S7.

9-demethyl FR-901235 (8): Yellow solid. $[\alpha]^{24}_D$: 0 (*c* 0.23, MeOH); ESI(+)MS $[M+Na]^+$ *m/z* 353.1; NMR (600 MHz, DMSO-d_6) see Supporting Information, Table S8.

Chapter Four

Chapter 4: Authors contribution

Nirmal Chaudhary- Isolation and purification of the crude extract, characterization, structure elucidation, manuscript draft

Dr. Ernest Lacey – Fungal culture and extraction, bioassay

Dr. Andrew Piggott –Project co-supervision

Prof. Peter Karuso – DFT calculation, Manuscript revision, Project supervision

Structure revision of talaromycesone A and new phenalenones and polyesters from *Talaromyces stipitatus*

*Nirmal K. Chaudhary,[†] Ernest Lacey,[§,†] Andrew M. Piggott,[†] Peter Karuso[†,]**

[†]*Department of Molecular Sciences, Macquarie University, NSW 2109, Australia,*

[§]*Microbial Screening Technologies Pty. Ltd., Smithfield, NSW 2164, Australia*

* Corresponding author: peter.karuso@mq.edu.au

Abstract

Investigation of the secondary metabolites of the filamentous fungus *Talaromyces stipitatus* led to the isolation of three new phenalenone dimers bacillisporin I (**1**), talarohemiketal A (**2**), talaroazasone A (**3**), talaromacrolactone A (**4**) and talarolactone A (**5**) along with the reported oxyphenalenone dimers bacillisporin A (**6**), bacillisporin B (**7**), bacillisporin C (**8**), *epi*-bacillisporin F (**9**), phenalenone monomer funalenone (**10**) and polyesters 15G256α (**11**), 15G256ν (**12**) and hydroxymellein (**13**). Moreover, assignment of 2D NMR correlations coupled with DFT calculations showed that talaromycesone A (**14**), is identical to talarolactone A but the original structure was misassigned. All the isolated compounds were tested for cytotoxicity, antibacterial and antifungal activities.

Introduction

The filamentous fungal genus *Talaromyces* (Trichocomaceae) is a well-known fungal genus because of their ubiquitous distribution in nature and have been isolated from diverse habitats including soil, plants, sponges and foods.[1] *Talaromyces* species are important producers of diverse range of structurally unique polyketides such as tropolones[2] or oxyphenalenone dimers[3,4,5,6,7,8] or macrolide polyesters.[9,10] Our chemical investigation of a cryptically co-culturing fungus, *Talaromyces stipitatus,* had earlier led to the isolation of a suite of interesting metabolites including the talauxins, the amino acid conjugates of the well-studied metabolite duclauxin.[11] Continuing with this chemical investigation, we report the isolation of 13 more polyketide derived secondary metabolites, **1**-**13** belonging primarily to the phenalenones or polyesters structural classes. Phenalenones are fused tricyclic ring system of hydroxyl-perinapthenones or their oxygenated dimeric counterparts[12] that have been documented both from fungi and higher plants but via distinct biogenetic pathways.[13] Since, the discovery of the first naturally occurring phenalenones, atrovenetin and deoxyherquinone from the fungus *Penicillium atrovenetum* in 1959,[14] approximately one hundred analogs have been discovered so far from a number of fungal species including *Penicillium*, *Talaromyces*, *Gremmeniella, Phaeosphaeria, Nigrospora, Godronia, Coniothyrium, Aspergillus, Scytalidium, Roesleria, Verticillium, Paecilomyces, Neonectria, Gilmaniella, Polytolpa, Sirococcus* and *Sclerophora*.[12] Similarly, polyester compounds have been previously isolated from a number of ascomycete fungi such as *Acremonium,*[15] *Hypoxylon,*[16] *Menisporopsis,*[17,18] *Penicillium,*[19] *Scedesporium,*[20] *Talaromyces*[9,10] and from the basidiomycete fungus *Albatrellus confluens.*[21] The isolated compounds included new secondary metabolites, **1**-**5** including an unusual bisoxyphenalenone dimer, talarohemiketal (**2**); an azaphenalenone talaroazasone (**3**) a macrolide polyester talaromacrolactone A (**4**) and two bisoxyphenalenone dimers (**1** and **5**).

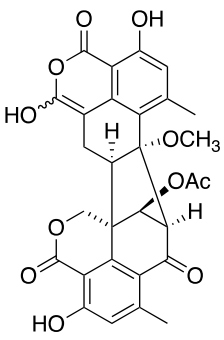

Bacillisporin I (**1**)

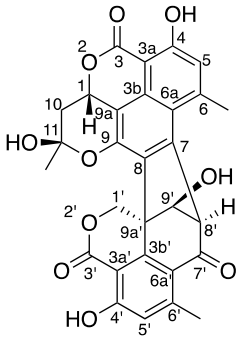

Talarohemiketal A (**2**)

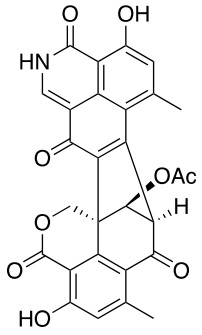

Talaroazasone A (**3**)

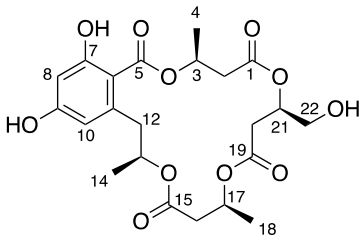

Talaromacrolactone A (**4**)

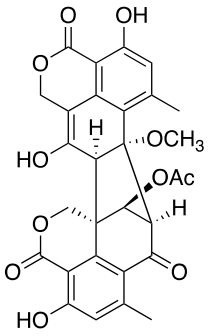

Talarolactone A (**5**)

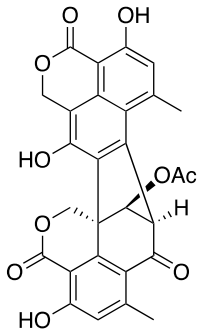

Bacillisporin A (**6**)

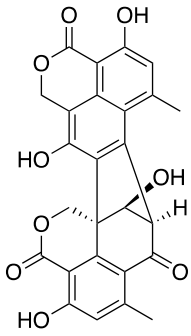

Bacillisporin B (**7**)

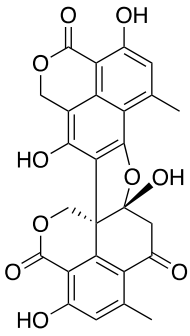

Bacillisporin C (**8**)

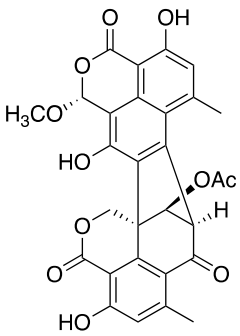

epi-Bacillisporin F (**9**)

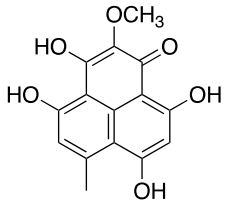

Funalenone (**10**)

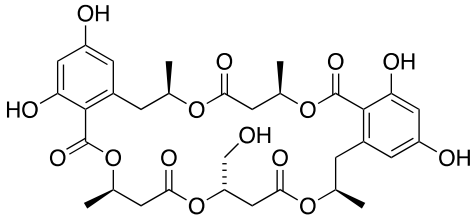

15G256 (**11**)

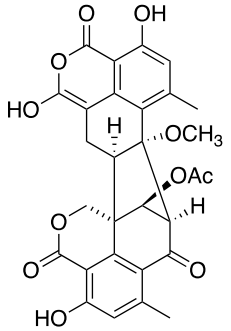

Talaromycesone A (**14**)

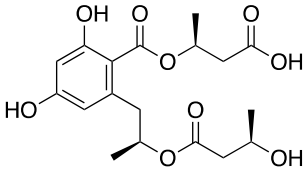

15G256 (**12**)

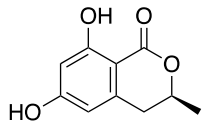

6-hydroxymellein (**13**)

Results and discussion

Media changes during the optimization study for *Aspergillus banksianus* on various agars had led to the emergence of a quiescent fungus identified as *Talaromyces stipitatus*. Culturing of this quiescent fungus on pearl barley followed by extraction of the pooled mycelial mass with acetone, removal of the solvent to an aqueous residue followed by partitioning with ethyl acetate yielded a crude extract. This crude extract was then defatted

to remove the non-polar lipids and the resulting fraction was then subjected to size exclusion chromatography on Sephadex LH-20. The Sephadex LH-20 fractionation yielded four fractions. Reverse phase HPLC purifications and characterization of the remaining crude extracts, following the initial isolation of 8 compounds,[11] yielded 13 more metabolites, **1-13**.

Bacillisporin I (**1**) was isolated as a pale-yellow solid mixture of two inseparable stereoisomers in the ratio of 1:1.25 (Supporting Information, Figure S1). The UV spectrum with absorbance maxima at 206, 236 and 352 nm was similar to the prototypical oxyphenalenone dimer duclauxin indicating the presence of an α,β-unsaturated carbonyl group mainly responsible for the characteristic UV spectrum of oxyphenalenone dimers.[4] The IR spectrum showed strong broad bands in the region around 3000-3400 cm^{-1} indicating the presence of chelated hydroxyl groups. At least two different carbonyl groups present were observed as absorption bands at 1748 cm^{-1} and 1716 cm^{-1} in the IR spectrum. The ESIMS revealed $[M+H]^+$, $[M–H_2O+H]^+$ and $[M–H]^-$ ions at *m/z* 533, 515 and 531 respectively indicating a molecular weight of 532. Although, the LC-MS indicated only one compound, the ^1H and ^{13}C NMR spectrum revealed two set of protons in the ratio of 1:1.25. In the ^1H NMR spectrum, each of these stereoisomers showed the presence of 20 protons including 4 exchangeable protons whereas the ^{13}C NMR spectrum showed 28 carbons (Table 1) each suggesting a molecular formula of $C_{29}H_{24}O_{11}$. This was confirmed by HRMS for the $[M–H]^-$ ion (Δmmu = +0.2 ppm). The resemblance of the ^1H NMR spectrum with duclauxin was very clear. Comparison of the ^1H NMR chemical shifts, showed the presence of two additional exchangeable protons in bacillisporin I and that the methoxide and H-8 proton were missing. The chemical shifts for C-7 and C-8 indicated an extra double bond between these two carbons. Introduction of this double bond resulted in enolization of C-9 carbonyl (δ_C 150.6 cf. 193.9 for duclauxin). Hence, significant differences in the chemical

shifts between duclauxin[11] and bacillisporin I occur around C-1, C-3, C-7, C-8 and C-9. The rest of the ^{1}H and ^{13}C NMR spectra were quite similar. The ^{13}C NMR chemical shift for C-1 (δ_C 92.4) is typical of a hemi-ketal.[22] The reversible opening of this ring led to epimerization of C-1 and an inseparable diastereomeric mixture. These deductions together with the observed 2D NMR correlations (Supporting Information, Table S1), led to the assignment of the structure as **1**.

Talarohemiketal A (**2**) was isolated as a yellow solid. The UV spectrum with absorbance maxima at 208, 236, and 353 nm was characteristic of an oxyphenalenone dimer. The IR spectrum showed the presence of absorption bands at 3462 and 1747 cm^{-1} indicating the presence of hydroxyl and carbonyl groups respectively. A molecular formula of $C_{29}H_{22}O_{10}$ was assigned based on the observed HRMS for the $[M+H]^+$ ion (Δmmu = +1.5 ppm). The ^{1}H NMR spectrum revealed resonances for two aromatic protons (δ_H 6.97 and 6.83), two methyls (δ_H 2.97 and 2.43), an oxymethylene (δ_H 5.09) and an oxymethine (δ_H 5.83) whereas the ^{13}C NMR spectrum revealed resonances for two oxy carbonyls (δ_C 167.7 and 169.9) and a ketone carbonyl (δ_C 192.6) characteristic of an oxyphenalenone dimer. However, additional proton resonances were observed including an aliphatic methyl singlet (δ_H 1.63), an aliphatic methylene (δ_H 2.16 and 2.50) and an alcoholic hydroxyl (δ_H 7.26). Assignment of 2D NMR correlations as shown in Figure 1, confirmed the structure as **2,** an unusual bis (oxaphenalenone) fused hemiketal (C-11, δ_C 100.0). The absolute configuration was assigned by comparison with the reported compound talaroketals B owing to their identical ECD spectrum (Supporting Information, Figure S28) and similar specific optical rotations (+231 cf. +197).[8]

Talaroazasone A (**3**) was also isolated as a yellow solid. The UV spectrum showed absorbance maxima at 214, 236 316, 374 and 452 nm similar as desacetyldesmethyltalauxin V. Additional absorbance maxima at 452 nm compared to most other oxyphenalenones,

clearly indicated the presence of an extended conjugated system in this molecule. The IR spectrum showed broad bands in the region around 3200 cm^{-1} indicating the presence of chelated hydroxyl groups. At least two different carbonyl groups were indicated by sharp and strong absorption bands at 1748 cm^{-1} and 1716 cm^{-1}. The ESI-MS revealed $[M+H]^+$, $[M+Na]^+$ and $[M–H]^-$ ions at *m/z* values of 514, 526 and 512 respectively suggesting an odd molecular weight of 513, indicative of the presence of an odd number of nitrogen atom(s). The ^1H NMR spectrum contained 16 protons on carbon and 3 exchangeable protons. The ^{13}C NMR spectrum showed 28 carbons (Table 1 and Supporting Information, Table S3) suggesting a molecular formula of $C_{28}H_{19}NO_9$ if only one nitrogen was present. This was confirmed by HRMS for the $[M+H]^+$ peak at *m/z* 514.1130 (Δmmu = –0.6 ppm). The ^1H and ^{13}C NMR spectra of **3** was somewhat similar to desacetyldesmethyltalauxin V[11] except the amino acid resonances were missing. The presence of an NH at δ_H 13.25 suggested this was the ammonia adduct of duclauxin that had eliminated methanol.

Talaromacrolactone A (**4**) was isolated as an off white solid. The ESI-MS revealed $[M+H]^+$, $[M+NH_4]^+$, $[M+Na]^+$, $[M–H]^-$ and $[2M–H]^-$ ions at *m/z* values of 469, 491, 467 and 935 respectively indicating a molecular weight of 468. The ^1H NMR spectrum contained 28 protons whereas the ^{13}C NMR spectrum showed 22 carbons suggesting a molecular formula of $C_{22}H_{28}O_{11}$. The presence of one tetra-substituted aromatic ring with two meta-coupled aromatic protons and three ester carbonyls in the ^1H and ^{13}C NMR spectra (Table S4) suggested a macrocyclic ester related to 15G256α and analogs. The UV spectrum with characteristic absorbance maxima at 215, 270 and 302 nm clearly indicated the presence of a 2,4-dihydroxybenzoate motif.[23] The two aromatic proton s showed weak W-couplings to the carbonyl carbon at δ_C 168.5 in the HMBC correlation. The molecular formula was confirmed by a HRMS for the $[M+Na]^+$ ion (Δmmu = –1.0 ppm). This molecular formula indicated an index of hydrogen deficiency of 9. An isochromanone with this molecular

formula has not been previously reported. Three different CH_3-CH-CH_2- and a single -CH_2-CH-CH_2- spin systems were established from the COSY correlations. These spin systems were interconnected with each other through an ester linkage and the HMBC correlations arising from each of the methine proton of these spin systems established a macrocyclic ring. A terminal methylene of the spin system -CH_2-CH-CH_2- was connected to a hydroxyl group as evident from its ^{13}C NMR chemical shift at δ_C 72.6. Thus, the structure was established as a macrocyclic polyester. Absolute configuration of **4** was assigned to be the same as that of the reported analogs based on biogenetic considerations and because of their negative optical rotation like all other reported macrocyclic polyesters. The observed ^{1}H and ^{13}C NMR chemical shifts and the key 2D NMR correlations are assigned in Table S4 **(**Supporting Information). A plausible biogenetic pathway of **4** could be the condensation of 6-hydroxymellein with 3-units of 3-hydroxybutyric acid, in which the methyl of the central 3-hydroxybutyric acid residue is oxidized to an alcohol (Figure 2).

Talarolactone A (**5**) was isolated as an off-white solid. The UV spectrum with absorbance maxima at 208, 242 and 362 nm was diagnostic of an α,β-unsaturation carbonyl functional group responsible for the characteristic UV spectrum of oxyphenalenone dimers.[4] The IR spectrum showed a strong band around 3148 cm^{-1} indicating the presence of chelated hydroxyl groups. At least two different types of carbonyl group present were suggested by the presence of sharp and strong absorption bands at 1748 and 1674 cm^{-1}. The ESI-MS of the compound revealed $[M+H]^+$, $[M+NH_4]^+$, $[M+Na]^+$ and $[M–H]^-$ ions at *m/z* 549, 566, 571 and 547 respectively indicating a molecular weight of 548. The ^{1}H NMR spectrum contained 21 protons on carbon and 3 exchangeable protons. The ^{13}C NMR spectrum showed 29 carbons suggesting a probable molecular formula of $C_{29}H_{24}O_{11}$ assuming no other elements are present. A review of the literature revealed that talaromycesone A (**14**) could be a possible match. The ^{1}H and ^{13}C NMR spectra were identical with that reported in the

literature when run in the same solvent (acetone-d_6) (supporting information, Table S5b).[6] Moreover, the specific optical rotations also matched in sign and magnitude(observed value +55 *cf.* reported value +25).[6] The difference in the optical rotation value might be attributed to the differences in purity. It appeared the reported structure assigned to talaromycesone A may be incorrect. The structure **14** assigned by Wu, *et al.;* was based on a long-range coupling between the H_2-9 methylene protons, (δ_C 65.4) to C-1. However, **14** does not explain the chemical shift for the methylene protons (δ_H 4.79 and 5.05) which appears too downfield. A chemical shift of 65.4 ppm is also not consistent with C-9 in the **14** but more appropriate to C-1 in our structure, **5**. In addition, in **14***.;* a HMBC correlation from H_2-9 methylene proton to C-7 is expected but it is not observed. A key correlation that supports the reassigned structure, **5** is the observation of a HMBC correlation from this methylene (δ_C 65.4) to C-6a consistent with a W-coupling; which otherwise is unexplainable by the reported structure, **14**. Also, the observed coupling constant of 2.1 Hz is perfectly consistent to a $^5J_{HH}$ W-coupling constant taking into account the presence of a double bond between the H-8 proton H_2-1 protons as in the revised structure whereas a vicinal coupling as in the reported structure should have resulted in a $^3J_{HH}$ value of ~7 Hz instead. Moreover, although the ^{13}C NMR spectrum reported by Wu *et al.* in the supporting information shows carbon resonances both at δ_C 150.7 and δ_C 165.0 but their tabulated data has no ^{13}C NMR peak at δ_C 150.7 whereas δ_C 165.0 is assigned twice to C-3 and C-4'.

This was further confirmed by DFT isotropic shielding calculations which showed better fit of the observed ^{13}C NMR chemical shifts on our proposed structure (coefficient of regression, $R^2 > 0.99$) unlike the published structure. (coefficient of regression, $R^2 < 0.95$) (Supporting Information, Figure S2).

Talarolactone A reacted with hexylamine at room temperature to spontaneously give a reversible red coloration in dimethyl sulfoxide. Attempts to characterize the red product were futile as it reverted to talarolactone A on HPLC purification.

Bacillisporin A (**6**) was isolated as a white solid. The UV spectrum indicated the presence of an α,β-unsaturated carbonyl group with absorbance maxima observed at 206, 230, 272, 320 and 350 nm typical of oxyphenalenone dimers. The ESI-MS revealed $[M+H]^+$, $[2M+Na]^+$, $[M–H]^–$ and $[2M–H]^–$ ions at *m/z* 517, 1055, 515, and 1031 respectively indicating a molecular weight of 516. The ^1H and ^{13}C NMR spectrum revealed 20 protons and 28 carbon resonances suggesting a probable molecular formula of $C_{28}H_{20}O_{10}$. The ^1H NMR spectrum was very similar to bacillisporin I except that C-1 is now a methylene (δ_H 5.66 and 5.70). This corresponded to the known compound bacillisporin A (**6**). Comparison of the observed chemical shifts of this compound with that of bacillisporin A[4] aided by the observed 2D NMR correlations (Supporting Information, Table S6) further confirmed its structure as bacillisporin A. Moreover, the observed specific optical rotation $[\alpha]^{24}_D = +417$ (c 0.92, MeOH) is in agreement with that reported in the literature, $[\alpha]^{24}_D = +484$ (c 0.583, acetone)[4] suggesting the same absolute configuration. Bacillisporin A has been previously isolated from the fungus *Talaromyces bacillisporus*[4,5] *and Penicillium* sp. JP-1, an endophytic fungus associated with the mangrove plant *Aegiceras corniculatum.*[24] Bacillisporin A is reported to have strong activity against the MCF-7 and NCI-H460 cell lines whereas only moderate activity against SF-268 cells.[5]

Bacillisporin B (**7**) was isolated as off-white compound. The UV spectrum was again characteristic of oxyphenalenones with absorbance maxima observed at 207, 232, 272, 322 and 350 nm suggesting the presence of an α,β-unsaturated carbonyl group. The ESI-MS revealed $[M+H]^+$ and $[M–H]^–$ ions at *m/z* 475 and 473 respectively indicating a molecular weight of 474. The ^1H and ^{13}C NMR spectrum revealed 18 and 26 resonances respectively

suggesting a probable molecular formula of $C_{26}H_{18}O_9$. The ^1H and ^{13}C NMR spectra was similar to bacillisporin A except that the resonances responsible for the acetate group were missing from both the ^{13}C and ^1H NMR spectra. Moreover, the difference in the molecular mass of these two compounds (42 amu) was also in agreement with the fact that this compound is a desacetyl analog of bacillisporin A i.e., bacillisporin B. Assignment of the observed key COSY, HMBC and ROESY correlations (Supporting Information, Table S7) also confirmed the structure as bacillisporin B. Additionally, the observed optical rotation $[\alpha]^{24}_D$ = +369 (c 0.09, MeOH) value was in agreement with the value reported in the literature, $[\alpha]^{27}_D$ = +512 (c 0.144, THF)[4] suggesting the same absolute configuration. Bacillisporin B has been first reported in 1980 by Yamakazi *et al.*[4] and subsequently by Dethoup *et al.* in 2006.[5] Bacillisporin B is reported to have moderate cytotoxicity against the cell lines MCF-7, NCI-H460 and SF-268 cell lines.[5]

Bacillisporin C (**8**) was isolated as a pale-yellow compound. The UV spectrum was characteristic of an α,β-unsaturated carbonyl group with absorbance maxima observed at 225, 232, 270, 315, 343 and 352 nm and hence suggestive of an oxyphenalenone scaffold. The ESI-MS revealed $[M+H]^+$ and $[M–H]^–$ ions at *m/z* 491 and 489 respectively indicating a molecular weight of 490. The ^1H and ^{13}C NMR spectra indicated resonances for 18 protons and 26 carbons respectively suggesting a probable molecular formula of $C_{26}H_{18}O_{10}$. The presence of two pairs of oxymethylene protons was indicated by two AB quartets at δ_H 5.46, 5.62; δ_C 66.7 and δ_H 4.60, 4.91; δ_C 68.7 whereas the third methylene was an aliphatic (at δ_H 3.08, 3.24; δ_C 48.5). Literature review revealed that the only oxyphenalenone with three pairs of methylenes with the molecular formula of $C_{26}H_{18}O_{10}$ was bacillisporin C. The observed chemical shifts of the protons and carbons (Supporting Information, Table S8) was identical with that reported for bacillisporin C.[4] However, some of the chemical shift values have been wrongly assigned in the literature.[5] In particular, the authors have interchanged

the chemical shifts for the two aromatic protons (H-5 with H-5' and vice-versa) and the two methyl groups (6-CH_3 with 6'-CH_3 and vice-versa) resulting in the subsequent interchange of the ^{13}C chemical shifts around their periphery (C-3a, C-4, C-5, C-6 and C-6a with C-3a', C-4', C-5', C-6' and C-6a') respectively and vice-versa. Also, the observed optical rotation $[\alpha]^{25}_{D} = +438$ (c 0.37, acetone) value is in agreement with those reported in the literature, $[\alpha]^{28}_{D} = +451$ (c 0.20, acetone)[4] suggesting the same absolute configuration as the reported one. Bacillisporin C has been previously isolated from the fungus *Talaromyces bacillisporus*[5,4] and the endophytic fungus *Penicillium* sp. JP-1 associated with the mangrove plant *Aegiceras corniculatum*[24] and another unidentified mangrove endophytic fungus SBE-14.[25] Bacillisporin C has moderate cytotoxicity against the cell lines MCF-7, NCI-H460 and SF-268.[5]

epi -Bacillisporin F (**9**) was isolated as a pale-yellow solid. The ESI-MS revealed $[M+H]^+$, $[M-3H_2O+Na]^+$, $[2M+Na]^+$, $[M–H]^–$, $[M+HCOONa–H]^–$, $[M+HCOONa+Na–2H]^–$ and $[2M–H]^–$ ions at *m/z* 547, 515, 1115, 545, 613, 635 and 1091 respectively indicating a molecular weight of 546. The resemblance of the observed NMR spectra (Supporting Information, Table S9**)** with that of **1** (Supporting Information, Table S1) suggested that the compound was closely related to **1**. The only notable difference was the presence of a methoxy group (δ_H 3.56) instead of a hydroxyl group. This was further supported by a corresponding mass difference of 14 amu between these two molecules. The rest of the ^1H and ^{13}C NMR spectra were quite similar. Observed ECD spectrum of **9** was perfectly identical with that reported for bacillisporin F and *epi*-bacillisporin F which were virtually the same.[7] However, the reported chemical shifts for bacillisporin F and *epi*-bacillisporin F were slightly different, particularly around the methoxy group and the methine H-1.[7] Comparison of the observed chemical shifts of **9** (for example, 1-methoxy, δ_H 3.56) closely

matched with that of *epi*-bacillisporin F (δ_H 3.58), rather than bacillisporin F (δ_H 3.47) thereby suggesting a 3*R* configuration at C-1.[7]

Funalenone (**10**) was isolated as a yellow powder. The UV spectrum showed absorbance maxima at 217, 251 and 330 nm indicative of a phenalenone monomer.[24,26] The ESI-MS revealed $[M+H]^+$ and $[M–H]^–$ ions at *m/z* 289 and 287 respectively indicating a molecular weight of 288. The ^{1}H NMR spectrum revealed two aromatic protons, a methyl group and a methoxy group whereas the ^{13}C NMR spectrum revealed 15 resonances of which 11 were aromatic quaternary resonances. Four of the quaternary carbons were oxygenated as evident from their chemical shifts. As three hydrogens were missing in the ^{1}H NMR spectrum, three of these quaternary carbons were assumed to be attached to hydroxyl residues while the remaining one was a carbonyl carbon. Some of the carbon resonances observed were broad suggesting that they were an equilibrium of interconverting tautomers. Similarity of the observed chemical shifts of the ^{1}H and the ^{13}C NMR spectra (Supporting Information, Table S10) with that of funalenone[27] confirmed its structure. Funalenone, a collagenase inhibitor was first isolated from the *Aspergillus niger* FO-5904.[27]

15G256α (**11**) was isolated as colorless solid. The UV spectrum showed spectral pattern characteristic of a 2,4-dihydroxybenzoate motif with absorbance maxima at 214, 256 and 300 nm.[23] This was supported by two sets of meta-coupled (2.3 Hz) aromatic protons (Supporting Information, Table S11). The ESI-MS revealed $[M+H]^+$, $[M+NH_4]^+$, $[M+Na]^+$ and $[M–H]^—$ ions at *m/z* 663, 680, 685 and 661 respectively indicating a molecular weight of 662. The ^{1}H NMR spectrum indicated 38 protons whereas the ^{13}C NMR spectrum showed 32 carbons suggesting a molecular formula of $C_{32}H_{38}O_{15}$. This formula indicated 14 degrees of unsaturation. The ^{13}C NMR spectrum accounted for two aromatic rings and five ester carbonyls leaving one degree of unsaturation unaccounted for. This suggested that **11** was a macrocyclic lactone (polyester). A search of literature for natural products with a

macrocyclic pentalactone and this molecular formula led to 15G256α as a possible match. Comparison of the observed chemical shifts of the ^{1}H and the ^{13}C NMR spectra with that reported for 15G256α in literature[16] substantiated this match. This together with the observed 2D NMR correlations further confirmed the identity of the compound as 15G256α. It was first reported from the culture of a terrestrial fungus *Penicillium verruculosum* F-4542 in 1992 as NG-O12 and shown to possess nerve growth factor (NGF) potentiator activity.[23] It was reported again from *Penicillium verruculosum* in 1993 as BK233-A and shown to possess antifungual activity ascribed to inhibition of cell-wall formation.[19] Additionally, the authors showed that the absolute configuration of C-3 in all the 3-hydroxybutyric acid residues was *R* by acid catalyzed ethanolysis, dervatization with *S*-phenylethylisocyanate followed by GC-separation of the diastereomers.[19] Subsequently, 15G256α was also isolated from the marine fungi *Hypoxylon oceanicum* LL-15G256[28] and *Calcarisporium* sp. KF525[29] as well as the wetland soil-derived fungus *Talaromyces flavus.*[9]

15G256ν (**12**) was isolated as an off white solid. The UV spectrum was similar to **11** with absorbance maxima at 215, 262 and 300 nm.[23] The ESI-MS revealed $[M+NH_4]^+$, $[M+Na]^+$, $[2M+Na]^+$, $[M–H]^-$ and $[2M–H]^-$ ions at *m/z* 402, 407, 791, 383 and 767 respectively indicating a molecular weight of 384. The ^{1}H NMR spectrum indicated 24 protons whereas the ^{13}C NMR spectrum showed 18 carbons suggesting a molecular formula of $C_{18}H_{24}O_9$. Comparison of the chemical shifts of the ^{1}H and the ^{13}C NMR spectra with that of the literature[16] aided by the observed 2D NMR correlations (Supporting Information, Table S12) confirmed its structure as 15G256**ν** (**12**). It was first reported from the marine fungus *Hypoxylon oceanicum*[16] and subsequently from the soil-derived fungus *Talaromyces flavus*.[9]

6-hydroxymellein (**13**) was isolated as off white solid. UV spectral pattern suggested the presence of an 2,4-dihydroxybenzoate motif with absorbance maxima observed at 215, 270

and 302 nm.[23] The ESI-MS revealed $[M+H]^+$, $[2M+Na]^+$, $[M–H]^–$ and $[2M–H]^–$ ions at *m/z* 195, 411, 193 and 387 respectively indicating a molecular weight of 194. The ^{1}H NMR spectrum contained 10 protons whereas the ^{13}C NMR spectrum showed 10 carbons suggesting a molecular formula of $C_{10}H_{10}O_4$. The ^{1}H NMR revealed a methyl doublet (δ_H 1.38; $^3J_{HH}$ 6.3 Hz), an oxymethine multiplet (δ_H 4.67), a pair of methylene protons as doublet of doublet (δ_H 2.79 and 2.91), two meta-coupled ($^4J_{HH}$ 2.3 Hz) aromatic protons (δ_H 6.23 and 6.18) and two exchangeables (δ_H 10.64 and 11.12). A search of literature for a compound with this molecular formula led to 6-hydroxymellein as a possible match. Comparison of the observed chemical shifts of the ^{1}H and the ^{13}C NMR spectra with that reported for 6-hydroxymellein in the literature[16] confirmed this. Together with the observed 2D NMR correlations (Supporting Information, Table S13), **13** was confirmed as 6-hydroxymellein.

Phenalenones have been reported to possess antimicrobial, cytotoxic and anticholinergic activities. Among the polyesters, the cyclic analogs are reported to possess antifungal activities owing to their cell-wall biosynthesis inhibitory activity whereas the linear polyesters are devoid of such activity.[16] These reported bioactive properties of the reported phenalenones and macrocyclic polyesters prompted us to screen compounds **1**-**13** for antibacterial, anticancer, antifungal and antiprotozoal activities, the results of which are summarizes in Table 2. The isolated phenalenones are analogs of duclauxin whose biosynthesis have been discussed in the preceding chapter of this thesis. The macrocyclic polyesters are produced by the condensation of hydroxymellein (**13**) with 3-hydroxybutyric acid as shown in Figure 2 based on Schlingmann's proposal.[16]

Conclusion

Chemical investigation of the quiescent fungus, *Talaromyces stipitatus* arising from the media optimization of a novel *Aspergillus* (*A. banksianus)* led to the isolation of 13

polyketide derived natural products-the phenalenones and the polyesters. This unique pattern of secondary metabolite distribution was suggestive of a *Talaromyces* sp., specifically *T. stipitatus.* This is the only species reported to produce both phenalenones and polyesters. [4, 6, 8, 9] This was later confirmed by morphological examination. Based on this work and our earlier report on talauxins,[11] we speculate that talaromycesone A, the major metabolite of *T. stipitatus* and duclauxin probably governs the products of all other oxyphenalenones dimers. Duclauxin, the biogenetic precursor for several other oxyphenalenone dimers such as talauxins,[11] duclauxamide A1,[30] bacillisporin H,[7] talaroketals[8] and talaroazasone A (**3**), owing to its strong electrophilic nature couples with nucleophiles like ammonia, amino acids and botryodiplodin thereby increasing the chemical diversity. Similarly, the reported anticancer compounds bacillisporin A and B are likely to be ex-vivo metabolites probably arising from talaromycesone A during the isolation process. Bioassay results of the tested compounds **5**-**6**, **8**-**12** have revealed that bacillisporin A (**6**) and *epi*-Bacillisporin (**9**) antibacterial activities.

EXPERIMENTAL

General experimental procedures

Size exclusion chromatography (SEC) was performed using Sephadex LH-20 (GE Healthcare Bio-Sciences Corp.). Thin-layer chromatography (TLC) was performed using pre-coated silica gel GF254 plates (Merck, Darmstadt, Germany) with various solvent systems and spots were visualized with UV light (254 nm). Preparative and semi-preparative HPLC separations were performed on a Gilson HPLC system, equipped with a Gilson 215 liquid handler, 819 injection module, 322 pump, 506C system interface and Gilson single variable wavelength UV-Vis 152 detector by reverse phase chromatography using a gradient of acetonitrile (Sigma Aldrich, USA) and water containing 0.025% HPLC grade TFA (Sigma Aldrich, USA) unless mentioned otherwise. Phenomenex Hydro-RP (250 × 22.4

mm, 10 μm) and Phenomenex Hydro-RP (250 × 10 mm, 5 μm) columns were used for preparative and semi-preparative purifications. UV-visible readings were taken on an Eppendorf UV-visible spectrophotometer (Model- Biospectrometer® Kinetic). Optical rotations were recorded in MeOH using a JASCO P-1020 Polarimeter (Jasco Corp., Japan). ECD spectra were taken on a Jasco J-810 spectropolarimeter; model CDF-426S/426L peltier type CD/Fluorescence simultaneous measurement attachment (Jasco Corp., Japan). The IR spectra were measured on a Thermo Scientific Nicolet iS10 ATR FTIR spectrometer as neat films. ^{1}H NMR, ^{13}C NMR and 2D NMR spectra were recorded in deuterated DMSO using a Bruker AVANCE II 600 MHz NMR spectrometer (Bruker Corp.). The ESIMS spectra were recorded using Agilent 6130 single quadrupole mass spectrometer (Agilent Corp., USA). HR-ESIMS data were obtained using a Q Exactive Plus hybrid quadrupole-orbitrap mass spectrometer (Thermo Scientific, Germany).

Biological Material

Media changes during the optimization study for the cultivation of a new *Aspergillus* sp., (*A. banksianus*) collected from Collaroy, New South Wales, Australia, on various agars led to the emergence of a quiescent fungal culture identified as *Talaromyces stipitatus*.

Extraction and Isolation

T. stipitatus was cultivated for extraction on grain pearl barley in Erlenmeyer flasks (100 g; 40 × 250 mL) at 24 °C for 14 days and pooled (3900× g) then extracted with acetone (2 × 5 L) for 2 h on a rotatory platform at 100 rpm. The macerated solid was removed by filtration and the filtrate concentrated to an aqueous concentrate (146 g) by rotatory evaporation. The concentrate was partitioned against ethyl acetate (2 × 2 L) then evaporated to dryness to provide an organic extract (56.9 g). The extract was

dissolved in methanol (360 mL), diluted with distilled water (140 mL) and de-fatted by partition against hexane (2 × 500 mL) to provide a crude extract (34.5 g).

A portion of the crude extract (9.0 g) was dissolved in 5 mL of 50:50 % v/v of MeOH/$CHCl_3$ and loaded onto a Sephadex LH-20 column approximately 24 × 12.2 cm. The sample loaded in the column was subjected to fractionation with the 50:50 % v/v of MeOH/$CHCl_3$ at a flow rate of 3 mL/min for approximately 40 h. The eluted fractions were then subjected to TLC and based on the results from TLC, the fractions were combined into four initial fractions, S1 to S4. Fraction S1 was mostly viscous polymeric material and was not further investigated. Fractions S2-S4 were pre-treated on a C_{18} SPE cartridge by washing with 10% methanol/water and eluting with 90% methanol/water, before reversed phase HPLC purification (acetonitrile/water).

Preparative HPLC purification of Fraction S2 yielded 15G256α (**11**; 23 mg; t_R 17.5 min), Fraction S3 yielded bacillisporin I (**1**; 10 mg; t_R 28.9min), talarohemiketal A (**2**; 2 mg; t_R 26.5 min), talaroazasone A (**4**; 15 mg; t_R 25.6 min), talalaromacrolactone A (**4**; 14 mg; t_R 25.3min), talalarolactone A (**5**; 55 mg; t_R 23.6min), bacillisporin A (**6**; 21 mg; t_R 29.0 min), bacillisporin B (**7**; 6 mg; t_R 23.2 min), bacillisporin C (**8**; 34 mg; t_R 23.0 min), *epi*-Bacillisporin F (**9**; 11 mg; t_R 29.2 min), whereas fraction S4 yielded funalenone (**10**; 35 mg; t_R 14.2 min), hydroxymellein (**13**; 4 mg; t_R 24.8 min) and 15G256υ (**12**; 27 mg; t_R 14.8 min).

Spectroscopic data

Bacillisporin I (1): Yellow solid; $[\alpha]^{24}_D$ +456 (c 0.24, MeOH); UV (MeOH) λ_{max} (log ε) 206 (4.37), 232 (4.64), 268 (4.23), 316 (3.99), 352 (3.94) nm; ECD (c 3.1×10^{-5} mg/mL; MeOH) λ(Δε) 222 (87.13), 237 (132.65), 301 (–51.71), 335 (10.15), 398 (–7.49); IR (ATR) ν_{max} 3446, 3151, 2975, 1748, 1716, 1667, 1601, 1568, 1507, 1470, 1454, 1430, 1362, 1319, 1267, 1212, 1187, 1126, 1090, 1045, 1023, 891, 867, 816, 803, 792, 762, 726, 701, 668,

603cm^{-1}; NMR (600 MHz, DMSO-*d*6) see Table 1 and Supporting Information, Table S1; HR-ESI(+)MS *m/z* 531.0934 $[M+H]^+$ (calcd for $C_{28}H_{19}O_{11}^+$, 531.0922).

Talarohemiketal A (2): Yellow solid; $[\alpha]^{24}_D$ +231 (c 0.39, MeOH); UV (MeOH) λ_{max} (log ε) 208 (4.79), 236 (4.73), 258 (4.42), 278 (4.23), 322 (–3.53) and 353 (4.07) nm; ECD (c 1.9 × 10^{-6} mg/mL MeOH) λ(Δε) 213 (–5.86), 229 (–2.30), 254 (–1.67), 278 (+3.98), 316 (+0.86), 361 (–1.72); IR (ATR) ν_{max} 3462, 2929, 2855, 1747, 1664, 1601, 1568, 1455, 1367, 1269, 1215, 1056, 816, 742 cm^{-1}; NMR (600 MHz, DMSO-*d*6) see Table 1 and Supporting Information, Table S2; HR-ESI(+)MS *m/z* 531.1294 $[M+H]^+$ (calcd for $C_{29}H_{23}O_{10}^+$, 531.1286).

Talaroazasone A (3): Yellow to orange solid; $[\alpha]^{24}_D$ –116 (c 0.57, MeOH); ECD (5.2×10^{-5} mg/mL MeOH) λ(Δε) 212 (–15.8), 244 (+19.72), 299 (–2.78), 325 (+2.55), 353 (+3.71), 377 (+4.30); UV (MeOH) λ_{max} (log ε) 219 (4.79), 241 (4.73), 273 (4.42), 317 (4.23), 378 (4.08) and 454 (4.07) nm; IR (ATR) ν_{max} 3446, 3173, 2971, 2358C 1748, 1716, 1667, 1601, 1567, 1507, 1470, 1454, 1431, 1361, 1321, 1267, 1212, 1160, 1126, 1090, 1043, 1023, 890, 867, 816, 762, 733, 668, 602, 573 cm^{-1}; NMR (600 MHz, DMSO-*d*$_6$) see Table 1 and Supporting Information, Table S3; HR-ESI(+)MS *m/z* 514.1130 $[M+H]^+$ (calcd for $C_{28}H_{20}NO_9^+$, 514.1133).

Talaromacrolactone A (4): Colorless solid; $[\alpha]^{24}_D$ –18.3 (c 0.46, MeOH); ECD (c 4.1×10^{-4} mg/mL, MeOH) λ(Δε) 219 (–5.81), 243 (5.67), 271 (–2.09), 336 (0.83), 379 (0.96), 400 (–0.24) ; UV (MeCN) λ_{max} (log ε) 217 (4.09), 259 (3.87), 302 (3.68) nm; IR (ATR) ν_{max} 3190, 2973, 1722, 1650, 1450, 1364, 1255, 1174, 1037, 990, 816, 760, 608 cm^{-1}; NMR (600 MHz, DMSO-*d*$_6$) see Table 1 and Supporting Information, Table S4; HR-ESI(+)MS *m/z* 491.1529 $[M+Na]^+$ (calcd for $C_{22}H_{28}O_{11}Na^+$, 491.1524).

Talarolactone A (5): Yellow solid; $[\alpha]^{24}_{D}$ +56 (c 0.57, MeOH); UV (MeOH) λ_{max} (log ε) 215 (4.59), 242 (4.72), 362 (3.80) nm; IR (ATR) ν_{max} 3446, 3173, 2971, 2358, 1748, 1716, 1667, 1601, 1567, 1507, 1470, 1454, 1431, 1361, 1321, 1267, 1212, 1160, 1126, 1090, 1043, 1023, 890, 867, 816, 762, 733, 668, 602, 573 cm^{-1}; NMR (600 MHz, DMSO-*d*6) see Supporting Information, Table S5.

Bacillisporin A (6): Off-white solid, $[\alpha]^{24}_{D}$: +417 (c 0.92, MeOH); NMR (600 MHz, DMSO-d_6) see Supporting Information, Table S6.

Bacillisporin B (7): Pale yellow solid, $[\alpha]^{24}_{D}$: +384 (c 0.41, MeOH); NMR (600 MHz, DMSO-d_6) see Supporting Information, Table S7.

Bacillisporin C (8): Yellow solid, $[\alpha]^{24}_{D}$: +449 (c 0.78, MeOH); NMR (600 MHz, DMSO-d_6) see Supporting Information, Table S8.

***epi*-Bacillisporin F** (9): Yellow solid; $[\alpha]^{24}_{D}$ +414 (c 0.66, MeOH); UV (MeOH) λ_{max} (log ε) 208 (4.59), 230 (4.73), 270 (4.45), 315 (4.04), 350 (3.98) nm; ECD (c 1.1×10^{-5} mg/mL; MeOH) λ(Δε) 222(–87.98), 242 (144.93), 301 (–52.17), 334 (12.01), 400 (–6.32); IR (ATR) ν_{max} 3432, 3173, 2977, 2895, 2836, 1748, 1716, 1667, 1602, 1568, 1507, 1469, 1454, 1431, 1362, 1319, 1267, 1212, 1186, 1161, 1126, 1091, 1045, 1023, 890, 868, 814, 802, 761, 748, 726, 704, 661, 649, 617, 602 cm^{-1}; NMR (600 MHz, DMSO-d_6) see Supporting Information Table S9; HR-ESI(+)MS $[M+H]^+$ *m/z* 545.1093 (calcd for $C_{29}H_{21}O_{11}$, 545.1078).

Funalenone (10): Yellow solid, NMR (600 MHz, DMSO-d_6) see Supporting Information, Table S10.

15G256α (11): Colorless solid, $[\alpha]^{24}_{D:}$ – 22.1 (c 0.67, MeOH); NMR (600 MHz, DMSO-

d$_6$) see Supporting Information, Table S11.

15G256ν (12): Colorless solid, $[\alpha]^{24}_{D:}$ – 19.6 (c 0.32, MeOH); NMR (600 MHz, DMSO-*d*$_6$) see Supporting Information, Table S12.

6-Hydroxymellein (13): Colorless oil, $[\alpha]^{24}_{D:}$ – 31.8 (c 0.49, MeOH); NMR (600 MHz, DMSO-*d*$_6$) see Supporting Information, Table S13**.**

Bioactivity Screening

Test compounds were dissolved in DMSO to provide 10 mg/mL stock solutions (or 1 mg/mL for compounds of limited quantities). An aliquot of each stock solution was transferred to the first lane of rows B to G in a 96-well microtiter plate and two-fold serially diluted across the 12 lanes of the plate to provide a 2,048-fold concentration gradient. Bioassay medium was added to an aliquot of each test solution to provide a 100-fold dilution into the final bioassay, thus yielding a test range of 100 to 0.05 μg/mL in 1% DMSO. Row A was used as the negative control (no inhibition) and Row H was used as the positive control (uninoculated).

CyTOX,[31] is an indicative bioassay platform for discovery of antitumor actives. NS-1 (ATCC TIB-18) mouse myeloma cells were inoculated in 96-well microtiter plates (190 μL) at 50,000 cells/mL in DMEM (Dulbecco's Modified Eagle Medium + 10% fetal bovine serum (FBS) + 1% penicillin/streptomycin (Life Technologies)) and incubated in 37 °C (5% CO_2) incubator. At 48 h, resazurin (250 μg/mL; 10 μL) was added to each well and the plates were incubated for a further 48 h. MIC end points were determined visually.

ProTOX,[31] is a generic bioassay platform for antibiotic discovery. *Bacillus subtilis* (ATCC 6633) and *Escherichia coli* (ATCC 25922) were used as indicative species for Gram positive and negative antibacterial activity, respectively. A bacterial suspension (50 mL in 250 mL flask) was prepared in nutrient broth by cultivation for 24 h at 100 rpm 250 rpm, 28 °C. The suspension was diluted to an absorbance of 0.01 absorbance units per mL, and 10 μL aliquots were added to the wells of a 96-well microtiter plate, which contained the test compounds dispersed in nutrient agar (Amyl) with resazurin (12.5 μg/mL). The plates were incubated at 28 °C for 48 h during which time the negative control wells change from a blue to light pink color. MIC end points were determined visually.

EuTOX,[31] is a generic bioassay platform for antifungal discovery. The yeasts *Candida albicans* (ATCC 10231) and *Saccharomyces cerevisiae* (ATCC 9763) were used as indicative species for antifungal activity. A yeast suspension (50 mL in 250 mL flask) was prepared in 1% malt extract broth by cultivation for 24 h at 250 rpm, 24 °C. The suspension was diluted to an absorbance of 0.005 and 0.03 absorbance units per mL for *C. albicans* and S. *cerevisiae*, respectively. Aliquots (20 μL and 30 μL) were applied to the wells of a 96-well microtiter plate, which contained the test compounds dispersed in malt extract agar containing bromocresol green (50 μg/mL). The plates were incubated at 24 °C for 48 h during which time the negative control wells change from a blue to yellow color. MIC end points were determined visually.

TriTOX,[31] is a bioassay focused on the discovery of inhibitors of the animal protozoan pathogen, *Tritrichomonas foetus* (strain KV-1). *T. foetus* were inoculated in 96-well microtiter plates (200 μL) at 4×10^4 cells/mL in *T. foetus* medium (0.2%

tryptone, Oxoid; 0.1% yeast extract, Difco; 0.25% glucose; 0.1% L-cysteine; 0.1% K_2HPO_4; 0.1% KH_2PO_4; 0.1% ascorbic acid; 0.01% $FeSO_4.7H_2O$; 1% penicillin/streptomycin, 10% new born calf serum (NBCS), Life Technologies). The plates were incubated in anaerobic jars (Oxoid AG25) containing an Anaerogen satchel (Oxoid AN25) in a 37 °C (5% CO_2) incubator. At 72 h, *T. foetus* proliferation was counted and % inhibition was graphed to determine the MIC values.

Conflicts of interest

There are no conflicts to declare.

Acknowledgements

We thank Dr M. McKay (APAF, Macquarie University) for the acquisition of HRMS data. This research was funded, in part, by the Australian Research Council (DP130103281 to PK and AMP; FT130100142 to AMP) and Macquarie University (iMQRES scholarship to NC).

References

(1) Zhai, M.-M.; Li, J.; Jiang, C.-X.; Shi, Y.-P.; Di, D.-L.; Crews, P.; Wu, Q.-X., *Nat. Prod. Bioprospect.* **2016,** 6, (1), 1-24.

(2) Birkinshaw, J. H.; Chambers, A. R.; Raistrick, H., *Biochem. J.* **1942,** 36, (1-2), 242.

(3) Shibata, S.; Ogihara, Y.; Tokutake, N.; Tanaka, O., *Tetrahedron Lett.* **1965**, (18), 1287-8.

(4) Yamazaki, M.; Okuyama, E., *Chem. Pharm. Bull.* **1980,** 28, (12), 3649-55.

(5) Dethoup, T.; Manoch, L.; Kijjoa, A.; Nascimento, M. S. J.; Puaparoj, P.; Silva, A. M. S.; Eaton, G.; Herz, W., *Planta Med.* **2006,** 72, (10), 957-960.

(6) Wu, B.; Ohlendorf, B.; Oesker, V.; Wiese, J.; Malien, S.; Schmaljohann, R.; Imhoff, J. F., *Mar. Biotechnol.* **2015,** 17, (1), 110-119.

(7) Zang, Y.; Genta-Jouve, G.; Escargueil, A. E.; Larsen, A. K.; Guedon, L.; Nay, B.; Prado, S., *J. Nat. Prod.* **2016,** 79, (12), 2991-2996.

(8) Zang, Y.; Genta-Jouve, G.; Retailleau, P.; Escargueil, A.; Mann, S.; Nay, B.; Prado, S., *Org. Biomol. Chem.* **2016,** 14, (9), 2691-2697.

(9) He, J.-W.; Mu, Z.-Q.; Gao, H.; Chen, G.-D.; Zhao, Q.; Hu, D.; Sun, J.-Z.; Li, X.-X.; Li, Y.; Liu, X.-Z., *Tetrahedron Lett.* **2014,** 70, (29), 4425-4430.

(10) Arai, M.; Tomoda, H.; Okuda, T.; Wang, H.; Tabata, N.; Masuma, R.; Yamaguchi, Y.; Omura, S., *J. Antibiot.* **2002,** 55, (2), 172-180.

(11) Chaudhary, N. K. Natural products from some filamentous fungi and other sources. PhD thesis, Macquarie University, Australia, 2017.

(12) Elsebai, M. F.; Saleem, M.; Tejesvi, M. V.; Kajula, M.; Mattila, S.; Mehiri, M.; Turpeinen, A.; Pirttila, A. M., *Nat. Prod. Rep.* **2014,** 31, (5), 628-645.

(13) Cooke, R.; Edwards, J., Naturally occurring phenalenones and related compounds. In *Fortschritte der Chemie organischer Naturstoffe/Progress in the Chemistry of Organic Natural Products*, Springer: 1981; pp 153-190.

(14) Barton, D.; De Mayo, P.; Morrison, G.; Raistrick, H., *Tetrahedron* **1959,** 6, (1), 48-62.

(15) Roy, K.; Chatterjee, S.; Deshmukh, S.; Vijayakumar, E.; Ganguli, B.; Fehlhaber, H.-W., *J. Antibiot.* **1996,** 49, (11), 1186-1187.

(16) Schlingmann, G.; Milne, L.; Carter, G., *Tetrahedron Lett.* **2002,** 58, (34), 6825-6835.

(17) Chinworrungsee, M.; Kittakoop, P.; Isaka, M.; Maithip, P.; Supothina, S.; Thebtaranonth, Y., *J. Nat. Prod.* **2004,** 67, (4), 689-692.

(18) Ruanglek, V.; Chokpaiboon, S.; Rattanaphan, N.; Madla, S.; Auncharoen, P.; Bunyapaiboonsri, T.; Isaka, M., *J. Antibiot.* **2007,** 60, (12), 748.

(19) Breinholt, J.; Jensen, G. W.; I, N. R.; Olsen, C. E.; Frisvad, J. C., *J. Antibiot.* **1993,** 46, (7), 1101-1108.

(20) Kondo, H., *Jpn Kokai Tokkyo Koho: JP 05032658* **1993**.

(21) Zhou, Z.-Y.; Liu, R.; Jiang, M.-Y.; Zhang, L.; Niu, Y.; Zhu, Y.-C.; Dong, Z.-J.; Liu, J.-K., *Chem. Pharm. Bull.* **2009,** 57, (9), 975-978.

(22) Boonyaketgoson, S.; Trisuwan, K.; Bussaban, B.; Rukachaisirikul, V.; Phongpaichit, S., *Tetrahedron Lett.* **2015,** 56, (36), 5076-5078.

(23) Ito, M.; Tsuchida, Y.; Mizoue, K.; Hanada, K., *J. Antibiot.* **1992,** 45, (10), 1566-1572.

(24) Lin, Z.; Zhu, T.; Fang, Y.; Gu, Q.; Zhu, W., *Phytochemistry* **2008,** 69, (5), 1273-1278.

(25) Guo, Z.; Shao, C.; She, Z.; Cai, X.; Liu, F.; Vrijimoed, L. L. P.; Lin, Y., *Magn. Reson. Chem.* **2007,** 45, (5), 439-441.

(26) Shibata, T.; Nishikawa, M.; Tsurumi, Y.; Takase, S.; Terano, H.; Kohsaka, M., *J. Antibiot.* **1989,** 42, (9), 1356-1361.

(27) Inokoshi, J.; Shiomi, K.; Masuma, R.; Tanaka, H.; Yamada, H.; Omura, S., *J. Antibiot.* **1999,** 52, (12), 1095-1100.

(28) Schlingmann, G.; Milne, L.; Williams, D. R.; Carter, G. T., *J. Antibiot.* **1998,** 51, (3), 303-316.

(29) Silber, J.; Ohlendorf, B.; Labes, A.; Erhard, A.; Imhoff, J. F., *Marine drugs* **2013,** 11, (9), 3309-3323.

(30) Cao, P.; Yang, J.; Miao, C.-P.; Yan, Y.; Ma, Y.-T.; Li, X.-N.; Zhao, L.-X.; Huang, S.-X., *Org. Lett.* **2015,** 17, (5), 1146-1149.

(31) Lacey, H. J.; Vuong, D.; Pitt, J. I.; Lacey, E.; Piggott, A. M., *Aust. J. Chem.* **2016,** 69, (2), 152-160.

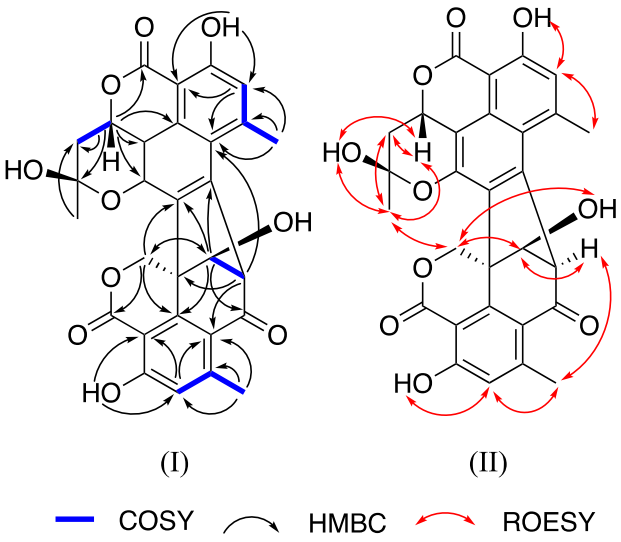

Figure 1: Key (I) HMBC, COSY correlations and (II) ROESY correlations in **2**

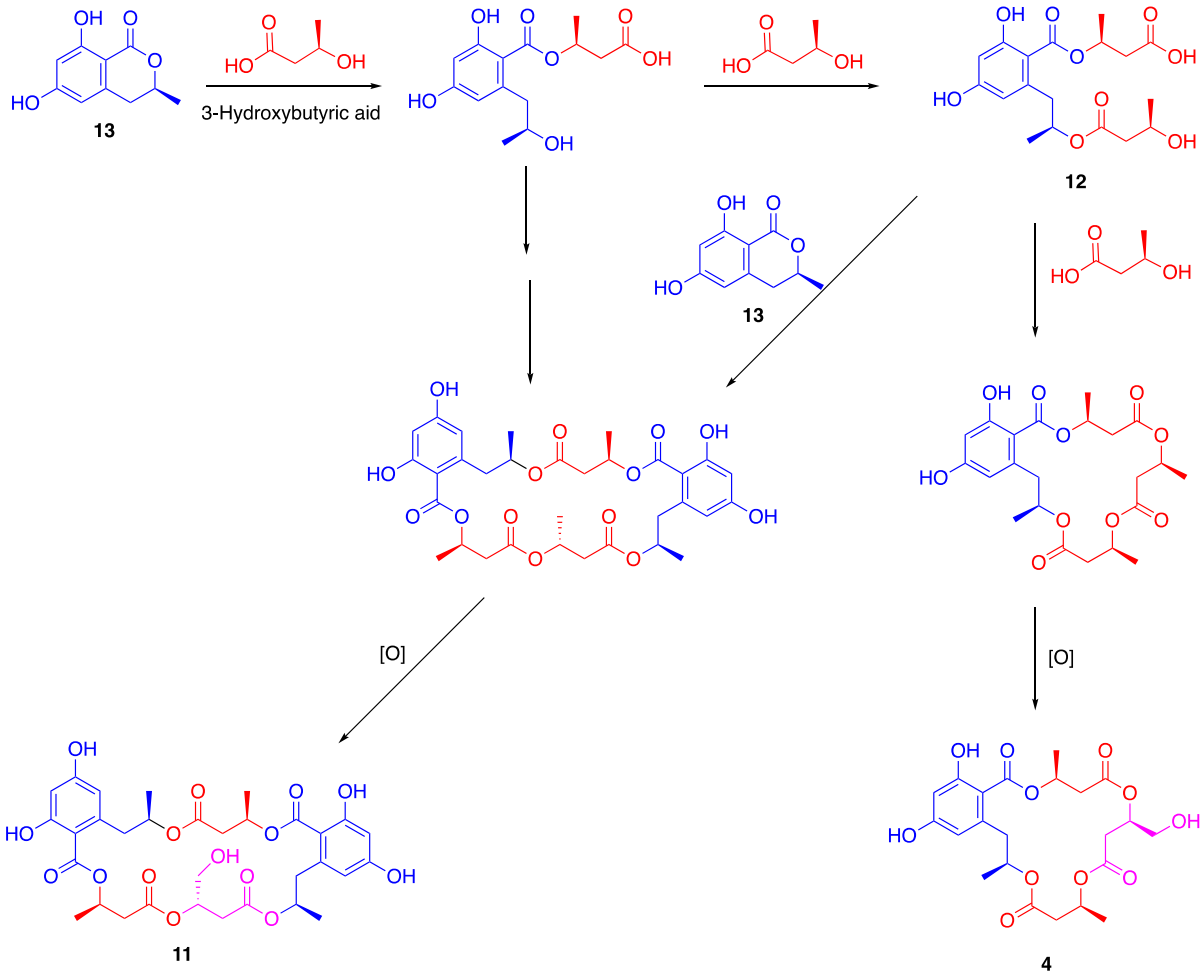

Figure 2: Proposed biogenesis of the new macrolide polyester **4** and reported polyesters isolated

Table 1: ^{1}H and ^{13}C NMR data of **1-3** in DMSO-d_6

Position	Bacillisporin I (**1**, Major isomer)		Bacillisporin I (**1**, Minor isomer)		Talarohemiketal A (**2**)		Talaroazasone A (**3**)	
	δ_C	δ_H, multi, (*J*, Hz)	δ_C	δ_H, multi, (*J*, Hz)	δ_C	δ_H, multi, (*J*, Hz)	δ_C	δ_H, multi, (*J*, Hz)
1	92.4	6.98, br s	92.5	7.00, br s	70.6	5.83, dd (*12.0, 5.9*)	141	8.41, d (*5.3*)
2								13.25, d (*5.3*)
3	169.1		169.0		169.9		166.1	
3a	97.4		97.3		98.9		108.1	
3b	130.5		130.7		130.7		135.3	
4	162.5		162.5		161.7		164.1	
5	119.1	6.99, br s	119.2	6.99, br s	119.3	6.97, br s	117.3	6.94, br s
6	146.2		146.2		146.1		148.9	
6a	118.4		118.3		118.6		113.9	
7	138		138.0		138.8		151.1	
8	134.1		134.1		132.7		139.4	
9	150.6		150.6		147.7		176.7	
9a	112.2		112.4		107.7		113.6	
6-CH_3	24.2	2.96, br s	24.3	2.95, br s			24.3	2.94, br s
1-OH		7.91, br s		8.07, br s				
4-OH		11.99, s		12.04, s				13.09, s
9-OH		10.54, s		10.41, s				
1'	68.7	5.09, d (*13.3*, *3.6*) 5.11, d (*13.3, 3.6*)	68.6	5.01, d (*13.0, 2.0*) 5.03, d (*13.0, 2.0*)	69.8	5.09, s		4.91, d (*12.2*) 5.00, d (*12.2*)
3'	167.2		167.3		167.7			
3a'	103.9		103.7		103.8			
3b'	146.4		146.6		147.7			
4'	163.2		163.3		163.2			
5'	120.2	6.90, br s	120.2	6.88, br s	119.8	6.83, br s		6.90, br s
6'	152.6		152.6		152.3			
6a'	116.5		116.3		116.8			
7'	191		191.0		192.6			
8'	61.3	5.01, br s	61.3	5.03, br s	64.5	4.80, br s		4.92, br s
9'	85.5	5.81, br s	85.2	5.82, br s	85.8	4.78, br s		5.73, s
9a'	47.9		48.1		49.4			
6'-CH_3	23.1	2.52, br s	23.0	2.49, br s	23.2	2.97, br s		2.51, br s
9'-$\underline{C}OCH_3$	170.0		170.0				170.1	
9'-$CO\underline{C}H_3$	20.6	1.98, s	20.7	2.02, s			20.8	2.03, s
4'-OH		11.96, s		11.97, s		12.01, br s		11.98, s
9'-OH						6.31, br s		
11					100.0			
12					36.4	2.16, dd (14.0, 12.0) 2.50, d (14.0)		
11-CH_3					27.7	1.63, s		
11-OH						7.26, br s		

Table 2: Antibacterial (ProTOX), antifungal (EuTOX), cytotoxicty (CyTOX), and antiprotozoan (TriTOX) minimum inhibitory concentrations (MICs) of compounds **1-13**.

Compound	ProTOX[a] (μg/mL)	EuTOX[b] (μg/mL)	CyTOX[c] (μg/mL)	TriTOX (μg/mL)
1	-	-	-	-
2	-	-	-	-
3	-	-	-	-
4	-	-	-	-
5	25	>200	50	100
6	1.6	>200	>100	50
7	-	-	-	-
8	50	>200	>100	>100
9	6.3	>200	50	>100
10	>100	>200	100	>100
11	25	>200	25	>100
12	50	>200	25	>100
13	-	-	-	-

[a] *Bacillus subtilis* (ATCC 6633), *Escherichia coli* (ATCC 25922)

[b] *Saccharomyces cerevisiae* (ATCC 9763), *Candida albicans* (ATCC 10231)

[c] mouse myeloma NS-1 cell line (ATCC TIB-18)

- Insufficient for bioassay

Supporting Information

Structure revision of talaromycesone A and new phenalenones and polyesters from *Talaromyces stipitatus*

Nirmal K. Chaudhary[†], *Ernest Lacey*[§,†], *Andrew M. Piggott*[†], *Peter Karuso*[†,*]

[†]*Department of Molecular Sciences, Macquarie University, NSW 2109, Australia*

[§]*Microbial Screening Technologies Pty. Ltd., Smithfield, NSW 2164, Australia*

* Corresponding author: peter.karuso@mq.edu.au

Table of Contents

A. NMR tables

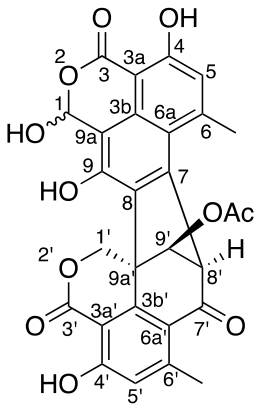

Bacillisporin I (**1**)

Table S1: NMR data of bacillisporin I (**1**) in DMSO-d_6

Position	Major isomer		Minor isomer		2D Correlations		
	δ_H, mult (*J*, Hz)	δ_C	δ_H, mult (*J*, Hz)	δ_C	^1H-^{13}C HMBC	COSY	ROESY
1	6.98, br s	92.4	7.00, br s	92.5	3, 3b, 9, 6a (w), 9a	1-OH	1-OH
3		169.1		169.0			
3a		97.4		97.3			
3b		130.5		130.7			
4		162.5		162.5			
5	6.99, br s	119.1	6.99, br s	119.2	3a, 6a, 6-CH_3, 3 (w)	6-CH_3(w)	6-CH_3, 4-OH
6		146.2		146.2			
6a		118.4		118.3			
7		138.0		138.0			
8		134.1		134.1			
9		150.6		150.6			
9a		112.2		112.4			
6-CH_3	2.96, br s	24.2	2.95, br s	24.3	5, 6, 6a, 3b (w)	5 (w)	5, 8'
1-OH	7.91, br s		8.07, br s			1	1
4-OH	11.99, s		12.04, s		3a, 4, 5, 6 (w)		5
9-OH	10.54, s		10.41, s		8, 9, 9a, 7 (w)		1
1'	5.09, d (*13.3*, *3.6*) 5.11, d (*13.3, 3.6*)	68.7	5.01, d (*13.0, 2.0*) 5.03, d (*13.0, 2.0*)	68.6	8, 3', 3b', 9', 9a', 6a' (w) 8, 3', 3b', 9', 9a', 6a' (w)		9', 9-OH 9', 9-OH
3'		167.2		167.3			
3a'		103.9		103.7			
3b'		146.4		146.6			
4'		163.2		163.3			

5'	6.90, br s	120.2	6.88, br s	120.2	3a', 6a', 6-CH_3', 3' (w)	6-CH_3'(w)	6-CH_3', 4-OH'
6’		152.6		152.6			
6a'		116.5		116.3			
7'		191.0		191.0			
8'	5.01, br s	61.3	5.03, br s	61.3	6a, 8, 6a', 9a', 6'	9'	6-CH_3, 9'
9'	5.81, br s	85.5	5.82, br s	85.2	7, 8, 7', 3b'	8'	8'
9a'		47.9		48.1			
6'-CH_3	2.52, br s	23.1	2.49, br s	23.0	5', 6', 6a', 3b' (w)	5' (w)	5'
9'- $\underline{C}OCH_3$		170.0		170.0			
9'-$CO\underline{CH_3}$	1.98, s	20.6	2.02, s	20.7	9'- $\underline{C}OCH_3$		
4'-OH	11.96, s		11.97, s		3a', 4', 5', 6' (w)		5'

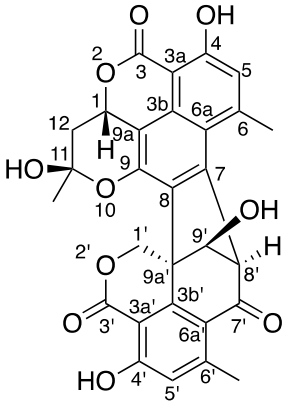

Talarohemiketal A (**2**)

Table S2: NMR data of talarohemiketal C (**2**) in DMSO-d_6

Position	δ_H, mult (*J*, Hz)	δ_C	^{1}H-^{13}C HMBC	COSY	ROESY
1	5.83, dd (*12.0, 5.9*)	70.6	3, 3b, 9, 6a (w), 9a, 11	12	12, 11-OH, 11-CH_3
3		169.9			
3a		98.9			
3b		130.7			
4		161.7			
5	6.97, br s	119.3	3a, 6a, 6-CH_3, 3 (w)	6-CH_3	6-CH_3, 4-OH
6		146.1			
6a		118.6			
7		138.8			
8		132.7			
9		147.7			

9a		107.7			
11		100.0			
12	2.16, dd (*14.0, 12.0*) 2.50, d (*14.0*)	36.4	1, 11, 9a, 11-CH_3	1	1, 11-CH_3
6-CH_3	2.97, br s	24.2	5, 6, 6a, 3b (w)	5 (w)	5, 8'
11-CH_3	1.63, s	27.7	11, 12		1, 12, 11-OH
4-OH	11.59, br s		3a, 4, 5, 6 (w)		5
11-OH	7.26, br s				1, 11-CH_3
1'	5.09, s	69.8	8, 3', 3b', 9', 9a', 6a' (w)		9', 9-OH, 11-CH_3
3'		167.7			
3a'		103.8			
3b'		147.7			
4'		163.2			
5'	6.83, br s	119.8	3a', 6a', 6-CH_3', 3'(w)	6-CH_3'	6-CH_3', 4-OH'
6’		152.3			
6a'		116.8			
7'		192.6			
8'	4.80, br s	64.5	6a, 8, 6a', 9a', 6'	9'	6-CH_3, 9'
9'	4.78, br s	85.8	7, 8, 7', 3b'	8'	8'
9a'		49.4			
6'-CH_3	2.47, br s	23.2	5', 6', 6a', 3b' (w)	5' (w)	5'
4'-OH	12.01, br s		3a', 4', 5', 6' (w)		5'
9'-OH	6.31, br s				

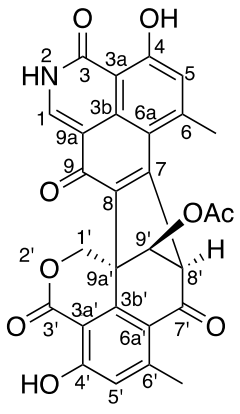

Talaroazasone A (**3**)

Table S3: NMR data of talaroazasone (**3**) in DMSO-d_6

Position	δ_H, multi (*J*, Hz)	δ_C	^1H-^{13}C HMBC	COSY	ROESY
1	8.41, d (*5.3*)	141.0	3, 3b, 9, 6a (w), 9a (w)	2	2
2	13.25, d (*5.3*)		3a, 9a	1	1
3		166.1			
3a		108.1			
3b		135.3			
4		164.1			
5	6.94, br s	117.3	3a, 6a, 6-CH_3, 3 (w)	6-CH_3 (w)	6-CH_3, 4-OH
6		148.9			
6a		113.9			
7		151.1			
8		139.4			
9		176.7			
9a		113.6			
6-CH_3	2.94, br s	24.3	5, 6, 6a, 3b (w)	5 (w)	5, 8'
4-OH	13.09, s		3a, 4, 5, 6 (w)		5
1'	4.91, d (*12.2*) 5.00, d (*12.2*)	68.0	8, 9a, 3', 3b', 9', 6a' (w)		9'
3'		167.3			
3a'		104.3			
3b'		146.5			
4'		163.3			
5'	6.90, br s	120.1	3a', 6a', 6-CH_3', 3' (w)	6-CH_3 '(w)	6-CH_3', 4-OH'
6'		152.7			
6a'		116.6			
7'		190.2			
8'	4.92, br s	62.8	6a, 8, 6a', 9', 9a', 6' (w)	9'	6-CH_3, 9'
9'	5.73, s	83.9	7, 8, 7', 3b', 1', 8', 9-$\underline{C}OCH_3$	8'	1', 8'
9a'		47.6			
6'-CH_3	2.51, br s	23.2	5', 6', 6a', 3b'	5' (w)	5'
9'-$\underline{C}OCH_3$		170.1			
9'-CO$\underline{CH_3}$	2.03, s	20.8	9'- $\underline{C}OCH_3$		
4'-OH	11.98, s		3a', 4', 5', 6' (w)		5'

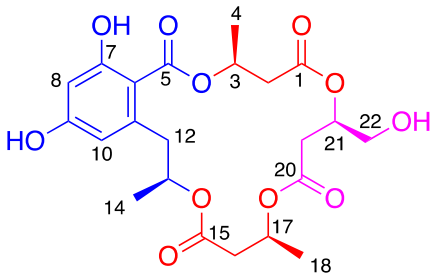

talaromacroclactone A (**4**)

Table S4: NMR data of talaromacroclactone A (**4**) in DMSO-d_6

Position	δ_H, mult (*J*, Hz)	δ_C	^1H-^{13}C HMBC	COSY	ROESY
1		169.5			
2	2.72, m 2.78, m	40.0[b]	1, 3, 4	3	3, 4
3	5.39, m	67.9	1, 2, 4	2, 4	2, 4
4	1.32, d (*6.3*)	19.5	2, 3	3	2, 3
5		168.3			
6		109.0			
7		159.9			
8	6.18, d (*2.3*)	101.2	6, 7, 9, 10, 5 (w)	10	7-OH
9		160.4			
10	6.15, d (*2.3*)	110.3	6, 8, 9, 12, 5 (w)	8	12, 13, 14
11		139.5			
12	2.81, m 2.77, m	40.2[b]	6, 10, 11, 13, 14	13	10, 13, 14
13	4.96, m	70.4	11, 12, 15, 14	12, 14	10, 12, 14
14	1.13, d (*6.3*)	19.7	12, 13	13	12, 13, 10
15		170.3			
16	2.19, dd (*14.7*, *6.7*) 2.30, dd (*14.7*, *6.7*)	44.3	15, 17, 18	17	17, 18
17	3.91, q (*6.5*)	63.3	15, 16, 19, 18	16, 18	16, 18
18	0.99, d (*6.3*)	23.0	16, 17	17	16, 17
19		175.1			
20	2.44, br d (*18.3*) 3.03, dd (*18.3*, *6.7*)	34.2	19, 21, 22	21	21, 22
21	5.39, m	70.6	1, 19, 20, 22	20, 22	20, 22
22	4.28, br d (*10.7*) 4.49, dd (*10.7*, *4.7*)	72.6	20, 21	21	20, 21
7-OH	10.39, s		6 (w), 8 (w)		8
9-OH	9.93, s				
22-OH	[a]				

[a] Not observed; [b] Masked under DMSO-d_6 peak

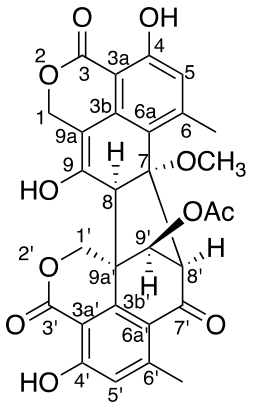

Talarolactone (**5**)

Table S5a: NMR data of talarolactone (**5**) in DMSO-d_6

Position	δ_H, mult (*J*, Hz)	δ_C	^{1}H-^{13}C HMBC	COSY	ROESY
1a	4.72, dd (*13.4, 2.2*)	64.5	3 (w), 3b (w), 6a (w), 9, 9a		9-OH
1b	4.90, d (*13.4*)		3, 3b, 9, 6a, 9a, 8 (w), 9' (w)		9-OH
3		169.3			
3a		100.4			
3b		137.4			
4		160.8			
5	6.46, d (*0.6*)	115.9	3a, 6a, 6-CH_3, 3 (w)	6-CH_3 (w)	6-CH_3, 4-OH
6		147.5			
6a		117.5			
7		86.2			
8	3.82, d (*2.2*)	55.9	6a, 7, 9, 9a, 1', 3b', 8', 9', 9a'		1', 7-OCH_3
9		150.5			
9a		98.6			
6-CH_3	2.45, d (*0.6*)	20.7	5, 6, 6a	5 (w)	5, 8'
7-OCH_3	2.85, s	51.6	7		8
4-OH	10.91, s		3a, 4, 5, 6 (w)		5
9-OH	10.29, s		8, 9, 9a, 3b (w)		1, 1'
1'	5.00, d (*11.9*) 5.12, d (*11.9*)	70.0	3', 3b', 6a', 9', 9a'		8, 9', 9-OH
3'		167.3			
3a'		105.1			
3b'		144.3			
4'		163.1			
5'	6.70, d (*0.7*)	119.5	3a', 6a', 6-CH_3', 3' (w)	6-CH_3 '(w)	6-CH_3', 4-OH'
6'		149.6			
6a'		121.0			
7'		191.5			

8'	4.00, br s	67.7	6a, 7, 8, 6a', 7', 9', 9a', 1' (w), 5' (w), 6' (w)	9'	6-CH_3, 9'
9'	5.15, br s	76.3	7, 8, 7', 3b'	8'	8'
9a'		50.6			
6'-CH_3	1.94, d (*0.7*)	21.2	5', 6', 6a'	5' (w)	5'
9'-$\underline{C}OCH_3$		169.7			
9'-$COCH_3$	2.15, s	20.9	9'-$\underline{C}OCH_3$		
4'-OH	11.72, s		3a', 4', 5', 6' (w)		5'

Table S5b: Comparison of NMR data of talarolactone (**5**) in acetone-d_6

Position	Observed values		Literature values	
	δ_H, mult (*J*, Hz)	**δ_C**	**δ_H, mult (*J*, Hz)**	**δ_C**
1	4.79, dd (*13.6*, *2.1*) 5.05, dd (*13.6*, *0.8*)	65.4		170.5
3		170.5		165.0
3a		101.5		101.6
3b		137.9		137.9
4		162.6		162.7
5	6.48, d (*0.8*)	117.4	6.49, d (*0.5*)	117.5
6		149.1		149.1
6a		118.7		118.7
7		87.8		87.8
8	4.02, d (*2.1*)	57.5	4.03, d (*1.9*)	57.6
9		150.5 br	4.83, dd (*13.9*, *1.9*) 5.08, dd (*13.9*, *0.9*)	65.4
9a		100.9		100.8
6-CH_3	2.55, d (*0.8*)	21.5	2.58, d (*0.5*)	21.5
7-OCH_3	2.95, s	51.2	2.98, s	51.2
4-OH	11.12, s			
9-OH	9.05, br s			
1'	5.21, d (*12.1*) 5.07, d (*12.1*)	71.6	5.22, d (*12.2*) 5.10, d (*12.2*)	71.6
3'		169.0		169.0
3a'		106.0		106.0
3b'		145.4		145.4
4'		165.0 br		165.0
5'	6.66, d (*0.8*)	120.6	6.67, d (*0.5*)	120.2
6'		151.4		151.3
6a'		122.2		122.2
7'		192.2		192.2
8'	4.14, s	69.1	4.16, s	69.1
9'	5.17, br s	77.6	5.19, s	77.7

9a'		53.0		53.0
6'-CH_3	2.03, d (*0.8*)	22.0	2.06, d (*0.5*)	22.0
9'-$\underline{C}OCH_3$		170.3		170.3
9'-$CO\underline{CH_3}$	2.15, s	20.9	2.19, s	20.9
4'-OH	11.86, br s			

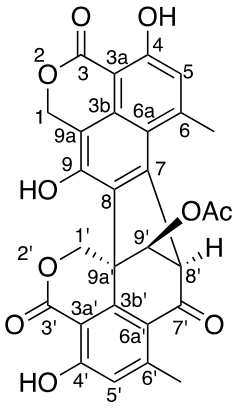

Bacillisporin A (**6**)

Table S6: NMR data of bacillisporin A (**6**) in DMSO-d_6

Position	δ_H, multi (*J*, Hz)	δ_C	^1H-^{13}C HMBC	COSY	ROESY
1	5.70, d (*15.2*) 5.66, d (*15.2*)	66.8	3, 3b, 9, 6a, 9a		9-OH
3		169.3			
3a		97.6			
3b		131.5			
4		161.7			
5	6.96, br s	119.5	3a, 6a, 6-CH_3	6-CH_3 (w)	6-CH_3, 4-OH
6		145.8			
6a		118.6			
7		136.0			
8		134.3			
9		148.3			
9a		110.3			
6-CH_3	2.93, br s	24.3	5, 6, 6a	5 (w)	5, 8'
4-OH	11.87, s		3a, 4, 5		5
9-OH	10.14, s		8, 9, 9a, 7 (w)		1, 1'
1'	5.03, d (*12.3*) 5.11, d (*12.3*)	68.7	3', 3b', 6a', 9', 9a'		9-OH, 9'
3'		167.4			
3a'		103.8			

3b'		146.6			
4'		163.3			
5'	6.89, br s	120.2	3a', 6a', 6-CH_3'	6-CH_3'(w)	6-CH_3', 4-OH'
6'		152.7			
6a'		116.4			
7'		191.2			
8'	4.99, br s	61.2	6a, 8, 6a', 9a', 5'	9'	9'
9'	5.80, br s	85.3	7, 8, 7', 3b'	8'	6-CH_3, 8'
9a'		48.0			
6'-CH_3	2.49, br s	23.2	5', 6', 6a'	5' (w)	5'
9'-$\underline{C}OCH_3$		170.1			
9'-CO$\underline{CH_3}$	2.00, s	20.8	9'-$\underline{C}OCH_3$		
4'-OH	11.95, s		3a', 4', 5'		5'

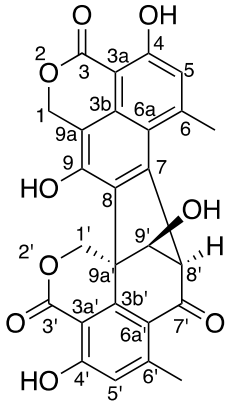

Bacillisporin B (**7**)

Table S7: NMR data of bacillisporin B (**7**) in DMSO-d_6

Position	δ_H, mult (*J*, Hz)	δ_C	^1H-^{13}C HMBC	COSY	ROESY
1	5.71, d (*15.0*) 5.64, d (*15.0*)	66.8	3, 3b, 9, 6a, 9a		9-OH
3		169.4			
3a		97.5			
3b		131.3			
4		161.5			
5	6.95, br s	119.1	3a, 6a, 6-CH_3, 3 (w)	6-CH_3 (w)	6-CH_3, 4-OH
6		145.9			
6a		119.1			
7		137.3			
8		134.8			
9		148.9			
9a		109.7			

6-CH_3	2.96 br s	24.4	5, 6, 6a	5 (w)	5, 8'
4-OH	11.85, br s				
9-OH	9.94 s		8, 9, 9a, 7 (w)		1, 1'
1'	5.12 d (*13.9*) 4.97 d (*13.9*)	70.1	3', 3b', 6a', 9', 9a'		9-OH, 9'
3'		167.9			
3a'		103.8			
3b'		147.8			
4'		163.1			
5'	6.83 br s	119.7	3a', 6a', 6-CH_3', 3' (w)	6-CH_3'(w)	6-CH_3', 4-OH'
6'		152.3			
6a'		116.8			
7'		192.8			
8'	4.81 br s	64.6	6a, 8, 6a', 9a', 5'	9'	9'
9'	4.76 br s	85.3	7, 8, 7', 3b'	8'	6-CH_3, 8'
9a'		49.6			
6'-CH_3	2.48 br s	23.2	5', 6', 6a'	5' (w)	5'
4'-OH	11.99 s		3a', 4', 5'		5'
9'-OH	[a]				

[a] Not observed

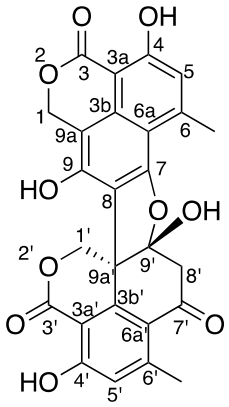

Bacillisporin C (**8**)

Table S8: NMR data of bacillisporin C (**8**) in DMSO-d_6

Position	δ_H, mult (*J*, Hz)	δ_C	^{1}H-^{13}C HMBC	COSY	ROESY
1	5.46, d (*14.3*) 5.62, d (*14.3*)	66.7	3, 3b, 9, 6a, 9a, 8 (w)		9-OH
3		169.6			
3a		96.8 br			
3b		132.0			
4		162.6			
5	6.81, br s	117.0	3a, 6a, 6-CH_3, 6 (w)	6-CH_3	6-CH_3, 4-OH
6		145.9			
6a		108.6 br			
7		155.1			
8		113.8			
9		150.2			
9a		102.1			
6-CH_3	2.74, br s	23.1	5, 6, 6a, 3b (w), 9a (w), 4 (w), 7 (w)	5 (w)	5 (w), 8'
4-OH	11.64, br s				5
9-OH	9.87, br s		8', 9', 9a', 7 (w)		1
1'	4.60, d (*11.3*) 4.91, d (*11.3*)	68.7	8, 3a', 3b', 6a' (w)		9'-OH
3'		168.9			
3a'		109.5			
3b'		144.2			
4'		162.8			
5'	6.97, br s	119.9	3a', 6a', 6-CH_3'	6-CH_3'	6-CH_3', 4-OH'
6'		148.6			
6a'		121.0			
7'		193.2			
8'	3.08 d (*15.5*) 3.24 d (*15.5*)	48.5	6a', 9a', 9', 7', 1'(w)		9'-OH, 6-CH_3
9'		111.4			
9a'		48.5			
6'-CH_3	2.55, br s	22.9	5', 6', 6a',	5' (w)	5' (w)
4'-OH	11.85, s		3a', 4', 5', 3b' (w)		5'
9'-OH	8.63, s				1', 8'

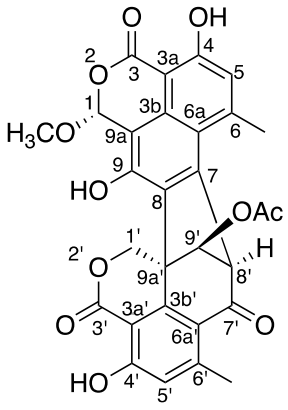

epi-Bacillisporin F (**9**)

Table S9: NMR data of epi-bacillisporin F (**9**) in DMSO-d_6

Position	δ_H, mult (*J*, Hz)	δ_C	^1H-^{13}C HMBC	COSY	ROESY
1	6.68, br	98.1	3, 3b, 9, 6a, 9a		1-OCH_3
3		168.4			
3a		97.0			
3b		130.8			
4		162.7			
5	7.00, br s	119.1	3a, 6a, 6-CH_3, 3 (w)	6-CH_3	6-CH_3, 4-OH
6		145.8			
6a		118.3			
7		138.8			
8		134.1			
9		151.3			
9a		109.7			
1-OCH_3	3.56, s	55.3	1		1
6-CH_3	2.96, br s	24.2	5, 6, 6a	5 (w)	5, 8'
4-OH	11.85, s		3a, 4, 5		5
9-OH	10.71, s		8, 9, 9a, 7 (w)		1, 1'
1'	5.02, d (*12.0*) 5.11, d (*12.0*)	68.7	3', 3b', 6a', 9', 9a'		9', 9-OH
3'		167.2			
3a'		103.9			
3b'		146.3			
4'		163.2			
5'	6.90, br s	120.3	3a', 6a', 6-CH_3', 3 (w)	6-CH_3'(w)	6-CH_3', 4-OH'
6’		152.8			
6a'		116.5			
7'		190.9			

8'	5.01, br s	61.4	6a, 8, 6a', 9a', 5'	9'	6-CH_3, 9'
9'	5.82, br s	85.4	7, 8, 7', 3b'	8'	8'
9a'		47.9			
6'-CH_3	2.48, br s	23.2	5', 6', 6a'	5' (w)	5'
9'-$\underline{C}OCH_3$		169.7			
9'-$CO\underline{CH_3}$	2.02, s	20.7	9'-$\underline{C}OCH_3$		
4'-OH	11.95, s		3a', 4', 5'		5'

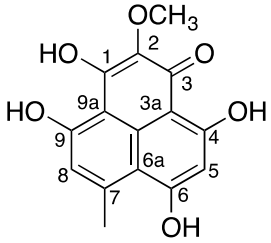

Funalenone (**10**)

Table S10: NMR data of funalenone (**10**) in DMSO-d_6

Position	δ_H, multi (*J*, Hz)	δ_C	^1H-^{13}C HMBC	COSY	ROESY
1		168.4			
2		132.7			
3		163.3			
3a		105.6			
3b		127.2			
4		165.2			
5	6.79, br s	116.8	3a, 4, 6, 6a	6-CH_3 (w)	6-CH_3 (w)
6		146.8			
6a		110.3			
7		165.9			
8	6.43, br s	99.9	6a, 7, 9, 9a		7-OH
9		170.3			
9a		102.4			
6-CH_3	2.80, br s	25.4	5, 6, 6a	5 (w)	5 (w)
2-OCH_3	3.80, s	59.7	2		
4-OH	[a]				
7-OH	11.66, br s		6a, 7, 8		8
9-OH	[a]				
2-OH	[a]				

[a]Not observed

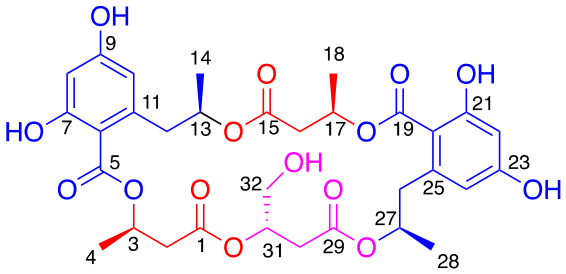

15G256α (**11**)

Table S11: NMR data of 15G256α (**11**) in DMSO-d_6

Position	δ_H, mult (*J*, Hz)	δ_C	^{1}H-^{13}C HMBC	COSY	ROESY
1		169.4			
2	2.73	39.5	3, 4	3	3, 4
3	5.33, m	67.7	2, 4, 5	2, 4	2, 4
4	1.30, d (*6.2*)	19.3	2, 3	3	2, 3
5		167.9			
6		109.1			
7		160.4			
8	6.21, d (*2.3*)	101.3	6, 7, 9, 10, 5 (w)	10	7-OH, 9-OH
9		159.9			
10	6.18, d (*2.3*)	110.1	6, 8, 9, 11, 5 (w)	8	12, 13, 14, 9-OH
11		139.1			
12	3.04, dd (*13.5*, *5.8*) 2.65,	39.7	6, 10, 11, 13, 14	13	10, 13, 14
13	4.91, m	71.0	11,12, 14, 15	12, 14	12, 14
14	1.05, d (*6.2*)	18.7	12, 13	13	12, 13
15		169.3			
16	2.61, 2.69,	40.0	17, 18	17	17, 18
17	5.31, m	68.0	16, 18	18	16, 18
18	1.31, d (*6.2*)	19.3	16, 17	17	16, 17
19		168.0			
20		110.0			
21		159.2			
22	6.21, d (*2.3*)	101.2	20, 21, 23, 24, 19 (w)	24	21-OH, 23-OH
23		160.1			
24	6.19, d (*2.3*)	109.7	20, 22, 23, 25, 19 (w)	22	26, 27, 28, 23-OH
25		138.9			
26	2.99, dd (*13.5*, *6.6*) 2.73,	39.3	20, 24, 25, 27, 28	27	24, 27, 28
27	4.89, m	71.3	25, 26, 28, 29	26, 28	24, 26, 28
28	1.09, d (*6.2*)	19.0	26, 27	27	24, 26, 27
29		169.0			

30	2.51, dd (*13.5*, *3.7*) 2.67,	35.4	31, 32	31	31, 32
31	5.10, m	71.2	1, 30, 32,	30, 32	30, 32
32	3.46, dd (*6.6*, *3.7*)	61.4	30, 31	31, 32-OH	30, 31, 32-OH
7-OH	9.91, s		6, 7, 8	9-OH	8
9-OH	10.30, s		8, 9, 10	7-OH	8, 10
21-OH	10.16, s		20, 21, 22	23-OH	22
23-OH	9.82, s		22, 23, 24	21-OH	22, 24
32-OH	[a]				

[a] Not observed

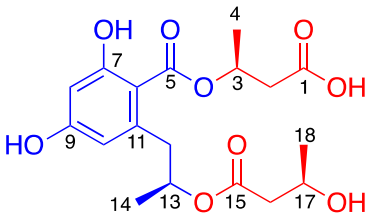

15G256υ(**12**)

Table S12: NMR data of 15G256ν (**12**) in DMSO-d_6

Position	δ_H, mult (*J*, Hz)	δ_C	^{1}H-^{13}C HMBC	COSY	ROESY
1		171.6			
2	2.64, d (*6.6*)	40.1	1, 3, 4	3	3, 4
3	5.35, m	68.4	1, 2, 4	2, 4	2, 4
4	0.97, d (*6.3*)	19.5	2, 3	3	2, 3
5		168.6			
6		108.4			
7		160.6			
8	6.17, d (*2.2*)	101.2	6, 7, 9, 10, 5 (w)	10	7-OH
9		160.6			
10	6.15, d (*2.2*)	110.6	6, 8, 9, 11, 12, 5 (w)	8	12, 13, 14
11		140.0			
12	2.76, dd (*14.0*, *8.4*) 2.91, dd (*14.0*, *4.9*)	40.4	6, 10, 11, 13, 14	13	10, 13, 15
13	4.99, m	70.4	11, 12, 14, 15	12, 14	12, 14
14	1.16, d (*6.3*)	19.8	12, 13	13	10, 12, 13
15		170.3			
16	2.18, dd (*14.0*, *6.7*) 2.30, dd (*14.0*, *6.7*)	44.3	15, 17, 18	17	17, 18
17	3.90, m	63.3	15, 16, 18	16, 18	16, 18
18	1.33, d (*6.3*)	23.1	16, 17	17	16, 17
1-OH	a				
7-OH	10.56, s		6, 7, 8		8
9-OH	9.99, br s				

[a] Not observed

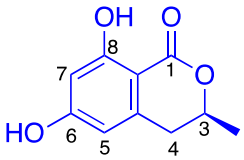

6-hydroxymellein (**13**)

Table S13: NMR data of 6-hydroxymellein (**13**) in DMSO-d_6

Position	δ_H, multi (J, Hz)	δ_C	^1H-^{13}C HMBC	COSY	ROESY
1		169.5			
3	4.67, m	75.4	1, 4a, 3-CH_3	4, 3-CH_3	4, 5, 3-CH_3
4	2.79, dd (*16.4*, *11.4*) 2.91, dd (*16.4*, *3.2*)	33.8	3, 5, 3-CH_3, 6 (w), 8a (w)	3, 3-CH_3 (w)	3, 5, 3-CH_3
4a		142.3			
5	6.23, br s	106.9	4, 6, 7, 4a, 8a	7	6-OH, 3, 4
6		163.4			
7	6.18, br s	100.9	5, 6, 8, 8a, 1 (w)	5	6-OH, 8-OH
8		164.5			
8a		100.1			
3-CH_3	1.38, d (*6.3*)	20.3	3, 4, 4a (w)	4, 3-CH_3	4, 3-CH_3
6-OH	10.64, br s		5, 6, 7		5, 6, 7
8-OH	11.12, s		7, 8, 8a		7

B. Figures

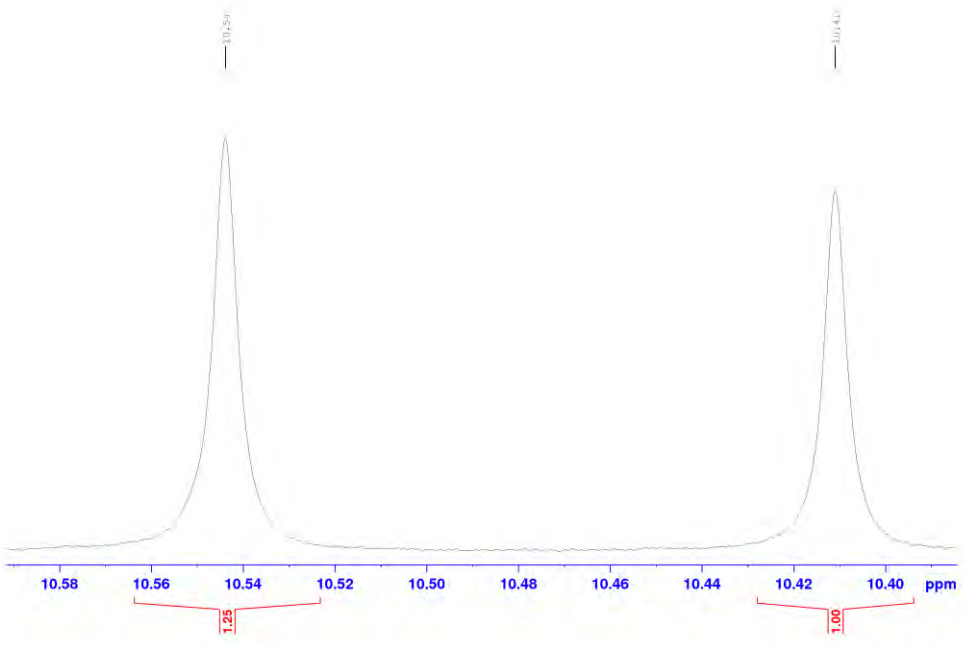

Figure S1: Section of the ^1H NMR spectrum of bacillisporin I (**1**) at H-9 showing the ratio of the minor isomer to the major isomer as 1: 1.25 in DMSO-d_6

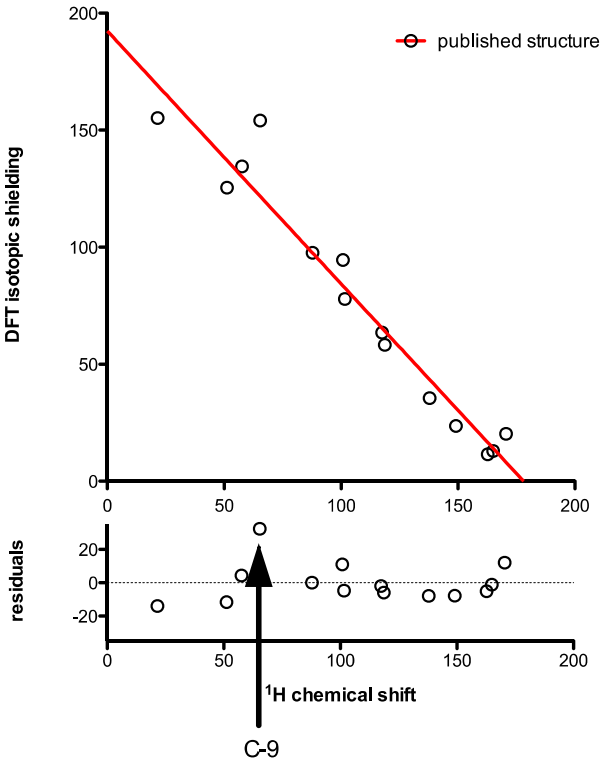

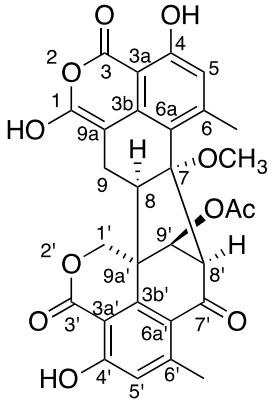

	published structure
Goodness of Fit	
Degrees of Freedom	12
R square	0.9465
Absolute Sum of Squares	1879
Sy.x	12.51

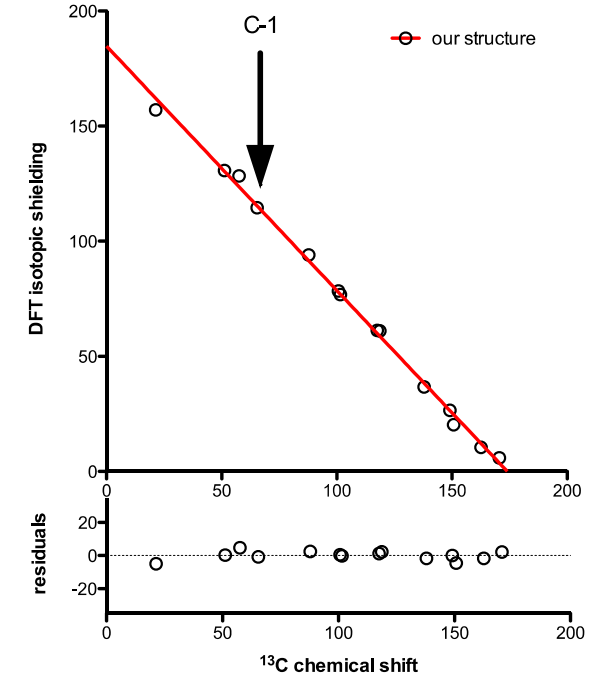

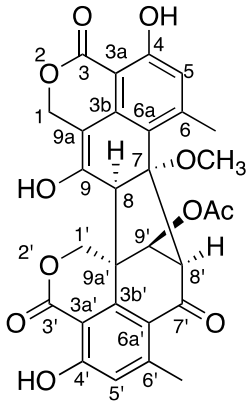

	our structure
Goodness of Fit	
Degrees of Freedom	12
R square	0.9970
Absolute Sum of Squares	91.11
Sy.x	2.755

Figure S2: DFT isotropic shielding calculations showing better fit of the observed ^{13}C chemical shifts for the proposed structure ($R^2 > 0.99$) compared to the published structure ($R^2 < 0.95$).

C. ^{1}H (600 MHz) and ^{13}C NMR (150 MHz) NMR spectra

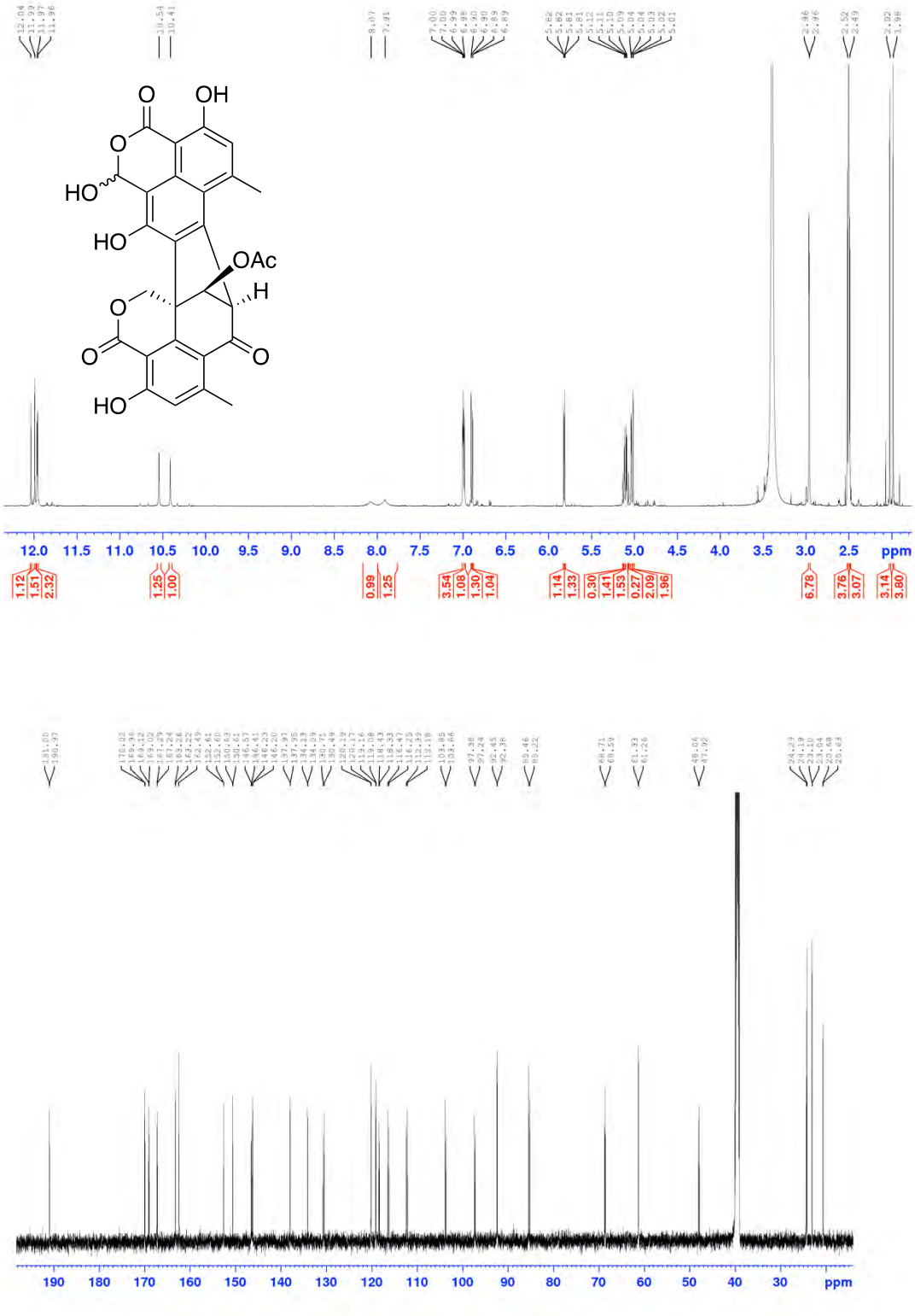

Figure S3: ^{1}H and ^{13}C NMR spectra of bacillisporin I (**1**) in DMSO-d_6

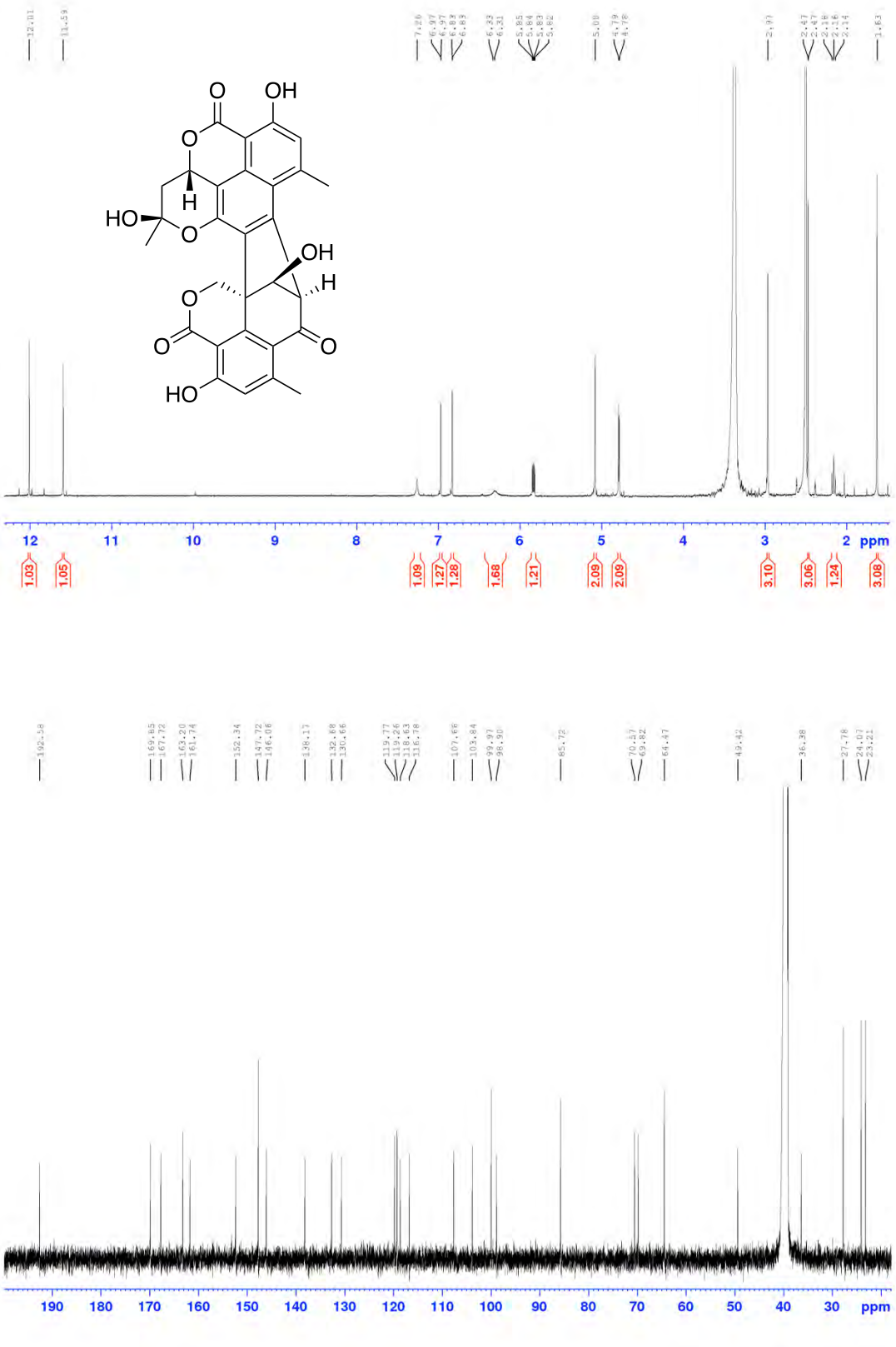

Figure S4: ^{1}H and ^{13}C NMR spectra of talarohemiketal (**2**) in DMSO-d_6

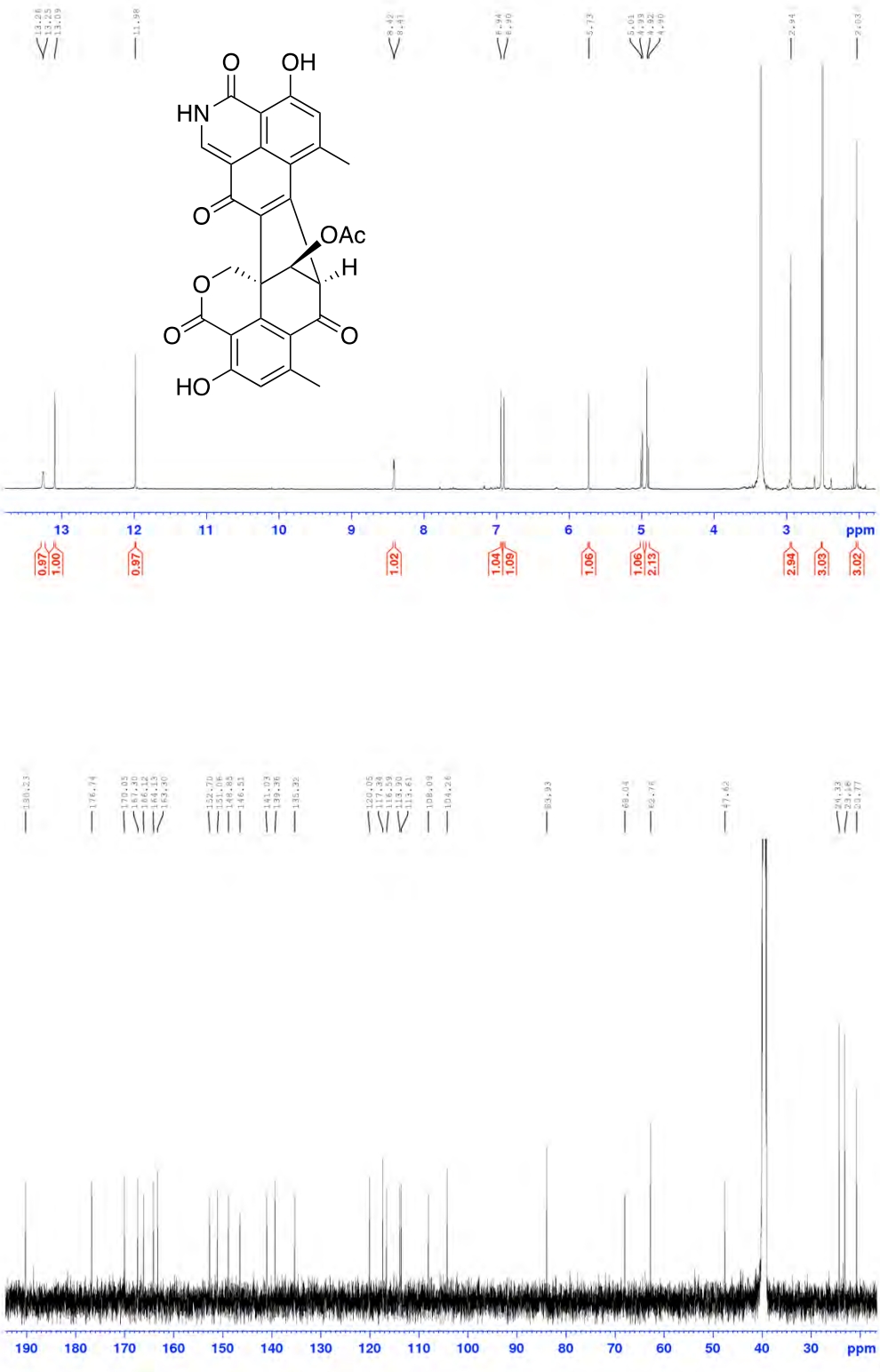

Figure S5: ^{1}H and ^{13}C NMR spectra of talaroazasone (**3**) in DMSO- d_6

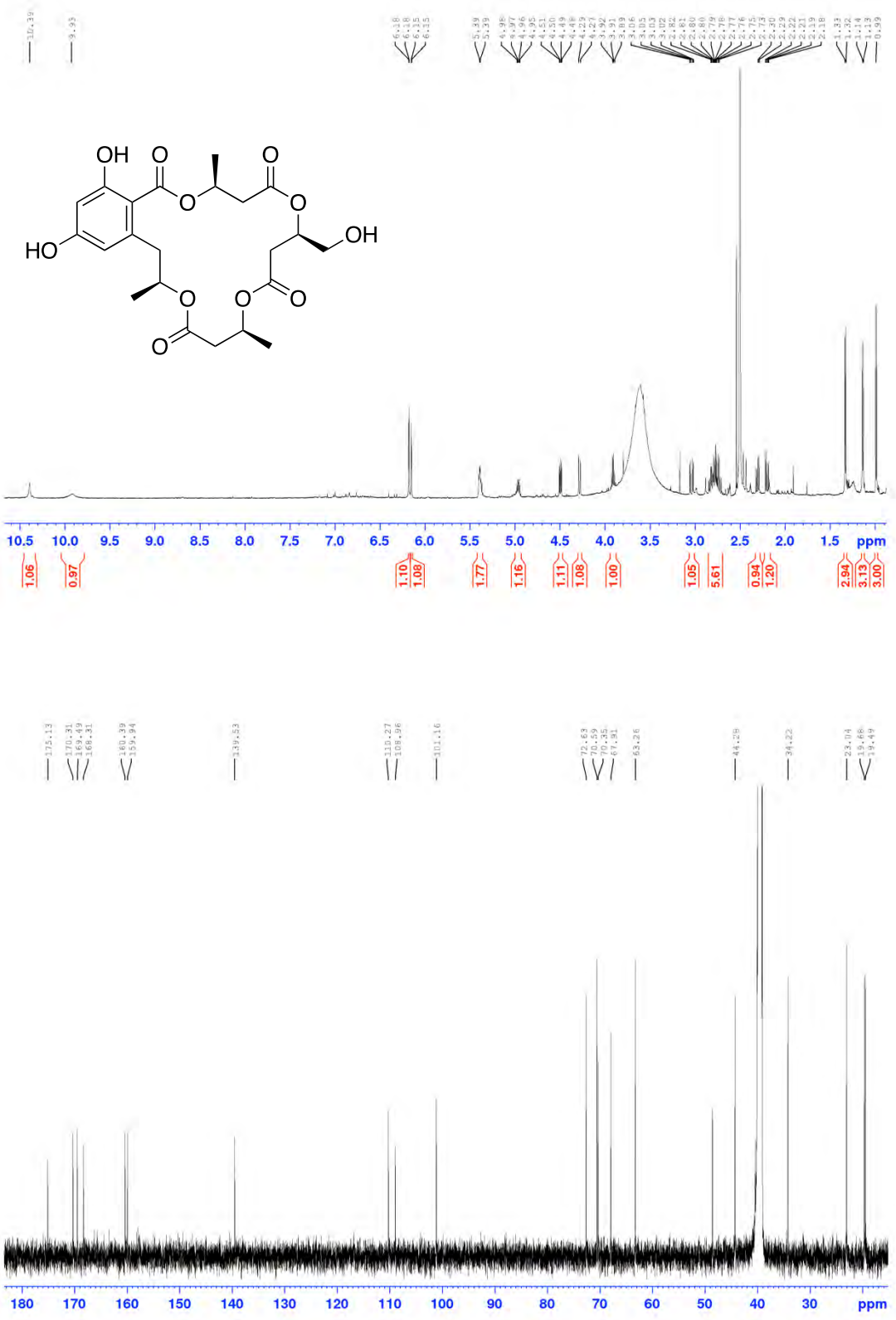

Figure S6: ^{1}H and ^{13}C NMR spectra of talaromacroclactone A (**4**) in DMSO-d_6

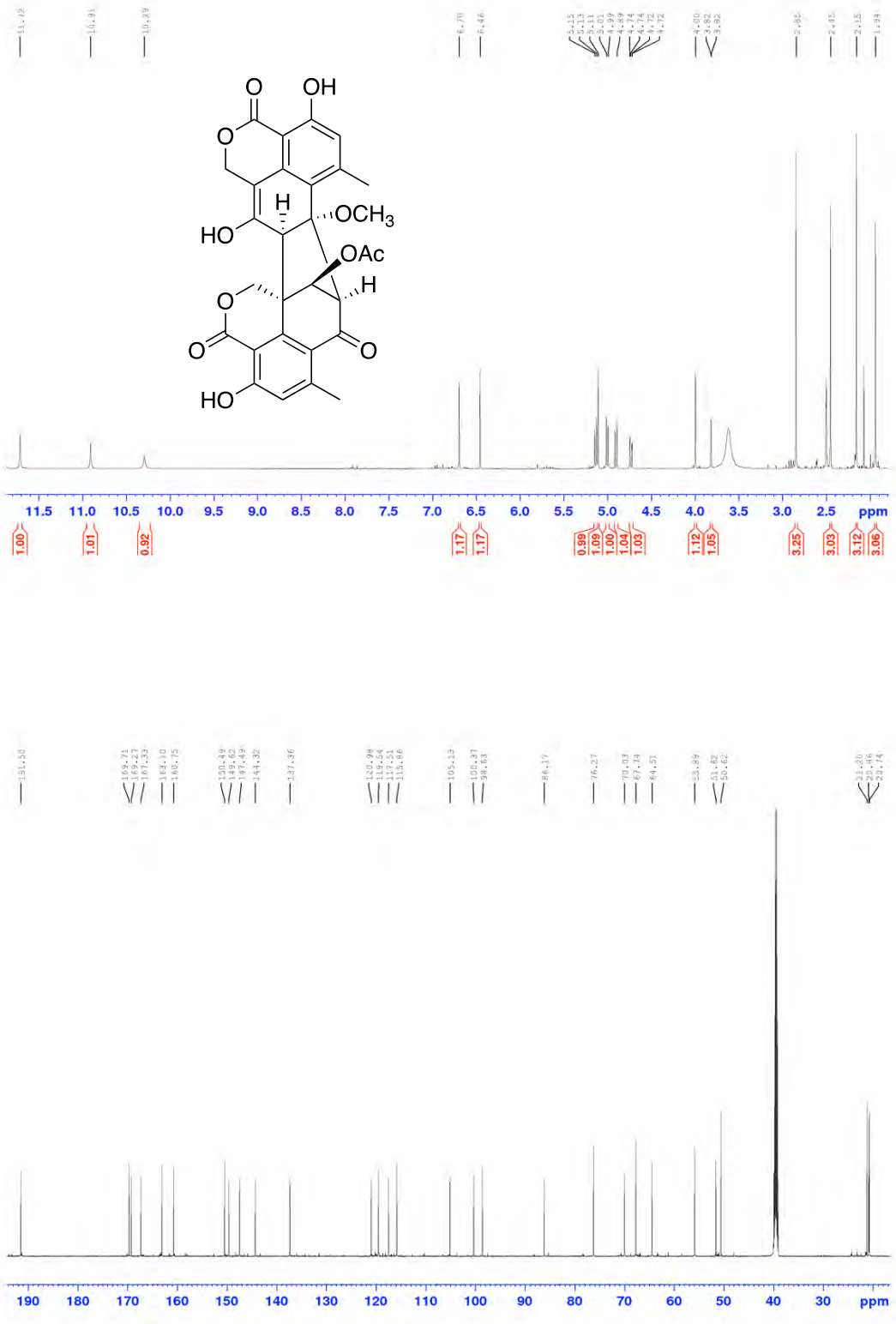

Figure S7a: ^{1}H and ^{13}C NMR spectra of talarolactone (**5**) in DMSO-d_6

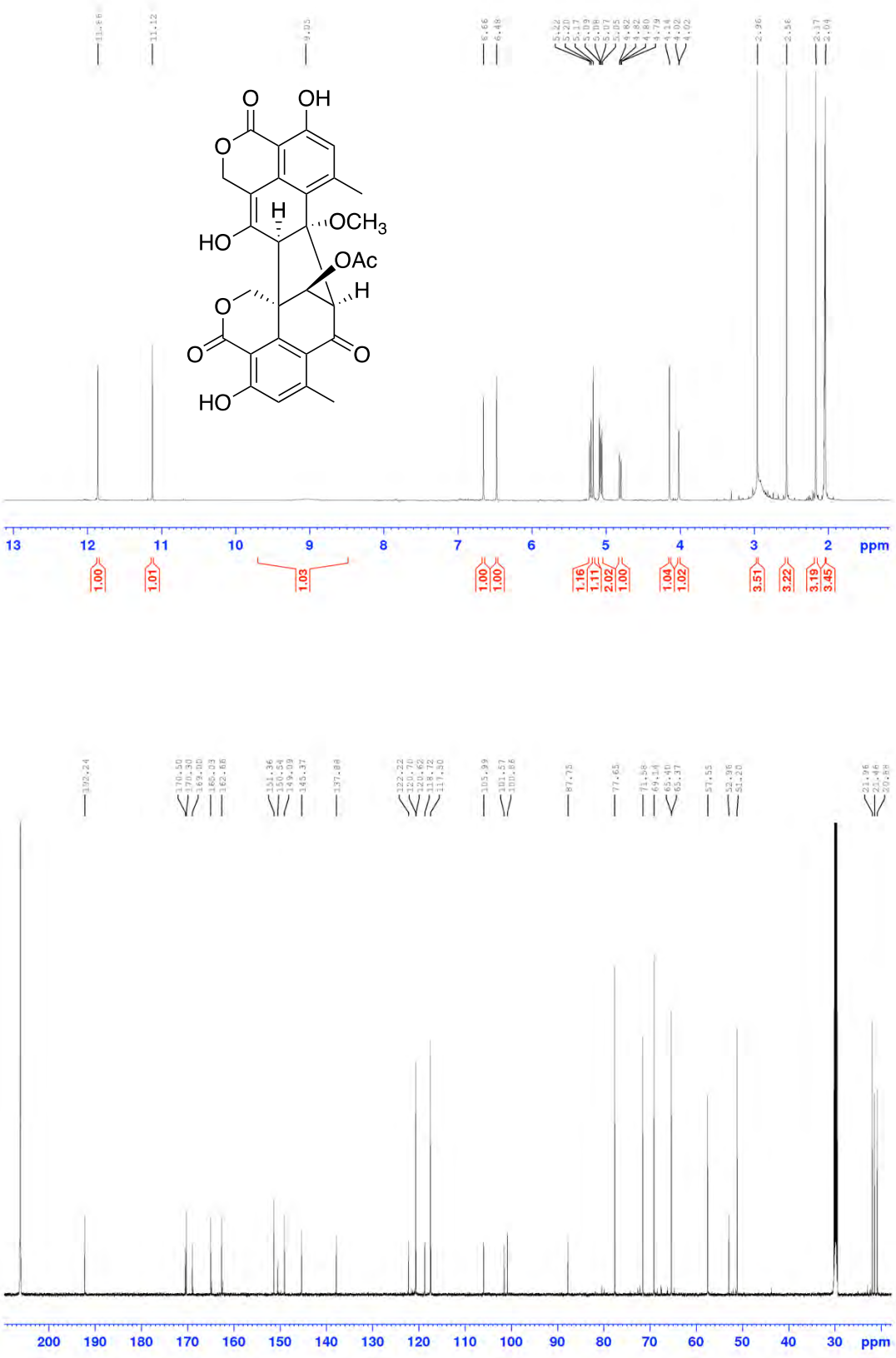

Figure S7b: ^{1}H and ^{13}C NMR spectra of talarolactone (**5**) in acetone-d_6

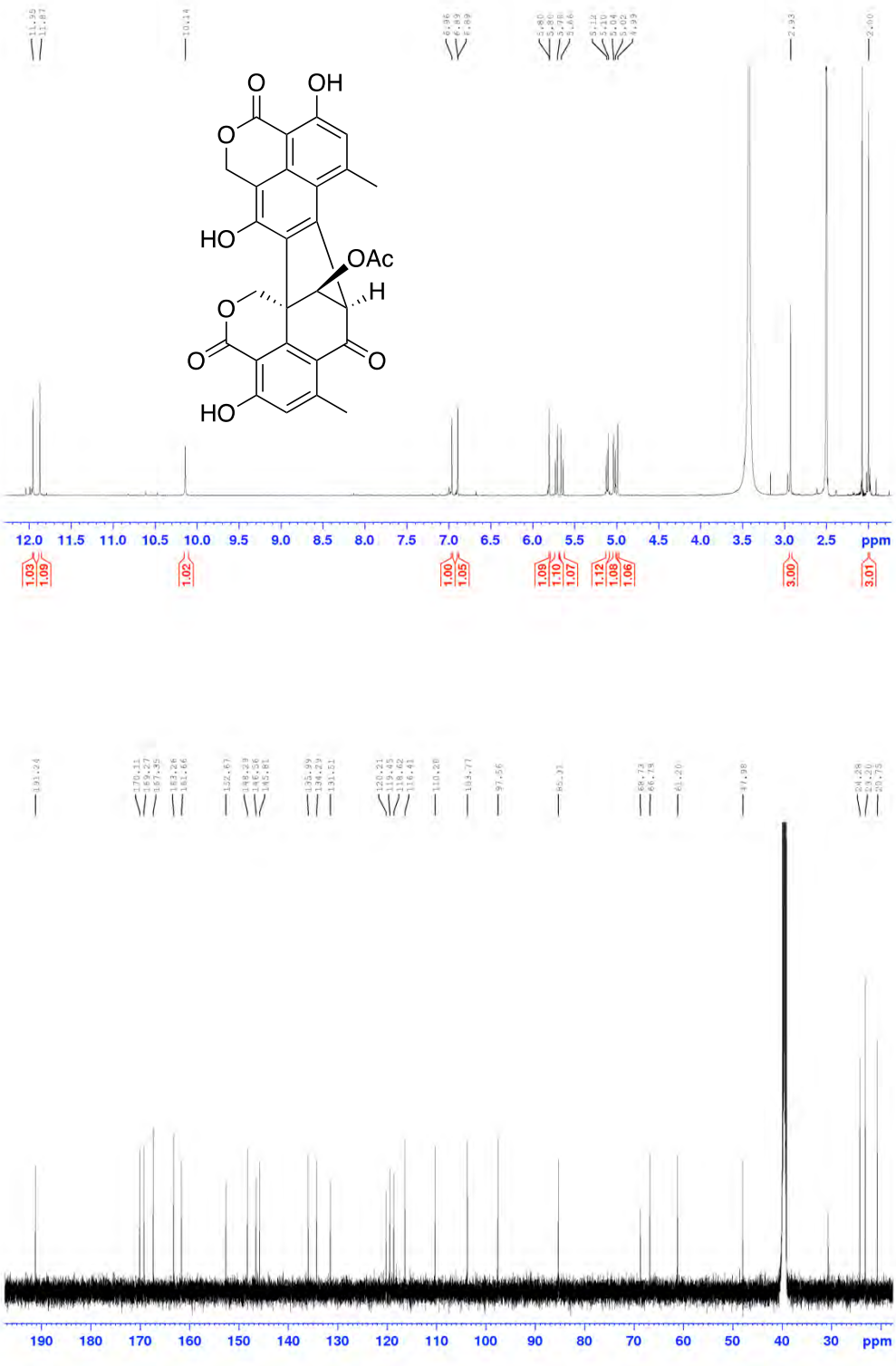

Figure S8: ^{1}H and ^{13}C NMR spectra of bacillisporin A (**6**) in DMSO-d_6

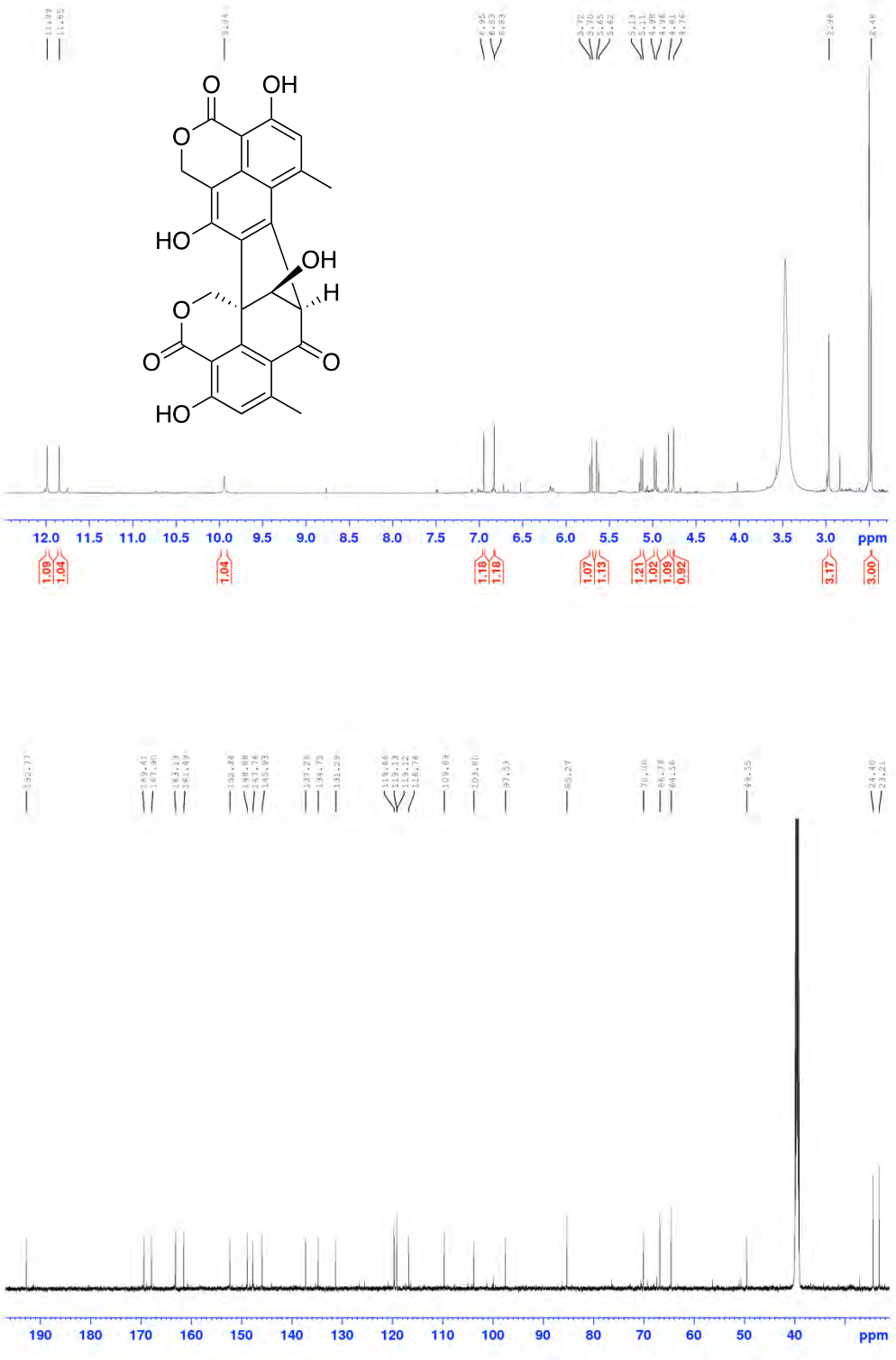

Figure S9: ^{1}H and ^{13}C NMR spectra of bacillisporin B (**7**) in DMSO-d_6

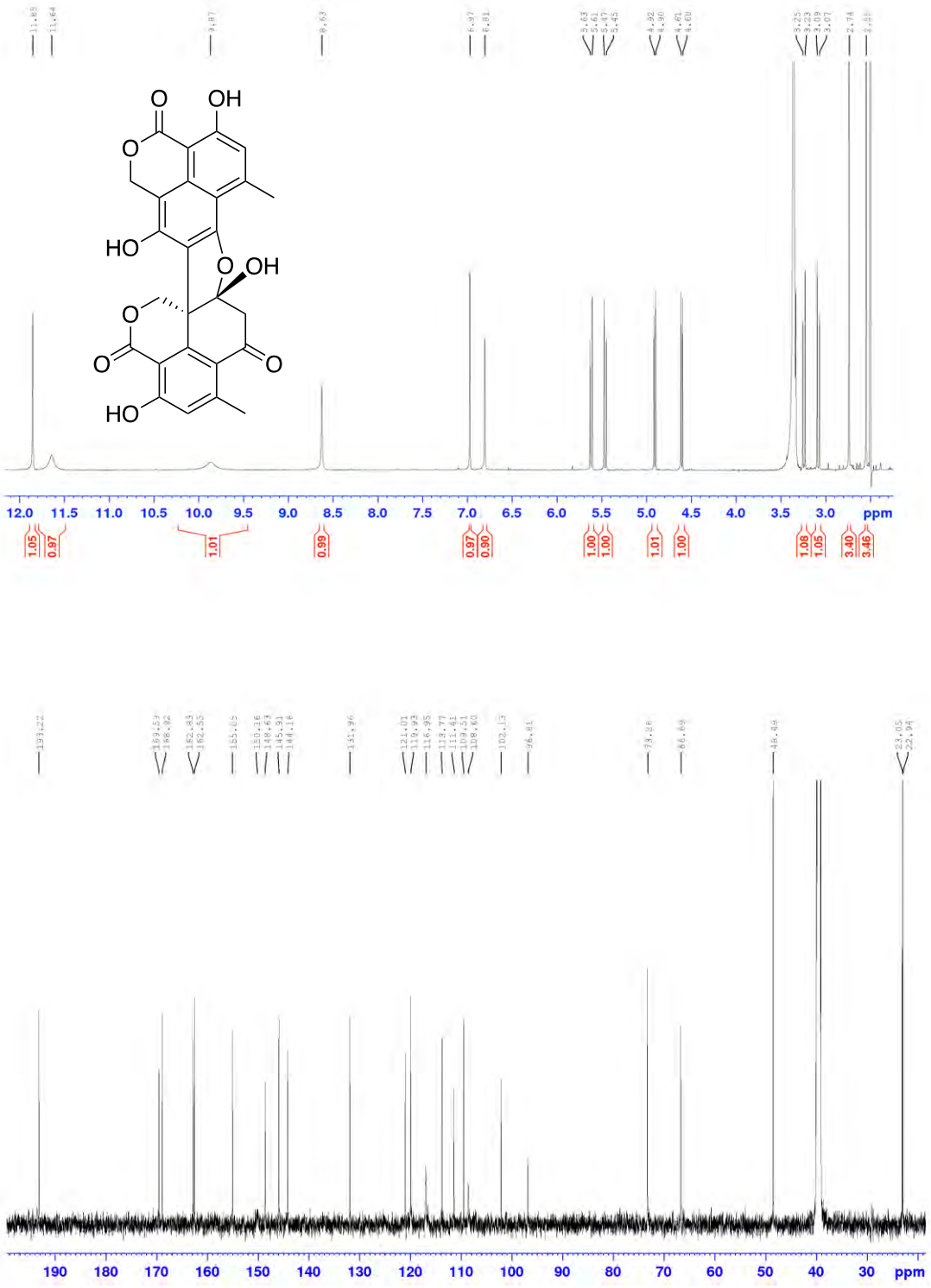

Figure S10: ^{1}H and ^{13}C NMR spectra of bacillisporin C (**8**) in DMSO-d_6

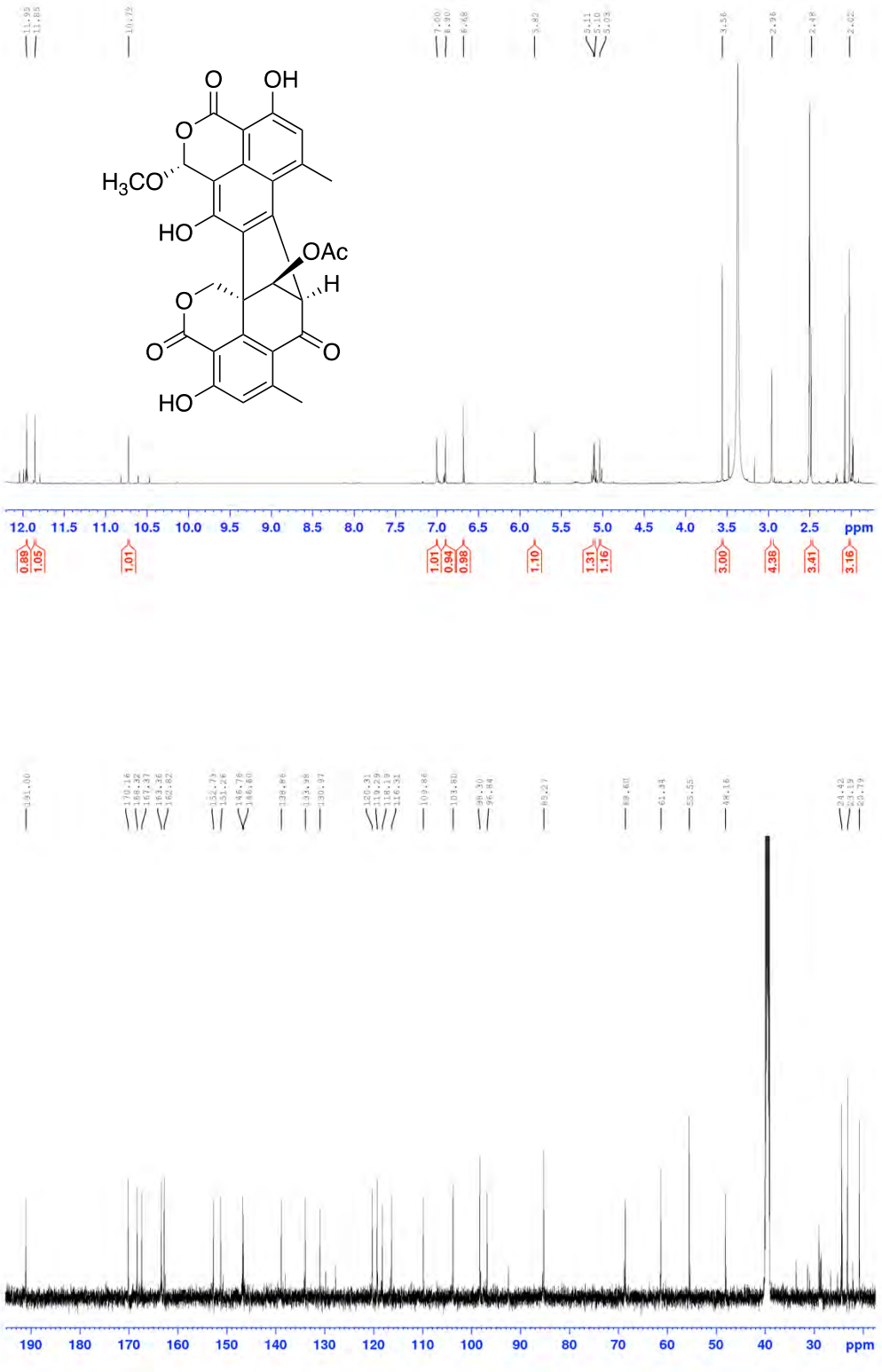

Figure S11: ^{1}H and ^{13}C NMR spectra of *epi*-bacillisporin F (**9**) in DMSO-d_6

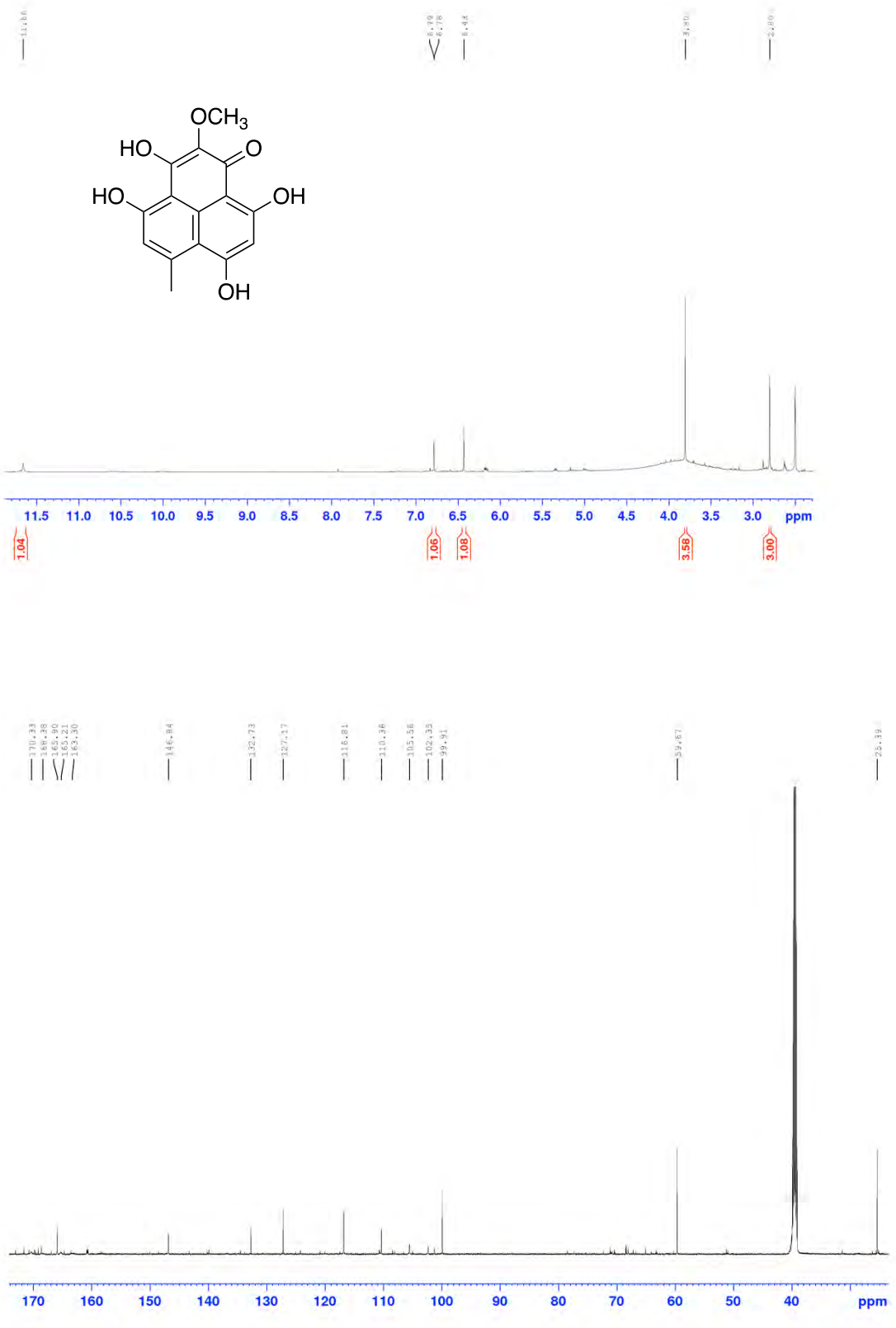

Figure S12: ^{1}H and ^{13}C NMR spectra of funalenone (**10**) in DMSO-d_6

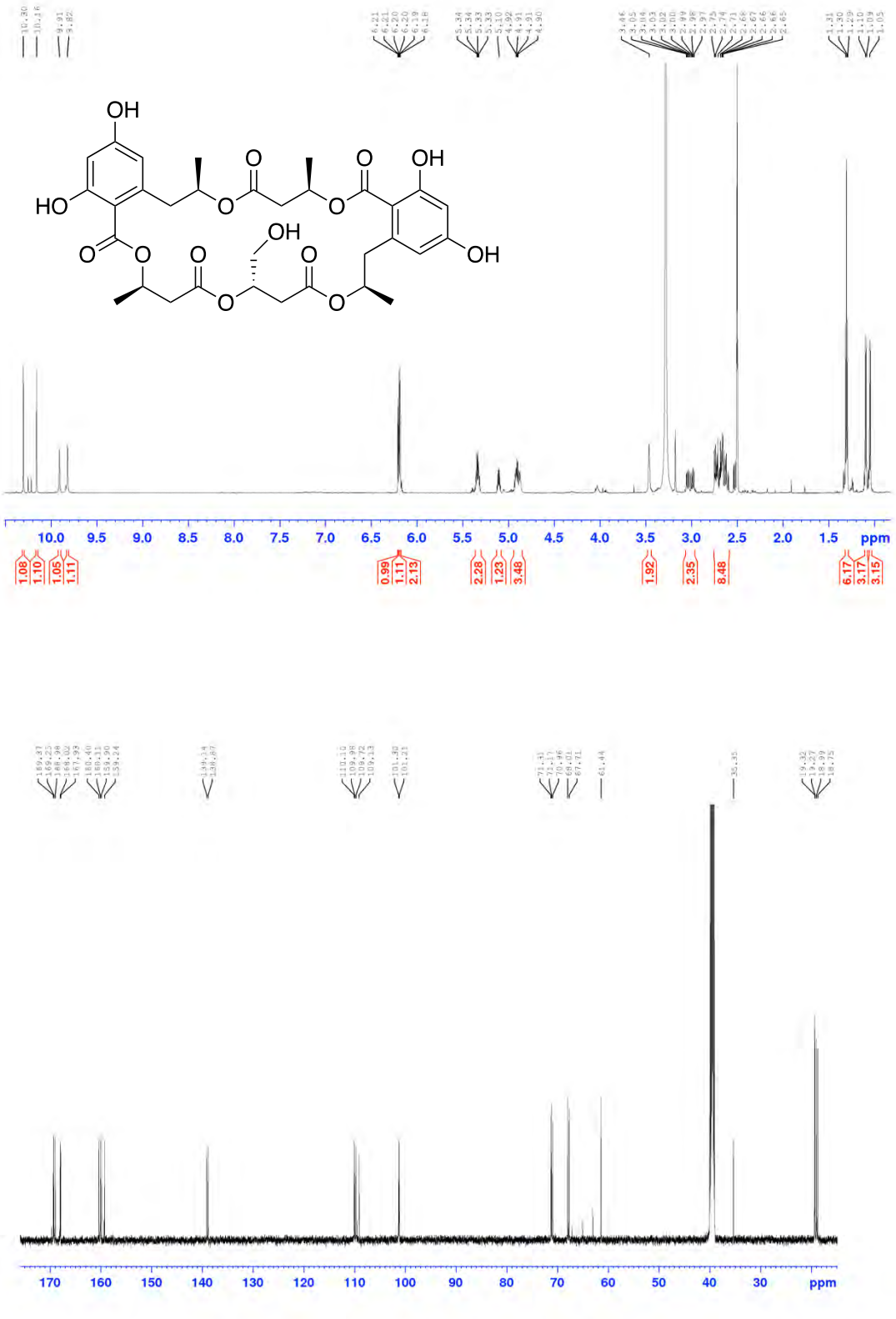

Figure S13: ^{1}H and ^{13}C NMR spectra of 15G256α (**11**) in DMSO-d_6

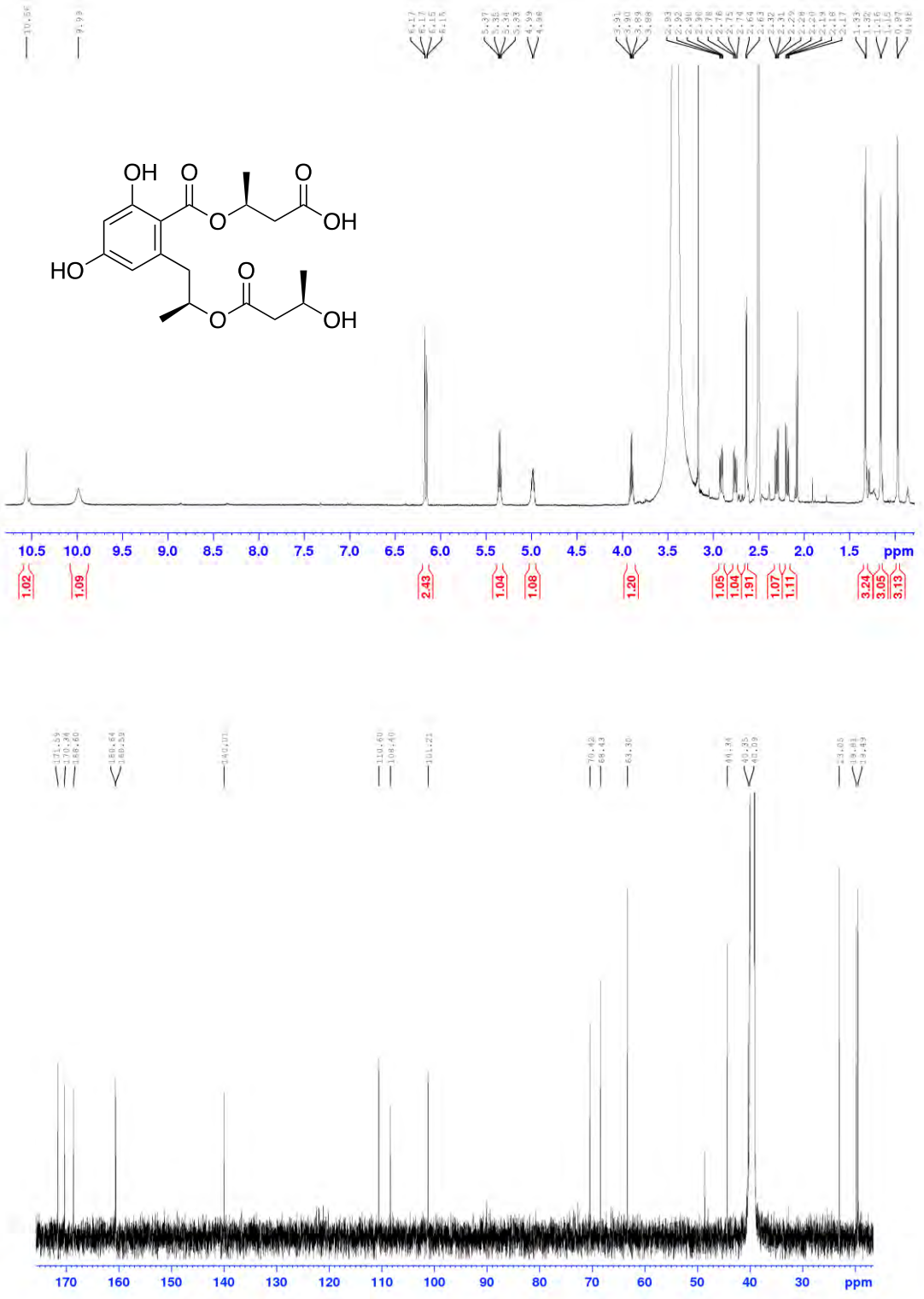

Figure S14: ^{1}H and ^{13}C NMR spectra of 15G256ν (**12**) in DMSO-d_6

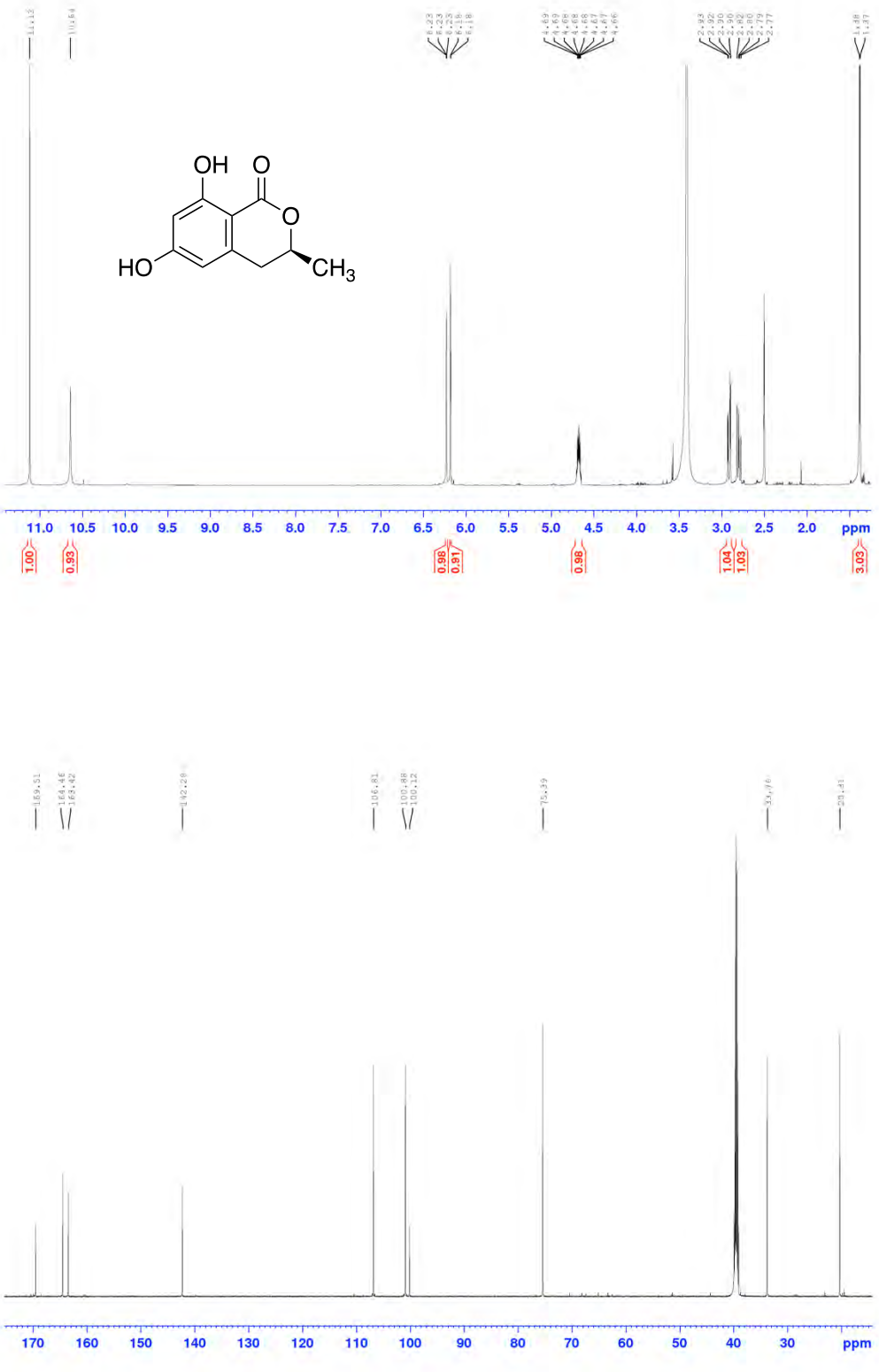

Figure S15: ^{1}H and ^{13}C NMR spectra of 6-hydroxymellein (**13**) in DMSO-d_6

D. UV-visible spectra

In-situ UV-visible spectra in acetonitrile-water gradient containing 0.05% formic acid

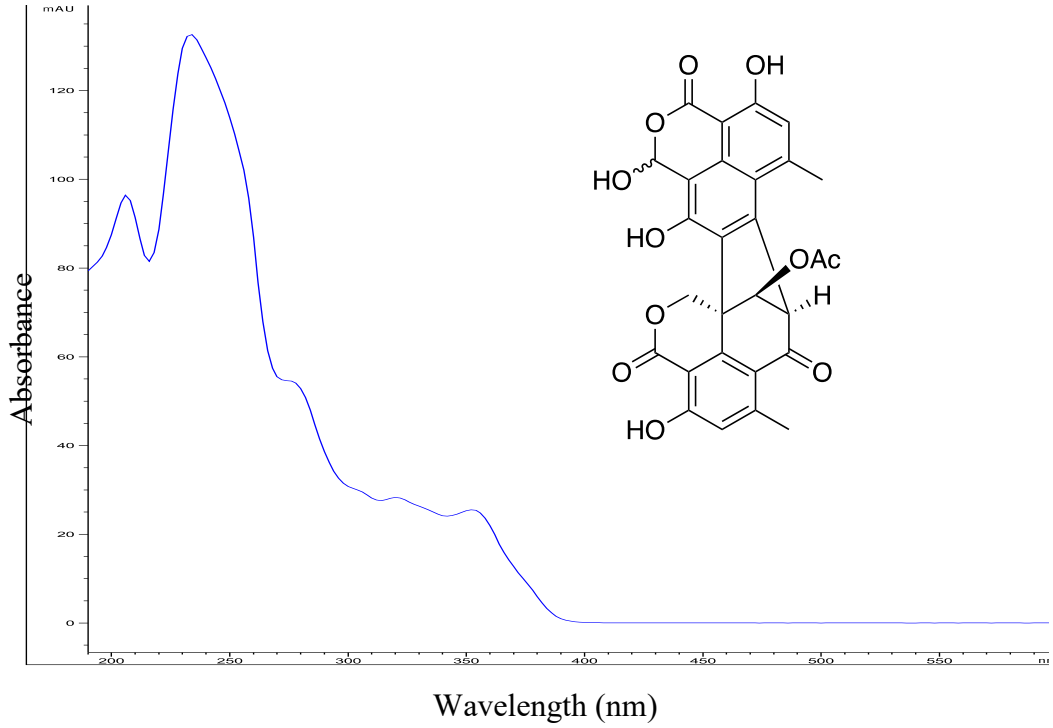

Figure S16: UV-visible spectrum of bacillisporin I (**1**)

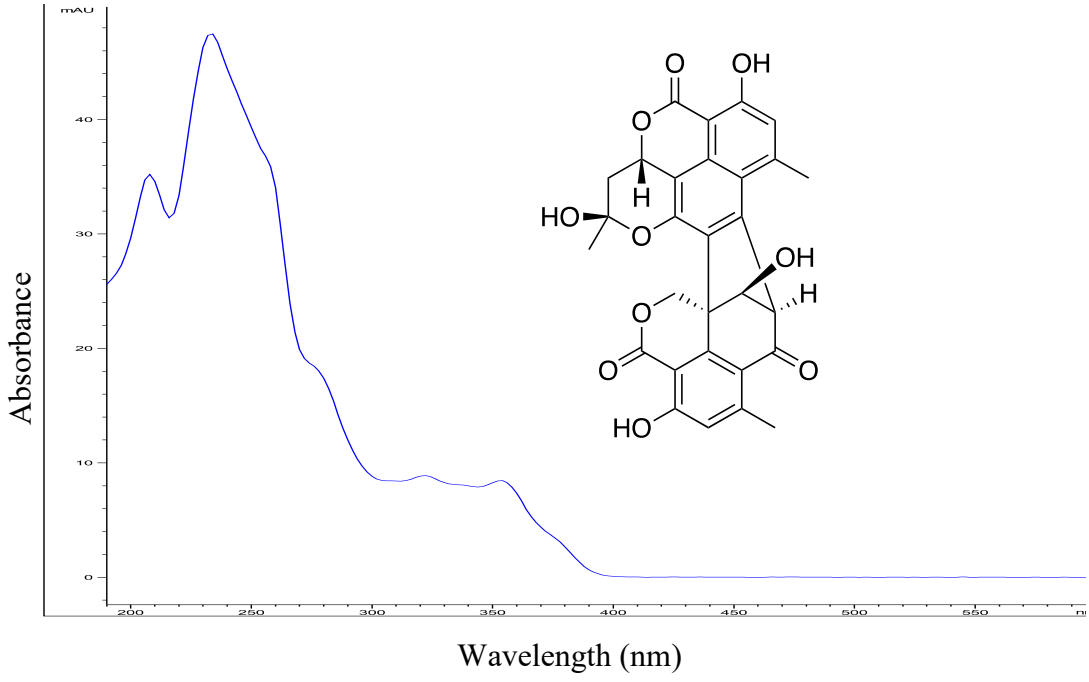

Figure S17: UV-visible spectrum of talarohemiketal (**2**)

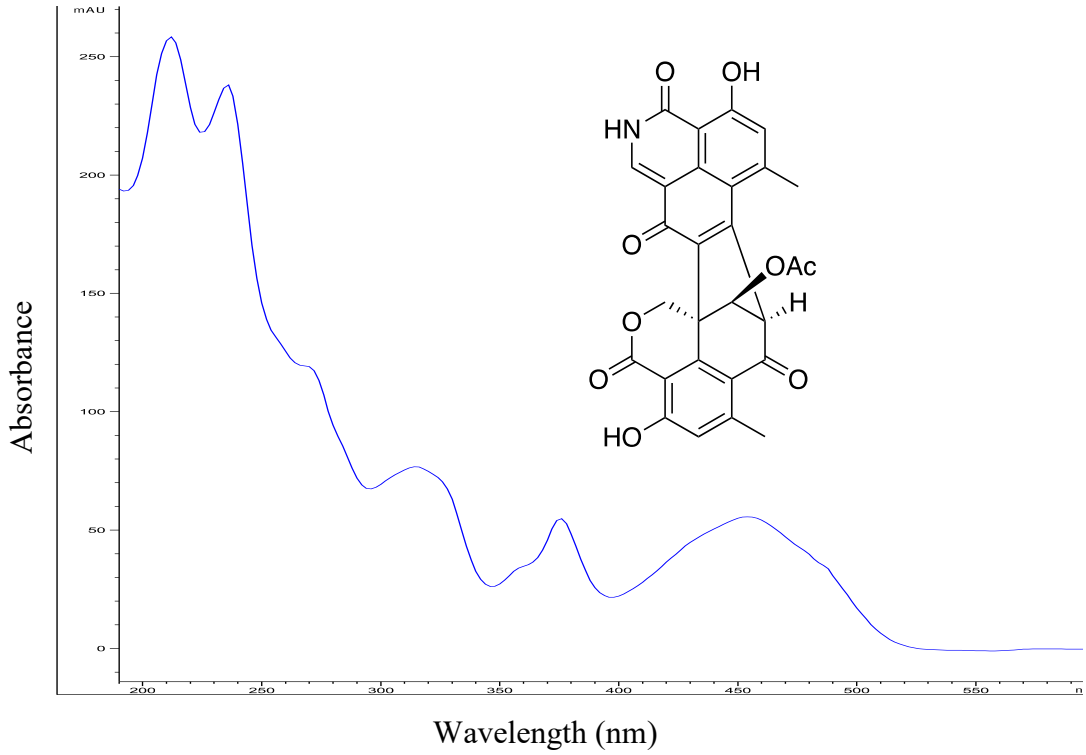

Figure S18: UV-visible spectrum of talaroazasone (**3**)

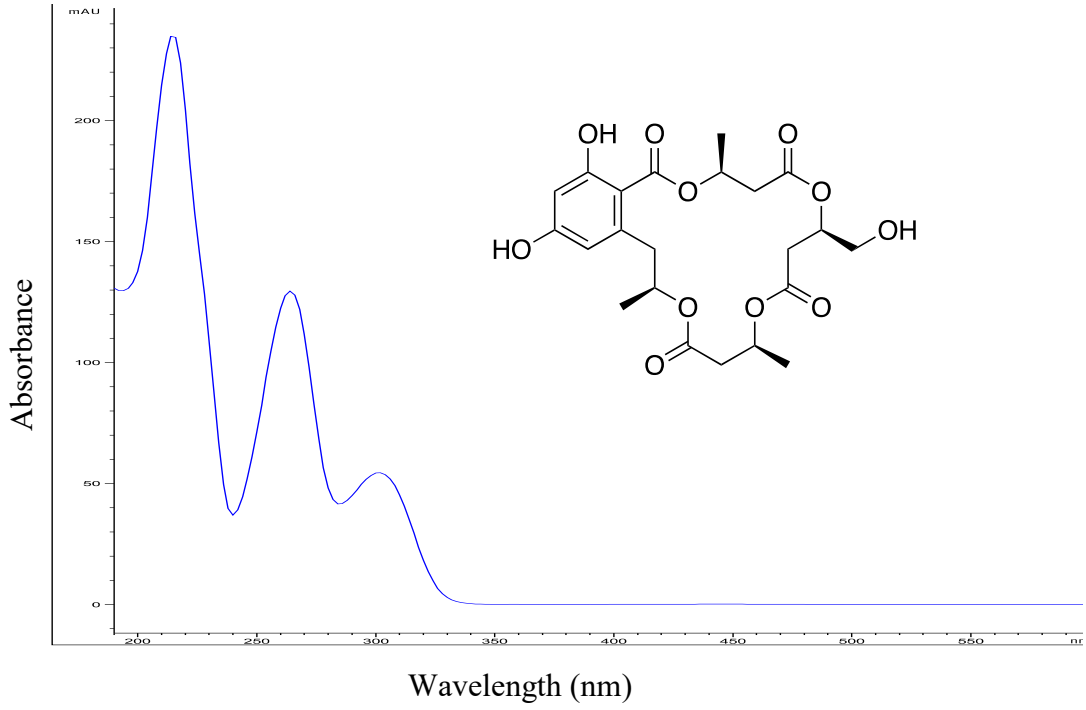

Figure S19: UV-visible spectrum of talaromacroclactone A (**4**)

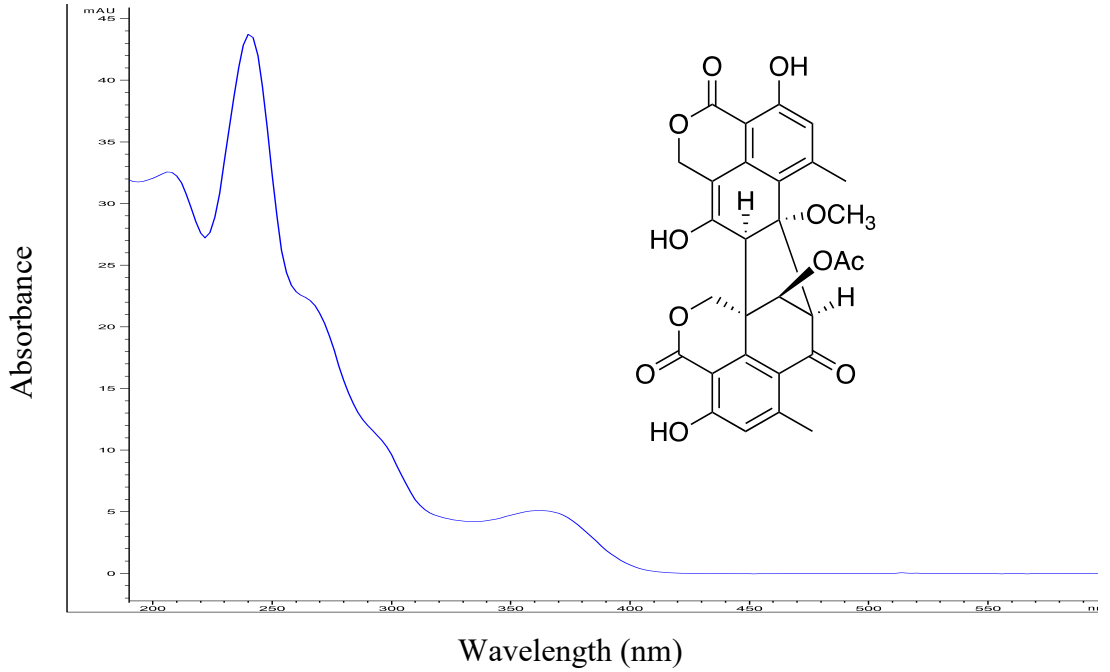

Figure S20: UV-visible spectrum of talarolactone (**5**)

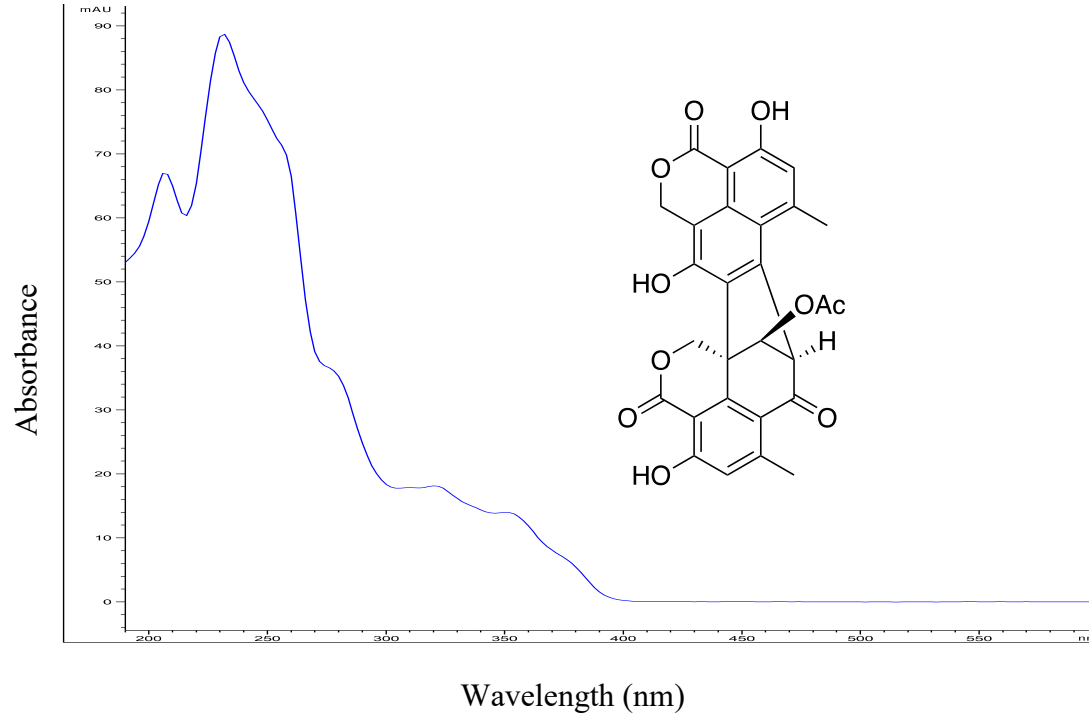

Figure S21: UV-visible spectrum of bacillisporin A (**6**)

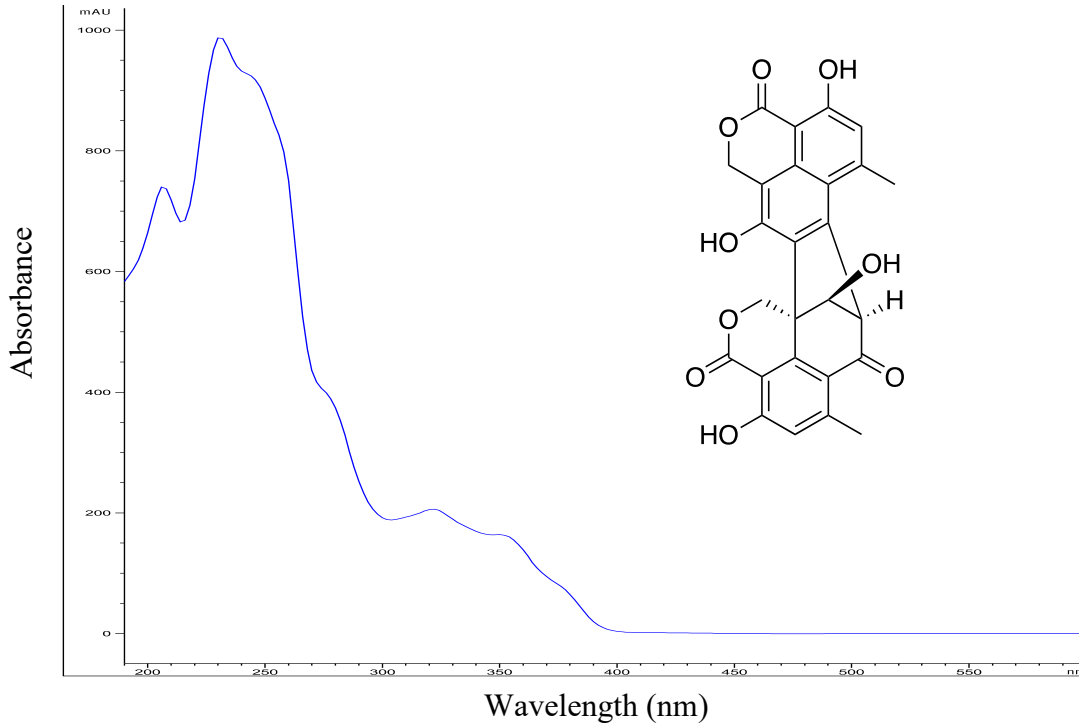

Figure S22: UV-visible spectrum of bacillisporin B (**7**)

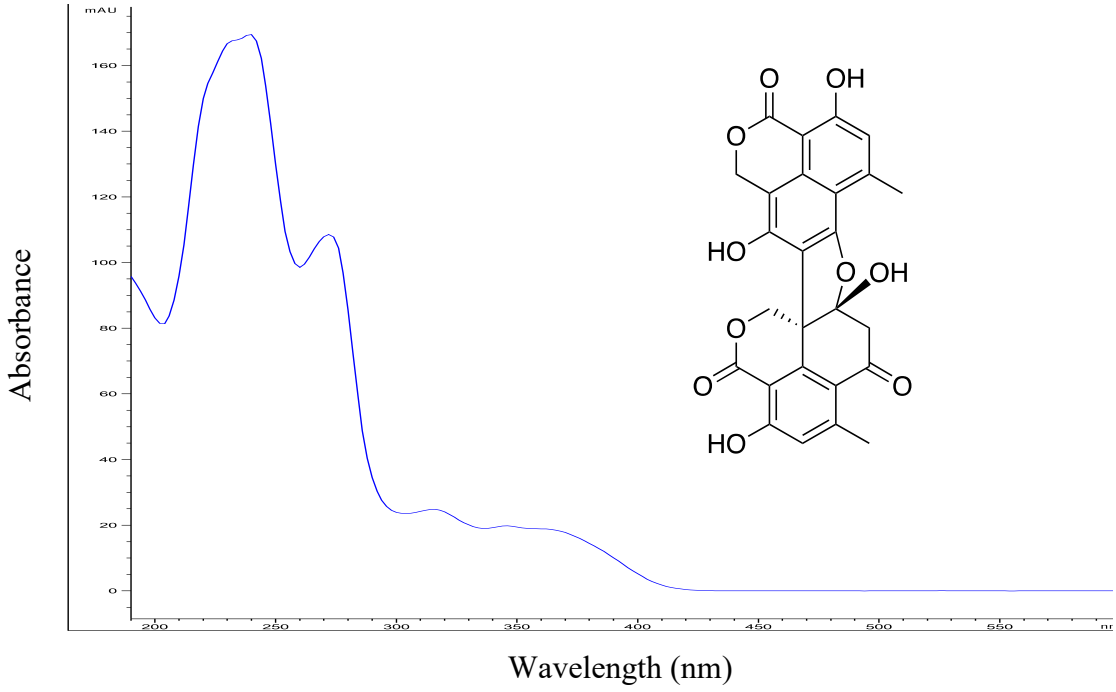

Figure S23: UV-visible spectrum of bacillisporin C (**8**)

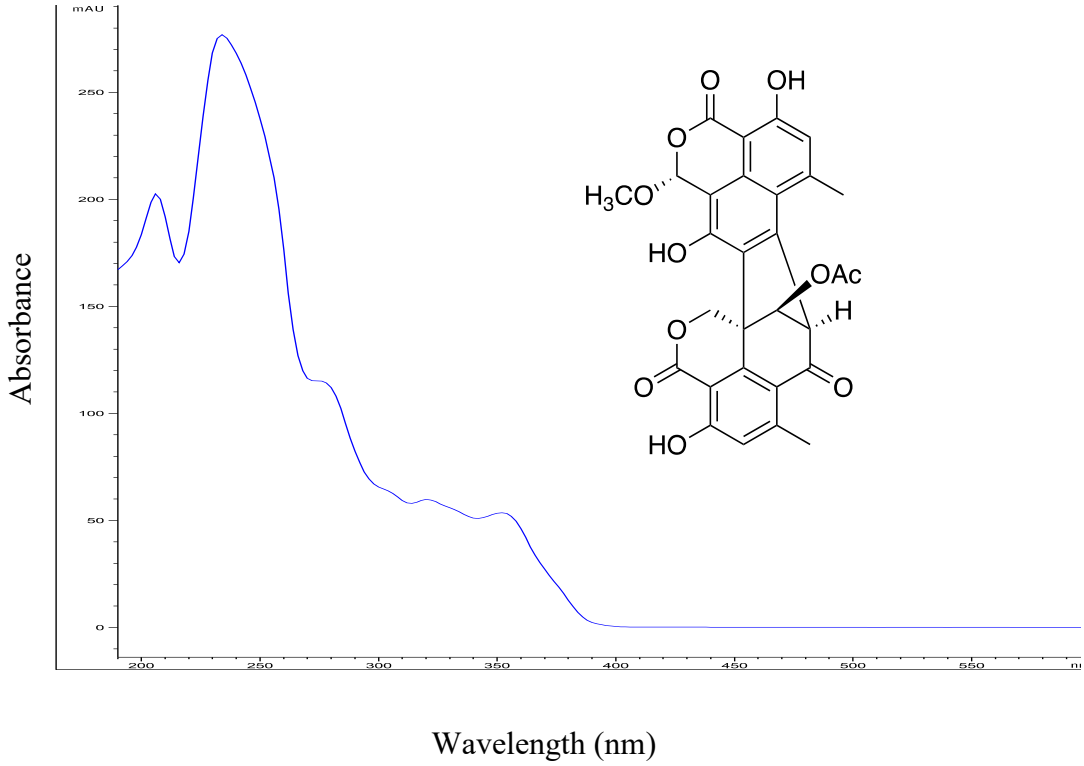

Wavelength (nm)

Figure S24: UV-visible spectrum of *epi*-bacillisporin F (**9**)

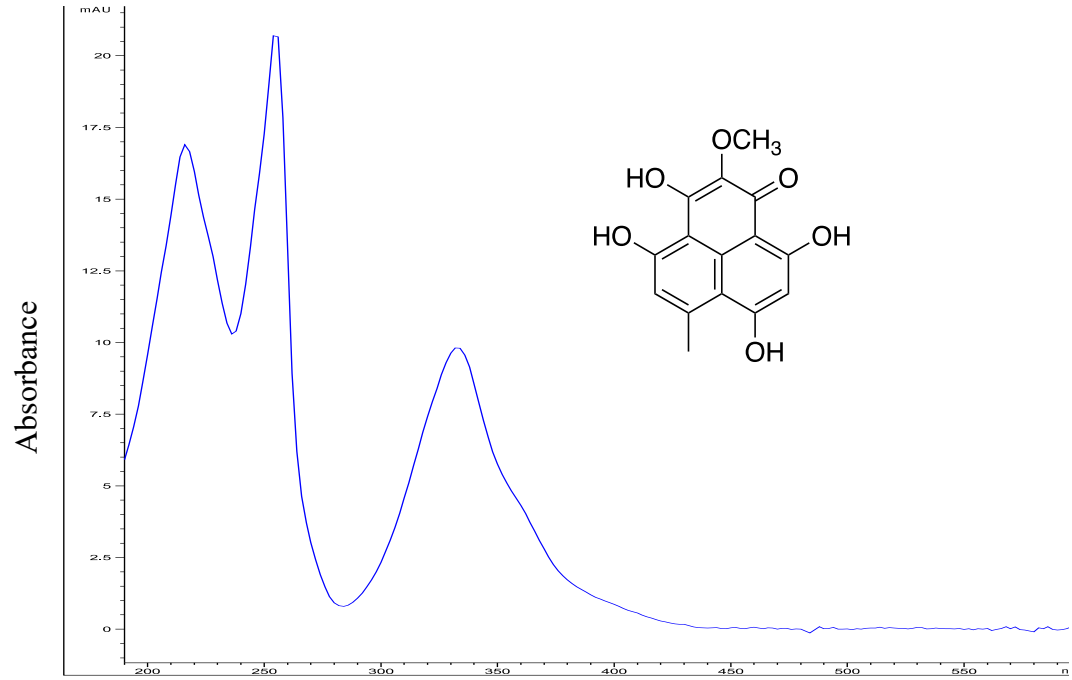

Wavelength (nm)

Figure S25: UV-visible spectrum of funalenone (**10**)

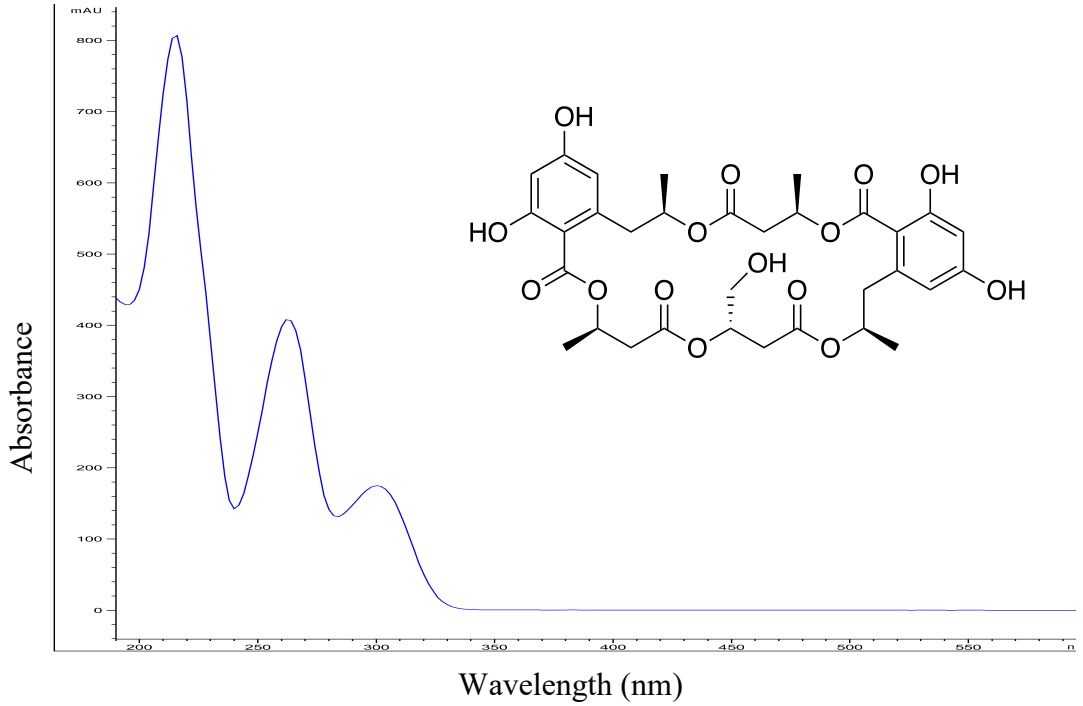

Figure S26: UV-visible spectrum of 15G256α (**11**)

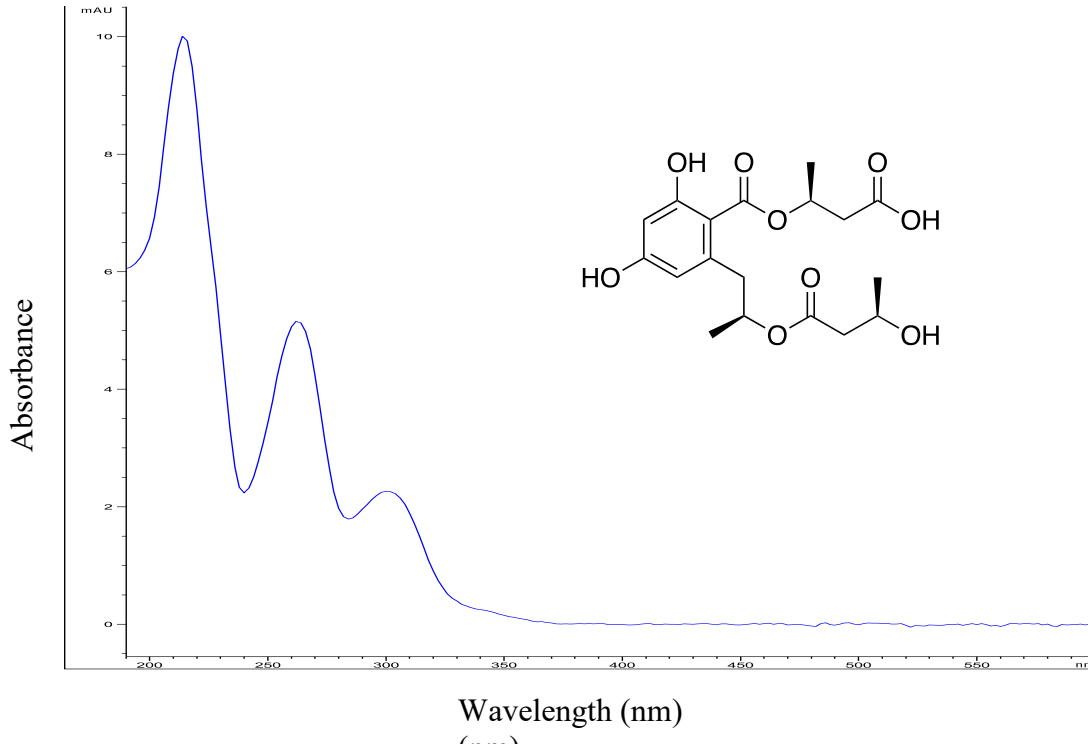

Figure S27: UV-visible spectrum of 15G256ν (**12**)

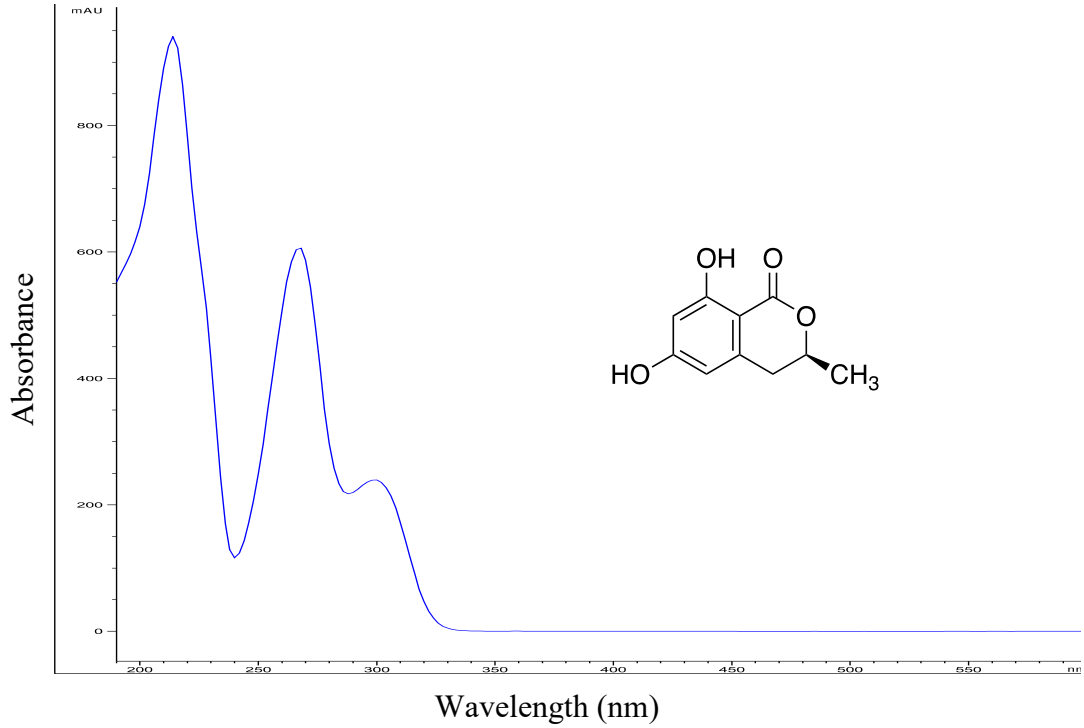

Figure S28: UV-visible spectrum of 6-hydroxymellein (**13**)

E. ECD spectra

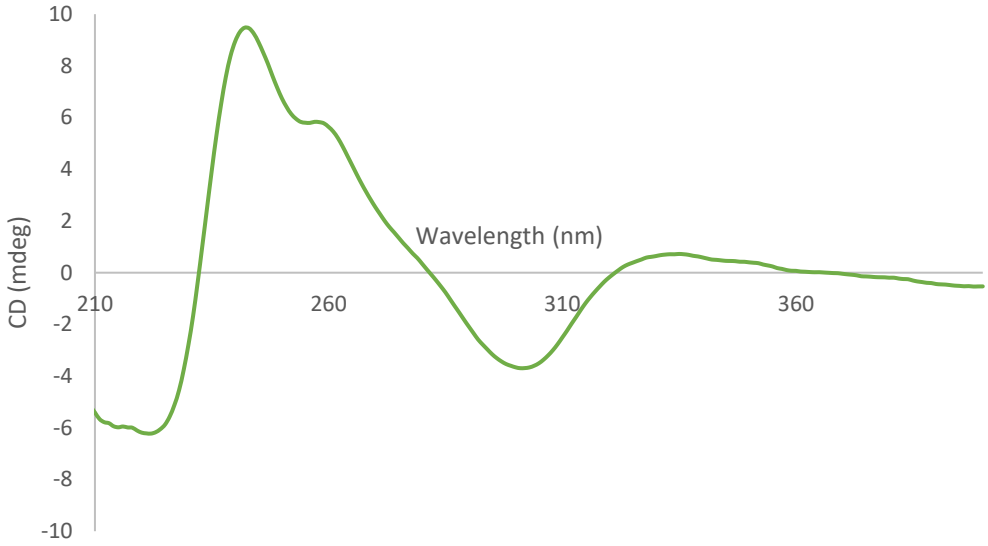

Figure S29: ECD spectrum of bacillisporin I (**1**) in MeOH

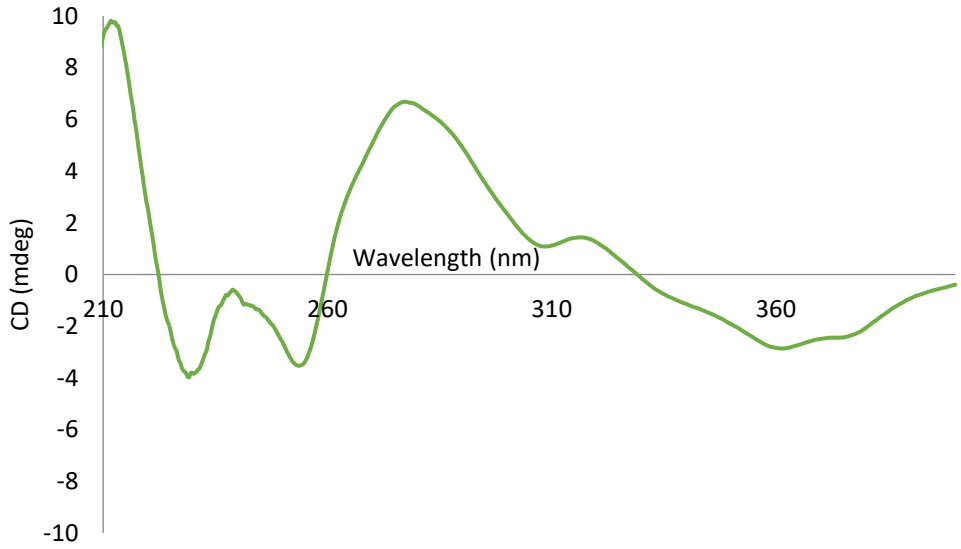

Figure S30: ECD spectrum of talarohemiketal A (**2**) in MeOH

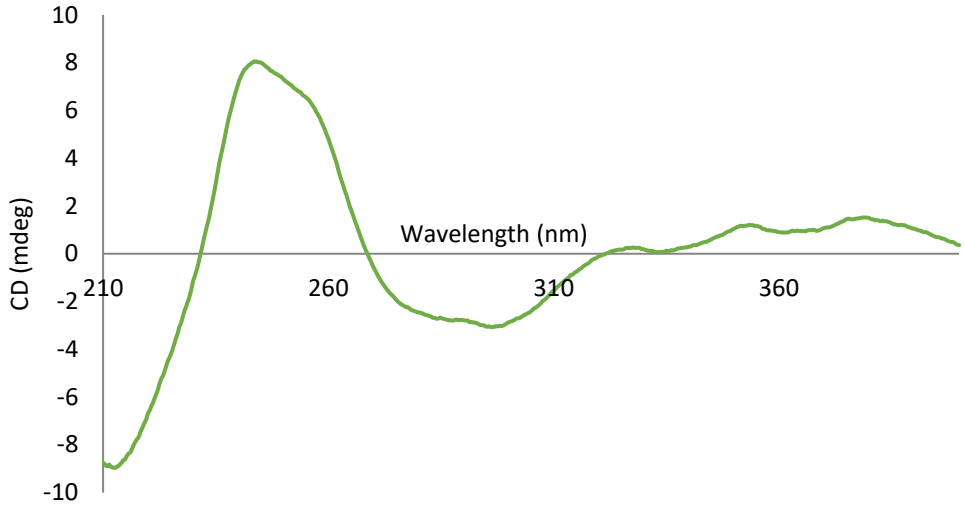

Figure S31: ECD spectrum of talaroazasone **(3)** in MeOH

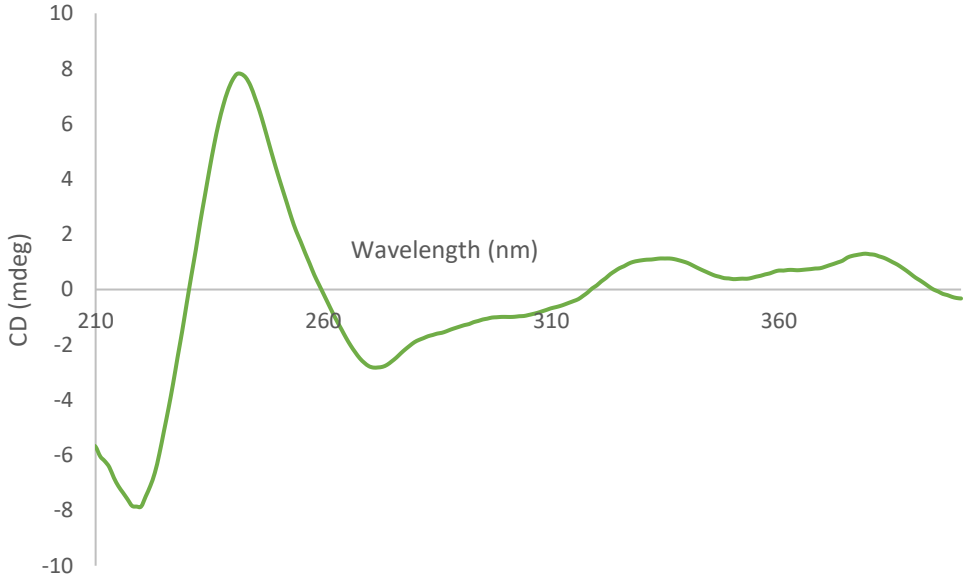

Figure S32: ECD spectrum of talaromacroclactone A (**4**) in MeOH

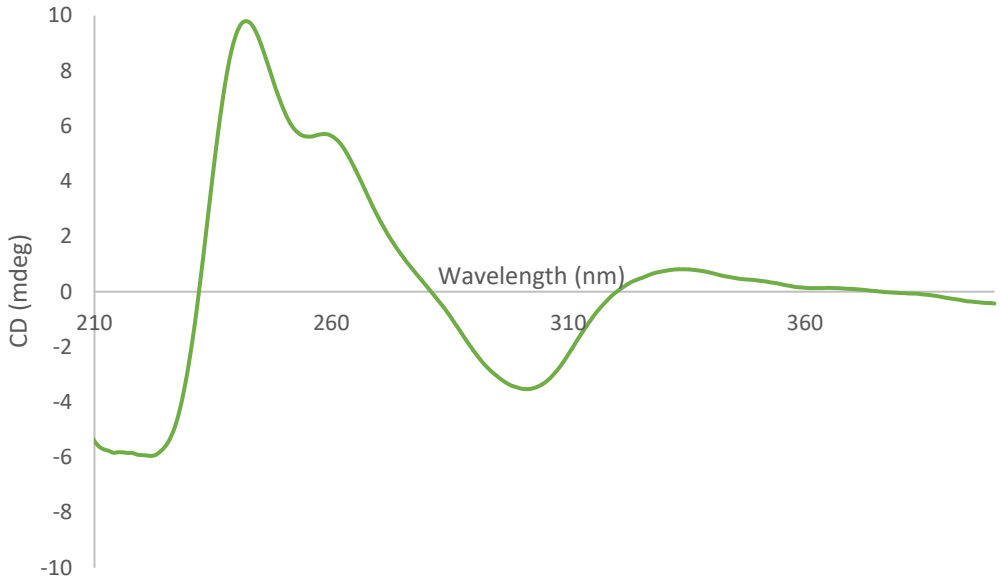

Figure S33: ECD spectrum of *epi*-bacillisporin F (**9**) in MeOH

Chapter Five

Chapter 5: Authors contribution

Nirmal Chaudhary- Isolation and purification of the crude extract, characterization, structure elucidation, manuscript draft

Dr. Ernest Lacey – Fungal culture and extraction

Dr. Andrew Piggott – Manuscript revision/Project co-supervision

Prof. Peter Karuso – Manuscript revision, Project supervision

Luteosteroside and luteolactones from an Australian fungus, *Aspergillus luteorubrus*

*Nirmal K. Chaudhary,[†] Ernest Lacey,[§,†] Andrew M. Piggott,[†] Peter Karuso[†,]**

[†]*Department of Molecular Sciences, Macquarie University, NSW 2109, Australia*

[§]*Microbial Screening Technologies Pty. Ltd., Smithfield, NSW 2164, Australia*

* Corresponding author: peter.karuso@mq.edu.au

Abstract

Exploration of the chemical diversity of the soil fungus, *Aspergillus luteorubrus*, led to the isolation of the metabolite luteosteroside A (**1**), luteolactones A-B (**2**-**3**) and the reported molecules aszonalenin (**4**), dihydrocandesolide (**5**) and viridicatumtoxin A (**6**). The structures of **1**-**6** were established by 2D NMR spectroscopy in conjunction with mass spectroscopy and the absolute configurations were determined from by comparisons of optical rotations and electronic circular dichroism data with literature data. The isolated compounds were then tested for cytotoxic, antibacterial and antifungal activities.

Introduction

The filamentous fungal genus *Aspergillus* are producers of a diverse range of bioactive metabolites. The hypolipidemic agent, lovastatin (*A. terreus*);[1] cholecystokinin antagonists, the asperlicins (*A. alliaceus*);[2] antifungal compounds, terrecyclic acid (*A. terreus*),[3] emestrin A and C (*A. striatus*),[4,5] fumitremorgin C and dehydrofumitremorgin C (*A. fumigatus & A. fischeri*);[6,7] anticancer compounds like terrein (*A. terreus*);[8] asperlin (*A. nidulan*s),[9] sequoiamonascin A (*A. parasiticus*),[10] norsolorinic acid (*A. nidulan*s, *A. parasiticus*),[11] austocystin D (*A. pseudoaustus*),[12,13] and stephacidin B (*A. ochraceous* & *A. westerdijkiae*)[14,15] are a few such examples. Recent genomic sequencing studies of *Aspergillus* sp. has revealed that the number of putative secondary metabolite genes far outnumber the metabolites discovered from them thereby suggesting the vast untapped potential of *Aspergillus* species.[16] Previous studies of Australian *Aspergillus* species, have led to the discovery of several new chemical scaffolds such as hankcockiamides A-F, a unique family of piperazines, from *A. hancockii*,[17] and kumbicins A-D, novel bis-indolyl benzenoids from *A. kumbius*.[18] Other notable chemical scaffolds from Australian strains of *Aspergillus* includes aspergillazines A-E from *A. unilateralis*,[19] aspergillicins A-E from a marine-derived strain of *A. carneus*,[20] and cottoquinazoline A and cotteslosins A-B from *A. versicolor*.[21] Continuing our chemical investigations and screening of the secondary metabolites of some Australian *Aspergilli*, a total of 7 natural products including 4 new compounds were isolated and characterized from the soil fungus *A. luteorubrus*. In contrast to the metabolite pattern of *A. banksianus,* wherein most metabolites belonged to a single biosynthetic class (isochromanones/isocoumarins) and diversification of the metabolite profile was achieved through conjugation of the major isochromanone with biosynthetically unrelated natural products and enantiodivergence.[22] The secondary metabolite pattern of *A. luteorubrus* followed the more commonly observed trend as with most *Aspergillus* sp. with

metabolites belonging to different structural classes including terpenoid, indole alkaloids, polyketides and mixture thereof.

Results and Discussion

A. luteorubrus was isolated from a soil sample collected at the White Mountains National Park, North Queensland, Australia. Preparative cultivation of *A. luteorubrus* was carried on rice resulted in a luxuriant growth of the fungus. The pooled mycelial mass was extracted into acetone, reduced to an aqueous concentrate, then partitioned against ethyl acetate to recover the organic metabolites. The crude extract was defatted and fractionated on a Sephadex LH-20 column, to yield four fractions. Fractions 2-4 contained small molecules (TLC) and were purified by reversed phase HPLC to yield 6 compounds, **1-6** in quantities sufficient for full spectroscopic characterization.

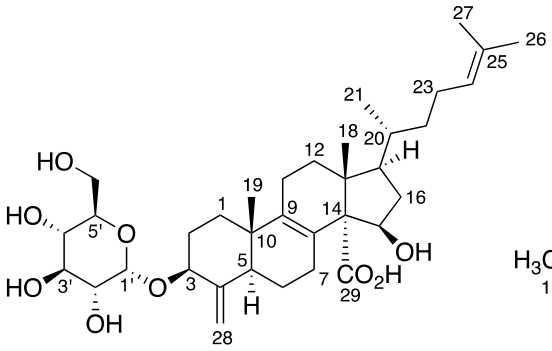

Luteosteroside A (**1**)

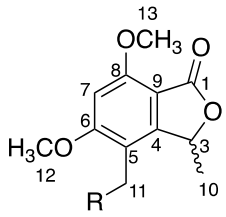

(±) Luteolactone A (**2**), R=H
(±) Luteolactone B (**3**), R=OH

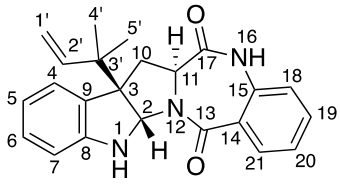

Aszonalenin (**4**)

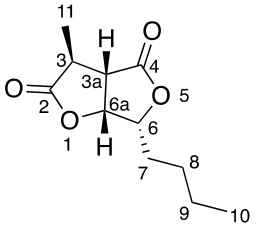

Dihydrocandesolide **(5)**

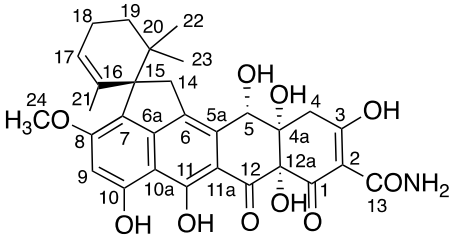

Viridicatumtoxin A (**6**)

Luteosteroside A (**1**) was isolated as a colorless amorphous solid. The IR spectrum showed absorption bands at 1698 cm^{-1} indicating the presence of a carbonyl group and at 3747 and 3364 cm^{-1} indicating the presence of hydroxyl groups. A molecular formula of $C_{35}H_{54}O_9$ was assigned based on the observed HRMS for the $[M–H]^-$ ion at *m/z* 617.3699 (Δmmu= 0.6 ppm) suggesting nine degrees of unsaturation. The ^1H and ^{13}C NMR spectra (Table 1) showed resonances for four methyl singlets (δ_H 0.83, 1.00, 1.56 and 1.64 with corresponding carbons at δ_C 18.6, 18.0, 17.5 and 25.5 respectively), one methyl doublet (δ_H 0.89 and δ_C 18.6), an olefinic methine triplet (δ_H 5.07, δ_C 124.8), a pair of broad singlets as terminal olefinic methylene (δ_H 5.17 and 4.60; δ_C 103.8), six oxymethines (δ_H 4.42, 3.96, 3.51, 3.40, 3.21 and 3.06 with corresponding carbons at δ_C 70.8, 74.3, 74.2, 73.1, 71.9 and 70.4 respectively), one oxymethylene (δ_H 3.40 and 3.54; δ_C 61.1) and one anomeric methine doublet (δ_H 4.84, δ_C 95.1) indicating the presence of a sugar unit. There were several overlapping resonances in the region (δ_H 0.98 ~ 2.8), which included 9 pairs of methylene protons and three methines. COSY correlations showed that four of the six oxymethines (δ_H 4.42, 3.51, 3.40 and 3.21), the only oxymethylene and the only anomeric methine constituted a single spin system which together with HMBC correlations from these protons further confirming the presence of hexose sugar. The ^{13}C NMR spectrum showed 35 resonances suggesting the presence of one carbonyl carbon (δ_C 176.1), three olefinic groups, of which a highly polarized pair (δ_C 103.8 and 150.1) constituted the two carbons involved in the exocyclic methylene. COSY correlations confirmed the presence of a -(OCH-CH_2)-CH-$CH(CH_3)$-CH_2-CH_2-CH= as another major spin system. The olefinic methine of this spin system (δ_C 124.8) showed a $^3J_{CH}$ correlation to two secondary methyls (δ_H 1.56, δ_C 17.5 and δ_H 1.64, δ_C 25.5) whereas the penultimate methylene (δ_C 24.2) showed $^3J_{CH}$ correlation to a non-protonated sp^2-hybridized carbon (δ_C 130.5) thereby suggesting the presence of a -$CH(CH_3)$-CH_2-CH_2-CH=$C(CH_3)_2$ side chain as in lanosterol. This together with the presence of nine methylenes, two angular methyl groups and four rings as defined by the remaining

unsaturation requirements was suggestive of a sterol skeleton. Other less extended spin systems identified by COSY correlations were -OCH-CH_2-CH_2-, -CH-CH_2-CH_2- and -CH_2-CH_2- and $^3J_{CH}$ correlations across all these spin systems established the sterol skeleton. The position of the exocyclic methylene was assigned to C-4 based on $^3J_{CH}$ correlations from H_2-4 olefinic protons to C-3 and C-5 and reciprocal $^3J_{CH}$ correlations from H-3 and H-5 to C-4. The position of the tetra-substituted double bond was assigned at the B/C ring juncture based on $^3J_{CH}$ correlations to C-9 (δ_C 138.3) from the methylene protons H_2-7 (δ_H 2.76, 1.83) and H_2-12 (δ_H 1.59, 2.11) and the angular methyl proton H_3-19 (δ_H 0.83) as well as correlations to C-8 from H_2-6 (δ_H 1.56), H_2-11 (δ_H 2.04, 2.14) and H-15 (δ_H 4.42). The $^3J_{CH}$ correlations to the carbonyl carbon (δ_C 176.1) from the H-15 oxymethine proton (δ_H 4.42) and the angular methyl proton H_3-18 (δ_H 1.00) helped in assigning the position of the carboxylic group to C-14 (δ_C 65.8).

Linkage between the glycone and the steroidal fragment was established by a $^3J_{CH}$ coupling between the anomeric proton (δ_H 4.84) with C-3 and anomeric carbon (δ_C 95.1) with H-3 methine proton (δ_H 3.96). A strong ROESY correlation between H_3-18 and H-20 and the absence of ROESY between H_3-18 and H-17 indicated that 18-CH_3 and C-17 side chain were on the same side of the steroidal skeleton. A strong ROESY correlation between H-15 and H-17 with no ROESY correlation to H_3-18 from either H-15 or H-17 indicated that H-15 and H-17 were on the opposite face as 18-CH_3 and C-17 side chain. Similarly, a strong ROESY correlation between H-3 and H-5 (Figure 1**)** with absence of any ROESY correlation from either of these protons to either H_3-19 or H-1' assigned their relative configuration. Similarly, the presence or absence of ROESY correlations starting at H-1' to the subsequent carbons assigned the relative configuration across the glycone moiety. Moreover, a small $^3J_{HH}$ coupling constant of 3.6 Hz between the anomeric proton (H-1') and the adjacent methine proton (H-2') indicated an α-anomer. The relative configuration of **1** from ROESY correlations was same as the reported compound ascosteroside. Moreover, the

measured specific optical rotation of **1** (+ 46, c 0.42 MeOH) and nature of the observed ECD spectra [(c 3.3 × 10^{-5} mg/mL, MeOH) λ(Δε) 233 (–27.3)] was very similar to that of ascosteroside (+ 43, c 0.20 MeOH) and ECD [(c not mentioned, MeOH) λ(Δε) 231 (–13.3)] suggesting same absolute configuration of as that of ascosteroside whose absolute configuration was determined by combination of NOE difference spectroscopy and application of the exciton chirality method.[23] Luteosteroside A (**1**) is the 18-methyl analog of the antibiotic PF 1032, reported from *Neosartorya* sp.

Luteolactone A (**2**) was isolated as a colorless solid. The UV spectrum was diagnostic of an isobenzofuranone chromophore with absorption maxima at 212 and 259 nm.[24] The IR spectrum showed absorption bands at 1734 cm^{-1} suggesting the presence of a carbonyl group. A molecular formula of $C_{12}H_{14}O_4$ was assigned based on the observed HRMS for the $[M+H]^+$ ion (Δmmu= –0.4 ppm). The ^1H NMR spectrum (Table 2) showed resonances for a singlet aromatic/olefinic methine (δ_H 6.58), two methyls (a doublet at δ_H 1.59 and a singlet at δ_H 2.18), two methoxy singlets (δ_H 3.92 and 4.04) and one oxymethine quartet (δ_H 5.40) whereas the ^{13}C NMR spectrum indicated the presence of a carbonyl (δ_C 168.4). A strong ROESY correlation between the methyl group (δ_H 2.18) and methoxy group (δ_H 4.04) suggested an ortho-regiochemistry. The position of carbonyl group (δ_C 168.4) was assigned based on the sole weak W-coupling from the aromatic proton which was also in agreement with the UV spectrum characteristic of an isobenzofuranone chromophore. $^3J_{CH}$ correlations from the protons confirmed the structure as **2**. The absolute configuration at the only stereocentre C-3 was concluded to be racemic as it showed zero optical rotation and the ECD spectrum was a flat line. Although, **2** has not been reported as a natural product, it has been synthesized as an intermediate in the synthesis of mycophenolic acid,[25] an isobenzofuranone based molecule with immunosuppressant and antimicrobial activities first isolated from the fungus *Penicillium brevicompactum.*[26] The spectral data of **2** was in close

agreement with the reported intermediate in the synthesis of mycophenolic acid.[25] However, natural products based on isobenzofuranone skeleton have been reported such as the austalides[27,28,29] and the marilones[30].

Luteolactone B (**3**) was isolated as a colorless solid. The UV spectrum was characteristic of an isobenzofuranone chromophore with absorption maxima at 213 and 256 nm. The IR spectrum showed absorption bands at 1734 and 3651 cm^{-1} indicating the presence of carbonyl and hydroxyl groups respectively. A molecular formula of $C_{12}H_{14}O_5$ was assigned based on the observed HRMS for the $[M+H]^+$ ion at *m/z* 239.0920 (Δmmu= 2.5 ppm). The ^1H NMR spectrum (Table 3) was very similar to luteolactone A except the presence of resonance for an oxymethylene group (δ_H 4.47) in place of a methyl singlet (δ_H 2.18) as **1**. $^3J_{CH}$ correlations to C-4, C-5 and C-6 from this oxymethylene assigned it to C-5 suggesting that **3** had a hydroxymethyl group instead of the 5-methyl group as in **2**. Also, the compound was concluded to be racemic as it showed zero optical rotation similar to **2**.

Aszonalenin (**4**) was obtained as a colorless solid. The UV spectrum showed absorption maxima at 238 and 328 nm. The IR spectrum showed absorption bands at 3747 and 1716 cm^{-1} indicating the presence of secondary amines and carbonyl groups respectively. The ESI(+)MS revealed a $[M+H]^+$ ion at *m/z* 374 suggesting an odd molecular mass of 373 which in turn suggested an odd number of nitrogens in the molecule. The ^1H and ^{13}C NMR spectra (Supporting Information, Table S1) revealed the presence of 23 protons and 23 carbons respectively suggesting a probable molecular formula of $C_{23}H_{23}N_3O_2$. The ^1H NMR spectrum showed the presence of two methyls (δ_H 0.96 and 1.05), eight aromatic/olefinic protons (δ_H 7.13, 6.61, 6.97, 6.64, 7.07, 7.48, 7.18 and 7.66) whereas the ^{13}C NMR spectrum revealed the presence of two amide carbonyls (δ_C 166.0 and 169.3). Search of literature for the molecular formula $C_{23}H_{23}N_3O_2$ with the above spectral features suggested aszonalenin

as a probable match. This was further confirmed by 2D NMR correlations. Comparison of the observed ECD spectra with the reported ECD spectra suggested 2*S*,3*R*,11*S*-aszonalenin.[31]

Dihydrocandesolide (**5**) was obtained as a colorless solid. The ^{1}H NMR spectrum showed the presence of a methyl doublet (δ_H 1.45, $^{3}J_{HH}$ = 7.8), a methyl triplet (δ_H 0.94, $^{3}J_{HH}$ = 7.2), a methine doublet of quartet (δ_H 3.06, $^{3}J_{HH}$ = 7.8, 1.3), a methine doublet of doublet (δ_H 3.14, $^{3}J_{HH}$ = 6.0, 1.3), an oxymethine doublet of doublet (δ_H 5.11, $^{3}J_{HH}$ = 6.0, 4.0), an oxymethine doublet of doublet of doublet (δ_H 4.55, $^{3}J_{HH}$ = 8.0, 5.3, 4.0), three pairs of methylene protons (δ_H 1.83/1.91, 1.47 and 1.40) whereas the ^{13}C NMR spectrum showed the presence of two carbonyls (δ_C 175.0 and 177.0) consistent with γ-lactones. COSY correlations established the presence of a single 2,3,4,5-tetrasubstituted n-nonane spin system and HMBC correlations (Supporting Information, Table S2) suggested dihydrocandesolide as a possible match. Comparison of the observed NMR data was a perfect match with the literature[32] including the coupling constant values. ROESY correlations established the relative configuration of the compound. The measured specific optical rotation of **6** (+36) was in close agreement with that reported for 3*S*,3a*S*,6*R*,6a*R*-dihydrocandesolide (+ 30,) thereby conforming its absolute configuration.[33]

Viridicatumtoxin A (**6**) was obtained as bright yellow solid. The UV spectrum showed absorption maxima at 236, 278, 332, 348 and 433 nm and was diagnostic of the viridicatumtoxin scaffold, a rare class of fungal polyketide closely related to the tetracycline antibiotic. The ESIMS at *m/z* 565.2 was consistent with $C_{30}H_{31}NO_{10}$ (viridicatumtoxin A). Comparison of the ^{1}H NMR and ^{13}C NMR spectra (Supporting Information, Table S3) showed similar chemical shifts despite the difference in the solvent used. Assignment of 2D NMR correlations further confirmed the structure as viridicatumtoxin A. Moreover, the

measured ECD spectrum (Supporting Information, Figure S16) was perfectly identical to that of the reported one and also the measured specific optical rotation (+ 28) was also in agreement with the reported value (+31) suggesting the same absolute configuration as the reported one.[34]

Conclusion

Investigation of the chemical diversity of the filamentous fungal species *A. luteorubrus* revealed the presence of 7 key metabolites with diverse chemical scaffolds. Luteolactones A and B were the major secondary metabolites with an isobenzofuranone scaffold and they could originate via orsellinic acid pathway which arises from 3 molecules of malonyl CoA and a molecule of acetyl CoA through acetate–malonate pathway. Luteosteroside A is a steroidal glycoside in which the steroidal moiety is derived from acetate-mevalonate pathway. Luteolic acid is an unusual fatty acid. Aszonalenin, an alkaloid is basically a product of shikimic acid pathway arising from the condensation of anthranillic acid with tryptophan followed by a reverse prenylation at C-3 position on the indole ring. Viridicatumtoxin A is a rare fungal tetracycline with potent antibiotic activity and biogenetic origin from 8 units of malonyl CoA with a unit of malanomoyl CoA to first yield a tetracycline scaffold followed by attachment and cyclization of a geranyl moiety to the ring C of tetracycline scaffold.[35]

EXPERIMENTAL

General

Thin-layer chromatography (TLC) was performed using pre-coated silica gel GF254 plates (Merck, Darmstadt, Germany) with various solvent systems and spots were visualised with UV light (254 nm). Preparative and semi-preparative HPLC separations were performed on

a Gilson HPLC system, equipped with a Gilson 215 liquid handler, 819 injection module, 322 pump, 506C system interface and Gilson single variable wavelength UV-Vis 152 detector by reversed phase chromatography using a gradient of acetonitrile (Sigma Aldrich, USA) and water unless mentioned otherwise. Phenomenex Hydro-RP (250 × 22.4 mm, 10 μm) and Phenomenex Hydro-RP (250 × 10 mm, 5 μm) columns were used for preparative and semi-preparative purifications respectively. UV-visible readings were taken on an Eppendorf UV-visible spectrophotometer (Biospectrometer Kinetic) in a 1 × 1 cm quartz cell. Optical rotations were recorded in MeOH using a JASCO P-1020 Polarimeter (Jasco Corp., Japan) in a 1 cm path length cell. ECD spectra were recorded on a Jasco J-1500 spectropolarimeter (Jasco Corp., Japan) in a 1 × 1 cm quartz cell. The IR spectra were recorded on a Thermo Scientific Nicolet iS10 ATR FTIR spectrometer as neat films. The ^{1}H NMR, ^{13}C NMR and 2D NMR spectra were recorded in deuterated DMSO or deuterated chloroform using a Bruker AVANCE II 500 MHz NMR spectrometer (Bruker Corp.). ESI-MS spectra were recorded using an Agilent 6130B single quadrupole mass spectrometer (Agilent Corp.). HR-ESIMS data were obtained using a Q Exactive Plus hybrid quadrupole orbitrap mass spectrometer (Thermo Scientific, Bremen, Germany).

Biological Material

A. luteorubrus was isolated from a soil sample collected from White Mountains National Park, North Queensland, Australia. as part of investigation of the diversity of the fungal family Trichocomaceae and was accessioned into the Commonwealth Scientific and Industrial Research Organisation (CSIRO) fungal collection as FRR 5427.

Extraction and Isolation

A. luteorubrus was cultivated for extraction on hydrated rice in Erlenmeyer flasks (100 g; 40 × 250 mL) at 24 °C for 14 days and pooled (2620 g) then extracted with acetone (2 × 3 L) for 2 h on a rotatory platform at 100 rpm. The macerated solid was removed by filtration and the filtrate concentrated to an aqueous concentrate (107 g) by rotatory evaporation. The concentrate was partitioned against ethyl acetate (2 × 1.5 L) then evaporated to dryness to provide an organic extract (14.9 g). The extract was dissolved in methanol (300 mL), diluted with distilled water (30 mL) and de-fatted by partition against hexane (2 × 300 mL) to provide a crude extract (4.7 g).

A portion of the crude extract of *A. luteorubrus* (2.5 g) was subjected to size exclusion chromatography on Sephadex LH-20 (methanol: chloroform, 1:1). Eluted fractions were combined based on TLC into four fractions, S1-S4. Fraction S1 was mostly viscous polymeric material and was not further investigated. Fractions S2-S4 were pre-treated on a C_{18} SPE cartridge by washing with 10% methanol/water and eluting with 90% methanol/water, before reversed phase HPLC purification (acetonitrile/water). Preparative HPLC purification of Fraction S2 yielded viridicatumtoxin A (**7**; 2 mg; t_R 36.1 min), luteosteroside A (**1**; 2 mg; t_R 30.6 min), luteolic acid (**4**; 2 mg; t_R 31.2 min), Preparative HPLC purification of Fraction S3 yielded luteosteroside A (**1**; 2 mg; t_R 30.6 min), aszonalenin (**5**; 3 mg; t_R 29.8 min), luteolactone A (**2**; 2 mg; t_R 25.3 min) and luteolactone B (**3**; 4 mg; t_R 13.2 min). Fraction S4 yielded aszonalenin (**5**; 3 mg; t_R 29.8 min), luteolactone A (**2**; 2 mg; t_R 25.3 min) and luteolactone B (**3**; 4 mg; t_R 13.2 min).

Spectroscopic data

Luteosteroside A (1): White solid; $[\alpha]^{24}_{D}$ + 46 (*c* 0.42, MeOH); ECD (c 3.3 × 10^{-5} mg/mL MeOH) λ(Δε) 233 (–27.3); UV (MeOH) λ_{max} (log ε) 235 (3.25) nm; IR (ATR) ν_{max} 3747, 3364, 2925, 2360, 1698, 1683, 1651, 1201, 1137, 1047, 1023, 1003, 824, 719, 626 cm^{-1}; NMR (600 MHz, DMSO-d_6) see Table 1; HR-ESI(–)MS *m/z* 617.3699 (calcd for $C_{35}H_{53}O_9^-$ 617.3695).

Luteolactone A (2): Colourless oil; $[\alpha]^{24}_{D}$ 0 (*c* 0.49, MeOH); UV (MeOH) λ_{max} (log ε) 212 (4.13), 259 (3.81) nm; IR (ATR) ν_{max} 2972, 1734, 1604, 1472, 1457, 1236, 1058, cm^{-1}; NMR (600 MHz, DMSO-d_6) see Table 2; HR-ESI(+)MS *m/z* 223.0964 (calcd for $C_{12}H_{15}O_4^+$, 223.0965).

Luteolactone B (3): Colourless oil; $[\alpha]^{24}_{D}$ 0 (*c* 0.74, MeOH); UV (MeOH) λ_{max} (log ε) 213 (4.17), 256 (3.87) nm; IR (ATR) ν_{max} 3651, 2972, 1734, 1602, 1472, 1457, 1340, 1236, 1056, cm^{-1}; NMR (600 MHz, DMSO-d_6) see Table 3; HR-ESI(+)MS *m/z* 239.0920 (calcd for $C_{12}H_{15}O_5^+$, 239.0914).

Aszonalenin (4): Off-white solid; $[\alpha]^{24}_{D}$ + 55 (*c* 0.15, MeOH); ECD (c 1.2 × 10^{-5} mg/mL MeOH) λ(Δε); 230 (–36.2), 252 (24.4), 277 (4.4), 304 (–8.0) NMR (600 MHz, DMSO-d_6) see Supporting Information, Table S1.

Dihydrocandesolide (5): Off-white solid; $[\alpha]^{24}_{D}$ + 36 (*c* 0.34, MeOH); ECD (c 2.1 × 10^{-4} mg/mL MeOH) λ(Δε); 229 (–12.1), 249 (17.9), 291 (–5.6); NMR (600 MHz, DMSO-d_6) see Supporting Information, Table S2.

Viridicatumtoxin A (6): Yellow solid; $[\alpha]^{24}_{D}$ + 28 (*c* 0.39, EtOH); ESI(+)MS *m/z* 565.2; NMR (600 MHz, DMSO-d_6) see Supporting Information, Table S3.

Conflicts of interest

There are no conflicts to declare.

Acknowledgement

We thank Dr M. McKay (APAF, Macquarie University) for the acquisition of HRMS data. This research was funded, in part, by the Australian Research Council (DP130103281 to PK and AMP; FT130100142 to AMP) and Macquarie University (iMQRES scholarship to NC).

References

(1) Alberts, A.; Chen, J.; Kuron, G.; Hunt, V.; Huff, J.; Hoffman, C.; Rothrock, J.; Lopez, M.; Joshua, H.; Harris, E. *Proc. Natl. Acad. Sci.* **1980,** *77* (7), 3957-3961.

(2) Goetz, M.; Monaghan, R.; Chang, R.; Ondeyka, J.; Chen, T.; Lotti, V. *J. Antibiot.* **1988,** *41* (7), 875-877.

(3) Visalakchi, S.; Muthumary, J. *Int. J. Pharma. Biosci.* **2010,** *1*, 1-9.

(4) Carberry, S.; Molloy, E.; Hammel, S.; O'Keeffe, G.; Jones, G. W.; Kavanagh, K.; Doyle, S. *Fungal Genet. Biol.* **2012,** *49* (4), 302-312.

(5) Kidd, J. G. *Science* **1947,** *105*, 511-513.

(6) Finefield, J. M.; Frisvad, J. C.; Sherman, D. H.; Williams, R. M. *J. Antibiot.* **2012,** *75* (4), 812-833.

(7) Zhao, S.; Smith, K. S.; Deveau, A. M.; Dieckhaus, C. M.; Johnson, M. A.; Macdonald, T. L.; Cook, J. M. *J. Med. Chem* **2002,** *45* (8), 1559-1562.

(8) Liao, W.-Y.; Shen, C.-N.; Lin, L.-H.; Yang, Y.-L.; Han, H.-Y.; Chen, J.-W.; Kuo, S.-C.; Wu, S.-H.; Liaw, C.-C. *J. Nat. Prod.* **2012,** *75* (4), 630-635.

(9) He, L.; Nan, M.-H.; Oh, H. C.; Kim, Y. H.; Jang, J. H.; Erikson, R. L.; Ahn, J. S.; Kim, B. Y. *Biochem. Bioph. Res. Co.* **2011,** *409* (3), 489-493.

(10) Stierle, D. B. S., Andrea A.; Bugni Timothy *J. Org. Chem.* **2003,** *68* (12), 4966-4969.

(11) Yamada, T.; Jinno, M.; Kikuchi, T.; Kajimoto, T.; Numata, A.; Tanaka, R. *J. Antibiot.* **2012,** *65* (8), 413-417.

(12) Chen, G.-D.; Li, Y.-J.; Gao, H.; Chen, Y.; Li, X.-X.; Li, J.; Guo, L.-D.; Cen, Y.-Z.; Yao, X.-S. *Planta Med.* **2012,** *78* (15), 1683-1689.

(13) Wang, C. C.; Chiang, Y. M.; Kuo, P. L.; Chang, J. K.; Hsu, Y. L. *Clini. Exp. Pharmacol. P.* **2008,** *35* (11), 1301-1308.

(14) Abraham, W.-R.; Arfmann, H.-A. *Phytochemistry* **1990,** *29* (3), 1025-1026.

(15) Yamazaki, M.; Suzuki, S.; Miyaki, K. *Chem. Pharm. Bull.* **1971,** *19* (8), 1739-1740.

(16) Sanchez, J. F.; Somoza, A. D.; Keller, N. P.; Wang, C. C. C. *Nat. Prod. Rep.* **2012,** *29* (3), 351-371.

(17) Pitt, J. I.; Lange, L.; Lacey, A. E.; Vuong, D.; Midgley, D. J.; Greenfield, P.; Bradbury, M. I.; Lacey, E.; Busk, P. K.; Pilgaard, B.; Chooi, Y.-H.; Piggott, A. M. *PLoS One* **2017,** *12* (4), e0170254.

(18) Lacey, H. J.; Vuong, D.; Pitt, J. I.; Lacey, E.; Piggott, A. M. *Aust. J. Chem.* **2016,** *69* (2), 152-160.

(19) Capon, R. J.; Ratnayake, R.; Stewart, M.; Lacey, E.; Tennant, S.; Gill, J. H. *Org. Biomol. Chem.* **2005,** *3* (1), 123-129.

(20) Capon, R. J.; Skene, C.; Stewart, M.; Ford, J.; Richard, A.; Williams, L.; Lacey, E.; Gill, J. H.; Heiland, K.; Friedel, T. *Org. Biomol. Chem.* **2003,** *1* (11), 1856-1862.

(21) Ibrahim, S. R.; Mohamed, G. A.; Ross, S. A. *Z. Naturforsch. C Bio. Sci.* **2017,** *72* (5-6), 155-160.

(22) Chaudhary, N. K. Natural products from some filamentous fungi and other sources. PhD thesis, Macquarie University, Australia, 2017.

(23) Leet, J. E.; Huang, S.; Klohr, S. E.; McBrien, K. D. *J. Antibiot.* **1996,** *49* (6), 553-559.

(24) Zhuravleva, O. I.; Sobolevskaya, M. P.; Leshchenko, E. V.; Kirichuk, N. N.; Denisenko, V. A.; Dmitrenok, P. S.; Dyshlovoy, S. A.; Zakharenko, A. M.; Kim, N. Y.; Afiyatullov, S. S. *J. Nat. Prod.* **2014,** *77* (6), 1390-1395.

(25) Watanabe, M.; Masao, T.; Hamada, Y.; Iwao, M.; Furukawa, S. *Chem. Pharm. Bull.* **1989,** *37* (11), 2948-2951.

(26) Bentley, R. *Chem. Rev.* **2000,** *100* (10), 3801-3826.

(27) Horak, R. M.; Steyn, P. S.; Van Rooyen, P. H.; Vleggaar, R.; Rabie, C. J. *J. Chem. Soc. Chem. Commun.* **1981,** (24), 1265-1267.

(28) Horak, R. M.; Steyn, P. S.; Vleggaar, R.; Rabie, C. J. *J. Chem. Soc. Perkin Trans. I* **1985**, 363-367.

(29) Zhou, Y.; Mándi, A.; Debbab, A.; Wray, V.; Schulz, B.; Müller, W. E.; Lin, W.; Proksch, P.; Kurtán, T.; Aly, A. H. *Eur. J. Org. Chem.* **2011,** *2011* (30), 6009-6019.

(30) Almeida, C.; Kehraus, S.; Prudêncio, M.; König, G. M. *Beilstein J. Org. Chem.* **2011,** *7*, 1636.

(31) Yin, W.-B.; Cheng, J.; Li, S.-M. *Org. Biomol. Chem.* **2009,** *7* (10), 2202-2207.

(32) Li, Y.; Teng, Z.; Parkin, K. L.; Wang, Q.; Zhang, Q.; Luo, W.; Ma, D.; Zhao, M. *J. Agri. Food Chem.* **2014,** *62* (33), 8392-8401.

(33) Nubbemeyer, U. *J. Org. Chem.* **1996,** *61* (11), 3677-3686.

(34) Shang, Z.; Salim, A. A.; Khalil, Z.; Quezada, M.; Bernhardt, P. V.; Capon, R. J. *J. Org. Chem.* **2015,** *80* (24), 12501-12508.

(35) Chooi, Y.-H.; Cacho, R.; Tang, Y. *Chem. Biol.* **2010,** *17* (5), 483-494.

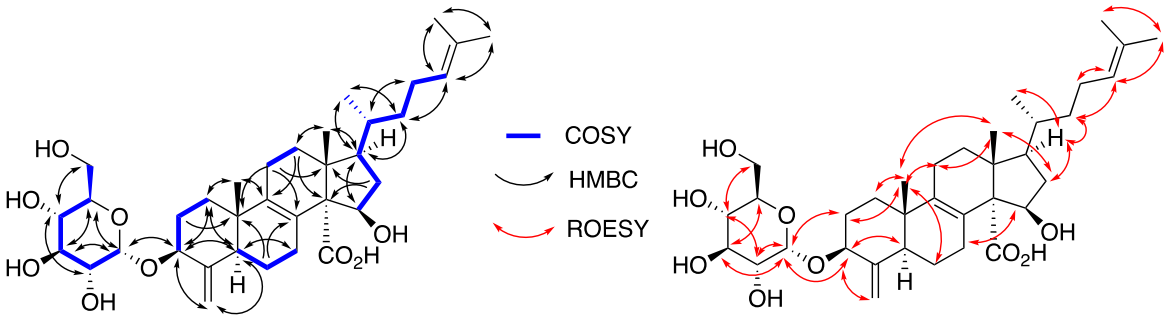

Figure 1: Key COSY, HMBC and ROESY correlations in luteosteroside A (**1**)

Table 1: NMR data for luteosteroside A (**1**) in DMSO-d_6

Position	δ_C, type	δ_H, mult (*J*, Hz)	^1H-^{13}C HMBC	COSY	ROESY
1	34.7, CH_2	α 1.26, m	2, 3, 19	1β, 2α, 2β	1β, 2α, 2β,19
		β 1.81, m	3, 5, 10	1α, 2α, 2β	1α, 2α, 2β
2	28.0, CH_2	β 1.26, m	3, 4, 10	2α, 1, 3	1α, 2α, 3, 19,1'
		α 2.04, m	1, 4, 10	2β, 1, 3	1α, 2β
3	74.3, CH	3.96, m	2, 4, 28, 1'	3, 2α, 2β	1α, 2α, 5', 5, 28, 1', 2'
4	150.1, C				
5	46.2, CH	1.85, m	1, 4, 6, 10, 19, 28	6	3, 6, 7β
6	20.6, CH_2	1.56, m	5, 8, 10	5, 7α, 7β	5, 7, 19
7	25.4, CH_2	α 1.87, m	8, 9	6	6, 7β, 15
		β 2.76, m	5, 6, 8	6	6, 7α, 15
8	127.5, C				
9	138.4, C				
10	39.0, C				
11	23.0, CH_2	β 2.04, m	8, 9	11α, 12α	12α, 12β, 18, 19
		α 2.14, m	9, 13	11β,12β	12α, 12β, 19
12	32.2, CH_2	β 1.59, m	9, 11, 13, 14,	12α, 11α	11α,11β, 12β, 17, 21
		α 2.11, dd (8.4, 12.4)	18	12α, 11β	11α,11β, 12α, 17, 18, 21
13	45.8, C				
14	65.7, C				
15	70.8, CH	4.42, br d (7.1)	13, 16, 17, 29	16α, 16β	7α, 7β, 16α, 16β
16	43.4, CH_2	β 1.35, dd (9.2, 13.4)	15, 18, 16 15, 16, 17	15, 17, 16α, 22	15, 17, 16α
		α 2.46, m		15, 17, 16β	15, 18, 16β

17	49.9, CH	1.33, m	16, 18	16, 20	12α, 12β, 21, 23, 16α, 22
18	18.0, CH_3	1.00, s	12, 13, 14, 17		11β, 12α, 12β, 16β, 17, 19, 20, 21, 23
19	18.6, CH_3	0.83, s	1, 5, 9, 10		2β, 6, 11α,11β, 18, 28a, 28b
20	34.9, CH	1.48, m	17, 22	17, 21, 22	18, 21, 22
21	18.5, CH_3	0.89, d (6.4)	17, 20, 22	20	12α, 12β, 17, 18, 20, 23
22	35.8, CH_2	0.99, m 1.35, m	17, 20, 21, 23, 24	21, 23	20, 23, 16β
23	24.2, CH_2	1.83, m 1.94, m	21, 22, 24, 25	22, 24	20, 21, 22, 24
24	124.8, CH	5.07, t (7.1)	22, 23, 26, 27	23	22, 23, 26
25	130.5, C				
26	25.5, CH_3	1.64, s	24, 25, 27		24, 27
27	17.5, CH_3	1.56, s	24, 25, 26		26
28	103.6, CH_2	a 4.60, s	3, 4, 5	28b	19, 28b
		b 5.17, s	3, 4, 5	28a	19, 28a, 3'
29	176.1, C				
1'	95.1, CH	4.84, d (3.6)	3, 3', 5'	2', 3'	2, 3, 2'
2'	71.9, CH	3.21, dd (9.6, 3.6)	3',	1', 3'	1', 4'
3'	73.2, CH	3.51, m	2', 5'	2', 4'	1', 5'
4'	73.1, CH	3.39, m	6'	3', 5'	2', 6'
5'	70.4, CH	3.06, m	3', 6'	4', 6'	3', 6'
6'	61.1, CH_2	3.40, m 3.54, m	1', 3', 4'	5'	4', 5'

Table 2: NMR data for luteolactone A (**2**) in $CDCl_3$

Position	δ_C, type	δ_H, mult (*J*, Hz)	^1H-^{13}C HMBC	COSY	ROESY
1	167.3, C				
3	76.4, CH	5.40, q (6.7)	1, 4, 5, 9	10	10, 11
4	153.1, C				
5	120.6, C				
6	164.4, C				
7	98.1, CH	6.58, s	5, 6, 8, 9		12
8	157.7, C				
9	109.8, C				
10	8.7, CH_3	1.59, d (6.7)	3, 4	3	3, 11
11	20.8, CH_3	2.18, s	4a 5, 6		3, 10
12	62.3, CH_3	4.04, s	6		7
13	56.2, CH_3	3.92, s	8		7

Table 3: NMR data for luteolactone B (**3**) in DMSO-d_6

Position	δ_C, type	δ_H, mult (*J*, Hz)	^1H-^{13}C HMBC	COSY	ROESY
1	167.3, C				
3	76.3, CH	5.53, q (6.6)	1, 4, 5, 9	10	10, 11
4	155.4, C				
5	123.0, C				
6	164.2, C				
7	100.2, CH	7.03, s	5, 6, 8, 9		12
8	157.6, C				
9	108.8, C				
10	20.2, CH_3	1.54, d (6.6)	3, 4	3	3, 11
11	51.4, CH_2	4.47, s	4, 5, 6		3, 10
12	62.7, CH_3	3.95, s	6		7
13	56.5, CH_3	3.90, s	8		7
11-OH					

Supporting Information

Luteosteroside and luteolactones from an Australian fungus, *Aspergillus luteorubrus*

Nirmal K. Chaudhary[†], *Ernest Lacey*[§,†], *Andrew M. Piggott*[†], *Peter Karuso*[†,*]

[†]*Department of Molecular Sciences, Macquarie University, NSW 2109, Australia*

[§]*Microbial Screening Technologies Pty. Ltd., Smithfield, NSW 2164, Australia*

* Corresponding author: peter.karuso@mq.edu.au

Table of Contents

A. NMR tables

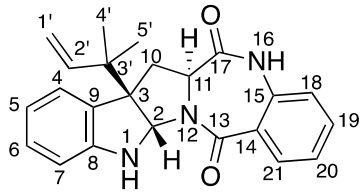

Table S1: NMR data for aszonalenin (**4**) in DMSO-d_6

Position	δ_C, type	δ_H, mult (*J*, Hz)	^{1}H-^{13}C HMBC	COSY	ROESY
1		6.65, brs			2, 7
2	80.7, CH	5.47, s	3, 8, 9, 10, 11, 3'		1, 7, 2', 4', 5'
3	60.1, C				
4	124.7, CH	7.13, d (7.4)	3, 5, 6, 8, 9	5	5, 10a, 4', 5'
5	117.5, CH	6.61, dd (7.4, 7.5)	4, 6, 7, 9	4, 6	4, 6, 10b (w)
6	128.1, CH	6.97, dd (7.5, 8.0)	4, 5, 7, 8	5, 7	5, 7
7	108.8, CH	6.64, d (8.0)	5, 6, 8, 9	6	1, 2, 6
8	149.3, C				
9	131.2, C				
10	33.0, CH_2	a 2.30, dd (13.8, 9.0) b 3.30, m (13.8, 7.2)	2, 3, 9, 11, 17 2, 3, 9, 11, 17, 3'	11	10b, 11, 4, 5' 10 a, 4', 5', 5(w)
11	56.6, CH	3.98, dd (9.3, 9.0)	2, 3, 10, 13, 17	10	10a
13	166.0, C				
14	126.9, C				
15	135.5, C				
16		10.59, s	11, 14, 15, 17, 18		18
17	169.3, C				
18	121.0, CH	7.07, dd (7.6, 1.3)	14, 15, 19, 20	19	16, 19
19	132.4, CH	7.48, ddd (7.6, 7.6, 1.3)	15, 18, 20, 21	18, 20	18, 20
20	124.0, CH	7.18, ddd	14, 18, 19, 21	19, 21	19, 21

		(7.6, 7.6, 1.3)			
21	130.2, CH	7.66, dd (7.6, 1.3)	13, 14, 15, 19, 20	20	20
1'	113.7, CH_2	5.06, br d (23.2) 5.87, br d (16.7)	2', 3', 4'(w), 5'(w)	2'	2', 4', 5'
2'	144.3, CH	6.10, dd (17.5, 10.8)	1', 3', 4'(w), 5'(w)	1'	1', 4', 5', 2
3'	41.2, C				
4'	22.4, CH_3	0.96, s	3, 2', 3', 5', 1'(w)		5', 10a, 10b
5'	22.4, CH_3	1.05, s	3, 2', 3',4', 1'(w)		10a, 4'

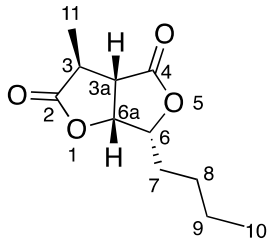

Table S2: NMR data for dihydrocandesolide (**5**) in $CDCl_3$

Position	δ_C, type	δ_H, mult (*J*, Hz)	^1H-^{13}C HMBC	COSY	ROESY
2	177.0, C				
3	38.6, CH	3.06, dq (7.8, 1.3)	3a, 4, 6a, 10	3a, 10	11
3a	49.1, CH	3.14, dd (6.0, 1.3)	3, 4, 6a, 6, 11	3, 6a	6a, 11
4	175.0, C				
6	82.5, CH	4.55, ddd (8.0, 5.3, 4.0)	4, 7, 8, 3a, 6a	6a, 8	6a, 7
6a	78.5, CH	5.11, dd (6.0, 4.0)	3, 3a, 4, 6, 7	6, 3a	3a, 6
7	28.7, CH_2	a 1.83, m	6, 9	8	8
		b 1.91, m	6, 6a, 8	6, 8	8, 6
8	27.7, CH_2	1.47, m	6, 8, 9, 10	7,9	7, 9
9	22.5, CH_2	1.40, m	7, 8, 10	8, 10	8, 10
10	14.1, CH_3	0.94, t (7.2)	8, 9	9	9
11	17.4, CH_3	1.45, d (7.8)	3, 3a	3	3, 3a

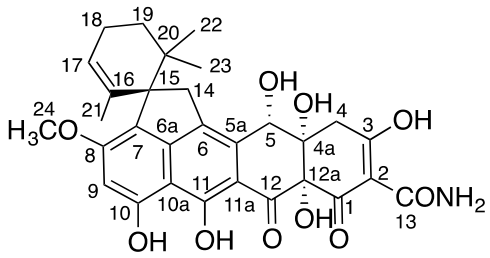

Table S3: NMR data for viridicatumtoxin A (**6**) in DMSO-d_6

Position	δ_C, type	δ_H, mult (*J*, Hz)	^{1}H-^{13}C HMBC	COSY	ROESY
1	192.0, C				
2	98.5, C				
3	193.4, C				
4	28.6, CH_2	β 2.79, br d α 2.82, br s	2, 3, 5, 4a, 12a 2, 3, 5, 4a, 12a	4α 4β	5
4a	68.7, C				
5	64.3, C		4, 6, 11a, 12a		4
6	128.3, C				
6a	147.3, C				
7	107.6, C				
8	158.6, C				
9	99.2, CH	6.67, s	7, 8, 10, 15, 10a		24
10	157.4, C				
10a	119.2, C				
11	165.6, C				
11a	105.5, C				
12	195.9, C				
12a	81.8, C				
13	173.0, C				
14	39.4, CH_2	α 1.06, s β 1.12, s	6, 7, 15, 16, 20, 5a, 6a, 10a, 11a		22, 23
15	58.3, C				
16	137.4, C				
17	119.9, CH	5.39, s	15, 19, 21	18	18, 21
18	33.4, CH_2	1.29, m	16, 17, 20, 22	17, 19	17, 19

		1.74, m			
19	22.4, CH_2	1.97,	15, 17	18	18, 22, 23
20	38.4, C	2.13,			
21	21.0, CH_3	1.43, s	15, 16, 17		17, 24
22	24.1, CH_3	0.86, s	15, 18, 20, 23		23, 14
23	25.7, CH_3	0.44, s	15, 18, 20, 22		22, 14
24	55.4, OCH_3	3.78, s	8		9, 21
3-OH		18.24, br s			
4a-OH		[a]			
5-OH		6.75, br s			
10-OH		12.31, br s			
11-OH		14.66, br s			
12a-OH		[a]			
13-NH_2		8.81, br s 9.68, br s			

[a]Not assignable

B. ^{1}H (600 MHz) and ^{13}C NMR (150 MHz) NMR spectra

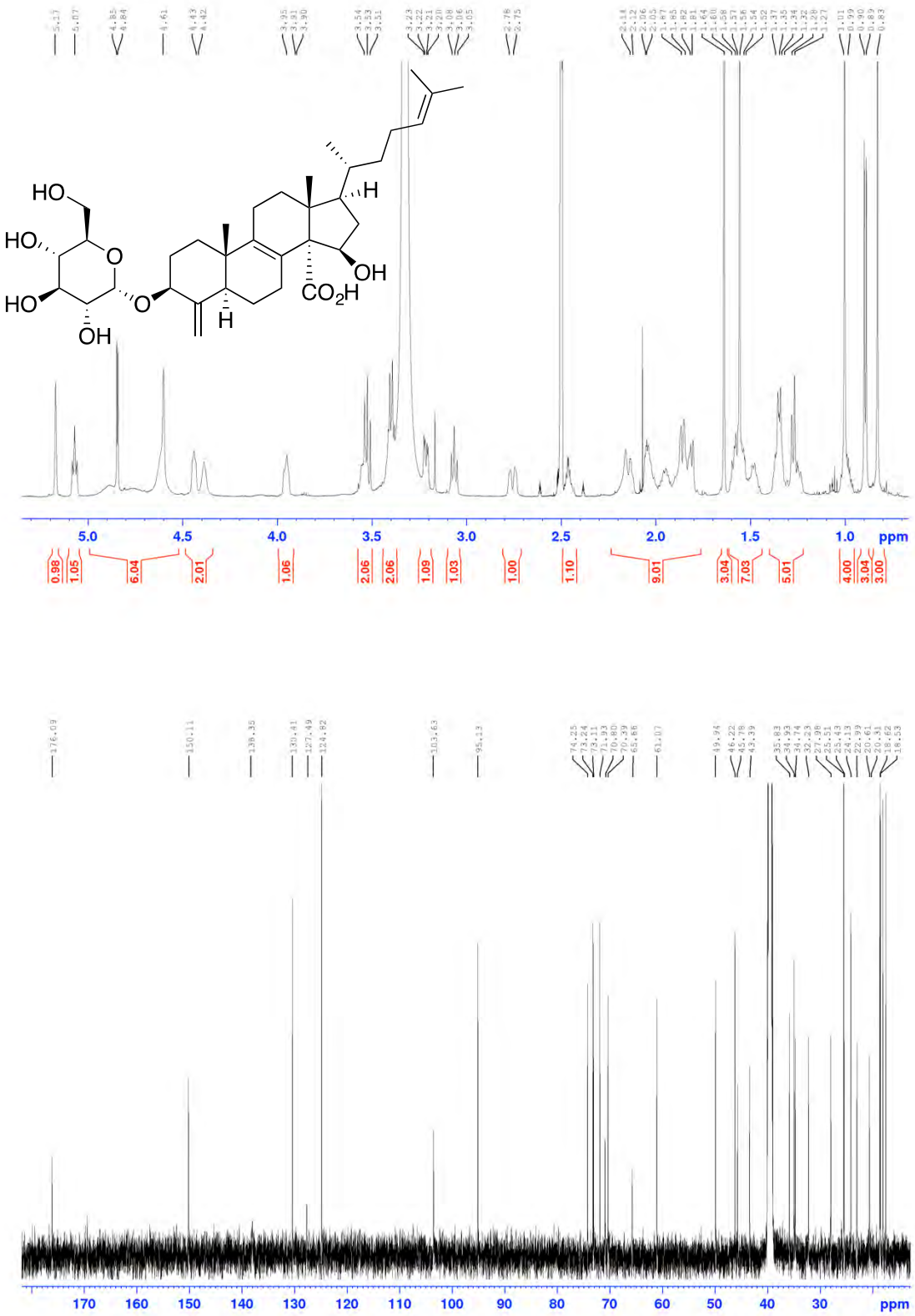

Figure S1: ^{1}H and ^{13}C NMR spectra of luteosteroside A (**1**) in DMSO-d_6

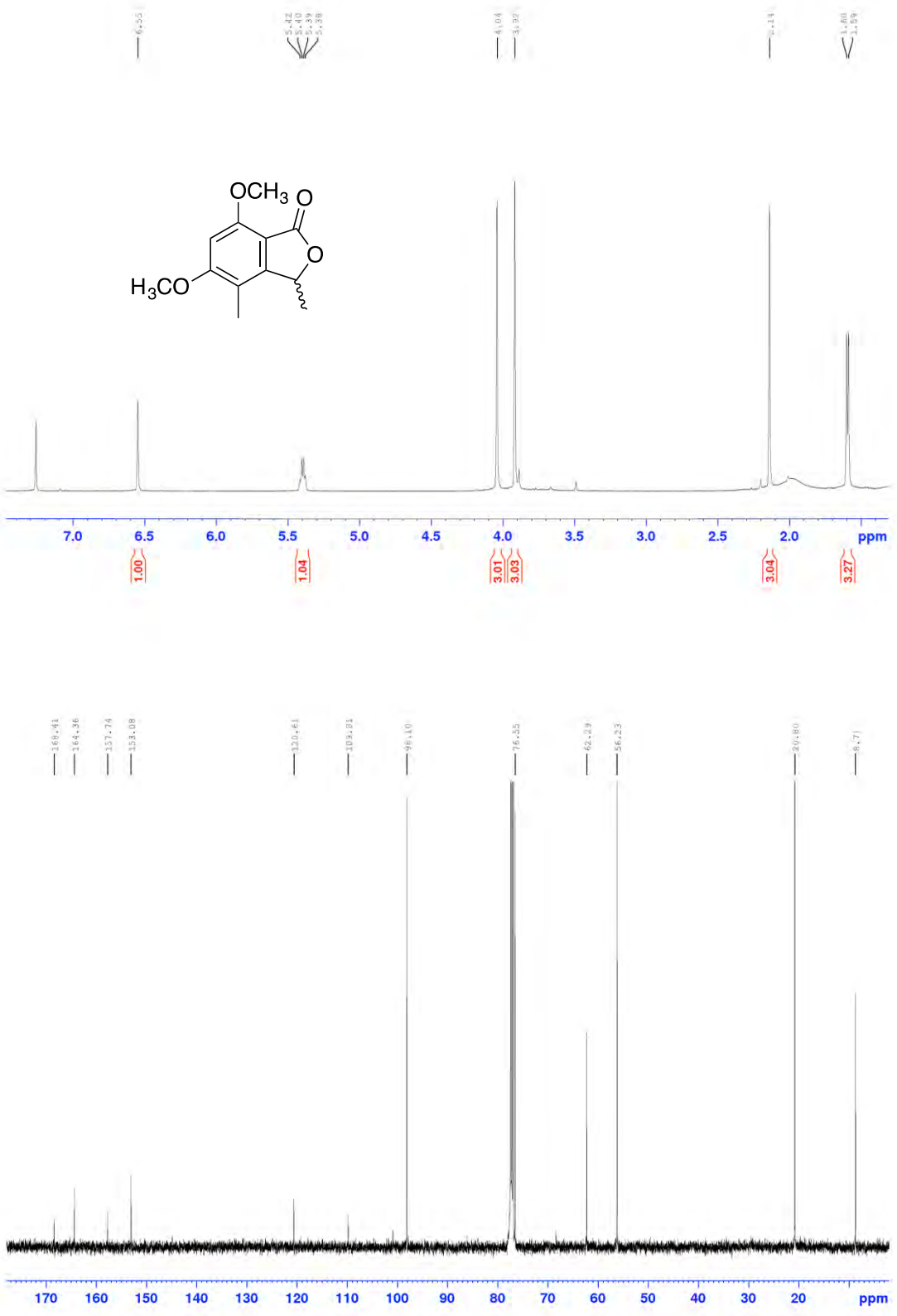

Figure S2: ^{1}H and ^{13}C NMR spectra of luteolactone A (**2**) in $CDCl_3$

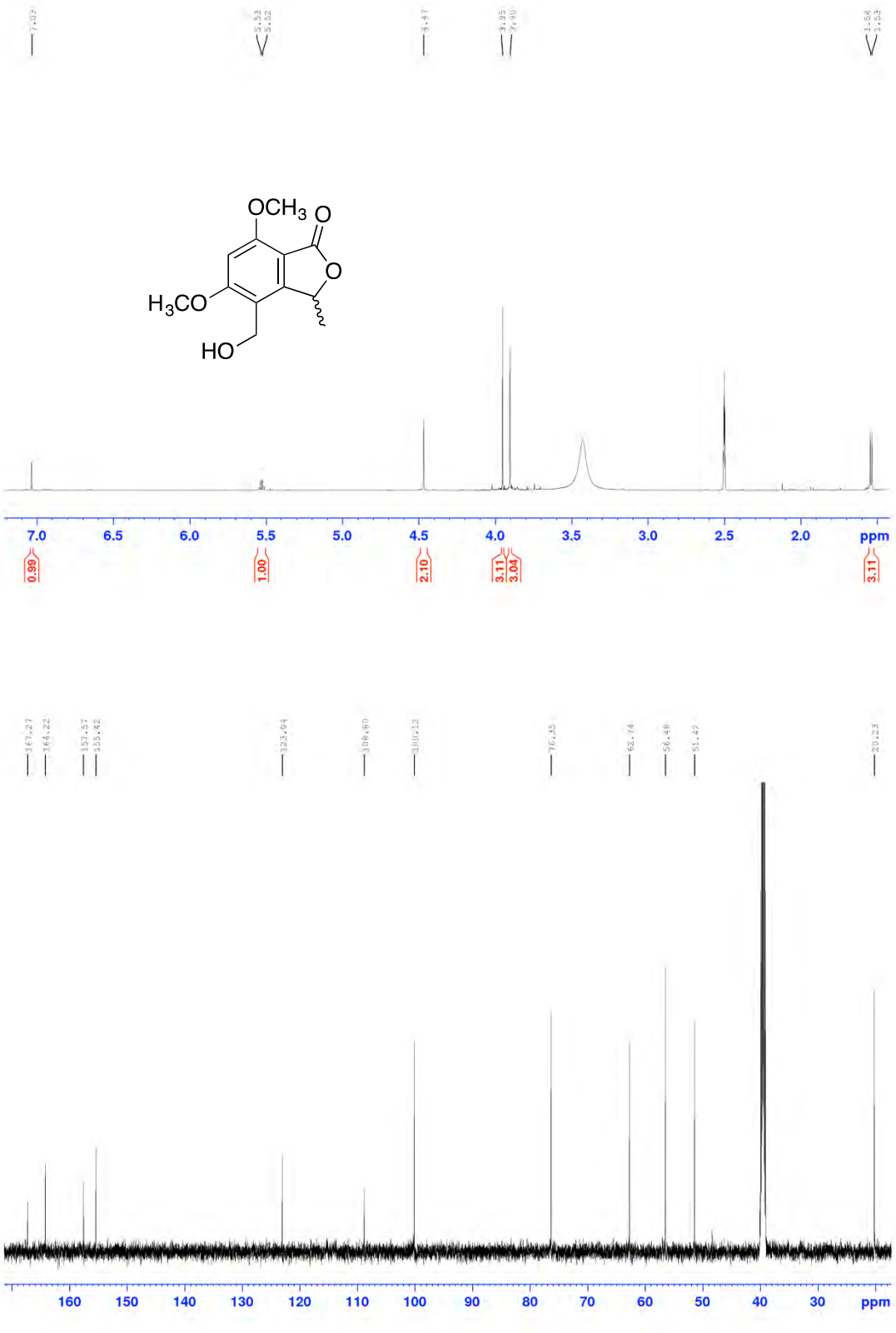

Figure S3: ^{1}H and ^{13}C NMR spectra of luteolactone B (**3**) in DMSO-d_6

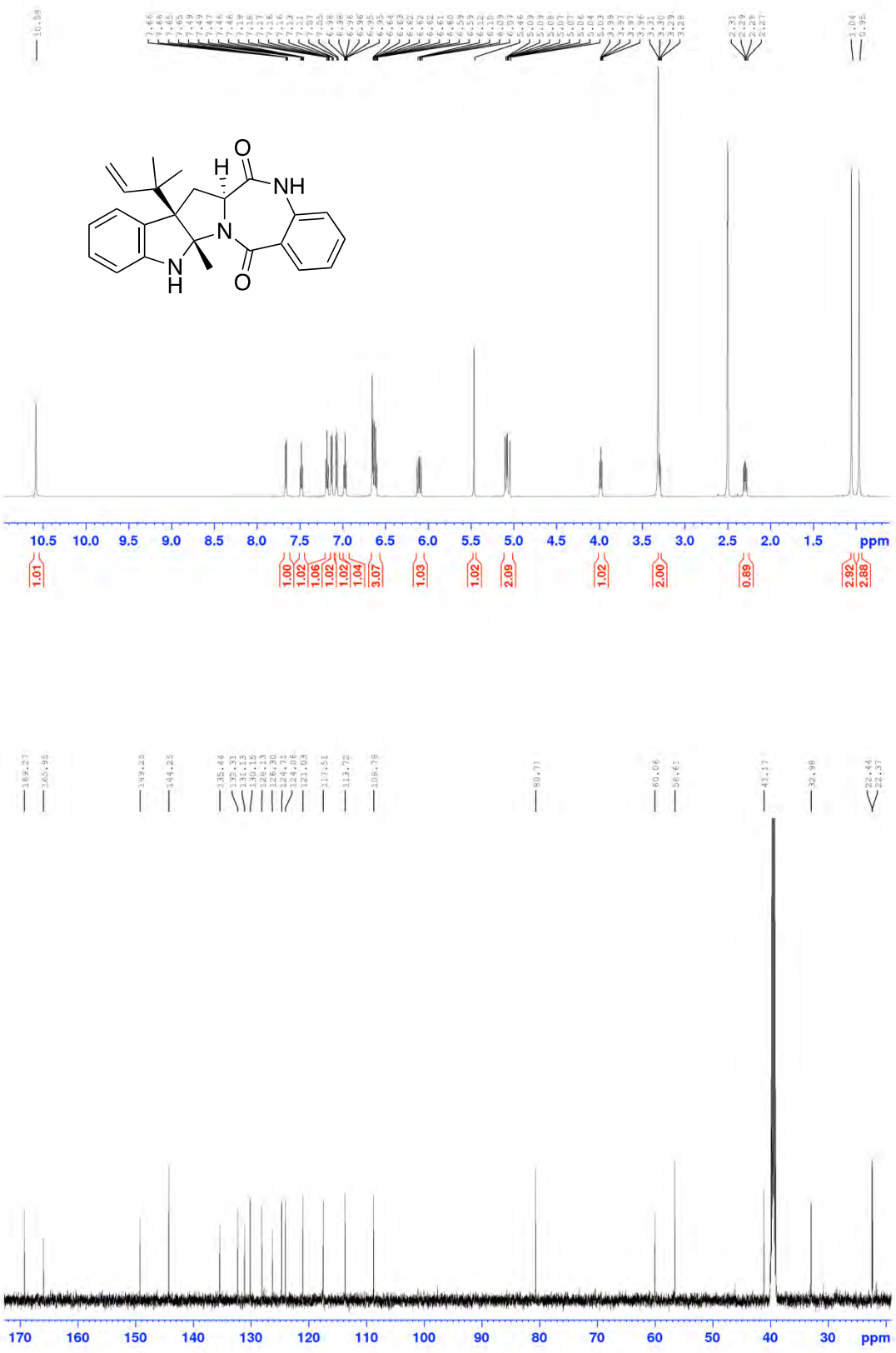

Figure S4: ^{1}H and ^{13}C NMR spectra of aszonalenin (**4**) in DMSO-d_6

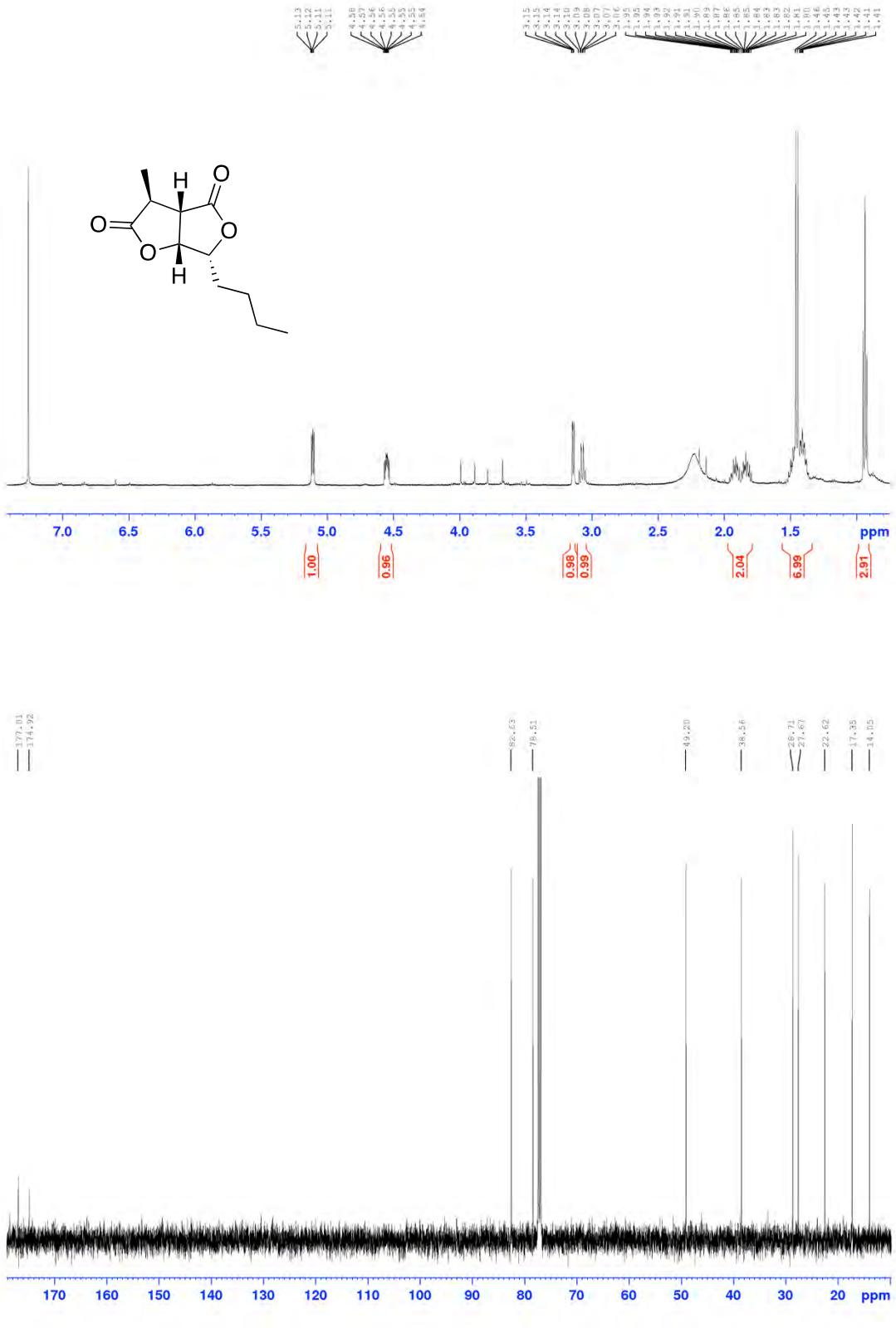

Figure S5: ^{1}H and ^{13}C NMR spectra of dihydrocandesolide (**5**) in $CDCl_3$

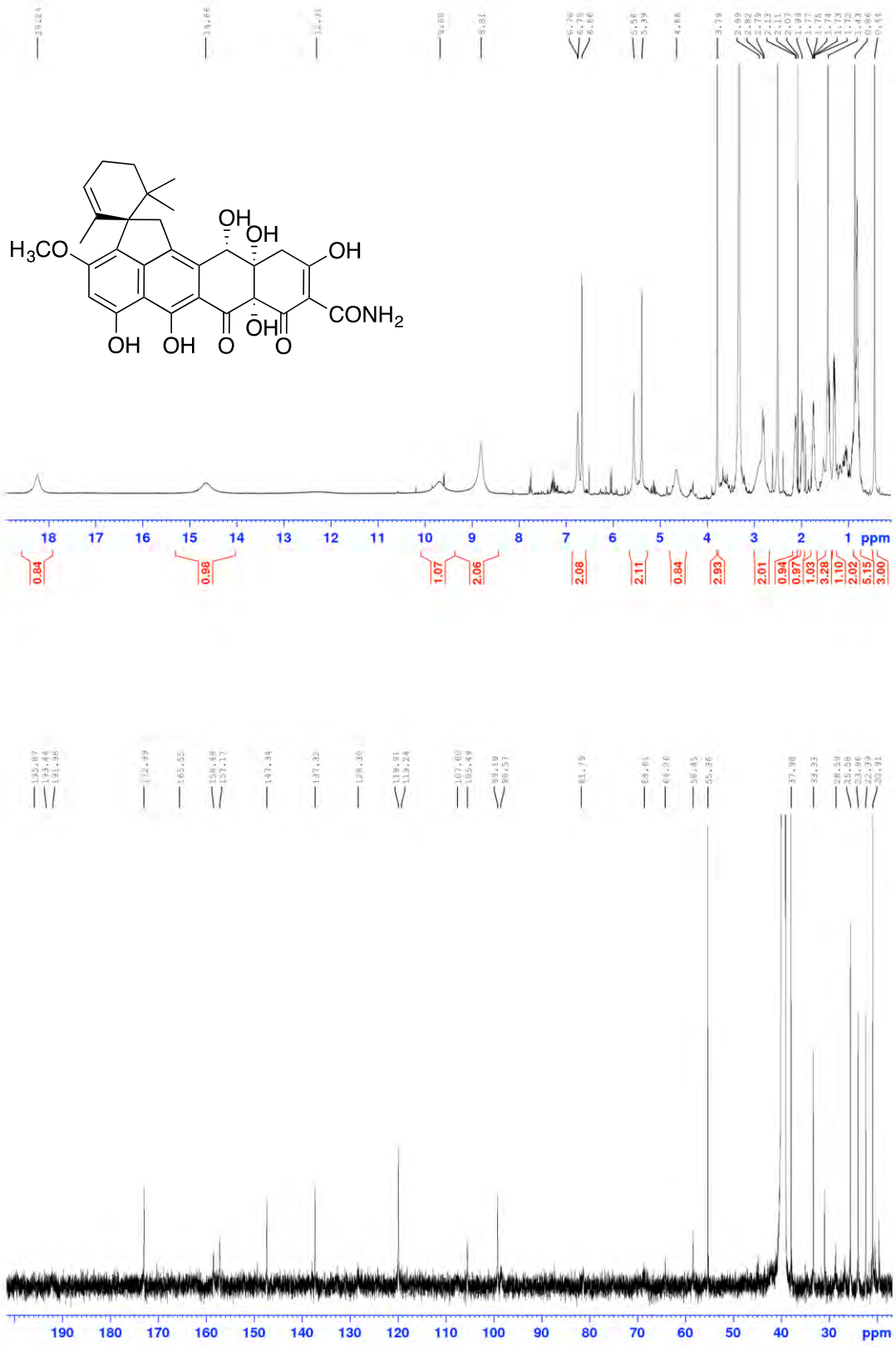

Figure S6: ^{1}H and ^{13}C NMR spectra of viridicatumtoxin (**6**) in DMSO-d_6

C. UV-visible spectra

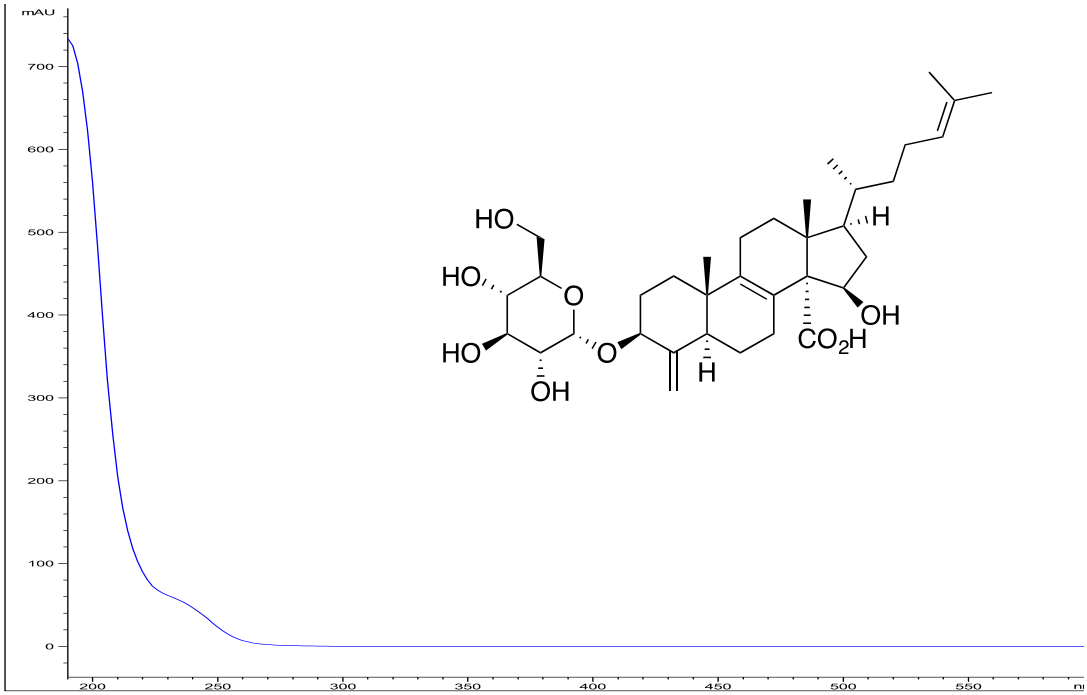

Figure S7: UV- visible spectrum of luteosteroside A (**1**).

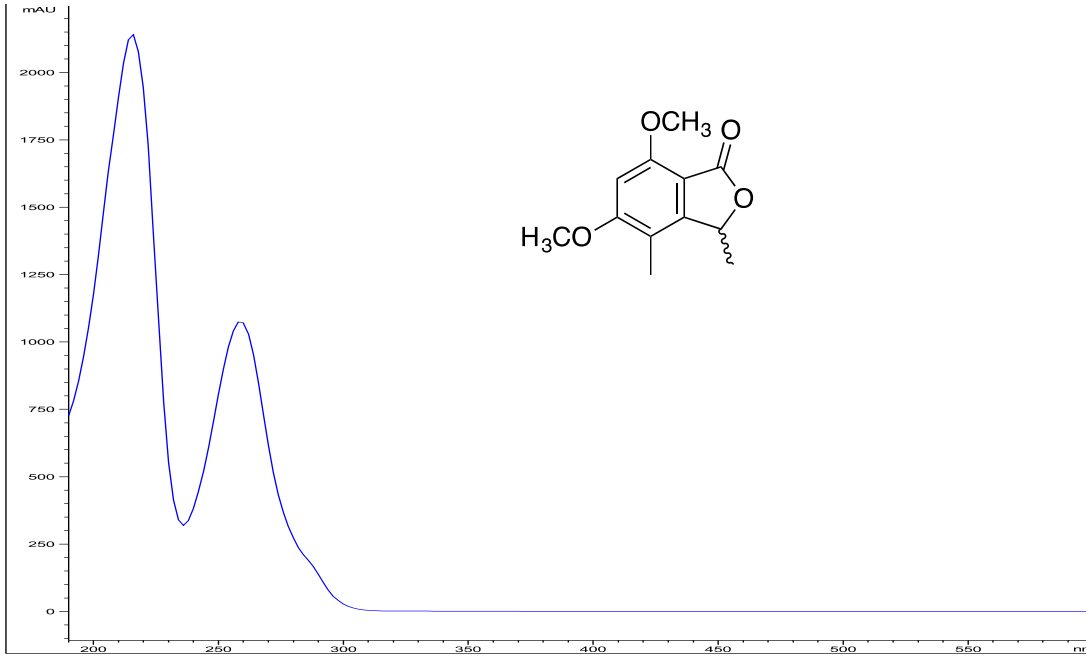

Figure S8: UV- visible spectrum of luteolactone A (**2**).

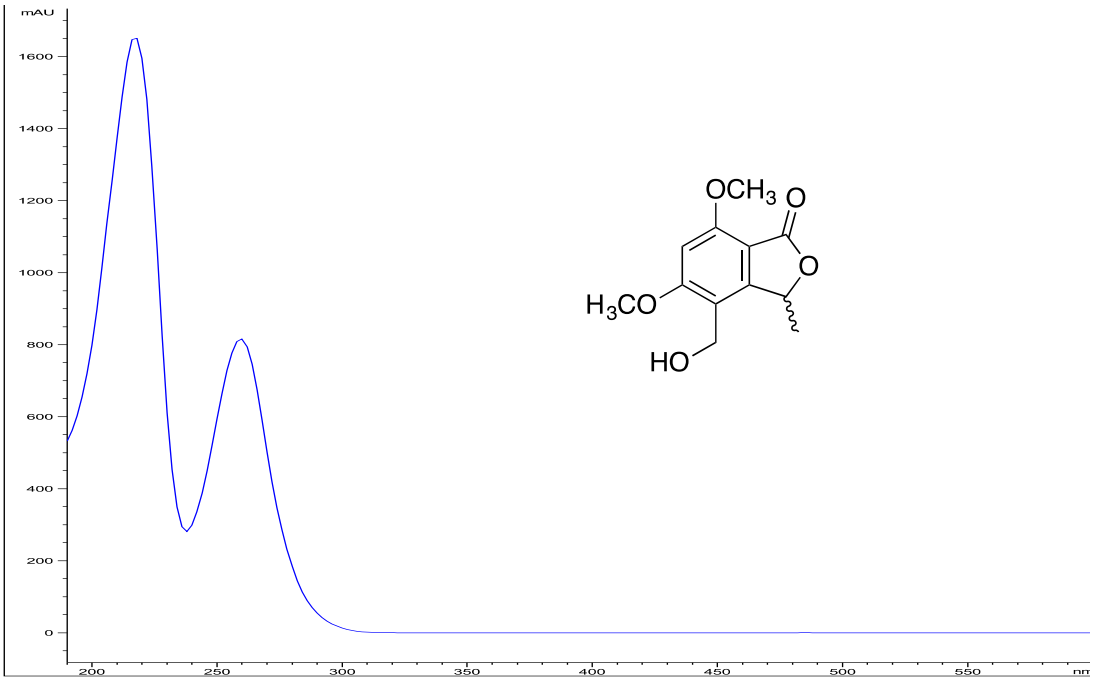

Figure S9: UV- visible spectrum of luteolactone B (**3**).

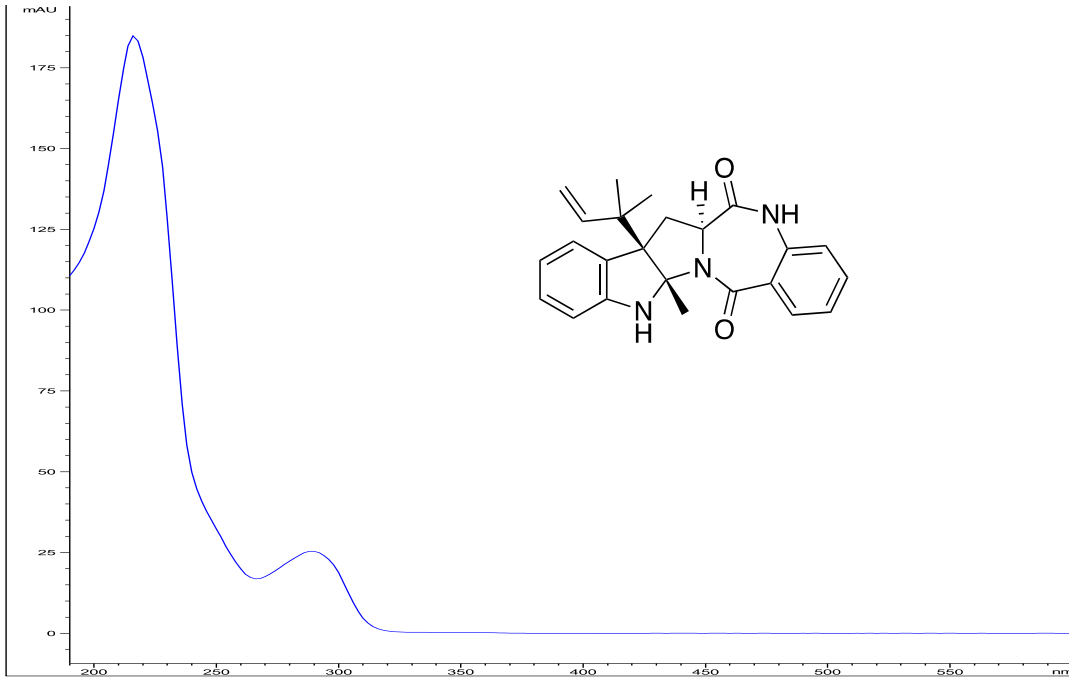

Figure S10: UV- visible spectrum of aszonalenin (**4**).

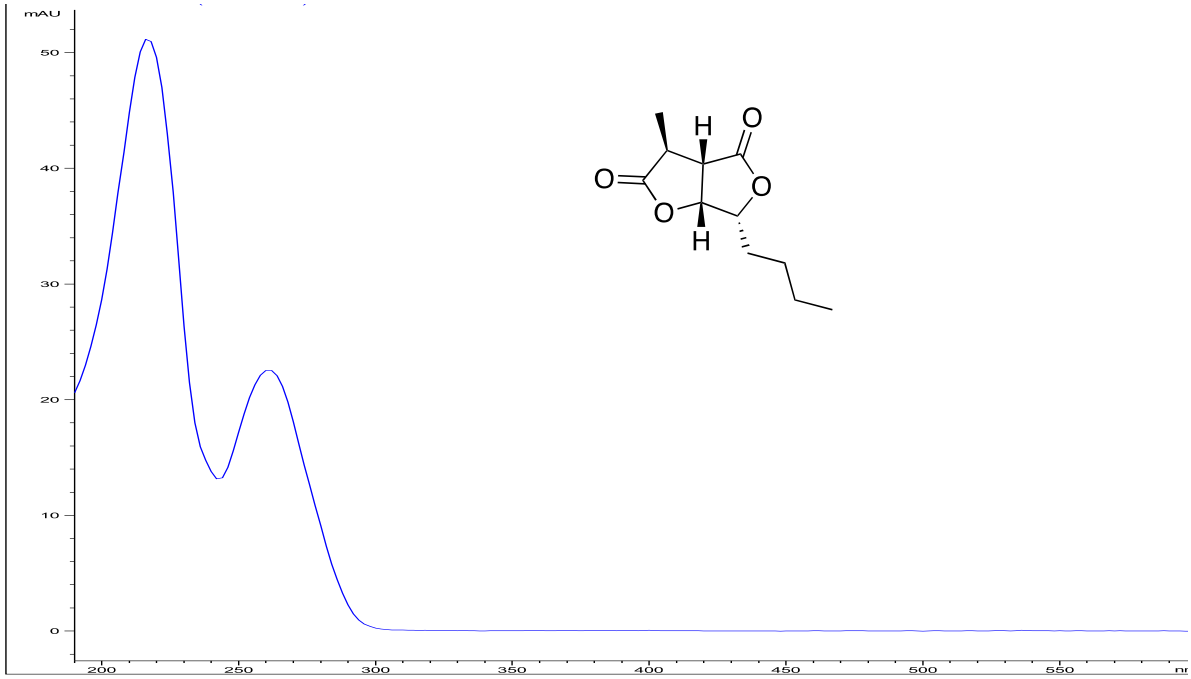

Figure S11: UV- visible spectrum of dihydrocandesolide (**5**).

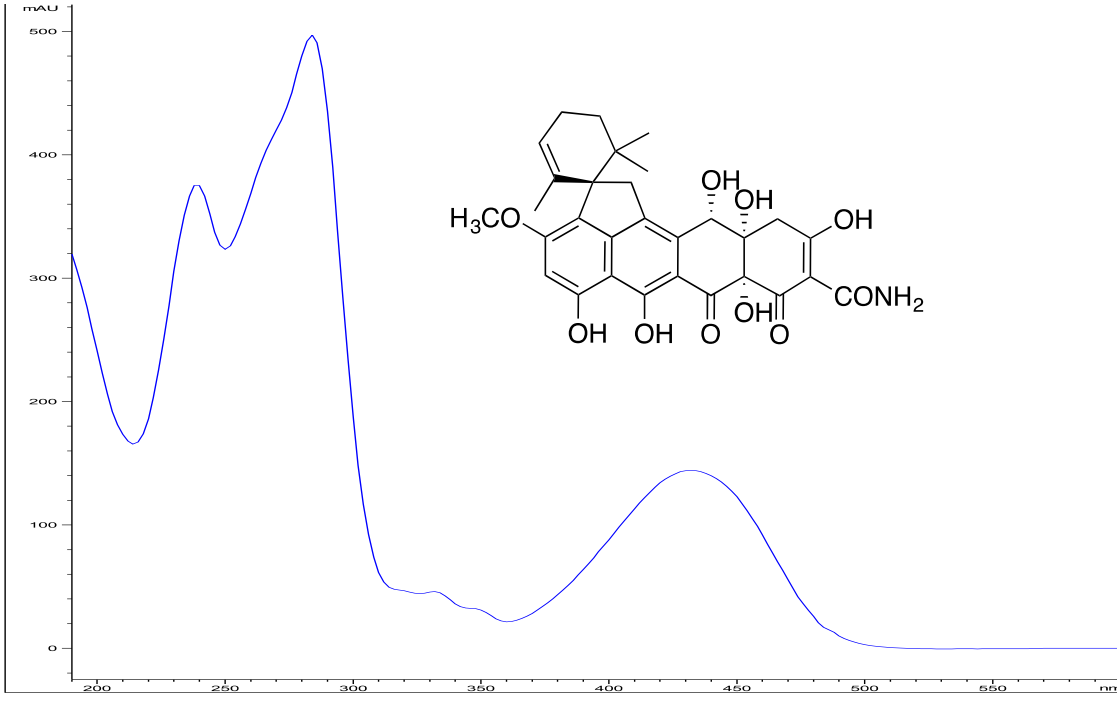

Figure S12: UV- visible spectrum of viridicatumtoxin A (**6**).

D. ECD spectra

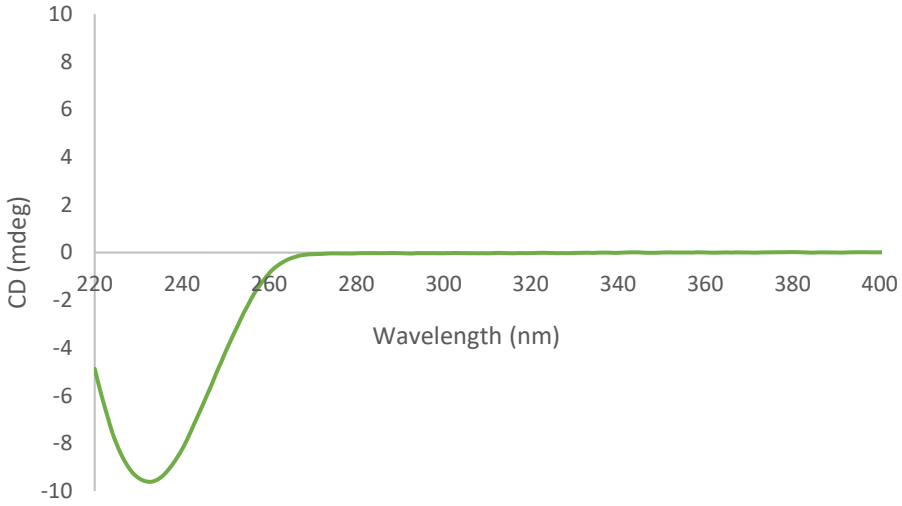

Figure S13: ECD spectrum of luteosteroside A (**1**) in MeOH.

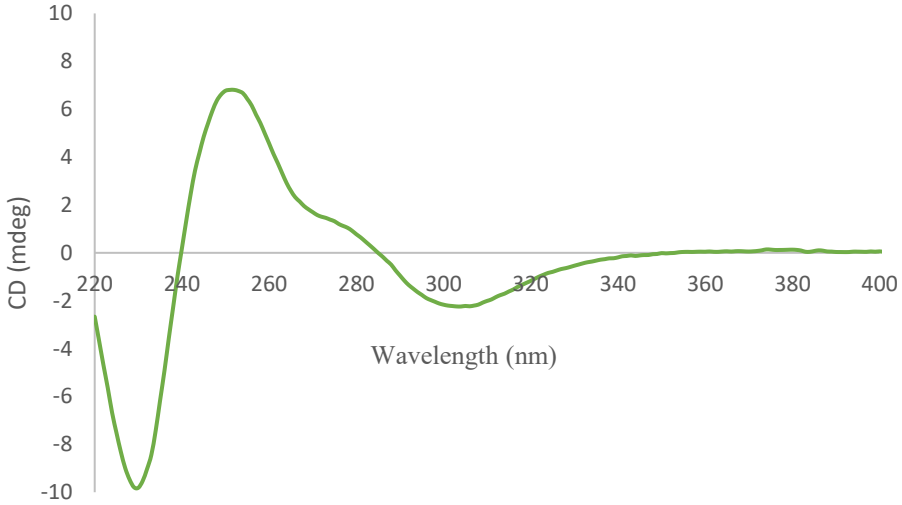

Figure S14: ECD spectrum of aszonalenin (**4**) in MeOH.

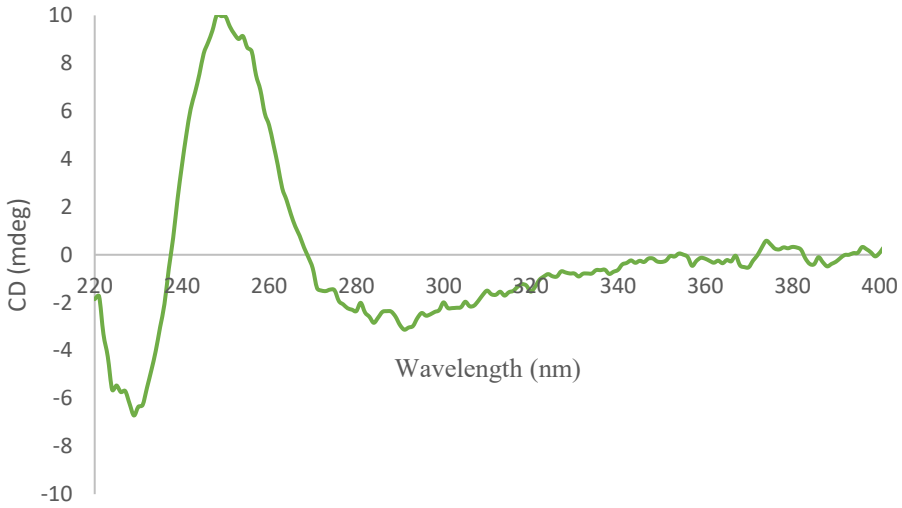

Figure S15: ECD spectrum of dihydrocandesolide (**5**) in MeOH.

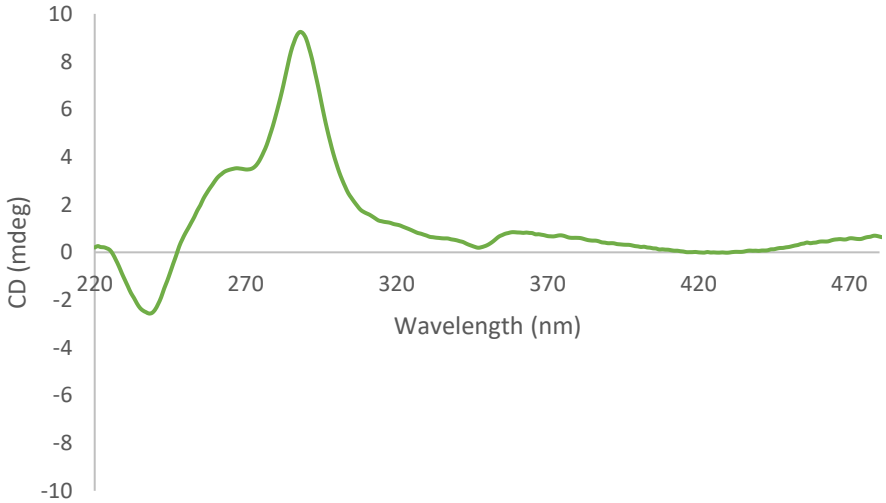

Figure S16: ECD spectrum of viridicatumtoxin (**6**) in MeOH.

Chapter six

Chapter 6: Authors contribution

Nirmal Chaudhary- Isolation and purification of the crude extract, characterization, structure elucidation, manuscript draft

Prof. Walter C. Taylor- Provided crude sample

Prof. Lewis N. Mander- Provided crude sample

Prof. Peter Karuso – Manuscript revision, Project supervision

Isolation and structure elucidation of new alkaloids from the tropical rainforest tree *Galbulimima baccata*

*Nirmal K. Chaudhary,[†] Walter C. Taylor, [‡] Lewis N. Mander,[§] Peter Karuso[†,]**

[†]*Department of Molecular Sciences, Macquarie University, NSW 2109, Australia*

[‡] *School of Chemistry, University of Sydney, NSW 2006, Australia,*

[§] *Research School of Chemistry, Australian National University, Canberra ACT 0200, Australia*

* Corresponding author: peter.karuso@mq.edu.au

Abstract

The structures of three new alkaloids (**1**-**3**) and a new non-alkaloid (**4**) isolated from the tropical rain forest trees *Galbulimima baccata*, have been determined by 2D NMR spectroscopy. Amongst the alkaloids, 1 belongs to class II GB alkaloid and class III GB alkaloid whereas 1 has a different scaffold. Compound **4** is most likely a degradation product arising from the degradation of a class I GB alkaloid. These new molecules have shed further light on the biogenetic relationship among these structurally unique and complex group of alkaloids. Also, the isolation of an unprecedented *Galbulimima* scaffold has the potential to unravel new pathway in the biosynthesis of the GB alkaloids.

Introduction

The bark of the rain forest trees *Galbulimima baccata* and *Galbulimima belgraveana*, found in Northern Australia and Papua New Guinea, respectively, has been a rich source of bioactive alkaloids.[1,2] During the period from 1956 to 1965, Taylor and co-workers reported the isolation of 28 alkaloids from *G. belgraveana* and *G. baccata*,[3] for which the structures of 22 were determined through a combination of spectroscopic analysis, structural degradation and interconversion, and semi-synthesis. Mander and co-workers reported the structures for five of the remaining six alkaloids as well as another two new alkaloids based on a combination of NMR spectroscopy and single crystal X-ray crystallography.[4,5] The structure of the last of the original 28 GB alkaloids (GB 14; $C_{24}H_{33}NO_5$) has been reported recently along with six new alkaloids GB 21-26.[6]

In Papua New Guinea, *Galbulimima belgraveana* has been used traditionally and reported to have hallucinogenic and psychoactive properties.[7,8] The prototypical *Galbulimima* alkaloid, himbacine, has been found to have antispasmodic activity[9] and to be a potent cardio-selective muscarinic antagonist due to its ability to bind selectively to M_2/M_4 muscarinic receptors.[10] Consequently, it became a lead compound in the search for new drugs for the treatment of neurodegenerative conditions resulting in Vorapaxar, the first-in-class PAR-1 antagonistic drug.[11]

Galbulimima alkaloids are characterized by a common structural feature a *trans*-decalin system and a piperidine ring. *Galbulimima* alkaloids can be categorized into four classes (I-III and "miscellaneous") based on their structure (Figure 1).[3] Class I *Galbulimima* alkaloids has a δ-lactone ring annulated to a *trans*-decalin core (except GB 18 where there is no δ-lactone ring) bearing a piperidine ring. The more recently characterized GB alkaloids (GB 18 and GB 20), included in class I have a slightly different structural feature compared to the typical class I alkaloids. GB 18 and GB 20 does not have a Δ^7 double bond but instead

are cyclized to form a 7,20-annulation. Class II *Galbulimima* alkaloids have the piperidine ring linked to the decalin moiety via an additional bond resulting in a structurally more complex fused ring system. Class III *Galbulimima* alkaloids differs from II by connectivity between the piperidine unit and the *trans*-decalin system. Class IV (miscellaneous) includes all others. The allocation of GB 16 to class IV is arguable as the only difference from other class III members is the missing bond between C-19 and C-20. Now, after the characterization of the original 28 alkaloids, and the subsequent discovery of 8 more new alkaloids, the number of members in various *Galbulimima* alkaloid class i.e., class I (himbacine type), class II (himandrine), class III (himbadine and himgaline) and class IV (miscellaneous) has been revised to 10, 18, 4 and 4 respectively.[2,6]

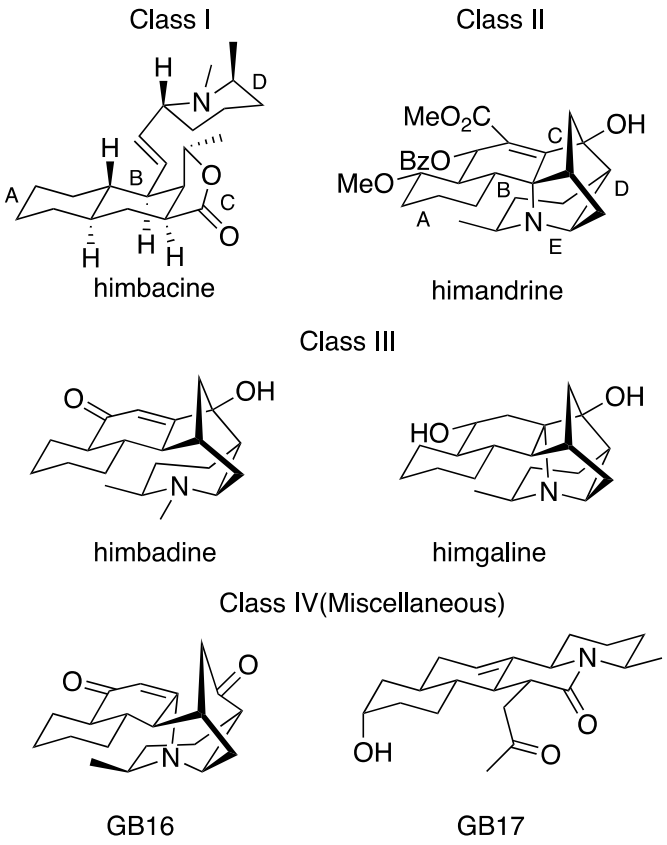

Figure 1: Classification of GB alkaloids

Galbulimima alkaloids have attracted considerable attention by synthetic chemists. Class I *Galbulimima* alkaloids are interesting because of their confirmed anticholinergic activity and potential use for the treatment of acute coronary syndrome, Alzheimer's disease and glaucoma. The Class II and III GB alkaloids have garnered attention as a result of their complex polycyclic architectures posing considerable challenge to their synthesis. The first racemic total synthesis of GB 13 (Class III) was reported by Mander in 2003[12] with further total syntheses from Movassaghi,[13,14] Chackalamannil,[15] Evans,[16] Sarpong,[17] and Ma.[18] The only Class II alkaloid to succumb to total synthesis is himandrine in 2009 by Movassaghi and coworkers.[19]

Despite the interesting biological activities, only few *Galbulimima* alkaloids have been systematically investigated. Moreover, the various biosynthetic schemes of the *Galbulimima* alkaloids proposed so far [1,4, 5, 14] reveals that some more potential intermediates may remain yet to be discovered. Conversely, the discovery of such potential intermediates and other new alkaloids could provide better understanding of the biosynthetic routes to these fascinating group of alkaloids.

Results and Discussion

Detailed LC-MS analysis of the remnants of the *Galbulimima baccata* extract revealed that there were still some new compounds that could be extracted in sufficient quantity for further studies. Hence, this exploration of *Galbulimima* alkaloids was undertaken which resulted in the isolation of four new chemical compounds, **1**-**4**, including an unprecedented scaffold, GB 28 and a unique class III scaffold with an unprecedented aromatic ring.

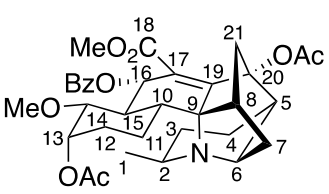

GB 27 (**1**)

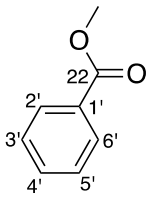

Benzoyl group

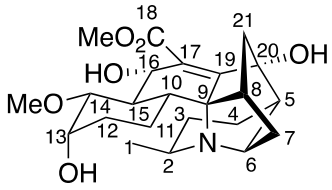

GB 28 (**2**)

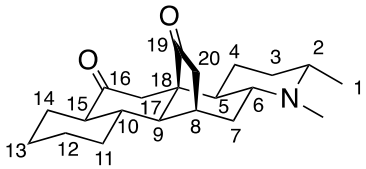

GB 29 (**3**)

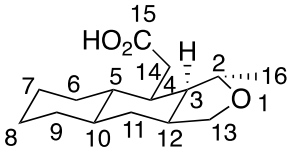

GB 30 (**4**)

GB 27 (**1**) was isolated as colorless crystalline solid. The UV spectrum showed absorption maxima at 195, 230 and 305 nm characteristic of the himandrine type (Class II) GB alkaloids.[20] The IR spectrum showed the presence of sharp absorption bands at 1737 and 1720 cm^{-1} indicating the presence of at least two carbonyl groups. A molecular formula of $C_{34}H_{41}NO_9$ was assigned based on the observed HRMS value for the $[M+H]^+$ ion (Δmmu 0.0) suggesting 15 degrees of unsaturation. The ^1H and ^{13}C NMR spectra in conjunction with the $^3J_{CH}$ and $^3J_{HH}$ correlations revealed resonances for a benzoyl group (five aromatic protons, 2 × δ_H 7.92, 2 × δ_H 7.44, 1 × δ_H 7.57; a non-protonated sp^2 carbon, δ_C 130.2; and a carbonyl carbon, δ_C 165.7) and a 2,5,6-trisubstituted piperidine ring (a methyl doublet, δ_H 1.81; two methylenes, δ_H 2.62/1.77 and 1.84/2.08; and three methines, δ_H 4.29, 3.13 and 4.11 constituting a single spin system) further confirming a class II GB alkaloid. The ^1H NMR spectrum also showed the resonances for a methyl ester (δ_H 3.65) and a methoxy group (δ_H 3.12) and two acetyl groups (δ_H 2.02 and 2.04) whereas the ^{13}C NMR spectrum revealed three more carbonyls, δ_C 170.3, 168.7 and 166.5. COSY correlations showed the presence of a 2,3,6-trisubstituted cyclohexylmethine spin system constituting the ring E of the GB scaffold. Also, COSY correlations showed the presence of a 2,3-disubstituted propyl (-CH_2-CH-CH_2-) fragment in continuum with the trisubstituted piperidine ring (ring A) forming a

single spin system. Key HMBC correlations (Figure 2) arising from the protons of this 2,3-disubstituted propyl fragment and selected protons from the cyclohexylmethine spin system established the structure of ring B, C and D. These deductions confirmed the structural formula of GB 27 as in **1**. A double bond was assigned between C-17 and C-19 based on their carbon chemical shifts, δ_C 124.1 and 140.9 respectively. The position of methyl ester was assigned to C-17 based on a $^3J_{CH}$ correlation from H-16 to the α, β-unsaturated ester carbonyl (δ_C 166.5). The position of the methoxy group was assigned to C-14 by $^3J_{CH}$ correlation from the methoxy protons whereas the two acetyl groups were assigned to C-13 and C-20 from the chemical shift of the carbons to which they were tethered. The relative configuration of **1** was assigned based on the observed ROESY correlations (Table 1) and the absolute configuration was assigned on the biogenetic assumption that all the GB alkaloids possess the same *S* configuration at C-2.[21]

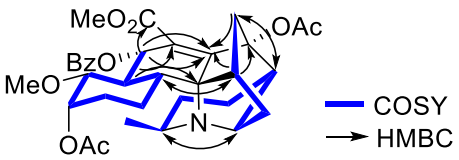

Figure 2: Key COSY and HMBC correlations in GB 27 (**1**)

GB 28 (**2**) was isolated as white solid. The UV spectrum showed absorption maximum at 213 nm. The IR spectrum showed the presence of a broad absorption band at 3376 cm^{-1} and a sharp absorption band at 1718 cm^{-1} indicating the presence of hydroxyl and carbonyl groups respectively. A molecular formula of $C_{23}H_{33}NO_6$ was assigned based on the observed HRMS, for the $[M+H]^+$ ion (Δmmu –0.7) suggesting 8 degrees of unsaturation. The UV spectrum was characteristic of a class III GB alkaloid. This was also consistent with the NMR spectral data. The ^1H and ^{13}C NMR spectra in conjunction with the $^3J_{CH}$ and $^3J_{HH}$ correlations suggested the presence of a 2,5,6-trisubstituted piperidine ring, suggestive of a

class II or III GB alkaloid. However, the absence of resonances for a benzoyl group unlike **1** further confirmed it as a class III scaffold. Also, the ^{1}H and ^{13}C NMR spectra lacked the resonances for the two acetyl groups unlike **1** but still showed the presence a methoxy group (δ_H 3.32) and a methyl ester (δ_H 3.59). Apart from these differences in substituents, the COSY correlations (Table 2) showed identical spin system and key HMBC correlations as **1** suggesting the same core structure. The position of the double bond, methyl ester and methoxy group were assigned as in **1** and found to be identical. Lack of resonances for acetyl groups and comparison of chemical shifts of C-13 (δ_C 62.2 cf. 65.6) and the bridgehead carbon C-20 (δ_C 79.0 cf. 84.2) with respect to **1** suggested that these two carbons were tethered to a hydroxy group rather than an acetyl group unlike in **1**. These deductions established the structural formula of GB 28 as **2.** The relative and absolute configuration of **2** was assigned based on the observed ROESY correlations and biogenetic considerations respectively as with **1**.

GB 29 (**3**) was isolated as off-white solid. The UV spectrum showed absorption maxima at 190 and 292 nm. The IR spectrum showed the presence of a sharp absorption band at 1739 cm^{-1} indicating the presence of a carbonyl group respectively. A molecular formula of $C_{21}H_{32}NO_2$ was assigned based on the observed HRMS, for the $[M+H]^+$ ion (Δmmu= –0.9) suggesting 7 degrees of unsaturation. The UV spectrum showed mainly end absorption. The low intensity absorption at λ_{max} of 292 with log ε value of 2.63 due to a $n\rightarrow\pi*$ was suggestive of the presence of a carbonyl group. Although the UV spectrum didn't match any of the three major classes of GB alkaloids, the ^{1}H and ^{13}C NMR spectra in conjunction with $^{3}J_{CH}$ and $^{3}J_{HH}$ correlations showed the presence of a 2,5,6-trisubstituted piperidine ring. The ^{13}C NMR spectrum showed the presence of only two carbonyls, both being ketones (δ_C 209.2 and 217.4) and thereby suggesting the absence of both acetyl and ester groups unlike in most

Galbulimima alkaloids. Also, COSY correlations confirmed the presence of a cyclohexylmethine spin fragment but unlike **1** and **2** rather than being discrete spin system, it formed a single continuous spin system up to the piperidine ring owing to C-9 now being protonated unlike **1**. These deductions in conjunction with key HMBC correlations (Figure 3) confirmed the structural formula as **3**. The relative stereochemistry was assigned from the observed ROESY correlations (Table 3) and the absolute configuration assigned assuming *S* configuration for all the GB alkaloids at C-2.[21] GB 29 has an unprecedented scaffold and could arise from GB 13 by an unprecedented mechanism involving bond migration as outlined in Scheme 1**.**

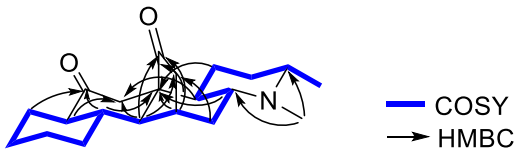

Figure 3: COSY and selected HMBC correlations in GB 29 (**3**)

GB 30 (**4**) was isolated as white solid. The IR spectrum showed the presence of a sharp absorption band at 1721 cm^{-1} indicating the presence of a carbonyl group. A molecular formula of $C_{15}H_{24}O_3$ was assigned based on the observed HRMS, for the $[M+H]^+$ ion at *m/z* 253.1651 (Δmmu –0.7) suggesting 7 degrees of unsaturation. The absence of nitrogen in the molecular formula itself indicated that it was not an alkaloid. The ^1H and ^{13}C NMR spectrum showed the presence of a carbonyl group (δ_C 178.2), a methyl doublet (δ_H 1.26, δ_C 21.1) attached to an oxymethine (δ_H 4.05, δ_C 73.5). However, the ^1H and ^{13}C NMR spectra in conjunction with $^3J_{HH}$ still revealed the presence of a *trans*-decalin ring and $^3J_{CH}$ correlations further confirmed the structure as **4**. The compound is possibly a degradation product of a class I GB alkaloid. Biogenetically, GB 30 could arise by the oxidative cleavage of the double bond of himbacine, himandravine or himbeline (Scheme 2). The relative stereochemistry was assigned based on ROESY correlations (Table 4) and the absolute

configuration was assigned same as himbacine based on direct comparison of observed optical rotation, ECD spectrum as well as biogenetic considerations.

Biosynthesis of *Galbulimima* alkaloids

In 1967, Ritchie and Taylor first proposed that *Galbulimima* alkaloids could be derived through polyketide pathway.[1] They concluded that these alkaloids could be either obtained from 9 acetates and 1 pyruvate or 10 acetates and a carbon unit without divulging much details. Bennet, a student of Jack Baldwin was the first to propose the possibility of cycloaddition in biosynthetic process suggesting that the *trans*-decalin moiety could arise from a Diels-Alder cycloaddition reaction. Since then, Movassaghi and Mander have also proposed their own hypothesis for biosynthesis of *Galbulimima* alkaloids.[22] Based on these hypotheses we have proposed biogenetic relationship among the GB alkaloids isolated till date including this work (Scheme I and II). GB 29 is an unprecedented scaffold and could arise from GB 13 via a rearrangement involving bond migration as depicted in Scheme I, an unprecedented biosynthetic route among GB alkaloids. GB 30 is not an alkaloid and could arise from the oxidative cleavage of Δ^7 double bond of class I GB alkaloids like himbeline, himbacine or himandravine. GB 28 could arise from hydroxylation of GB 8 and could be the precursor for himandridine. GB 27 could arise from the acetylation of either GB 6 or GB 7.

Conclusion

The present study has expanded the range of structures of this unusual family of polycyclic piperidine alkaloids as well as filled in some of the probable missing intermediates involved in the biosynthesis of these alkaloids. Moreover, isolation of GB 29, an unprecedented *Galbulimima* scaffold has unraveled an unprecedented route involving bond migration in the

biosynthesis of *Galbulimima* alkaloids. The isolation of GB 30, a non-alkaloid revealed that the Δ^7 unsaturated alkaloids could undergo degradation via oxidative cleavage.

EXPERIMENTAL

Thin-layer chromatography (TLC) was performed using pre-coated silica gel GF254 plates (Merck, Darmstadt, Germany) with various solvent systems and spots were visualized with UV light (254 nm). Preparative and semi-preparative HPLC separations were performed on a Gilson HPLC system, equipped with a Gilson 215 liquid handler, 819 injection module, 322 pump, 506C system interface and Gilson single variable wavelength UV-Vis 152 detector by reversed phase chromatography using a gradient of acetonitrile (Sigma Aldrich, USA) and water unless mentioned otherwise. Phenomenex Hydro-RP (250 × 22.4 mm, 10 μm) and Phenomenex Hydro-RP (250 × 10 mm, 5 μm) columns were used for preparative and semi-preparative purifications respectively. UV-visible absorbance readings were taken on an Eppendorf UV-visible spectrophotometer (Biospectrometer Kinetic) in a 1 × 1 cm quartz cell. Optical rotations were recorded in MeOH unless otherwise stated using a Jasco P-1020 Polarimeter (Jasco Corp., Japan) in a 1 cm path length cell. The ECD spectra were recorded on a Jasco J-1500 spectropolarimeter (Jasco Corp., Japan) in a 1 × 1 cm quartz cell. The IR spectra were recorded on a Thermo Scientific Nicolet iS10 ATR FTIR spectrometer. The ^{1}H NMR, ^{13}C NMR and 2D NMR spectra were recorded in deuterated DMSO or deuterated chloroform using a Bruker Avance II 500 MHz NMR spectrometer (Bruker Corp.). The ESI-MS spectra were recorded using an Agilent 6130 B single quadrupole mass spectrometer (Agilent Corp.). The HR-ESIMS data were obtained using a Q Exactive Plus hybrid quadrupole orbitrap mass spectrometer (Thermo Scientific, Bremen, Germany).

Spectroscopic data

GB 27 (1)*:* Colorless crystals; $[\alpha]^{24}_{D}$ + 19 (*c* 0.34, MeOH); ECD (c 7.6 × 10^{-4} mg/mL, MeOH) λ_{max} ($\Delta\varepsilon$) 203 (–29.5), 229 (–5.34), 249 (5.1) nm; UV (MeOH) λ_{max} (log ε) 195 (4.21), 233 (3.77), 274 (2.67) nm; IR (ATR) ν_{max} 2984, 2902, 2361, 2339, 1737, 1720, 1267, 1237, 1218, 1067, 1048, 957, 722 cm^{-1}; NMR (500 MHz, $CDCl_3$) see Tables 5 and S5; HR-ESI(+)MS *m/z* 608.2860 $[M + H]^+$ (calcd for $C_{34}H_{42}NO_9^+$, 608.2860).

GB 28 (2)*:* Off-white to pale yellow solid; $[\alpha]^{24}_{D}$ –18 (*c* 0.25, MeOH); ECD (c 5.02 × 10^{-4} mg/mL, MeOH) λ_{max} ($\Delta\varepsilon$) 203 (–12.5), 239 (3.5) nm; UV (MeOH) λ_{max} (log ε) 213 (4.19) nm; IR (ATR) ν_{max} 3376, 2913, 2359, 2339, 1718, 1569, 1391, 1277, 1049, 1025, 820 cm^{-1}; NMR (500 MHz, DMSO-d_6) see Tables 6 and S6; HR-ESI(+)MS *m/z* 420.2379 $[M + H]^+$ (calcd for $C_{23}H_{34}NO_6^+$, 420.2386).

GB 29 (3)*:* Off-white solid; $[\alpha]^{24}_{D}$ –23 (*c* 1.01, MeOH); ECD (c 3.12 × 10^{-4} mg/mL, MeOH) λ_{max} ($\Delta\varepsilon$) 250 (–0.5), 290 (4.1), 311 (2.9), 322 (2.2) nm; UV (MeOH) λ_{max} (log ε) 190 (4.17), 292 (2.63) nm; IR (ATR) ν_{max} 2948, 2339, 2112, 1739, 1701, 1443, 1043, 903, 606 cm^{-1}; NMR (500 MHz, $CDCl_3$) see Tables 7 and S7; HR-ESI(+)MS *m/z* 330.2424 $[M + H]^+$ (calcd for $C_{21}H_{32}NO_2^+$, 330.2433).

GB 30 (4)*:* White solid; $[\alpha]^{24}_{D}$ + 18 (*c* 0.34, MeOH); ECD (c 2.86 × 10^{-2} mg/mL, MeOH) λ_{max} ($\Delta\varepsilon$) 220 (–11.1) nm; UV (MeOH) λ_{max} (log ε) 215 (2.98) nm; IR (ATR) ν_{max} 2673, 2972, 2911, 2360, 2339, 2028, 1721, 1406, 1218, 1056, 940, 836 cm^{-1}; NMR (500 MHz, $CDCl_3$) see Tables 8 and S8; HR-ESI(+)MS *m/z* 253.1651 $[M + H]^+$ (calcd for $C_{15}H_{25}O_3^+$, 253.1651).

Supplementary data

Supplementary data associated with this article can be found, in the online version, at

Acknowledgements

We thank Dr M. McKay (APAF, Macquarie University) for the acquisition of HRMS data. This research was funded, in part, by the Australian Research Council (DP130103281 to PK and AMP; FT130100142 to AMP) and Macquarie University (iMQRES scholarship to NC).

References

(1) Ritchie, E.; Taylor, W., *The Alkaloids: Chemistry and Physiology* **1967,** 9, 529-543.

(2) Ritchie, E.; Taylor, W., *The Alkaloids: Chemistry and Physiology* **1971,** 13, 227-271.

(3) Binns, S. V.; et, a., *Aust. J. Chem.* **1965,** 18, (4), 569-73.

(4) Bradford, T. A.; Willis, A. C.; White, J. M.; Herlt, A. J.; Taylor, W. C.; Mander, L. N., *Tetrahedron Lett.* **2011,** 52, (2), 188-191.

(5) Mander, L. N.; Willis, A. C.; Herlt, A. J.; Taylor, W. C., *Tetrahedron Lett.* **2009,** 50, (50), 7089-7092.

(6) Lan, P.; Herlt, A. J.; Willis, A. C.; Taylor, W. C.; Mander, L. N., *ACS Omega* **2018,** 3, (2), 1912-1921.

(7) Thomas, B., *J. Psychoactive Drugs* **2005,** 37, (1), 109-111.

(8) Thomas, B., *P. N. G. Med. J.* **2006,** 49, (1/2), 57.

(9) Gilani, A., *Fitoterapia* **1992,** 63, 238-242.

(10) Zhang, H.-M.; Li, D.-P.; Chen, S.-R.; Pan, H.-L., *J. Pharmacol. Exp. Ther.* **2005,** 313, (2), 697-704.

(11) Knight, E.; Robinson, E.; Smoktunowicz, N.; Chambers, R. C.; Aliev, A. E.; Inglis, G. G.; Chudasama, V.; Caddick, S., *Org. Biomol. Chem.* **2016,** 14, (12), 3264-3274.

(12) Mander, L. N.; McLachlan, M. M., *J. Am. Chem. Soc.* **2003,** 125, (9), 2400-2401.

(13) Movassaghi, M.; Hunt, D.; Tjandra, M., *Synfacts* **2006,** 2006, (12), 1201-1201.

(14) Movassaghi, M.; Hunt, D. K.; Tjandra, M., *J. Am. Chem. Soc.* **2006,** 128, (25), 8126-8127.

(15) Shah, U., *Enantioselective Total Synthesis of Galbulimima Alkaloids GB13 and Himgaline*. ProQuest: 2006.

(16) Evans, D. A.; Adams, D. J., *J. Am. Chem. Soc.* **2007,** 129, (5), 1048-1049.

(17) Larson, K. K.; Sarpong, R., *J. Am. Chem. Soc.* **2009,** 131, (37), 13244-13245.

(18) Zi, W.; Yu, S.; Ma, D., *Angew. Chem.* **2010,** 122, (34), 6023-6026.

(19) Movassaghi, M.; Tjandra, M.; Qi, J., *J. Am. Chem. Soc.* **2009,** 131, (28), 9648-9650.

(20) Guise, G. B.; Mander, L. N.; Prager, R. H.; Rasmussen, M.; Ritchie, E.; Taylor, W. C., *Aust. J. Chem.* **1967,** 20, (5), 1029-35.

(21) Willis, A. C.; O'Connor, P. D.; Taylor, W. C.; Mander, L. N., *Aust. J. Chem.* **2006,** 59, (9), 629-632.

(22) Rinner, U., Galbulimima Alkaloids. In *The Alkaloids: Chemistry and Biology*, Elsevier: 2017; Vol. 78, pp 109-166.

Biosynthesis of *Galbulimima* alkaloids

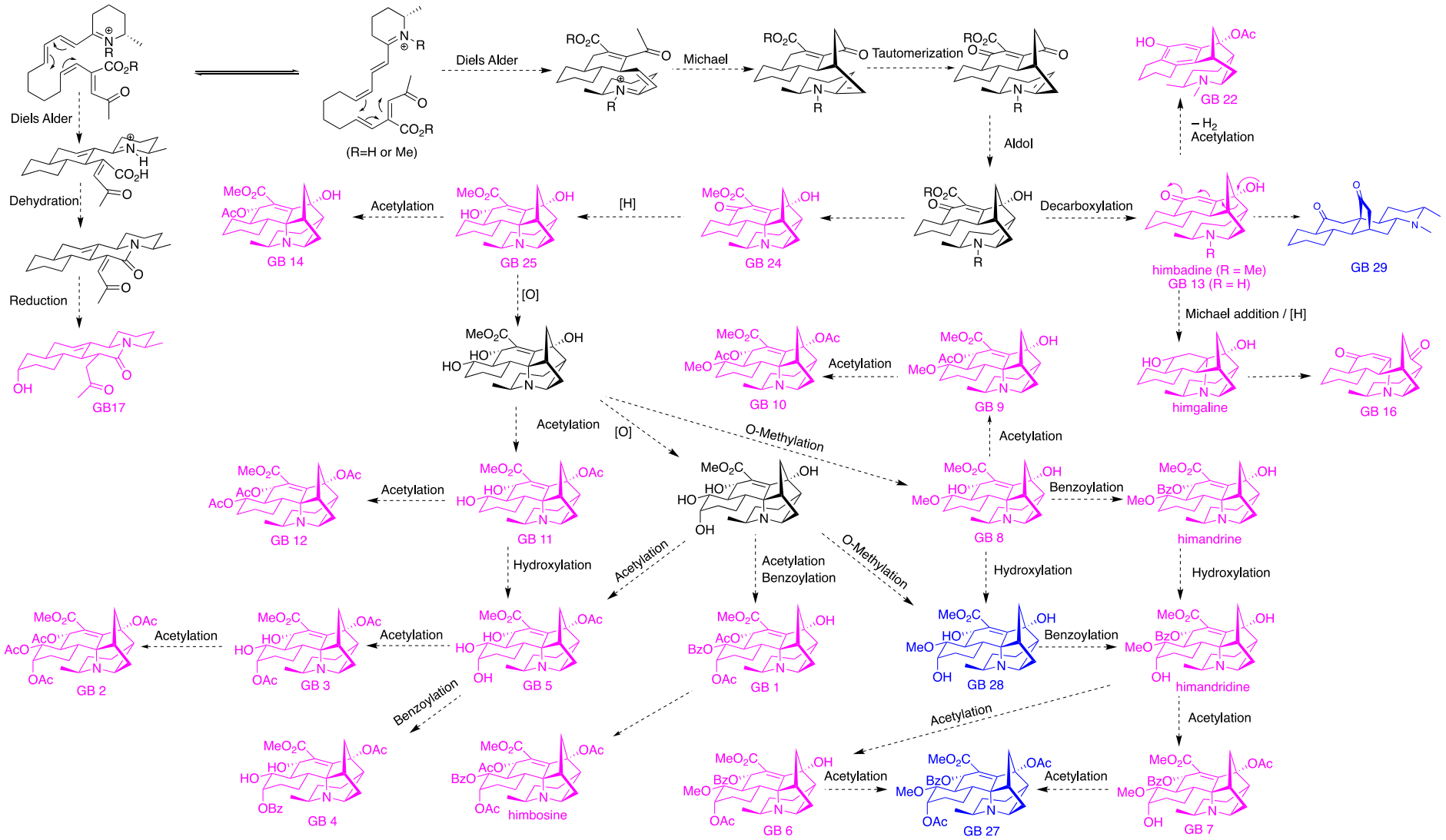

Scheme 1: Proposed biogenetic pathway of GB alkaloids (Class II, III, IV)

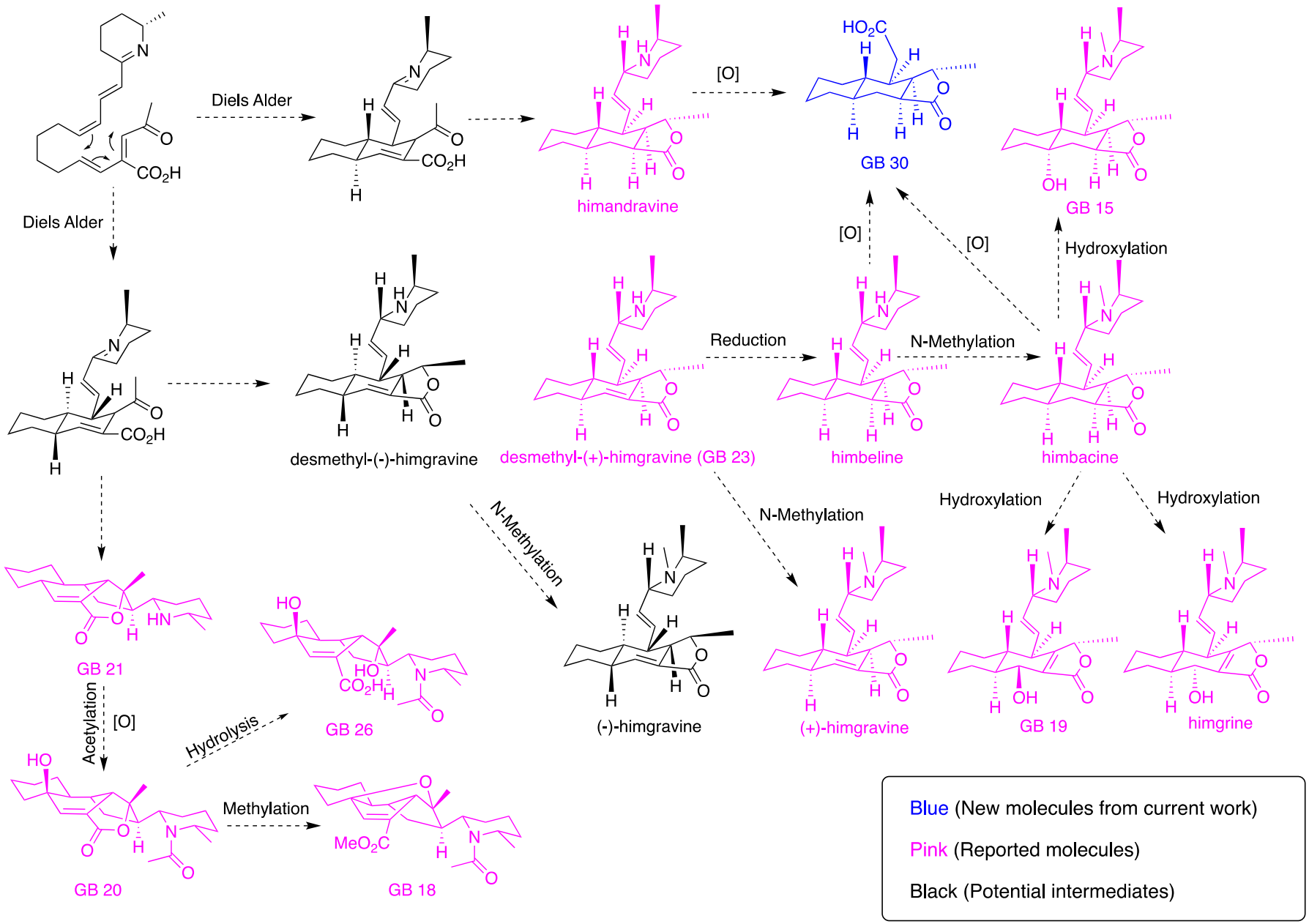

Scheme 2: Proposed biogenetic pathway of GB alkaloids (Class I)

Table 1: NMR data for GB 27 (**1**) in $CDCl_3$

Position	δ_C, type	δ_H, mult (*J*, Hz)	^1H-^{13}C HMBC	COSY	ROESY
1	20.5, CH_3	1.81, d (7.0)	2, 3	2	2, 3α, 6
2	60.1, CH	4.29, m	1, 3, 4, 6	1, 3	1, 3α, 3β, 6
3	25.0, CH_2	α 2.62, m	1, 2, 4, 5	2, 3β, 4	1, 2, 3α, 4α, 11α
		β 1.77, m	1, 2, 4, 5	2, 3α, 4	2, 3β, 4β, 11β
4	23.2, CH_2	β 1.81, m	2, 3, 5, 6, 20	3, 5, 4α	3β, 4α, 5
		α 2.08, m	2, 3, 5, 6, 20	3, 5, 4β	3α, 4β, 5, 8
5	38.8, CH	3.13, m	3, 4, 6, 7, 20, 21	6, 4	4α, 4β, 6, 8 7α, 7β
6	70.1, CH	4.11, m	4, 5, 7, 8	5, 7	5, 7α, 7β, 1
7	35.9, CH_2	α 1.96, m	5, 6, 8, 9, 21	6, 8, 7β	5, 6, 7β
		β 2.77, m	5, 6, 8, 9, 21	6, 8, 7α	5, 6, 7α
8	48.3, CH	2.70, m	6, 7, 9, 10, 19, 20, 21	7, 21	4α, 5, 10
9	71.9, C				
10	42.1, CH	1.86, m	8, 12, 14, 16	11, 15	8, 13, 15, 16
11	21.8, CH_2	α 1.80, m	9, 10, 12, 13, 15	11β, 12β	3α, 12α, 15
		β 2.20, m	9, 10, 12, 13, 15	11α, 12α	3β, 12β
12	27.9, CH_2	β 1.49, m	10, 11, 13, 14	11α, 12α	12α, 11β, 15
		α 2.20, m	10, 11, 13, 14	11β, 12β	12β, 11α
13	65.6, CH	5.46, m	11, 12, 14, 15, 13-$\underline{C}OCH_3$	12, 14	10, 14, 16
14	84.6, CH	3.15, m	10, 12, 16	13, 15	13, 16
15	39.6, CH	2.83, m	13, 14, 17, 9	14, 16	10, 11α, 12β
16	71.0, CH	6.07, m	10, 14, 15, 17, 18, 19	15	10, 13, 14

17	124.1, C				
18	166.5, C				
19	140.9, C				
20	84.2, C				
21	41.6, CH_2	α 1.91, m	19, 20, 9, 8, 7, 5	8, 21β	21α
		β 2.74, m	19, 20, 9, 8, 7, 5	8, 21α	5, 21β
13-$\underline{C}OCH_3$	170.3, C				
13-$CO\underline{CH_3}$	21.3, C	2.04, s	13-$\underline{C}OCH_3$		
14-$O\underline{CH_3}$	57.3, C	3.12, s	14		14
18-$O\underline{CH_3}$	52.4, C	3.65, s	18		
20-$\underline{C}OCH_3$	168.7, C				
20-$CO\underline{CH_3}$	21.3, CH_3	2.02, s	20-$\underline{C}OCH_3$		
22	165.7, C				
1'	130.2, C				
2'	129.6, CH	7.92, m	22, 4', 6'	3'	3'
3'	128.6, CH	7.44, m	1', 5'	2', 4'	2', 4'
4'	133.3, CH	7.57, m	2', 6'	3', 5'	3', 5'
5'	128.6, CH	7.44, m	1', 3'	4', 6'	4', 6'
6'	129.6, CH	7.92, m	22, 2', 6'	5'	5'

Table 2: NMR data for GB 28 (**2**) in DMSO-*d*$_6$

Position	δ_C, type	δ_H, mult (*J*, Hz)	^{1}H-^{13}C HMBC	COSY	ROESY
1	23.1, CH_3	1.23, d (*7.3*)	2, 3	2	2, 3β, 11α, 11β, 12, 15
2	54.4, CH	3.23, m	1, 3, 9	1, 3	1, 3α, 3β, 4α, 6
3	26.4, CH_2	α 1.01, m	1, 2, 3, 4	2, 4, 3β	4α, 2, 11α
		β 2.24, m	1, 2, 3, 4	2, 4, 3α	1, 2, 11β
4	25.2, CH_2	α 1.54, m	2, 3, 5, 6, 20	3, 5, 4β	2, 3α, 5, 8
		β 2.23, m	2, 3, 5, 6, 20	3, 5, 4α	5, 8
5	47.5, CH	1.73, m	20	4, 6	4α, 4β, 6, 21α, 20-OH
6	68.2, CH	3.13, br s	8, 9, 20, 7 (w)	5, 7	2, 5, 7α, 7β
7	36.9, CH_2	α 1.39, m	5, 6, 9, 21	6, 8, 7β	6, 8, 7β
		β 1.65, m	5, 6, 9, 21	6, 8, 7α	6, 8, 7α
8	48.6, CH	2.01, m	6, 10, 20, 7(w)	7, 21	4α, 4β, 7α, 7β, 10
9	65.0, C				
10	42.2, CH	1.31, m	8, 9, 11, 12, 14	15, 11	8, 13, 16
11	20.1, CH_2	α 1.16, m	10, 13, 9	10, 12, 11β	1, 3α, 12α, 15
		β 1.75, m	10, 13, 9	10, 12, 11α	1, 3β, 12β
12	30.4, CH_2	α 1.31, m	10, 14	11, 13, 12β	11α, 12β
		β 1.77, m	10, 14	11, 13, 12α	11β, 12α, 15
13	62.2, CH	4.07, m	11, 15	12, 14	10, 14, 16
14	88.8, CH	3.05, dd (*10.0, 2.0*)	13, 15, 16, 14- O<u>C</u>H$_3$	13, 15	13, 16
15	40.9, CH	2.45, m	9, 11, 13, 17	10, 14, 16	10, 11α, 12β, 16-OH

16	71.7, CH	4.29, d (*7.7*)	14, 15, 17, 19, 21	15, 16-OH	10, 13, 14, 16-OH
17	117.6, C				
19	152.1, C				
20	79.0, C				
21	45.9, CH_2	α 1.38, m	5, 7, 17, 19, 20	8, 21β	21β
		β 1.53, m	5, 7, 17, 19, 20	8, 21α	5, 21α
18	169.6, C				
18- O$\underline{CH_3}$	50.9, CH_3	3.59, s	18		
14- OCH_3	55.4, CH_3	3.32, s	14		
13- OH		4.42, br s			
16- OH		3.75, d (*1.3*)	14, 17, 19	13	15, 16
20- OH		4.73, br s			5, 3, 4(w), 7(w)

Table 3: NMR data for GB 29 (**3**) in $CDCl_3$

Position	δ_C, type	δ_H, mult (*J*, Hz)	^1H-^{13}C HMBC	COSY	ROESY
1	16.8, CH_3	1.33, d (*6.0*)	2, 3	2	2, 3, N<u>C</u>H_3
2	54.2, CH	3.09, m	1, 3, 6	1, 3	1, 3
3	28.9, CH_2	1.96, m	1, 2, 4, 5	2, 4	2, 4
4	15.9, CH_2	α 1.69, m	2, 3, 5, 6, 18	3, 5, 4α	3, 5
		β 1.96, m	2, 3, 5, 6, 18	3, 5, 4β	3, 5
5	41.8, CH	1.83, m	3, 4, 6, 7, 9, 17, 19	4, 6	4, 6
6	58.1, CH	3.06, m	2, 4, 8, 18, N<u>C</u>H_3	5, 7	5, 7, 20α, N<u>C</u>H_3
7	31.3, CH_2	2.25, m	5, 9, 20	6, 8	5, 6, 8
8	30.5, CH	2.69, m	6, 7, 9, 10, 19	7, 20	7, 20α, 20β, 12β
9	47.5, CH	2.11, m	7, 10, 11, 20	8, 10	10
10	41.8, CH	1.01, m	8, 9, 11, 12, 14, 16, 18	9, 11, 15	9, 11α, 11β, 15, 11α, 11β, 12β, 20β
11	25.2, CH_2	α 1.11, m	9, 12, 13, 15	10, 12, 11β	10, 12β
		β 1.86, m	9, 12, 13, 15	10, 12, 11α	10, 12α
12	31.9, CH_2	α 1.10, m	10, 13, 14	11, 13, 12β	11α, 13α
		β 2.03, m	10, 13, 14	11, 13, 12α,	8, 10, 11β, 13β
13	25.4, CH_2	α 1.08, m	11, 12, 14, 15	12, 14, 13β	12α, 14α
		β 1.76, m	11, 12, 14, 15	12, 14, 13α	12β, 14β
14	24.9, CH_2	β 1.14, m	10, 12, 16	13, 15, 14β	13β, 15

		α 1.77, m	10, 12, 16	13, 15, 14α	13α
15	52.6, CH	1.87, m	9, 11, 13, 17	10, 14	10, 14β
16	209.2, C				
17	41.1, CH_2	α 2.37, m	5, 15, 16, 18, 19	18, 17β	20α
		β 2.62, m	5, 15, 16, 18, 19	18, 17α	
18	59.1, C				
19	217.4, C				
20	39.1, CH_2	α 2.10, m	7, 8, 9, 18	8, 20β	6, 8, 17α
		β 2.39, m	7, 8, 9, 18	8, 20α	8, 10
N$\underline{CH_3}$	39.8, CH_3	2.59, s			1, 2, 6

Table 4: NMR data for GB 30 (**4**) in $CDCl_3$

Position	δ_C, type	δ_H, mult (*J*, Hz)	^1H-^{13}C HMBC	COSY	ROESY
2	73.5, CH	4.05, dq (*8.7, 6.0*)	4, 12, 13, 3 (w)	3, 16	13β, 16, 5
3	49.7, CH	2.10, m	2, 5, 11, 13, 14, 16	2, 4, 12	4, 16, 13β, 14β
4	38.7, CH	2.11, m	2, 6, 15	3, 5, 14,	3, 10, 14β
5	41.4, CH	0.95, m	3, 7, 9, 11, 14	4, 6, 10	2, 6β, 7β, 10
6	30.2, CH_2	α 0.84, m	4, 8, 10	5, 7, 6β	7β
		β 1.77, m	4, 8, 10	5, 7, 6α	11β, 14β, 5
7	26.8, CH_2	β 1.22, m	5, 9	6, 8, 7α	6α, 8β, 9β
		α 1.77, m	5, 9	6, 8, 7β	6α, 8α
8	26.2, CH_2	α 1.20, m	6, 10	7, 9, 8β	7α
		β 1.68, m	6, 10	7, 9, 8α	5, 7β, 9β
9	34.2, CH_2	β 0.97, m	5, 7, 11	8, 10, 9α	7β
		α 1.61, m	5, 7, 11	8, 10, 9β	10, 11α
10	41.7, CH	1.06, m	4, 6, 8, 12	5, 9, 11	4, 5, 9α, 11α
11	35.3, CH_2	β 1.18, m	3, 5, 9, 13	10, 12, 11α,	6β, 11α, 12
		α 1.50, m	3, 5, 9, 13	10, 12, 11β,	10, 11β, 13α
12	41.5, CH	2.20, m	2, 3, 4, 10, 11	3, 11, 13	3, 11α, 13β
13	72.2, CH_2	α 3.49, d (*8.0*)	2, 3, 11, 10 (w)	12, 13β	12, 11, 13β
		β 3.78, dd (*8.0*, *4.1*)	2, 3, 11, 10 (w)	12, 13α,	2, 3, 12, 13α, 16
14	36.0, CH_2	β 2.59, d (*15.5, 4.5*)	3, 4, 5, 15	4, 14α,	3, 4, 6β, 14α,
		α 2.14, m	3, 4, 5, 15	4, 14β	14β
15	178.2, C				
16	21.1, CH_3	1.26, d (*6.0*)	1, 2		2, 3, 13β

Supporting Information

Isolation and structure elucidation of new alkaloids from the tropical rainforest tree *Galbulimima baccata*

Nirmal K. Chaudhary[†], *Walter C. Taylor*[‡], *Lewis N. Mander*[§], *Peter Karuso*[†,*]

[†]*Department of Molecular Sciences, Macquarie University, NSW 2109, Australia*

[‡] *School of Chemistry, University of Sydney, NSW 2006, Australia,*

[§] *Research School of Chemistry, Australian National University, Canberra ACT 0200, Australia*

* Corresponding author: peter.karuso@mq.edu.au

Table of Contents

A. NMR spectra

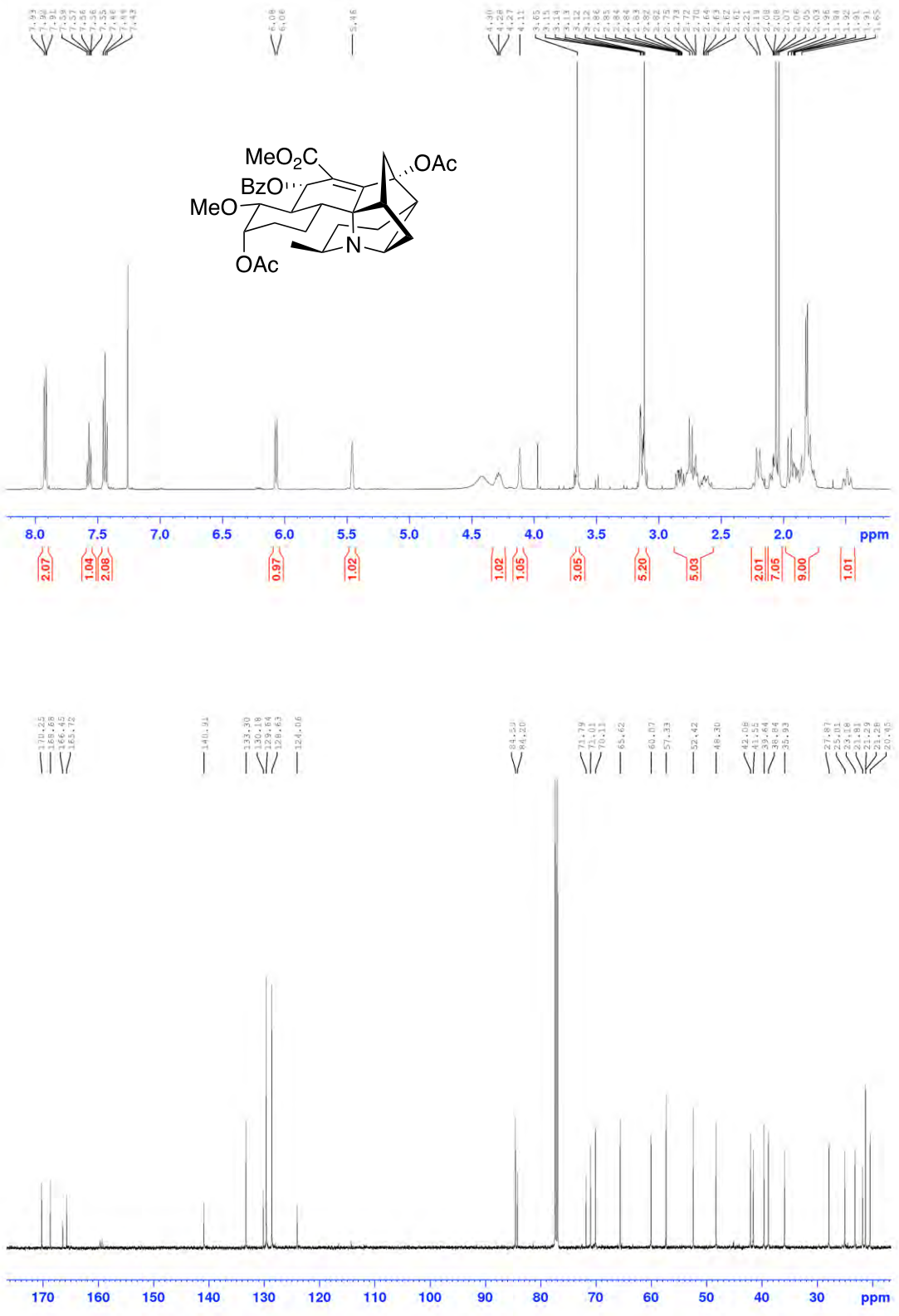

Figure S1(a): ^{1}H and ^{13}C NMR spectra of GB-27 (**1**) in $CDCl_3$

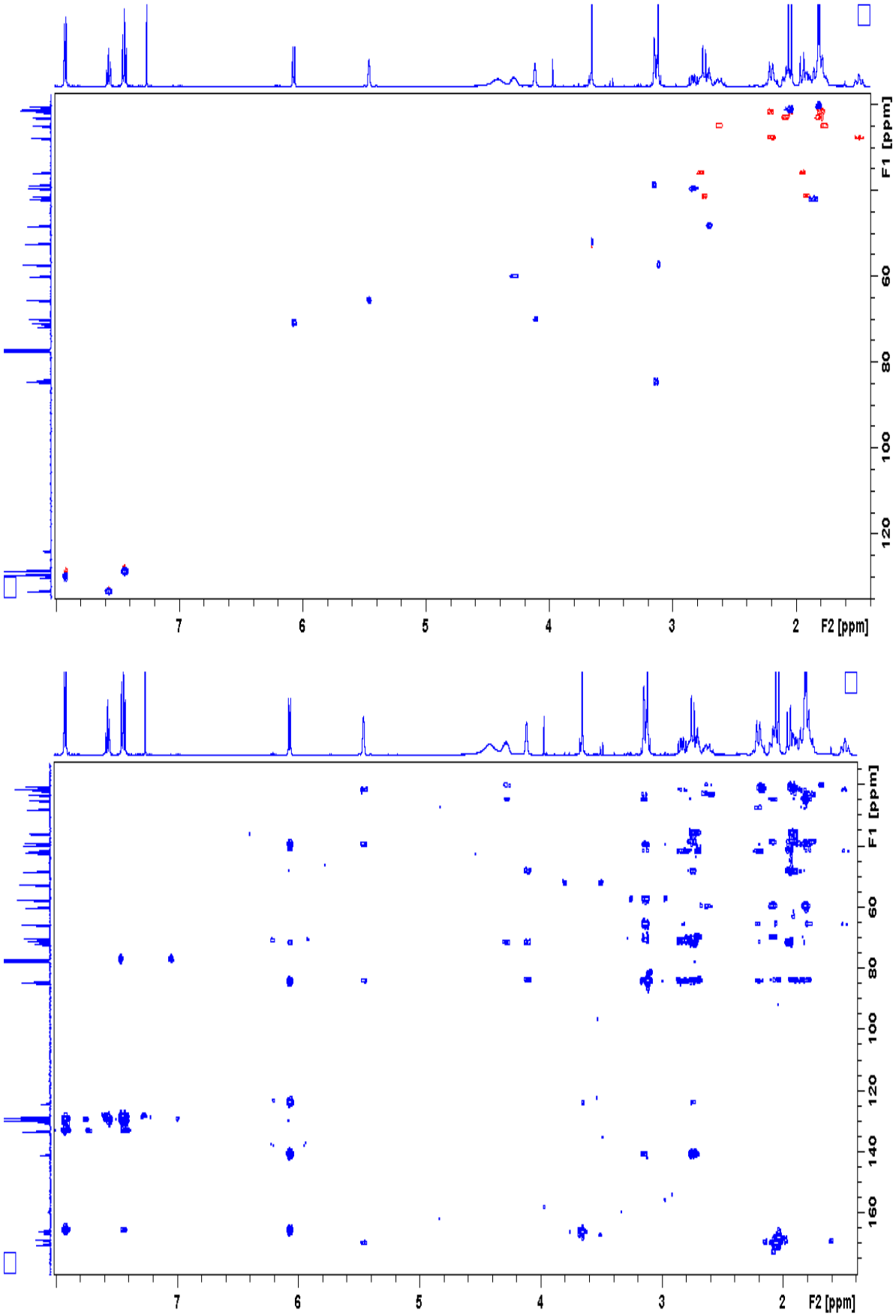

Figure S1(b): HSQC and HMBC spectra of GB-27 (**1**) in $CDCl_3$

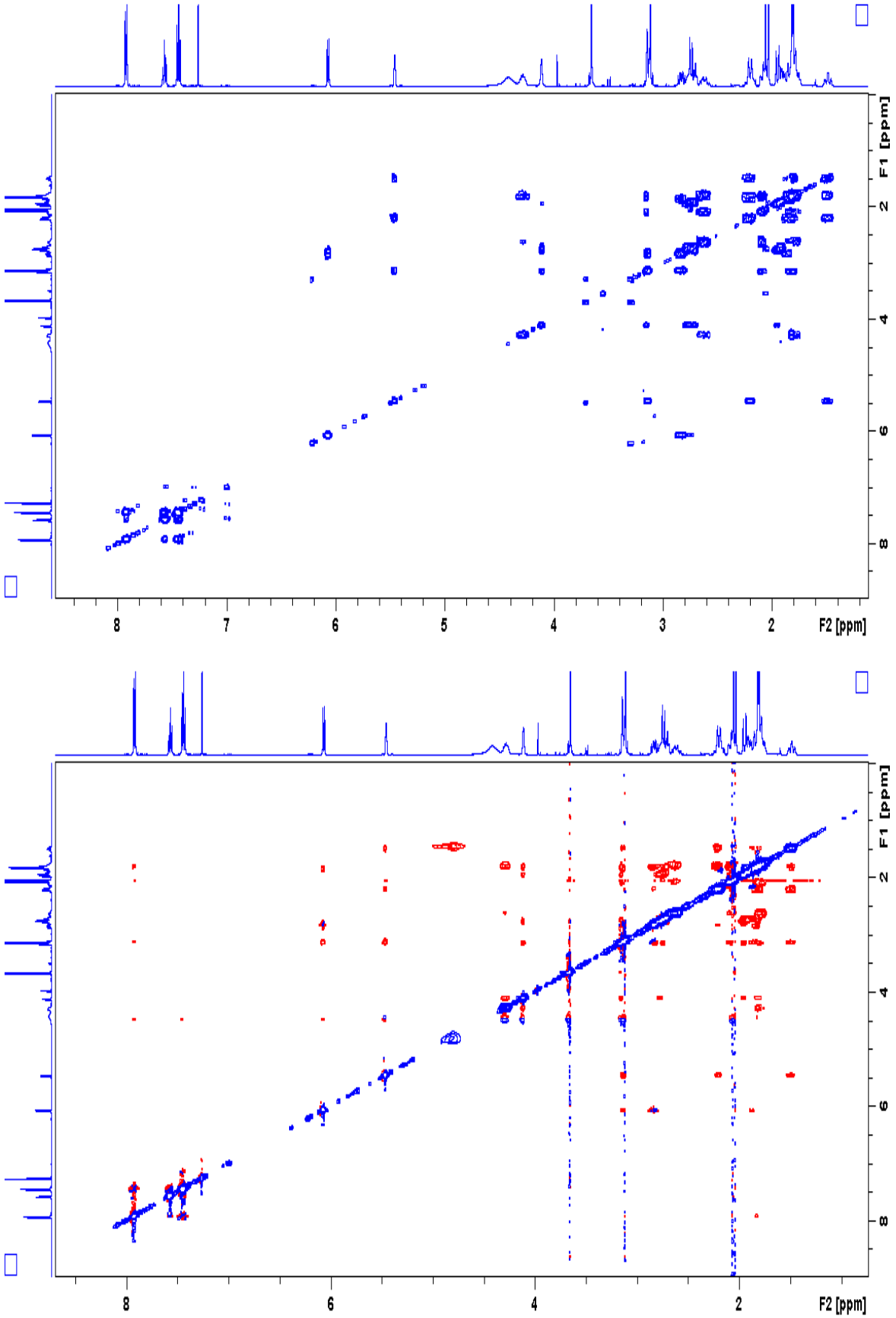

Figure S1(c): COSY and ROESY spectra of GB-27 (**1**) in $CDCl_3$

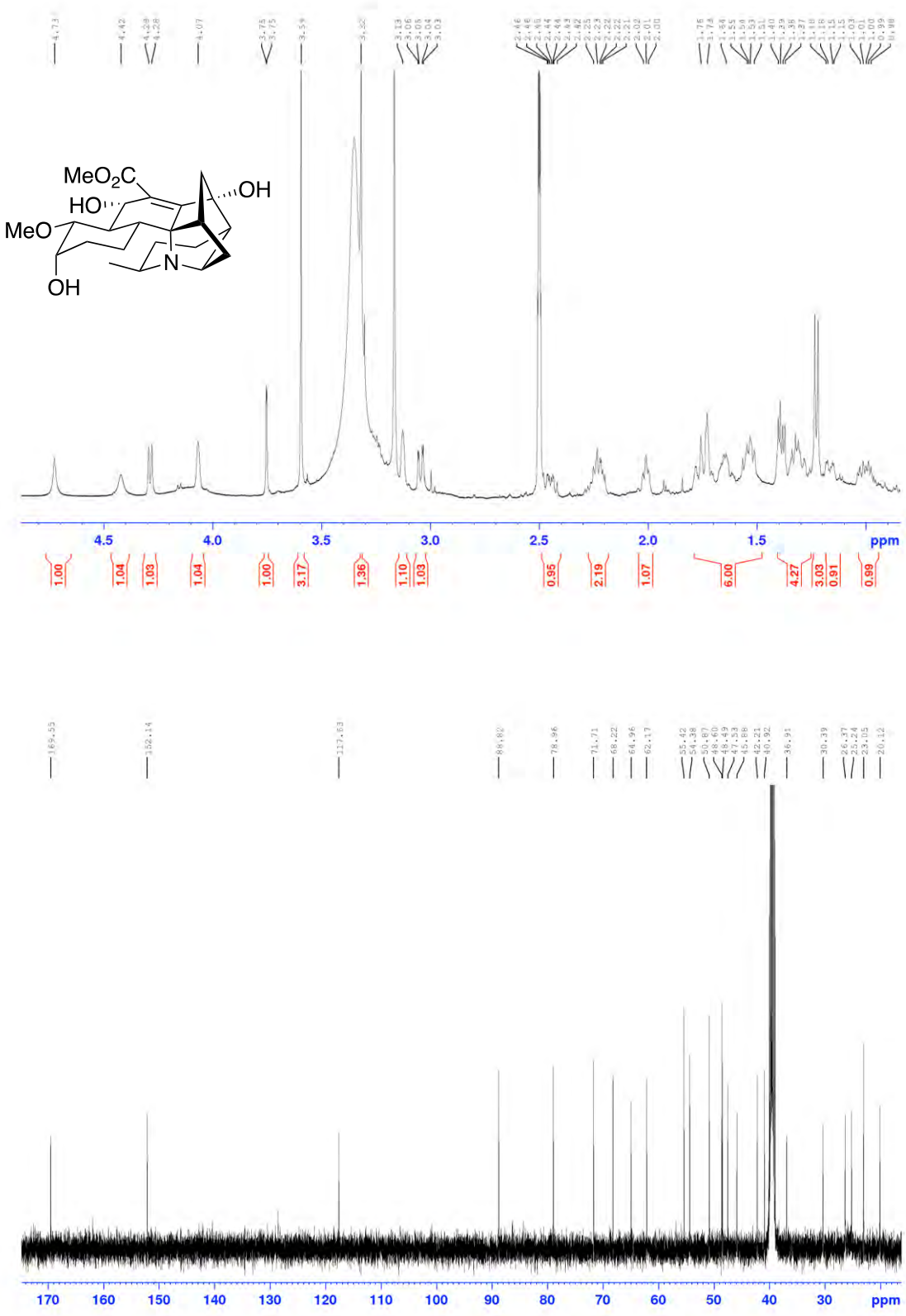

Figure S2(a): ^{1}H and ^{13}C NMR spectra of GB 28 (**2**) in DMSO-d_6

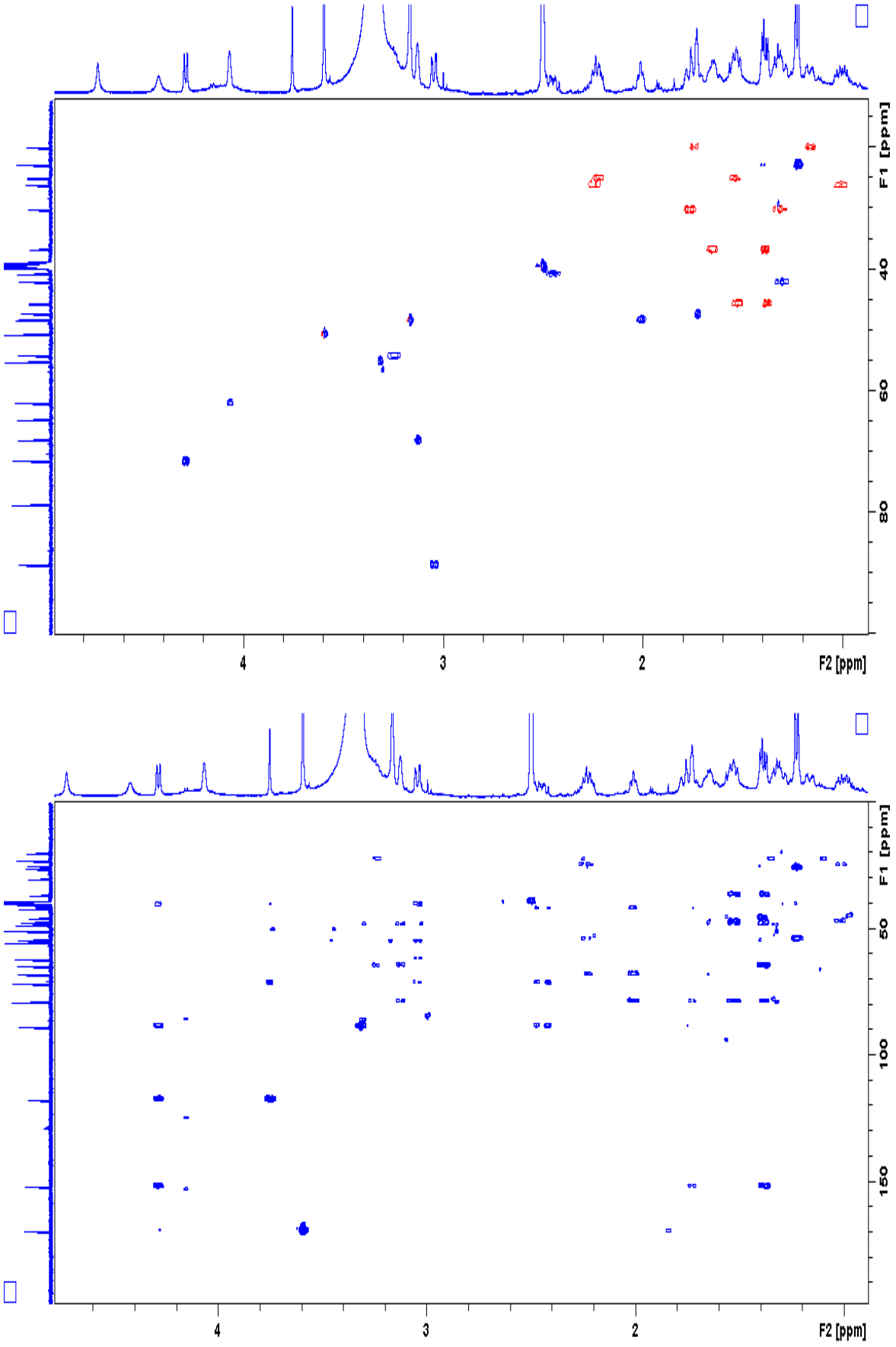

Figure S2(b): HSQC and HMBC spectra of GB 28 (**2**) in DMSO-d_6

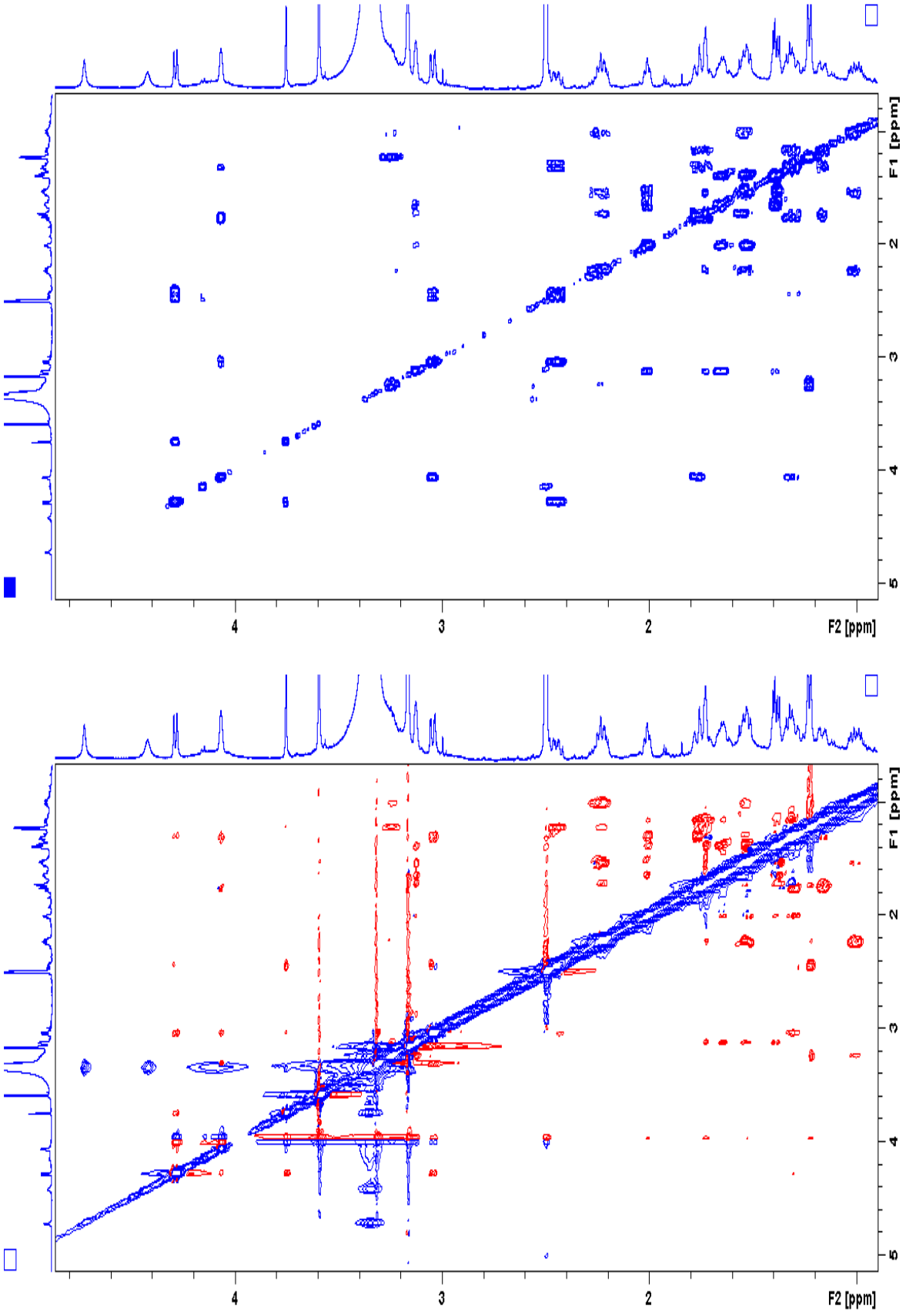

Figure S2(c): ^{1}H and ^{13}C NMR spectra of GB 28 (**2**) in DMSO-d_6

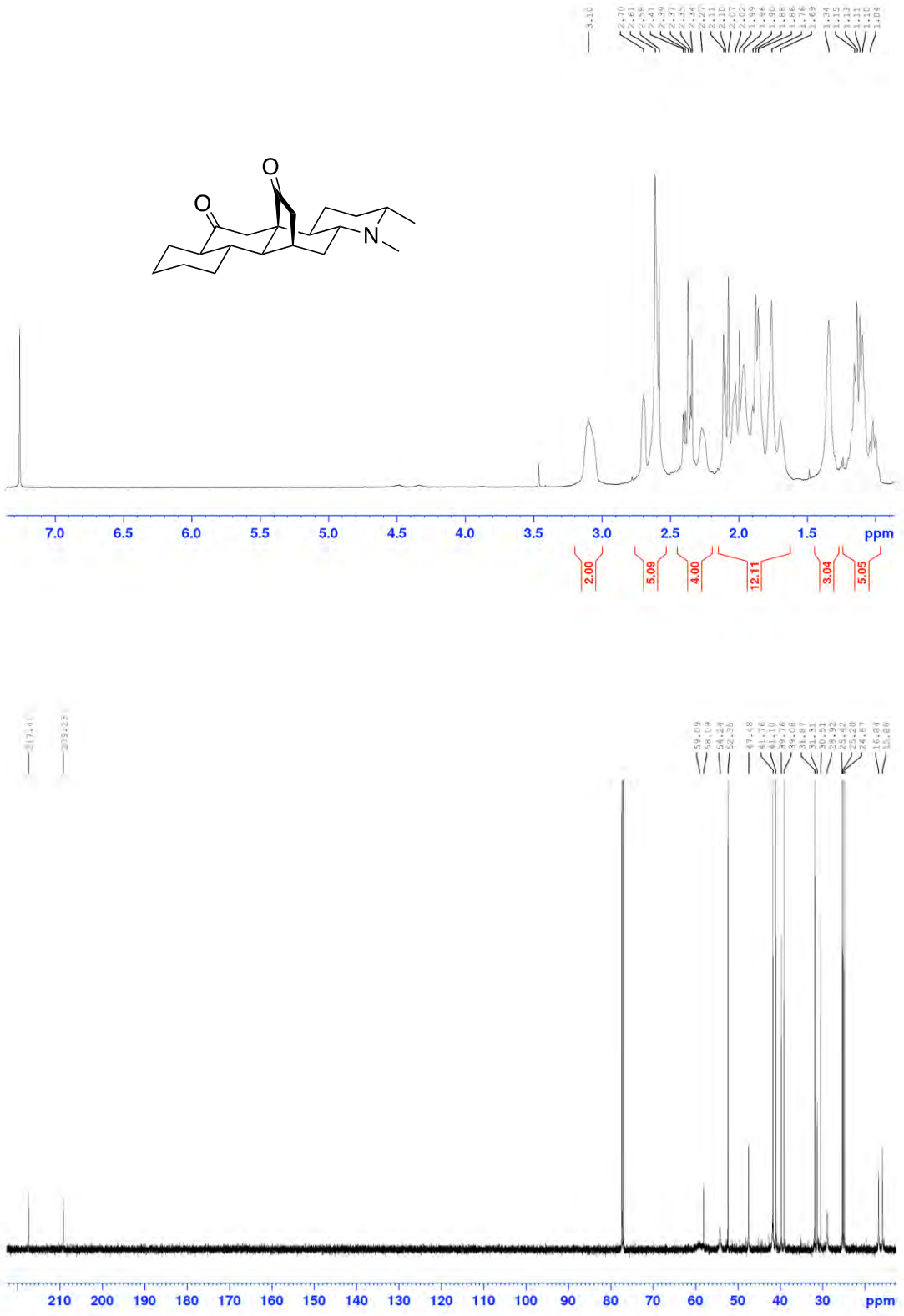

Figure S3 (a): ^{1}H and ^{13}C NMR spectra of GB-29 (**3**) in $CDCl_3$

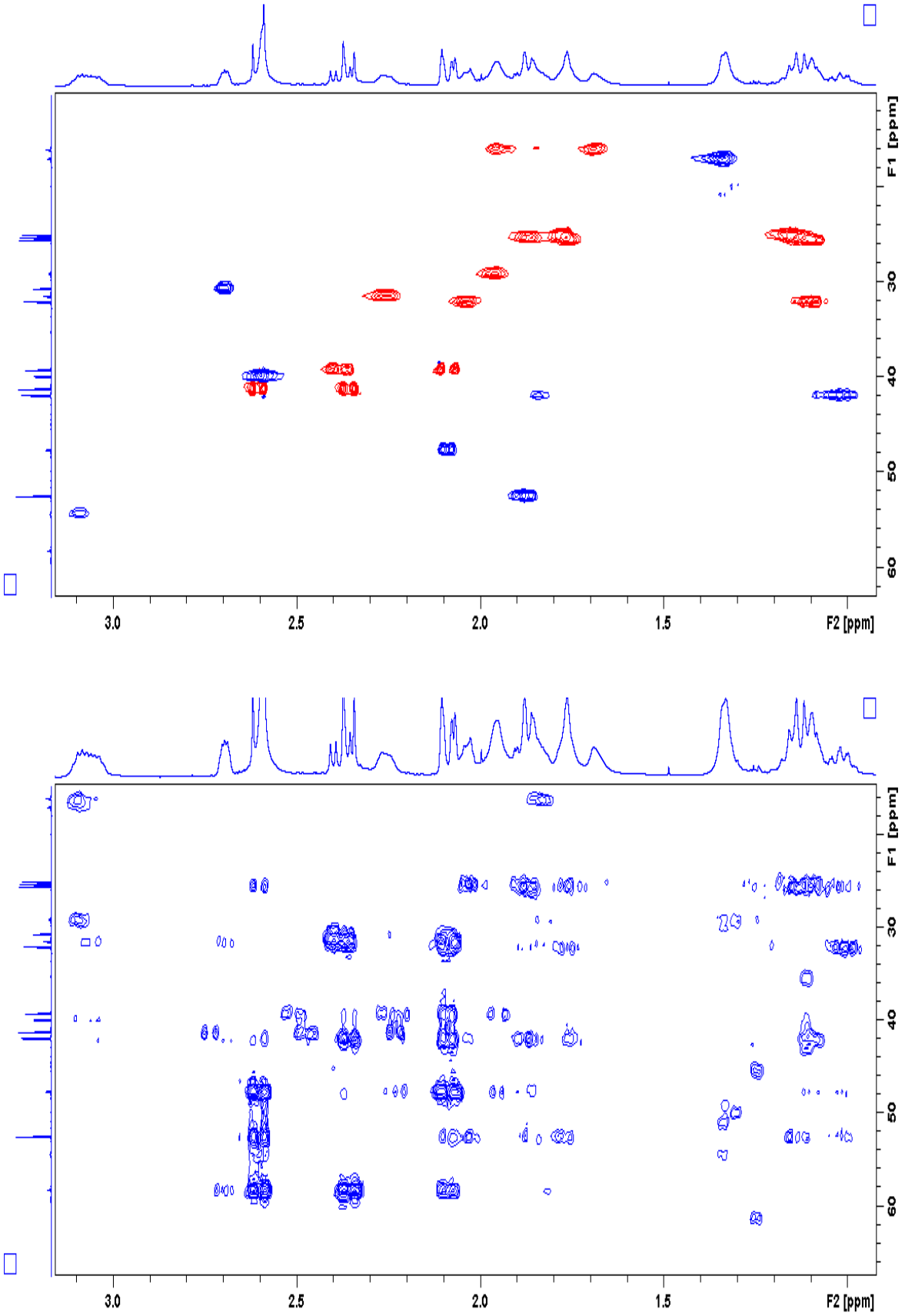

Figure S3 (b): HSQC and HMBC spectra of GB-29 (**3**) in $CDCl_3$

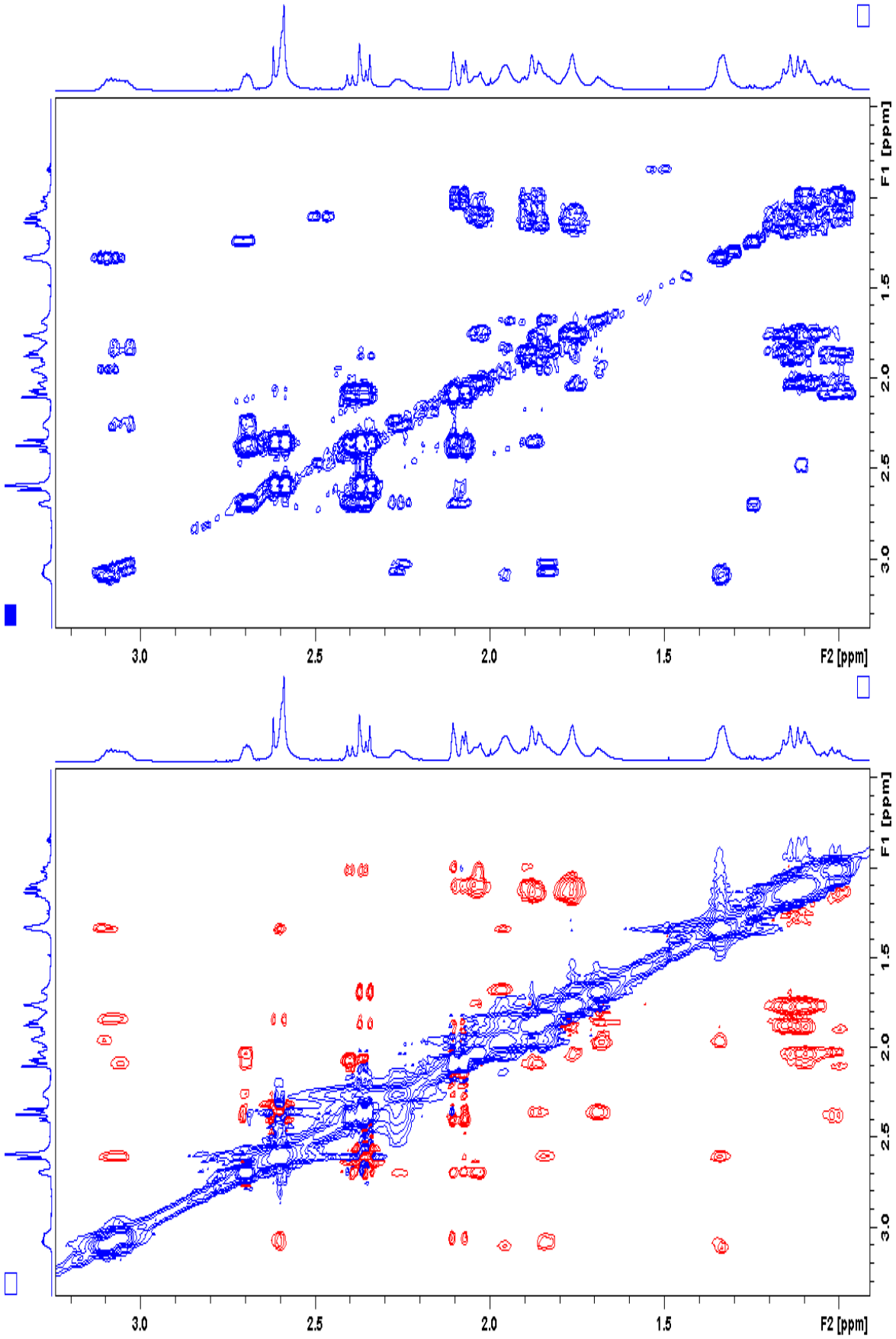

Figure S3 (c): COSY and ROESY spectra of GB-29 (**3**) in $CDCl_3$

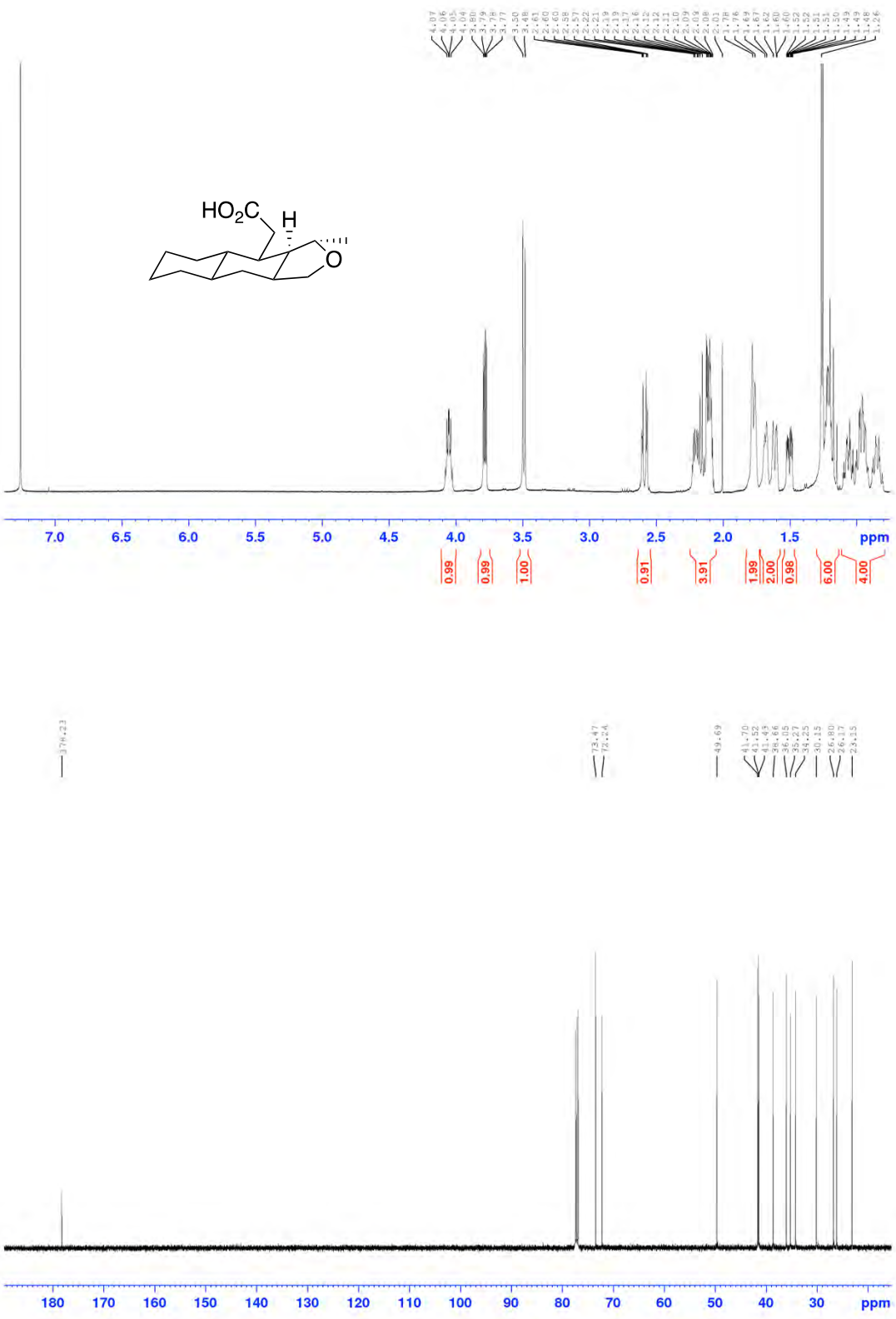

Figure S4 (a): ^{1}H and ^{13}C NMR spectra of GB-30 (**4**) in $CDCl_3$

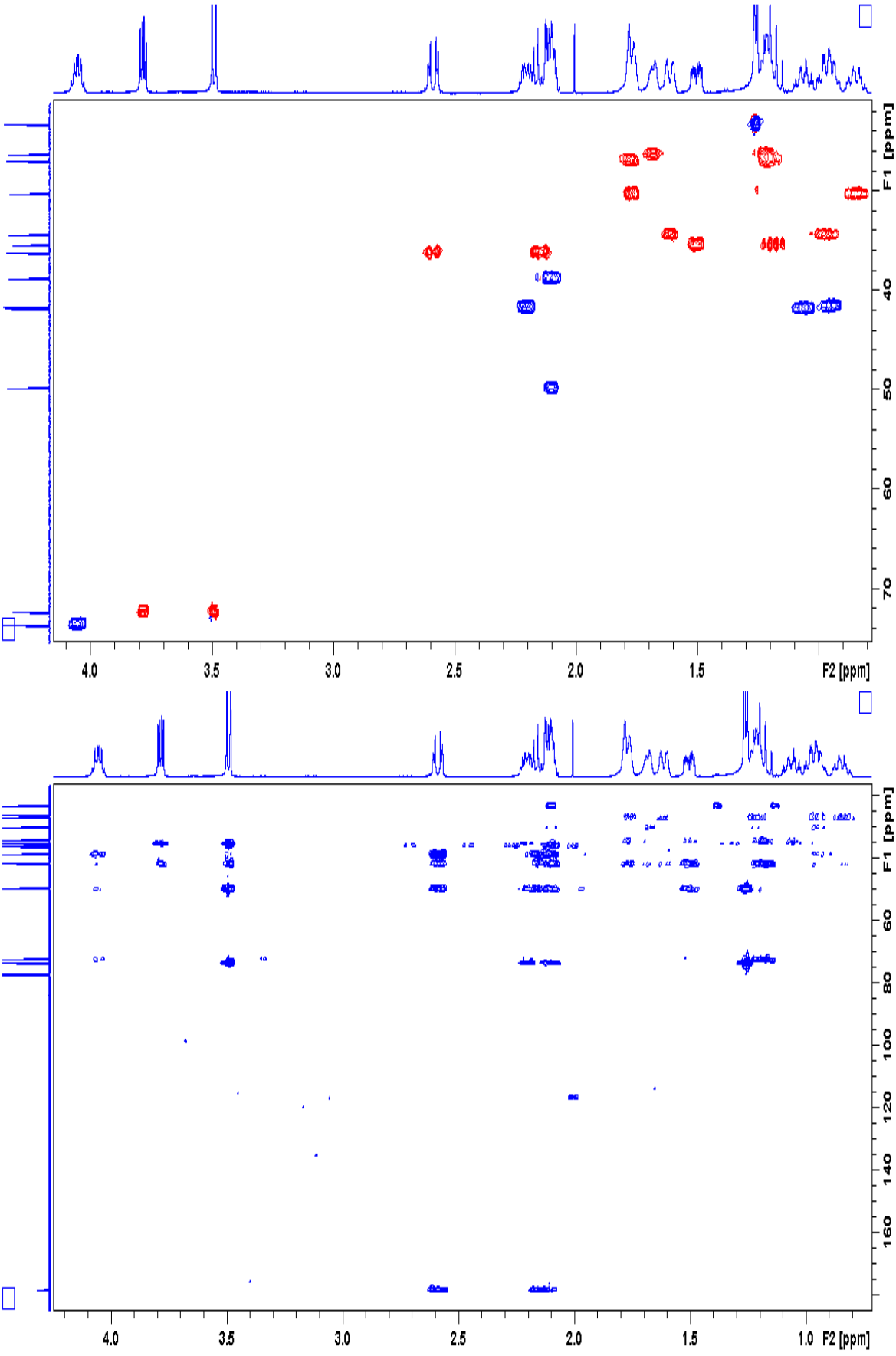

Figure S4 (b): HSQC and HMBC spectra of GB-30 (**4**) in $CDCl_3$

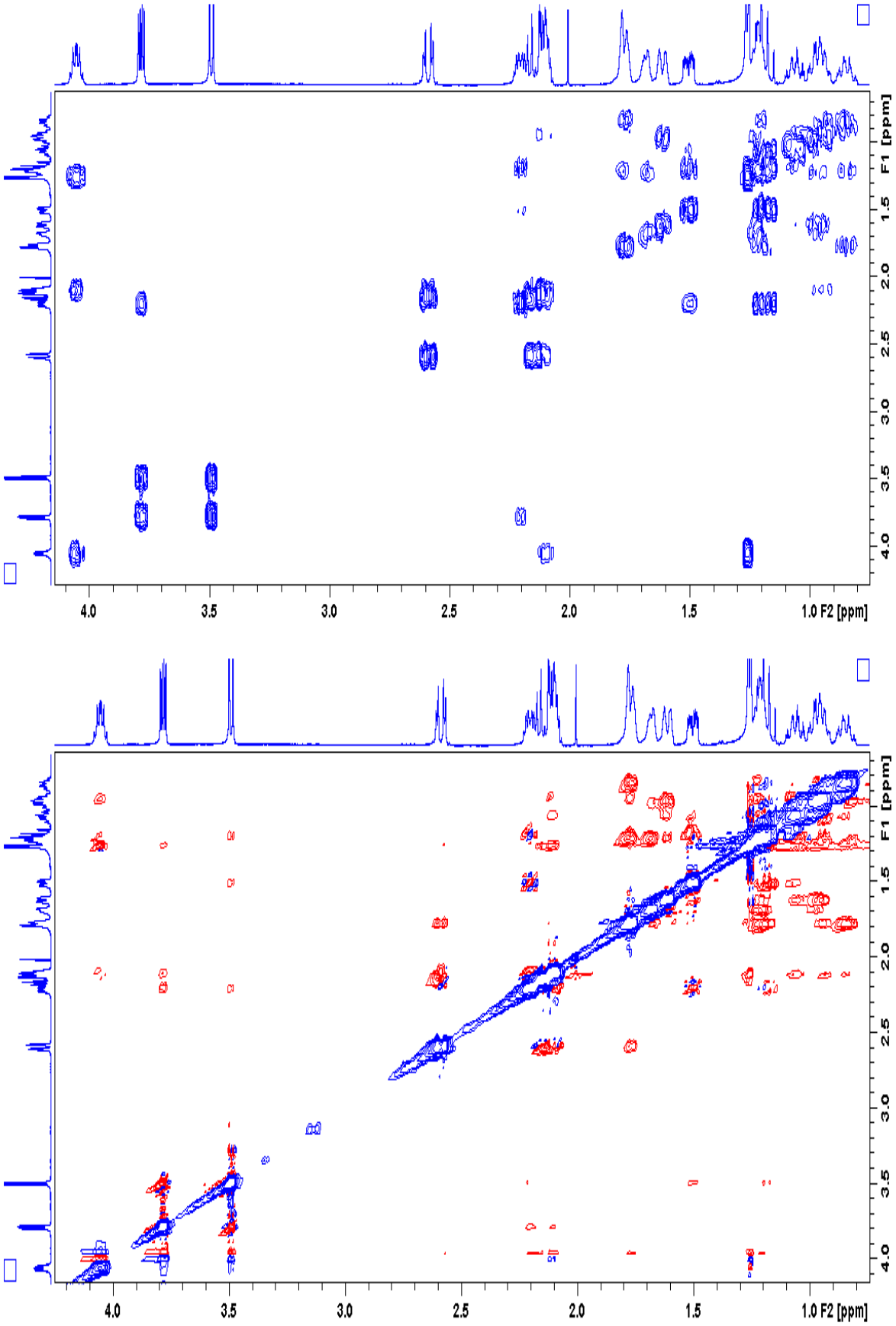

Figure S4 (c): COSY and ROESY spectra of GB-30 (**4**) in $CDCl_3$

B. UV-visible spectra

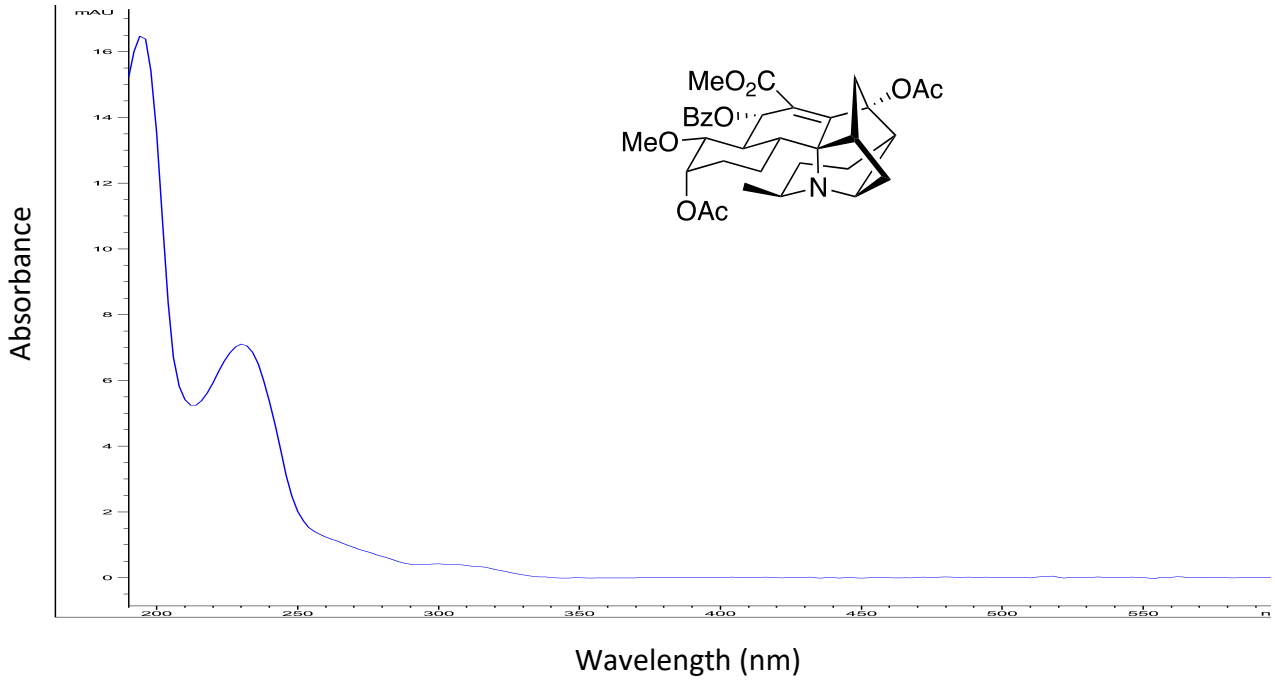

Figure S5: UV- visible spectrum of GB 27 (**1**).

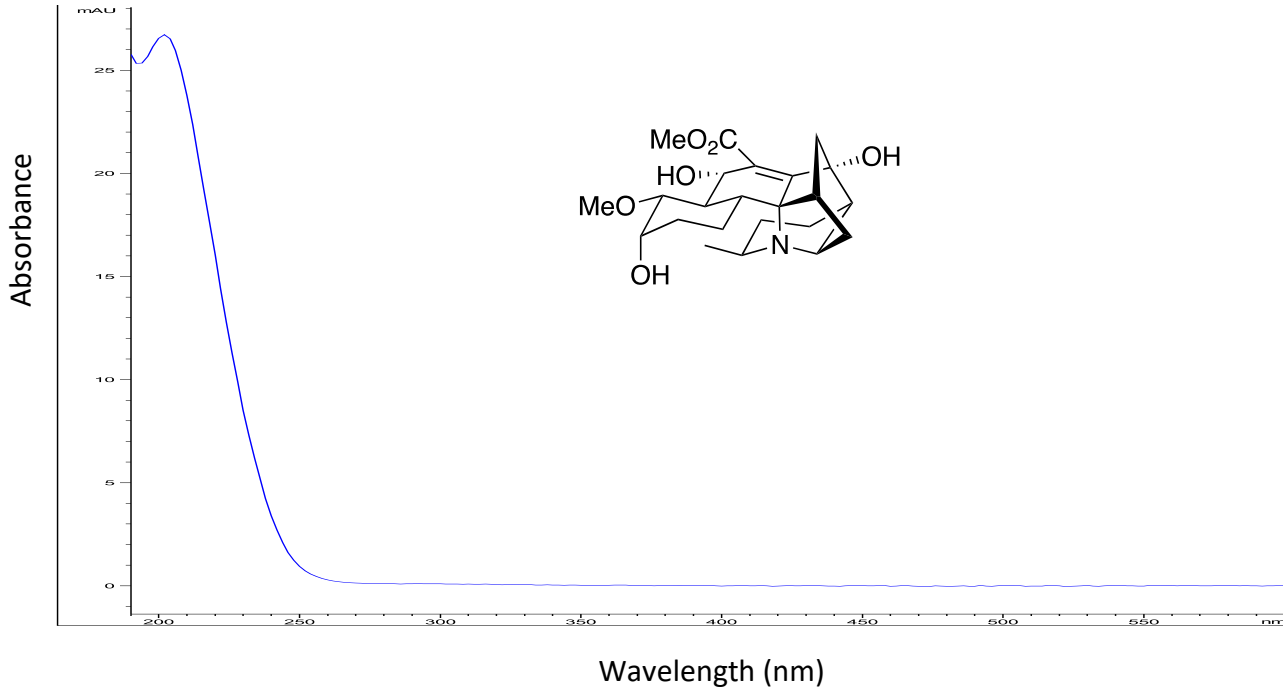

Figure S6: UV- visible spectrum of GB 28 (**2**).

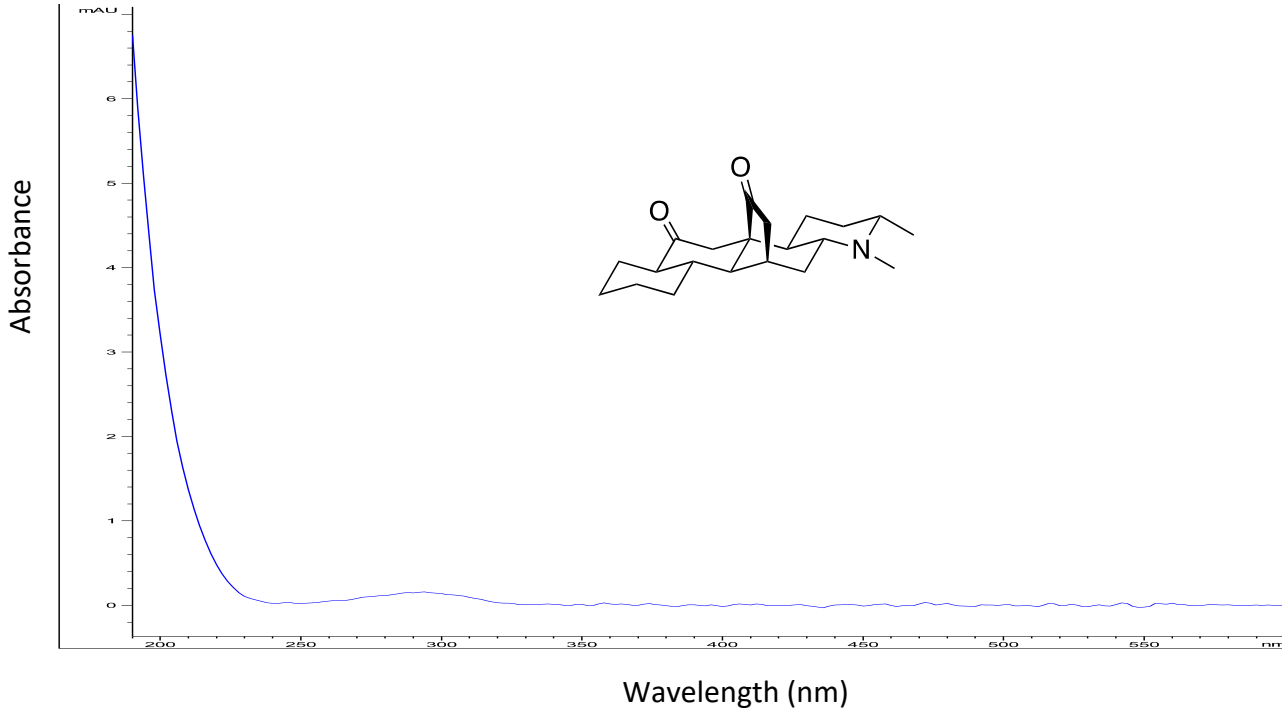

Figure S7: UV- visible spectrum of GB 29 (**3**).

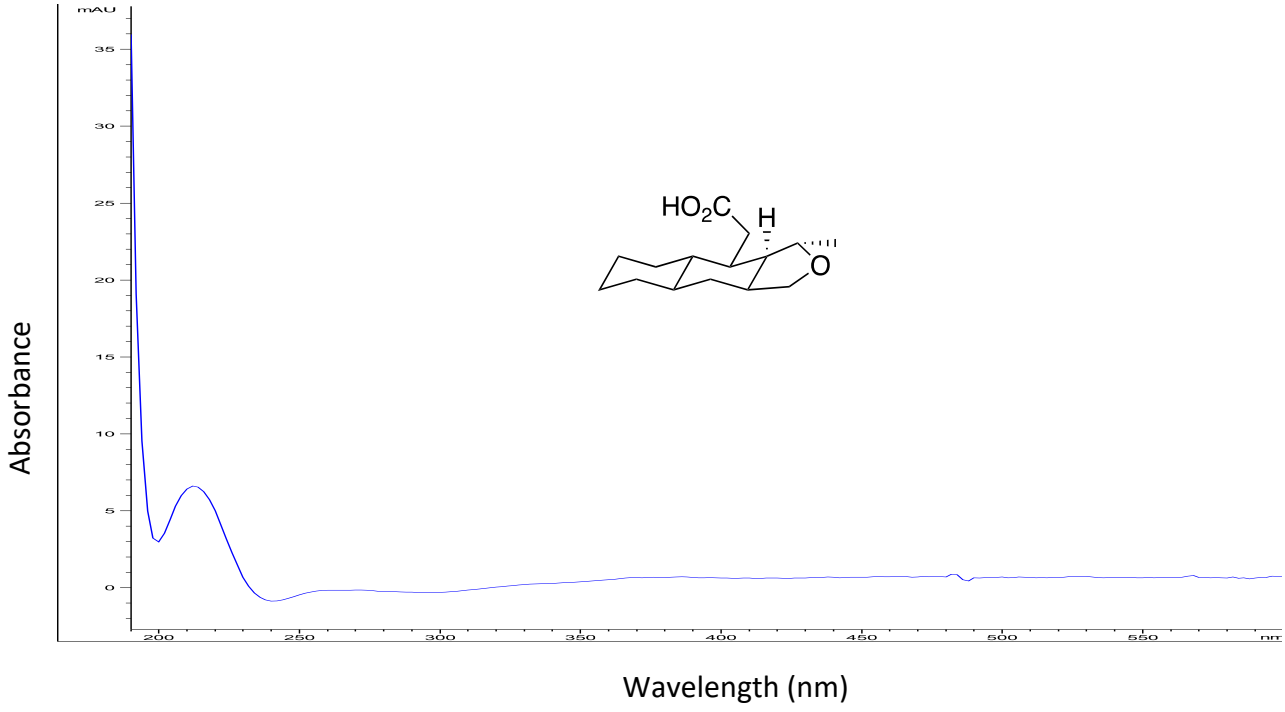

Figure S8: UV- visible spectrum of GB 30 (**4**).

C. ECD spectra

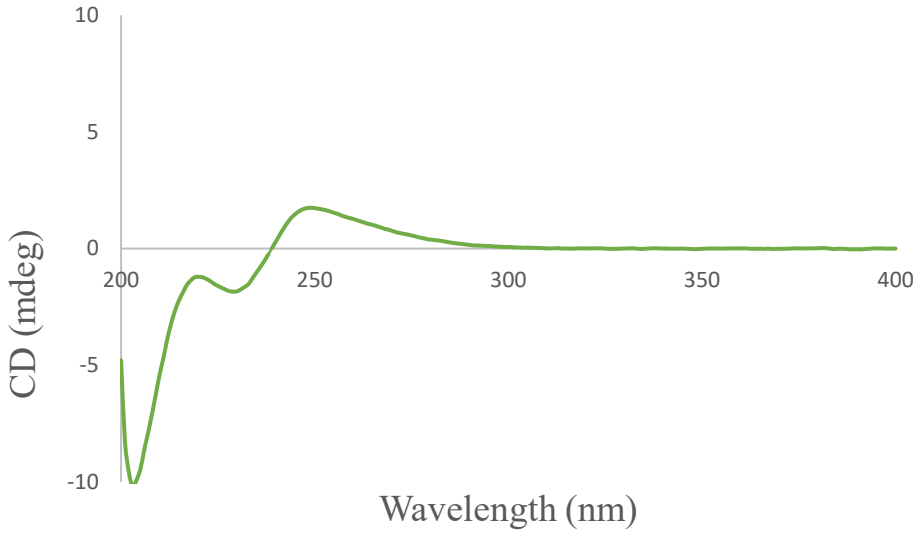

Figure S9: ECD spectrum of GB-27 (**1**) in MeOH.

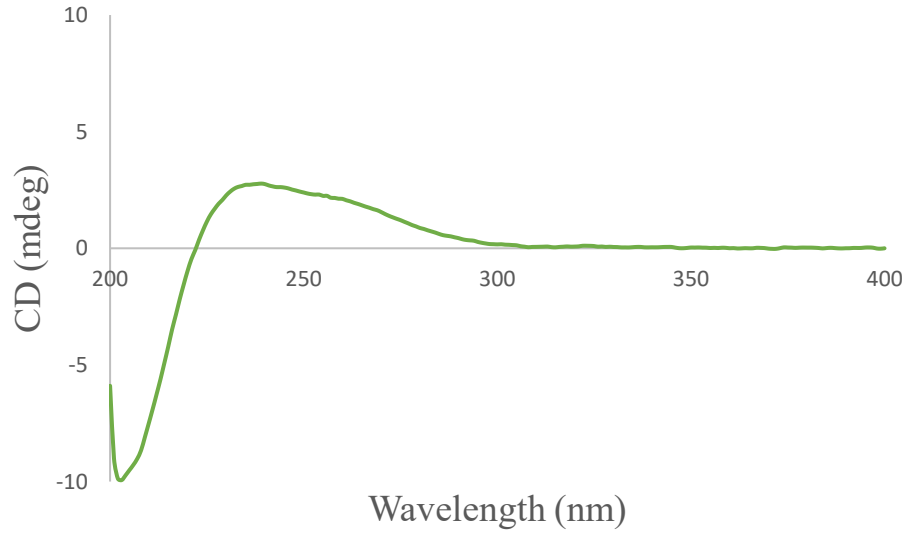

Figure S10: ECD spectrum of GB-28 (**2**) in MeOH.

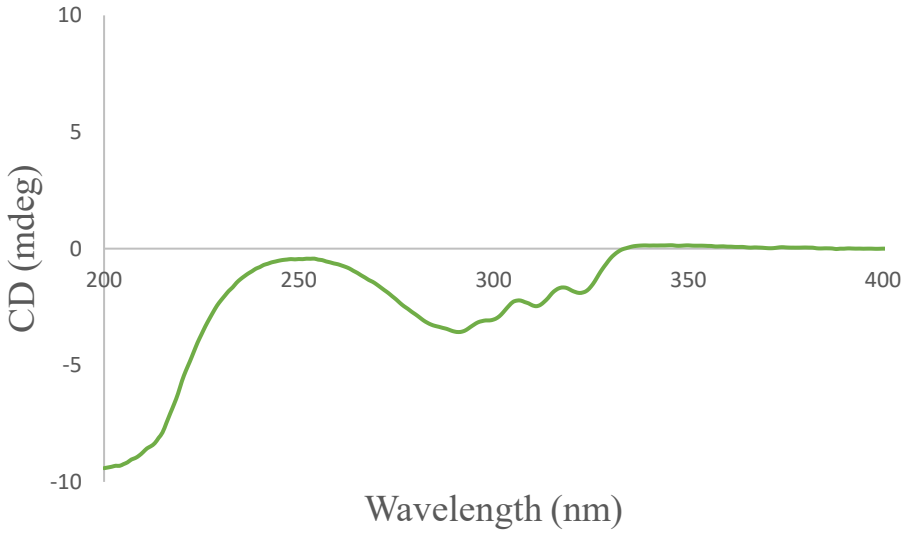

Figure S11: ECD spectrum of GB-29 (**3**) in MeOH.

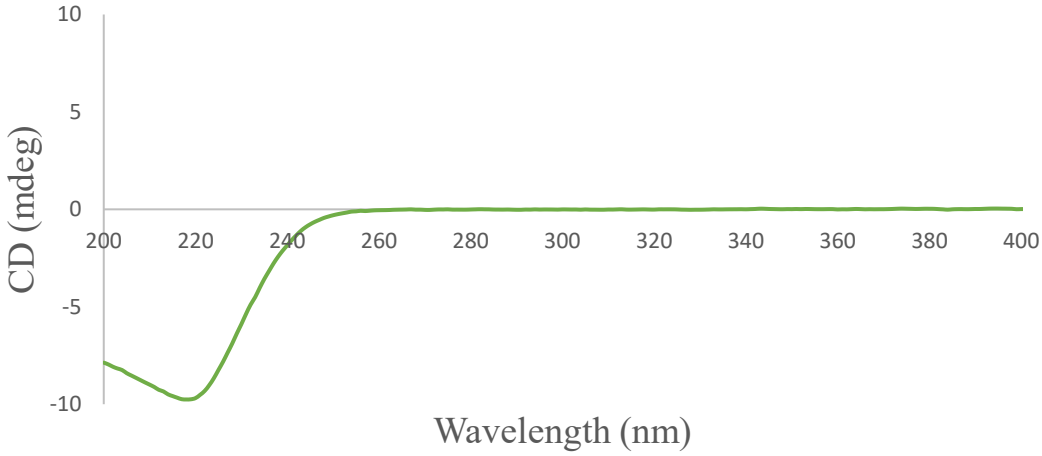

Figure S12: ECD spectrum of GB-30 (**4**) in MeOH.

Summary & Conclusion

Summary and Conclusion

The main goal of this study was discovery of novel natural products and screening of these compounds for potential pharmacological activity. Filamentous fungi have been identified as a promising source for such molecules. This study was primarily focussed on the three filamentous fungal species *Aspergillus banksianus*, *Talaromyces stipitatus* and *Aspergillus luteorubrus*. Additionally, novel alkaloids from *Galbulimima baccata* were isolated and characterized. The structures of all the compounds were established by 2D NMR spectroscopy whereas the stereochemical assignments were done by either ECD TDDFT calculations, coupling constant, ROESY correlations, comparison of optical rotations or ECD spectrum with literature or a combination thereof. The identified compounds were evaluated for their biological activities by our collaborator at Microbial Screening Technologies, Sydney with some compounds still under evaluation and their results awaited.

43 compounds including 22 new natural products with some having unprecedented structures were isolated from three different fungal strains. Additionally, the structure of one of the reported fungal metabolite talaromycesone A was revised. Also, 4 new alkaloids were isolated and characterized from *Galbulimima* baccata alongside several reported alkaloids not included in this thesis. The degradation product of talauxin V and 4 semi-synthetic talauxins, all new molecules, were also isolated and fully characterized. Biosynthetic schemes leading to most new molecules isolated have been proposed.

Chemical investigation of the novel *Aspergillus* species, *A. banksianus* revealed that isochromanones (isocoumarins) dominated the secondary metabolite profile and chemical diversity of the metabolite profile was increased by conjugation with other unrelated products such as orsellinates, anthraquinones, etc. The most abundant and the key metabolite

banksialactone A (**1**) acted as the direct precursor to several other unique natural products including the unprecedented conjugates illustrating the use of parallel biosynthetic pathways in Nature to generate hybrid metabolites. Biogenesis of the ester secondary metabolites **4-6** involves two polyketide synthase (PKS) pathways merging, whereas the *S*-hybrids **2** and **3** represent an apparent primary metabolite and secondary metabolite fusion. Among the 15 isolated secondary metabolites, 10 were new metabolites, including a rare sulphoxide compound (**3**). However, most of them did not show significant activities in the available bioassays, with only the ester hybrids exhibiting some antibiotic, antiprotozoal and cytotoxic activity warranting further investigation to fully understand their role in the ecology of *A. banksianus.*

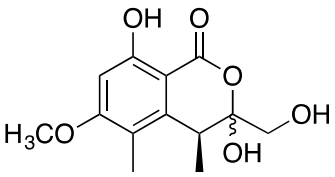

1

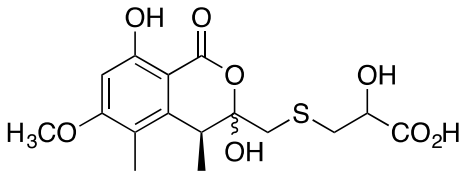

2

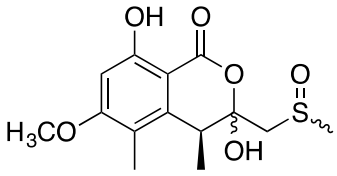

3

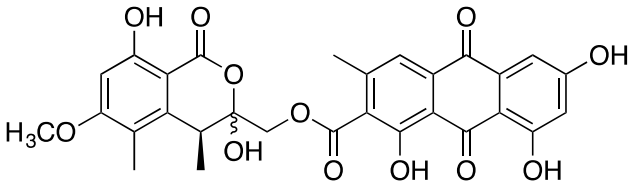

4

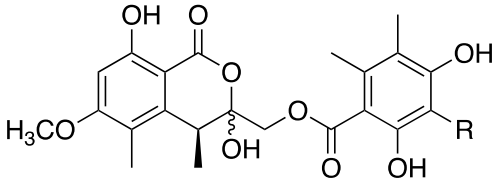

5, R=H;

6, R=CH_3

The detailed analysis of *Talaromyces stipitatus* resulted in a series of compounds with polyketide skeletons, the phenalenones and polyesters. A total of 21 compounds were isolated including nine new molecules and the structure of the reported metabolite talaromycesone A was revised. Most metabolites were structurally unique and complex with talarohemiketal (**7**) and the azaphenalenones, talauxins (**8**) and talaroazasone (**9**) being the

relatively rare ones. Additionally, a facile semi-synthesis of talauxins from their biogenetic precursor duclauxin (**10**) was established and a comprehensive biosynthetic pathway leading to the talauxins which also effectively explains biosynthesis of all other monomeric phenalenones and oxyphenalenone dimers is proposed. The only new macrocyclic polyester isolated was talaromacrolactone A (**11**). Among the compounds bioassayed so far, bacillisporin A and *epi*-Bacillisporin F had antibacterial activity whereas the monomer, *O*-desmethylfunalenone (**12**) displayed weak to moderate cytotoxic activity whereas the talauxins displayed no activity.

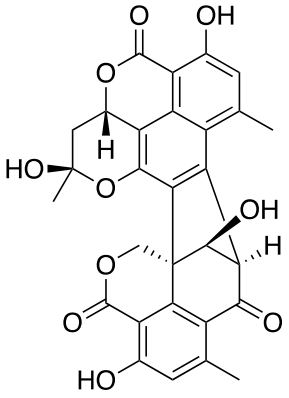

7

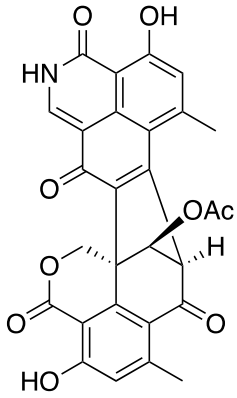

8

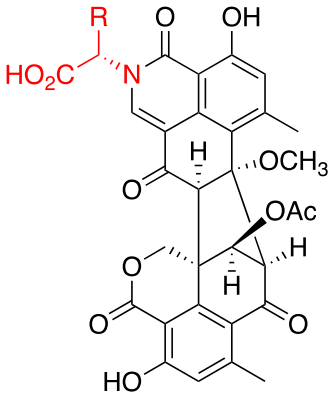

9

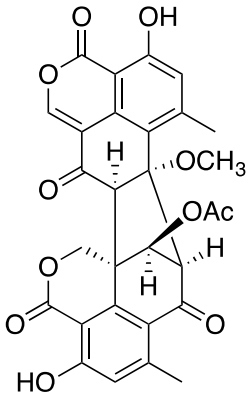

10

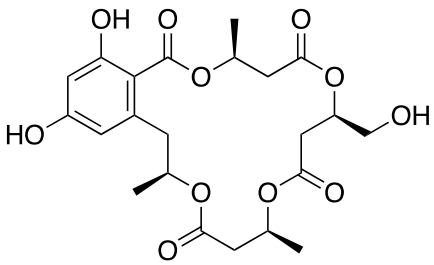

11

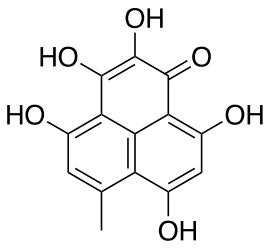

12

Chemical investigation of the filamentous fungal species *A. luteorubrus* revealed the presence of 6 key metabolites with diverse chemical scaffolds including a steroidal glycoside, luteosteroside A (**13**); benzoisofurans, luteolactones A (**14)** and B (**15**); a reverse prenylated alkaloid aszonalenin (**16**), dihydrocandesolide (**17**) and a rare fungal tetracycline antibiotic viridicatumtoxin A (**18**). Amongst these **1-3** were new natural products.

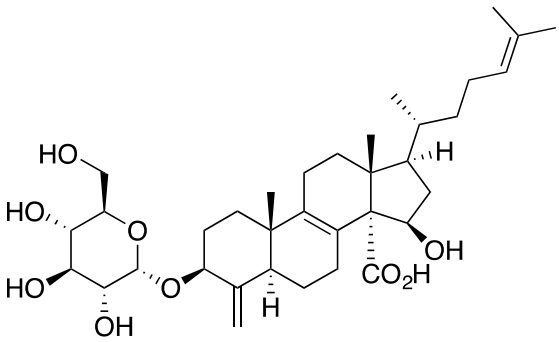

13

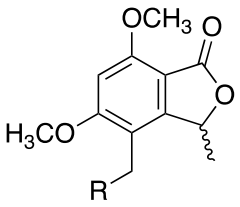

14, R=H

15, R=OH

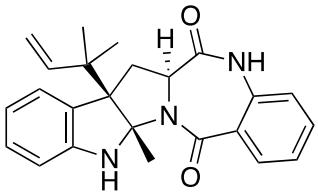

16

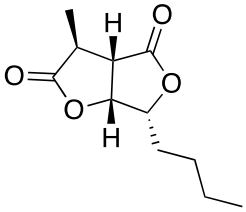

17

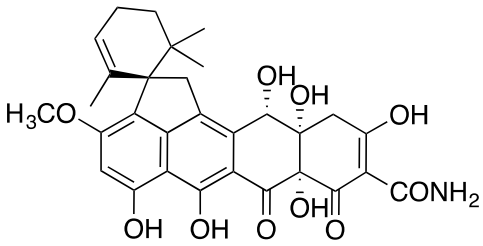

18

Investigation of the *Galbulimima* extract led to the discovery of 4 new unusual polycyclic compounds, **19-22**, including a few with unprecedented structural features. Alkaloid **21** has a different scaffold from all other GB alkaloids that has unraveled a new biosynthetic route involving a bond migration unlike in all other GB alkaloids. Compound **22**, unlike **19-21**, is not an alkaloid and could arise from the oxidation of class I GB alkaloid like himbacine, himbeline or himandravine. Isolation of these new molecules has provided some of the missing interlinks in the biosynthesis of GB alkaloids.

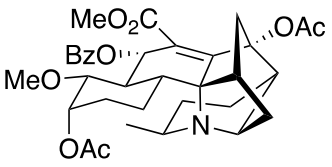

19

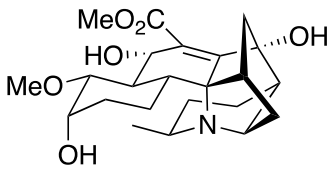

20

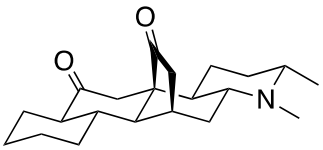

21

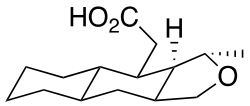

22

To conclude, the chemical investigation of three filamentous fungi and *Galbulimima* alkaloids has resulted in the discovery of 26 new natural products including some unprecedented structures. Additionally, 4 other new molecules were semi-synthesized or obtained as a degradation product. Some of these natural products have been screened for preliminary biological activity and so far, a few of them have shown moderate to weak biological activities. Some of these molecules are still being screened for bioactivity. The proposed biosynthetic pathways can help in the biomimetic synthesis of these natural products and their analogs in the future.